

International Atomic Energy Agency

INDC(NDS)-223/GF

INDC

INTERNATIONAL NUCLEAR DATA COMMITTEE

FUSION EVALUATED NUCLEAR DATA LIBRARY
(FENDL)

PROCEEDINGS OF THE IAEA SPECIALISTS' MEETING
ON FUSION EVALUATED NUCLEAR DATA LIBRARY (FENDL)
ORGANIZED BY THE
INTERNATIONAL ATOMIC ENERGY AGENCY
VIENNA, 8-11 MAY 1989

SUMMARY REPORT

Edited by

V. Goulo

August 1989

IAEA NUCLEAR DATA SECTION, WAGRAMERSTRASSE 5, A-1400 VIENNA

FUSION EVALUATED NUCLEAR DATA LIBRARY
(FENDL)

PROCEEDINGS OF THE IAEA SPECIALISTS' MEETING
ON FUSION EVALUATED NUCLEAR DATA LIBRARY (FENDL)
ORGANIZED BY THE
INTERNATIONAL ATOMIC ENERGY AGENCY
VIENNA, 8-11 MAY 1988

SUMMARY REPORT

Edited by

V. Goulo

August 1989

Abstract

The IAEA Nuclear Data Section, in cooperation with national laboratories and other interested institutions, has begun to assemble, process, and test the Fusion Evaluated Nuclear Data Library (FENDL) for use in international (ITER) and national/regional fusion reactor designs. This report includes a summary report on the second IAEA Specialists' Meeting on FENDL convened by the IAEA Nuclear Data Section from 8 to 11 May 1989 in Vienna with the objectives:

1. to analyse a "review kit" of evaluated nuclear-data intercomparisons with EXFOR data for the choice of files for FENDL; recommend the next actions with the "review kit", including double differential emission spectra of particles and gamma rays; recommend a verification procedure for processing codes and FENDL application libraries;
2. to review the status of special purpose libraries and plans for their development,
3. to analyse the results of a benchmark comparison for a lead sphere.
4. to discuss plans for future co-operation with national and regional nuclear data centres on the development of FENDL.

A number of unpublished papers from the prior specialists' meeting on this subject, held from 14 to 16 November 1987, are included here for convenient reference.

Reproduced by the IAEA in Austria
September 1989

Contents

| | | |
|------|---|----|
| 1. | Introduction. (V. Goulo, J. Schmidt). | 7 |
| 2. | Agenda. | 9 |
| 3. | Time-schedule of future FENDL activities (J. Schmidt, V. Goulo). | 11 |
| 4. | Report of Working Group I. Intercomparison of Evaluated (D. Larson). . . | 17 |
| 4.1. | Intercomparison of evaluations (D. Larson) | 17 |
| 4.2. | Status of evaluations and selection for FENDL-1 (V. Goulo). | 25 |
| 4.3. | Activation subgroup | 27 |
| 4.4. | List of Activation Reactions important for fusion (R. Forrest). . . | 28 |
| 4.5. | Dosimetry file | 33 |
| 5. | Report of Working Group II. Intercomparison of benchmark calculations (K. Sumita, E. Cheng). | 35 |
| 5.1. | Conclusions and Recommendations | 35 |
| 5.2. | Summary of Evaluated results for neutron leakage multiplication from the 22.5 cm TUD lead sphere. | 37 |
| 6. | Processing FENDL-1 into library applications (D. Muir). | 39 |
| 7. | Reports of participants: | |
| 7.1. | Ch. Dunford "Status of ENDF/B-VI" | 43 |
| 7.2. | H. Gruppelaar "The European Fusion File Project" | 46 |
| 7.3. | S. Igarasi "Guide to JENDL-3" | 47 |
| 7.4. | Pronyaev V.G., et al "Consistency of microscopic evaluations and integral experiments for some structural materials" | 50 |
| 7.5. | Forrest R.A. "Work on Fusion Activation in Harwell" | 57 |
| 7.6. | J. Kopecky "European Activation Library for Fusion Reactor Technology" | 62 |
| 7.7. | M. Mizumoto "Brief description of evaluation of lead isotopes for JENDL-3" | 66 |
| 7.8. | E.T. Cheng (USA), "Status of Lead Cross Sections and Benchmark Calculations" | 75 |

| | | |
|------|---|-----|
| 7.9 | H. Maekawa, K. Kosako, T. Suzuki, and A. Hasegawa (Japan), "Analytical Results on IAEA Benchmark Problem Based on TUD Pb Sphere Experiment" | 85 |
| 7.10 | H. Maekawa, Y. Oyama, S. Yamaguchi (Japan), "Preliminary Results of Time-of-Flight Experiment on Lead Slabs" | 91 |
| 7.11 | J. Yamamoto and K. Sumita (Japan), "Benchmark Calculations on a Lead Sphere". | 95 |
| 7.12 | U. Fischer (FRG), "Lead Sphere Benchmark Calculations" | 105 |
| 7.13 | S. Pelloni (Switzerland), "Effect of Double-Differential Lead Cross Sections on the Performance Parameters of Lead Spheres and Fusion Blankets" | 116 |
| 7.14 | D.V. Markovskij (USSR), "Neutron Multiplication in Lead in the Experiments with Neutron Generators" (presented by Pronjaev). . | 138 |
| 7.15 | D.V. Markovskij and A.A. Borisov, "Calculations of Spherical Models of Lead with a Source of 14 MeV Neutrons" (presented by Pronjaev) | 151 |

Reports submitted to the meeting and discussed by the participants

| | | |
|------|--|-----|
| 7.16 | A. Kumar (USA), "Results for IAEA Sponsored International Benchmark on 22.5 cm Thick Spherical Lead Shell". | 161 |
| 7.17 | S. Antonov (Bulgaria), K. Ilieva, J. Jordanova, K. Palova, and I. Popova, "TUD-Pb Computational Benchmark with 14 MeV Neutrons" | 168 |
| 8. | List of participants | 179 |
| 9. | Enclosure - Reports submitted for the IAEA Specialists' Meeting on FENDL, 14-16 November 1987: | |
| 9.1 | E.T. Cheng "Requirements of Nuclear Data Library for the ITER Design" | 185 |
| 9.2 | D.C. Larson, D.M. Hefrick, C.Y. Fu (ORNL) "Description of Evaluation for 50, 52, 53, ⁵⁴ Cr performed for ENDF/B-VI" | 187 |
| 9.3 | D.C. Larson, D.M. Hefrick, C.Y. Fu (ORNL) "Description of Evaluations for 58, 60, 61, 62, ⁶⁴ Ni performed for ENDF/B-VI". . . | 195 |
| 9.4 | D.C. Larson, D.M. Hefrick, C.Y. Fu (ORNL) "Description of Evaluations for 54, 56, 57, ⁵⁸ Fe performed for ENDF/B-VI". | 204 |
| 9.5 | D.C. Larson, D.M. Hefrick, C.Y. Fu (ORNL) "Description of Evaluations for ⁶³ , ⁶⁵ Cu performed for ENDF/B-VI" | 212 |

| | | |
|-----|--|-----|
| 9.6 | D.C. Larson, C.Y. Fu, D.M. Hetrick (ORNL) "Some notes on the calcuation of energy-angular correlated distributions with TNG and their representation in File 6 formats". | 220 |
| 9.7 | S.T. Perkins, E.F. Plecharty, R.J. Howerton, The Lawrence Livermore National Laboratory, " ⁹ Be Evaluation" presented by R.M. White. | 223 |
| 9.8 | K. Shibata "Status of Japanese Nuclear Data Evaluation for Fusion Application". | 237 |
| 9.9 | Forrest R.A. "The Activation Cross Section Library UKACT1 and the Inventory Code FISPACT". | 254 |

I. Introduction (V. Goulo, J. Schmidt).

Following the recommendations of the 16th INDC Meeting and the scientific programme for the development of a nuclear data base for fusion reactor technology agreed at the IAEA Advisory Group Meeting on Nuclear Data for Fusion Reactor Technology, 1-5 December, 1986, Gaussig, German Democratic Republic, IAEA NDS has convened two Specialists' Meetings on the Fusion Evaluated Nuclear Data Library (FENDL) in November 1987 and May 1989.

On 16-19 November 1987 IAEA/NDS convened a group of specialists to formulate a detailed programme and time-schedule for the development of the Fusion Evaluated Nuclear Data Library (FENDL) to meet the future needs of the ITER activity. The conclusions and recommendations of the meeting have been published in report INDC(NDS)-201/GF.

On 8-11 May 1989 the second IAEA Specialists' Meeting on FENDL and Benchmark Calculations was convened with the following objectives:

- analysis of cross-section intercomparisons and recommendations for the choice of files for inclusion in FENDL;
- recommendation of further actions for data intercomparison;
- review of the status of special purpose libraries;
- discussion of the results of calculational benchmarks on lead sphere measurements;
- recommendation of procedures for the fusion processing of FENDL into pointwise/multi-group/Monte Carlo libraries for applications.

The conclusions and recommendations of the meeting can be summarized as follows:

FENDL was agreed to serve as a reference library for use in national and international fusion activities. FENDL-1, the first version of the library, is planned to be finished by the end of 1990. It will consist of nuclear data files, selected from five national evaluated nuclear data libraries which already exist or are currently under development.

- the ENDF/B -VI library maintained by the National Nuclear Data Center at the Brookhaven National Laboratory;
- the BROND library maintained by the USSR Nuclear Data Center at the Physics and Energetics Institute in Obninsk;
- the JENDL-2 and -3 Japanese nuclear data libraries maintained by the JAERI Nuclear Data Center;
- the EFF-1 European Fusion File maintained by ECN Petten, Netherlands;
- the ENDF-84 library maintained by the Lawrence Livermore National Laboratory in the USA.

FENDL-1 will include evaluated nuclear data for the main elements and isotopes of the following fuel, blanket, structural and shielding materials:

H, D, T, Li-6, Li-7, Be-9, B-10, B-11, C-12, N, O, F, Si, Al, Ti, V, Cr-50, Cr-52, Cr-53, Cr-54, Mn-55, Fe-54, Fe-56, Fe-57, Fe-58, Co-59, Ni-58, Ni-60, Ni-61, Ni-62, Ni-64, Cu-63, Cu-65, Zr, Nb-93, Mo-92, Mo-94, Mo-95, Mo-96, Mo-97, Mo-98, Mo-100, Sn, Ba-134, Ba-135, Ba-136, Ba-137, W, and Pb.

The next version of FENDL-2, will contain in addition the following updated special-purpose libraries:

- the International Reactor Dosimetry File for use in neutron dosimetry maintained by the Nuclear Data Section with the support of the Institute für Radiumforschung und Kernphysik, Vienna;
- the Charged Particle Data Library DATLIB maintained by the Technical University in Graz;
- a large comprehensive activation data library covering several thousand activation reactions selected and compiled from various national files, and
- a library of gamma-ray interaction data.

The selection of nuclear data for the FENDL library was organized using the expertise of specialists from several national nuclear data centres and laboratories.

At the first IAEA Specialists' Meeting on FENDL (November 1987, Vienna), a preliminary choice of elements and isotopes was performed and a programme on benchmark calculations for nuclear data testing starting with the lead sphere measurements of the Technical University Dresden, GDR.

The second IAEA Specialists' Meeting on FENDL and Benchmark Calculations (May 1989, Vienna) has analyzed the differences between the evaluated nuclear data files for some of the main fusion reactor materials in comparison with experimental data from the international EXFOR-library. The first stage of intercomparison has included only neutron reaction cross sections. The next intercomparison exercise will be devoted to angular and energy neutron emission spectra, gamma production data, charged particle neutron production data, and activation cross sections. In the second phase of the FENDL project the results of these intercomparison exercises will be used to improve and complement the data contained in the FENDL-1 library and a second improved version of the library, FENDL-2, be developed by 1992 which is intended to serve as a reference file for fusion applications.

The preprocessing of microscopic data files into forms usable in neutronic and safety calculations will be conducted by IAEA/NDS with the support of the laboratories which contribute to the FENDL project. In particular, FENDL will be converted into a fine-mesh point data library and from this a multigroup data library for use in discrete ordinate codes and a library for use in Monte-Carlo code calculations will be prepared.

The integral testing of the data files is an important process to examine the quality of the FENDL-1 files. It will identify the deficiencies of FENDL-1 and suggest actions for improvement for the development of FENDL-2. The integral data testing has been started with the lead benchmark problem and will be continued to include the beryllium benchmark in 1989 due to the importance of the neutron multiplication reactions needed for the design of the near term experimental reactors. Beginning in 1990 high priority structural, blanket, and shield materials such as Fe, Cr, Ni, B, and C, will be considered in the international benchmark comparison activities. In addition to the benchmark data testing, the programme discussed at the second IAEA Specialists' Meeting on FENDL also includes calculational benchmarks for the verification of neutron transport codes.

2. Agenda

IAEA Specialists' Meeting
on
"THE FUSION EVALUATED NUCLEAR DATA LIBRARY (FENDL)
AND BENCHMARK CALCULATION"

IAEA Headquarters, Vienna
Meeting Room C0704, 8 - 11 May 1989

Opening, (Konshin V.A.),

D. Muir was selected as chairman of the meeting.

Section I. Reports on the status of national nuclear data
libraries.

-
1. Status of FENDL, common information on content, general presentation of "Review Kit"
(V. Goulo, NDS)
 2. Status of ENDF/B-VI
(Ch. Dunford, BNL, USA)
 3. The European Fusion File Project
(H. Gruppelaar, Petten)
 4. Guide to JENDL-3
(S. Igarasi, JAERI)
 5. Status of BROND
(V. Pronjaev, FEI, USSR)
 6. Status of dosimetry reaction cross section evaluations
(H. Vonach, IRK)
 7. Status of Charged Particle Neutron Production Data Library-DATLIB
(R. Feldbacher, Graz)
 8. UK activity on activation data
(R. Forrest, UK)
 9. REAC-activation data library
(J. Kopecky, Petten)

Working Group I: Intercomparison of Evaluations

Chairman D. Larson (ORNL, USA)

- 1) Detailed evaluation comparisons following "Review Kit".
Recommendations of choice for FENDL-1
- 2) Special Purpose Files

Working Group II: Inter-Comparison of Benchmark Calculations

Chairman: Prof. K. Sumita (Osaka)
Secretary: Dr. E.T. Cheng (San Diego, USA)

I. Reports presented by the participants

- (1) E.T. Cheng (USA), "Status of Lead Cross Sections and Benchmark Calculations"
- (2) H. Maekawa, K. Kosako, T. Suzuki, and A. Hasegawa (Japan), "Analytical Results on IAEA Benchmark Problem Based on TUD Pb Sphere Experiment"
- (3) H. Maekawa, Y. Oyama, S. Yamaguchi (Japan), "Preliminary Results of Time-of-Flight Experiment on Lead Slabs"
- (4) J. Yamamoto and K. Sumita (Japan), "Benchmark Calculations on a Lead Sphere"
- (5) U. Fischer (FRG), "Lead Sphere Benchmark Calculations"
- (6) U. Fischer (FRG), A. Schwenk-Ferrero, and E. Wiegner, "Neutron Multiplication in Lead: A Comparison Study Based on a New Computational Procedure and New Nuclear Data"
- (7) S. Pelloni (Switzerland), "Effect of Double-Differential Lead Cross Sections on the Performance Parameters of Lead Spheres and Fusion Blankets"
- (8) D.V. Markovskij (USSR), "Neutron Multiplication in Lead in the Experiments with Neutron Generators" (presented by Pronyaev)
- (9) D.V. Markovskij and A.A. Borisov, "Calculations of Spherical Models of Lead with a Source of 14 MeV Neutrons" (presented by Pronyaev)

II. Reports submitted to the meeting and discussed by the participants

- (1) A. Kumar (USA), "Results for IAEA Sponsored International Benchmark on 22.5 cm Thick Spherical Lead Shell"
- (2) S. Antonov (Bulgaria), K. Ilieva, J. Jordanova, K. Palova, and I. Popova, "TUD-Pb Computational Benchmark with 14 MeV Neutrons"

Thursday, 11 May

- (1) Report of WG I (review)
- (2) Report of WG II (review)
- (3) Summary, actions, recommendations
- (4) Date and place of next FENDL meetings.

3. Time-schedule of future FENDL activities
Chairmen: J.J. Schmidt and D. Muir
Secretary: V. Goulo

1. Actions for FENDL-1:

- 1.1 Participants: send all files identified for inclusion into FENDL-1 to IAEA/NDS till the end of 1989.
- 1.2 NDS: check these files and assemble them in ENDF/B -VI format to check the FENDL-1 library to be finalized by the end of 1990.
- 1.3 Bologna: send the EFF-1 file for Al in ENDF/B-V format ENDS.
- 1.4 NDS: translate the Bologna Al file into ENDF/B -VI format.
- 1.5 NDS: request corrected Si file from Dresden.
- 1.6 NDS: request selected JENDL-3 files from their evaluators only for review.
- 1.7 NDS: use the ENDF/B -VI gamma interaction data library for incorporation into FENDL-1.
- 1.8 NDS: translate the Graz charged particle nuclear data library from ECPL- into ENDF/B format using the format conversion programme of ENEA, Bologna (G. Panini).
- 1.9 NNDL/NDS: arrange a review of the main charged particle nuclear reactions relevant for DT - fusion reactors of the Graz charged particle nuclear data library at the next CSEWG - meeting to be held at Brookhaven, November 1989, by R. White, G. Hale and R. Feldbacher.
- 1.10 NDS/IRK Vienna: finish an updated version of the IRDF-library by March 1990.
- 1.11 Activation data library:
Kopecky, Forrest, Mann, Pronyaev:

(1) Send list of about 200 high priority reactions to be included into FENDL-1 to NDS by June 1989;

(2) Send evaluations for these reactions to NDS by November 1989 for review at the next FENDL meeting in 1990.

NDS: prepare plots of these evaluations two months prior to the next FENDL meeting in 1990.

2. Preprocessing of FENDL-1

- 2.1 The pre-processing of neutron data files for the FENDL-1 library into pointwise (PENDF) data files and the preparation of application data libraries will be done by NDS till October 1990.
- 2.2 PENDF should be converted into the following libraries for applications in fusion calculations:

- neutron and gamma multigroup cross sections (GENDF) for discrete ordinate codes and a library for Monte Carlo codes (ACE),
- multigroup covariance matrices library, and
- KERMA and DPA cross section library.

- 2.3 The pre-processing procedure of MF=6 (double differential particle and γ -ray emission spectra) should include verification of this procedure for the available modules of the NJOY-code system (Los Alamos) and the code GROUPXS (Petten). The meeting considered this task as urgent before starting the processing of all FENDL-files.
- 2.4 The pre-processing of data should be performed by NDS, but NDS certainly needs help in this task. NDS should obtain test cases of file processing from each of the major data file producers together with information on the computer software used. It was decided that test cases should be sent to NDS as pointed out in the table below till 30 June 1990.

| | Material | PENDF | GENDF | ACE |
|-----------|-------------------|-------|-------|-----|
| BROND | D and Nb | + | + | + |
| ENDF/B-VI | Fe-56 and/or Be-9 | + | + | + |
| EFF | Pb | + | + | + |
| JENDL | Mn-55 | + | + | + |

- 2.5 NDS should independently try the pre-processing of the EFF-Pb file into 175 VITAMIN-J groups with NJOY and GROUPXS to prepare transfer matrices from MF=6 data by 31 October 1989.

3. Benchmark data testing

- 3.1 Markovskij will report recent Kurchatov experimental Pb benchmark data at the planned Gaussig Fusion Benchmark Meeting in November 1989. The participants in the Pb benchmark intercomparison should complete their comparison between calculations and the new Kurchatov data and submit a report to the NDS by 31 December 1989.
- 3.2 Additional Pb -benchmark problems to be discussed at the Gaussig benchmark meeting:
- JAERI leakage spectra from slab geometry
 - Osaka 10 cm pulsed sphere leakage spectra.

Specifications and results of these measurements should be sent to NDS by the end of March 1990.

Action on NDS: to distribute this information to the benchmark intercomparison participants. Till 30 September 1990 NDS should collect the results of the new calculations to be discussed at the Chengdu Benchmark Meeting in October 1990.

- 3.3 Action on Maekawa, Markovskij: to send Be- benchmark data available from JAERI and Kurchatov Institute to NDS till 30 September 1989.

NDS to distribute this information plus GENDF and ACE data files for Be immediately and collect the results from the Benchmark intercomparison participants by 30 September 1990, to be discussed at the Chengdu Benchmark Meeting in October 1990.

- 3.4 The Chengdu Meeting should also consider shielding benchmarks and other blanket benchmarks. Home task to participants to identify needs for such benchmarks.

4. Neutronic codes verification

- 4.1 Analysis of the benchmark calculations on the lead sphere showed large differences between different codes used and even between results obtained with the same codes (e.g. ANISN). It is urgently necessary to find out about the reasons for these discrepancies. The following actions were agreed:

U. Fischer (KFK): repeat calculations with codes ONETRAN, ANTRAI and ONEDANT and submit a report on the findings to NDS by 1 October 1989.

H. Maekawa (JAERI): try to identify the reasons for the different results of the ANISN and BERMUDA codes and send a report to NDS by 1 October 1989.

NDS: conclude a research contract with Dr. Ilieva (Sofia) with the tasks to perform the Pb benchmark calculations with different codes, but one and the same EFF-Pb multigroup data set, and to perform further benchmark calculations with different codes, but same multigroup data set.

Cheng, Sumita, Markovskij, Zhou Delin: perform independent calculations of the Pb benchmark with the code ANISN and the EFF-Pb VITAMIN-J multigroup cross section data to be provided by Pelloni and submit reports to NDS by 31 December 1989.

5. Future meetings

1989

- 5.1 Review Meeting for the most important charged particle reactions occurring in the D-T fusion cycle during the CSEWG meeting at BNL, USA, on 13 November 1989,

- 5.2 Informal IAEA Meeting on Fusion Benchmarks with the tasks:

- to review Pb and Be benchmark specifications,
- to analyse the results of the neutronics codes intercomparison for the Pb benchmark,
- to analyse the results of the ANISN code calculations.

This should be a two day meeting to be held in conjunction with the XIXth International Symposium in Nuclear Physics - Nuclear Processes in Fusion Reactors, Gaussig, German Democratic Republic, 6 - 10 November 1989.

1990

5.3 Consultants Meeting on FENDL, Vienna, 4 days, June 1990 (tentative date) in conjunction with the Agency's Research Coordination Meeting on Measurement and Analysis of Double-Differential Neutron Emission Spectra, with the following main objectives:

- to finalize the review of FENDL-1, and
- to start preparation of FENDL-2,

and the following specific tasks:

- to discuss the problems encountered in FENDL-1 files,
- to review gamma production and DDCS data in FENDL-1 for ^{52}Cr , ^{56}Fe , ^{58}Ni and ^{208}Pb ,
- to review and approve charged particle nuclear data for incorporation into FENDL-1,
- to review and approve dosimetry neutron cross sections (IRDF update) for incorporation into FENDL-1,
- to review and approve activation cross sections for incorporation into FENDL-1,
- to define new evaluations to replace FENDL-1 files to be considered for FENDL-2.

The exact date of the meeting will depend upon preparation of graphs for DDCS, charged particle, dosimetry and activation cross section data and upon availability of new evaluations for FENDL-2.

5.4 Advisory Group Meeting on Fusion Benchmark Measurements and Calculations, Chengdu, South-West Institute of Nuclear Technology, China, 4 days, October 1990, with the following tasks:

- to review measurements and evaluations of $(n,2n)$ cross sections for Pb, Be and other benchmark materials,
- to discuss the available integral experiments for Pb, Be and other benchmark materials,
- to analyse the Pb and Be benchmark calculational results, and
- to discuss and specify candidates for other material benchmarks including shielding and other blanket benchmarks,

1991

5.5 Advisory Group Meeting on FENDL-2 and Benchmark Calculations, mid 1991, Vienna.

After 1991

5.6 1-2 meetings per year should be considered after 1991.

6. FENDL - NETWORK

During the meeting a proposal was made to use for the FENDL activity the MFE-NETWORK connection.

Action on Ch. Dunford: inform NDS whether this is possible.

7. Action on NDS: to submit information on the status of FENDL-1 and plans for FENDL-2 development for the ITER-Newsletter.

4. Report of Working Group I "Intercomparison of Evaluations"
(Chairman D. Larson)

4.1 Intercomparison of Evaluations (D. Larson)

Participants: D. Larson (Chairman), F. Mann, H. Gruppelaar, V. Goulo, V. Pronyaev, Ch. Dunford, H. Vonach, S. Igarasi, J. Kopecky, R. Forrest, G. Reffo, G. Panini, Zhou Delin.

Working Group I assembled, with the purpose of reviewing and comparing, available evaluations from the BROND, EFF, ENDF and JENDL libraries. Primary participants in this effort included H. Vonach, Zou Dhelein, G. Reffo, G. Panini, S. Igarasi, H. Gruppelaar, J. Kopecky, V. Pronyaev, R. Forrest, C. Dunford, D. Larson, and F. Mann. Two full working days were devoted by this group to critical reviews based primarily on the three volumes of plots of BROND vs ENDF/B-VI vs EXFOR experimental data produced by V. Goulo during a visit to Brookhaven National Laboratory. Plots of cross section comparison are prepared as IAEA(NDS) document and available from Nuclear Data Section upon request. Plots of selected evaluations from JENDL-2 and EFF were also available. As specific results of this review, selections were made for the FENDL-1 library from among the evaluations offered. The evaluations selected are listed in item 4.5 of this report. The primary criterion for these choices for FENDL-1 was completeness of the evaluations for fusion application purposes. The evaluation comparison exercise indicated differences between the BROND, JENDL, EFF and ENDF/B Libraries, but at present the most complete library is ENDF/B-VI, since it includes gamma-ray production, File 6 data including neutron, proton, alpha, gamma and recoil distributions, and will include uncertainty files. Evaluators for the various libraries agreed that this file intercomparison was a very useful exercise and will take its results back for further review and improvements of the individual files.

Since this was the first time evaluations from the four projects have been assembled for a mutual evaluation review, several suggestions were made for more information to allow more complete future reviews of the files. In particular, in addition to the resonance region (File 2) and cross section (File 3) plots which were available for review this time, for the next review it was felt to be very useful to have plots for File 6 data comparing (n,xn), (n,xp), (n,x α) and (n,x γ) energy distributions with available experimental data around 14 and 9 MeV. It would also be useful to have plots of binned cross sections versus experimental data in the resonance region, as the working group found it difficult to compare highly structured resonance region evaluations with averaged experimental data.

A summary of the results of the discussions and comparisons of the evaluated data libraries follows. Most of the comments are for BROND and ENDF, since plots comparing these evaluations with experimental data were available.

^{58}Ni

====

1. Different values of scattering radii were used for resonance region cross sections
2. ENDF/B-VI (V6) uses Reich-Moore (as does BROND) and more recent experimental data, with the resolved resonance region extending to 850 keV

3. Missed resonances in EFF above 450 keV
4. (n,2n) in BROND should use latest data
5. (n, γ) has too coarse an energy grid in V6 above 1 MeV
6. (n,p) in BROND too large above 14 MeV
7. (n, α) cross section in V6 may be too low at peak near 10 MeV, based on new data
8. (n, γ) Γ_γ may be too large for the 15.3 keV resonance (conclusion from Mito Conference paper) - may be 1.5 eV

⁶⁰Ni
====

1. BROND thermal values lower than BNL-325, V6, EFF
2. V6 has each reaction in File 6, including recoil and gamma spectra
3. EFF does not include effect of distant resonances
4. Glitch near 14 MeV in BROND (n,p)
5. (n,p) in EFF lower than in BROND and V6 below 14 MeV, but new preliminary data favour EFF
6. V6 misses low energy resonances present in BROND, EFF
7. V6 energy grid too coarse for (n, γ) above 1 MeV
8. V6 (n, γ) may have too little semi-direct contributions
9. (n, γ) in BROND lower than EFF, V6 but little data available
10. V6 has (n, α) shape different from BROND, EFF

⁵⁶Fe
====

1. BROND has negative angular distribution data in MT-58
2. V6 energy grid too coarse for (n, γ)
3. There may be an interpolation problem in BROND (n,p)
4. Shape difference between V6 and BROND (n, α) should be checked
5. Both BROND and V6 have photon production data
6. EFF will be ready late fall 1989

54Fe

====

1. Energy balance problem in MT=16 at 16 MeV for BROND
2. V6 misses narrow resonances from 3 - 50 keV
3. BROND total cross section low 500 - 700 keV
4. Inelastic cross section differences between V6 and BROND above 3 MeV
5. (n,2n) has differences above ~ 15 MeV, V6 may follow better experimental data set
6. V6 capture from 1 - 6 MeV should be checked
7. (n,p) in BROND may be too large at ≈ 10 MeV
8. (n,np) in V6 above experimental data, BROND agrees with experimental data

Pb

==

1. BROND - sum up test fails for disappearance cross section, normalisation problem for MF=6, MT=10
2. BROND has resolved resonances, EFF does not
3. Files should have MF= 4 and 5, but not MF= 6, or MF= 6 but not 4 and 5, all three (4,5,6) should not be present simultaneously
4. BROND has negative angular distribution data for MF=6, MT=10
5. BROND does not have gammas, recoils or charged particles in MF=6. Gammas are in File 12 - 15
6. BROND has some gammas which do not conserve energy
7. EFF has energy points in partial cross sections which must also be in total cross sections
8. EFF has MT=3,4 sum up problems
9. EFF has no gammas or recoils in MF=6 - gammas are in 12-15
10. Gamma-ray energy balance in BROND and EFF may have problems
11. BROND total cross section low below 100 keV, high from 0.8 - 1.6 MeV
12. EFF has glitch near 14 MeV in total
13. BROND elastic lower than EFF
14. Check (n,2n) near 14 MeV, BROND may be high, EFF may be low, JENDL is low
EFF will raise (n,2n) to 2.19 b at 14.1 MeV (Vonach's evaluation)
EFF does not have semi-direct capture at 14 MeV

⁵²Cr

====

A new, revised evaluation for BROND is in progress, including DDX, photon production, and resolved resonance region.

1. Thermal values for BROND are too low compared to BNL-325
2. V6 resolved resonance region awaits further discussion with GEEL prior to completion
3. BROND higher than V6 for elastic by ~ 10% for $E_n > 10$ MeV
4. BROND (n,n') goes to zero at 20 MeV, lower than V6 elsewhere
5. V6 (n,2n) higher than BROND, but recent IRK data agree with V6
6. V6 misses (n, γ) resonance below ~ 5 KeV
7. V6 energy grid too coarse for (n, γ) above ~ 1 MeV
8. BROND (n,np) too large at high energies as a consequence of low (n,n')

⁶Li

===

1. BROND and V6 differ in elastic cross section below 150 keV
2. Neither BROND nor V6 use File 6; both use Files 4,5
3. V6 is standard cross section at lower energies

⁷Li

===

1. BROND has a new file, main improvements below ~ 10 keV
2. Slight energy shift in 250 keV resonance for total cross section (BROND, V6)
3. Glitch in (n, γ) at 10 MeV in BROND
4. (n,d) cross sections differ in BROND, V6, but go through available data
5. Univ. Birmingham will provide DDX based on V6, EFF and V6 will use these data

⁵⁰Cr

====

1. Check BROND scattering radius - problem with low energy scattering
2. For V6, total cross section is for natural Cr above 4 MeV

3. BROND total inelastic has strange shape

4. BROND (n,p) may be too low

⁵³Cr

=====

1. Check BROND scattering radius as for ⁵⁰Cr

2. Comment 2 for ⁵⁰Cr applies

3. V6 (n,2n) may be too high

⁵⁴Cr

=====

1. Comments 1 and 2 for ⁵⁰Cr apply

2. BROND high energy cross section too large

3. BROND has no direct interaction contribution at high energies

⁵⁷Fe

=====

1. Total cross section for V6 above 200 keV is for natural iron

2. Resonance structure is missing in first inelastic level for V6

3. V6 should look at direct inelastic contribution (this may lower n, 2n)

4. Add more energy points in (n, γ) above 1 MeV

⁵⁸Fe

=====

1. BROND potential scattering may be low

2. V6 total cross section above 400 keV is for natural iron

3. V6 - check direct interaction (n,n'), may need more levels to raise (n,n') at high energies

4. Add more points in V6 (n, γ) above ~ 1 MeV

⁶¹Ni

=====

1. V6 misses low energy narrow resonances

2. Total cross section in V6 is for natural nickel above 70 keV

3. (n, γ) may be low in V6 near 14 MeV

4. V6 (n,np) may be high

^{62}Ni

====

1. V6 total cross section above 600 keV is for natural nickel
2. V6 - look at high energy capture
3. (n,γ) is important activation cross section

^{64}Ni

====

1. V6 total cross section above 600 keV is for natural nickel
2. V6 - check (n,γ) resonance parameters from 40 - 100 keV, strange looking plot

^{92}Mo

====

1. JENDL-2 (J-2) capture does not include direct capture (included in J-3)
2. J-2 has $(n,3n)$ energy balance problem

^{94}Mo

====

1. As for ^{92}Mo
2. (n,p) low compared to new data
3. (n,α) low compared to new data

^{95}Mo

====

1. As for ^{92}Mo
2. $(n,3n)$ energy balance problem in J-2
3. New (n,γ) data at 14 MeV are higher than J-2

^{96}Mo

====

1. As for ^{92}Mo
2. As for ^{92}Mo
3. J-2 total cross section may be low from 1-5 MeV

^{97}Mo

====

1. As for ^{92}Mo
2. As for ^{92}Mo
3. J-2 total (n,n') rises at 20 MeV
4. J-2 has dip in elastic scattering near 12 MeV
5. New (n,p) data near threshold are lower than J-2

Notifications: VG - ENDF/B-VI, J-2 - JENDL-2

^{98}Mo

====

1. As for ^{92}Mo
2. As for ^{92}Mo
3. New Russian data for (n, γ) lower than J-2 above 100 keV

^{100}Mo

====

1. As for ^{92}Mo
2. As for ^{92}Mo
3. J-2 total may be low from 500 keV to 6 MeV
4. J-2 check elastic scattering around 10 MeV
5. J-2 (n,n') increases at 20 MeV
6. J-2 (n,2n) is lower than experimental data at 14 MeV - important activation cross section
7. J-2 (n, γ) higher than experimental data from 500 keV to 6 MeV

^2H

==

1. J-2 thermal neutron capture higher than Mughabghab

V

=

1. J-2 has no direct capture contribution
2. J-2 total cross section higher than experimental data from thermal up to 150 eV

3. V6 fails to reproduce minimum in total cross section near 8 keV
4. General discrepancies in reproduction of total width resonance parameters
5. J-2 total cross section high from 1 - 4 MeV
6. J-2 (n, γ) higher than V6 up to 100 eV
7. V6 uses straight line for (n, γ) from 40 - 2000 eV
8. J-2 does not match experimental elastic scattering data from 500 - 1000 keV
9. No direct capture in J-2
10. J-2 has (n,p) problem below 4 MeV
11. V6 (n,np) very large
12. V6 (n,n't) much larger in J2 than V6
13. J-2 (n, α) threshold has problem - fixed in J-3

Be

==

1. V6 thermal (n, γ) disagrees with BNL-325
2. V6 (n,d₀) has energy balance problem at 20 MeV
3. (n, γ) plot looks strange for V6
4. V6 (n,2n) reduced by ~ 10% from V5
5. No covariance information available for V6, cooperation encouraged
6. EFF/Birmingham work going on for energy distributions

4.2 Status of Evaluations and selection for FENDL-1 (V.Goulo)

| Element | Evaluation source | Availability | Reviewed by | Corrected | Format ENDF/B | FENDL-1 choice |
|---------|-------------------|--------------|-------------|-----------|---------------|----------------------|
| H | ENDF/B-6 | A | Evaluator | Y | 6 | ENDF/B-6 |
| D | JENDL-2 | A | N | N | 6 | BROND |
| | ENDF/B-5 | N/A | N | N | 6 | |
| | BROND | A | N | N | 6 | |
| T | ENDF/B-6 | A | Evaluator | Y | 6 | V6 |
| Li-6 | ENDF/B-6 | A | CSEWG | Y | 6 | V6 |
| | BROND | A | N | N | 6 | |
| Li-7 | ENDF/B-6 | A | CSEWG | Y | 6 | V6/EFF |
| | BROND | A | N | N | 6 | |
| Be-9 | ENDF/B-6 | A | CSEWG | Y | 6 | V6 |
| | ENDF/B-5 | N/A* | | | | |
| B-10 | ENDF/B-6 | A | CSEWG | Y | 6 | V6 |
| | ENDF/B-5 | N/A* | | | | |
| B-11 | ENDF/B-6 | A | CSEWG | Y | 6 | V6 |
| C-12 | ENDF/B-6 | A | CSEWG | Y | 6 | V6 |
| N | ENDF/B-IV | A | Evaluator | Y | 6 | V6 (unless BROND) |
| O | ENDF/B-4 | A | - | - | 4 | V6 |
| F-19 | JENDL-2 | A | Evaluator | N | 6 | JENDL-2 |
| | ENDF/B-5 | N/A* | | | | |
| AL | EFF-1 | N/A | | | | EFF-1 |
| | ENDF/B-4 | A | - | - | 4 | |
| Si | BROND | A | CSEWG | N | 5 | BROND |
| | EFF-1 | N/A | | | | |
| Ti | ENDF/B-IV | A | Evaluator | Y | 6 | V6 |
| V-51 | JENDL-2 | A | Evaluator | N | 6 | V6 unless JENDL-3 |
| | ENDF/B-5 (ANL) | A | CSEWG | N | 6 | |
| Cr-0 | BROND | A | N | N | 6 | |
| | ENDF/B-5 | N/A* | | | | |
| Cr-50 | BROND | A | - | N | 6 | V6 |
| | ENDF/B-6 | A | CSEWG | N | 6 | |
| Cr-52 | BROND | A | - | N | 6 | V6 |
| | ENDF/B-6 | A | CSEWG | N | 6 | |
| Cr-53 | BROND | A | - | N | 6 | V6 |
| | ENDF/B-6 | A | CSEWG | N | 6 | |
| Cr-54 | BROND | A | - | N | 6 | V6 |
| | ENDF/B-6 | A | CSEWG | N | 6 | |
| Mn-55 | ENDF/B-6 (JAERI) | A | CSEWG | Y | 6 | V6/JENDL-3 |
| | ENDF/B-5 | N/A* | | | | |

| | | | | | | |
|-------|----------------------------|------------------|------------|--------|--------|-----------|
| Fe-0 | BROND ENDF/B-5 | A N/A* | - | N | 6 | |
| Fe-54 | BROND ENDF/B-VI | A A | - CSEWG | N Y | 6 6 | V6 |
| Fe-56 | BROND ENDF/B-VI | A A | - CSEWG | N Y | 6 6 | V6 |
| Fe-57 | BROND ENDF/B-VI | A A | - CSEWG | N Y | 6 6 | V6 |
| Fe-58 | BROND ENDF/B-VI | A A | - CSEWG | N Y | 6 6 | V6 |
| Co-59 | ENDF/B-VI ENDF/B-5 | A N/A* | CSEWG | Y | 6 | V6 |
| NI-0 | BROND ENDF/B-5 EFF-2 | A N/A* N/A | - | N | 6 | |
| NI-58 | BROND ENDF/B-6 EFF-2 | A A N/A | - CSEWG | N N | 6 6 | V6 |
| NI-60 | BROND ENDF/B-6 EFF-2 | A A N/A | - CSEWG | N N | 6 6 | V6 |
| NI-61 | BROND ENDF/B-6 EFF-2 | A A N/A | - CSEWG | N N | 6 6 | V6 |
| NI-62 | BROND ENDF/B-6 EFF-2 | A A N/A | - CSEWG | N N | 6 6 | V6 |
| NI-64 | BROND ENDF/B-6 EFF-2 | A A N/A | - CSEWG | N N | 6 6 | V6 |
| Cu-63 | ENDF-VI ENDF/B-5 | A N/A | CSEWG | Y | 6 | V6 |
| Cu-65 | ENDF-VI ENDF/B-5 | A N/A | CSEWG | Y | 6 | V6 |
| Zr | BROND ENDF/B-IV | N/A A | - | - | 6 | V6 |
| Nb | BROND ENDF/B-6 (ANL) | A END 89 | - | N | 6 | new BROND |
| Mo-0 | JENDL-2 ENDF/B-5 | A N/A* | Evaluator | N | 6 | |
| Mo-92 | JENDL-2 ENDF/B-5 | A N/A* | Evaluator | N | 6 | JENDL-2 |
| Mo-94 | JENDL-2 ENDF/B-5 | A N/A* | Evaluator | N | 6 | JENDL-2 |
| Mo-95 | JENDL-2 ENDF/B-5 | A N/A* | Evaluator | N | 6 | JENDL-2 |

| | | | | | | |
|--------|----------------------|---------------|-----------|--------|--------|---------|
| Mo-96 | JENDL-2 ENDF/B-5 | A N/A* | Evaluator | N | 6 | JENDL-2 |
| Mo-97 | JENDL-2 ENDF/B-5 | A N/A* | Evaluator | N | 6 | JENDL-2 |
| Mo-98 | JENDL-2 ENDF/B-5 | A N/A* | Evaluator | N | 6 | JENDL-2 |
| Mo-100 | JENDL-2 ENDF/B-5 | A N/A* | Evaluator | N | 6 | JENDL-2 |
| Sn | ENDL | END 89 | Evaluator | | | V6 |
| Ba-134 | ENDF/B-6 | A | Evaluator | Y | 6 | V6 |
| Ba-135 | ENDF/B-6 | A | Evaluator | Y | 6 | V6 |
| Ba-136 | ENDF/B-6 | A | Evaluator | Y | 6 | V6 |
| Ba-137 | ENDF/B-6 | A | Evaluator | Y | 6 | V6 |
| W | ENDF/B-6 | END 89 | | | | V6 |
| PB-0 | BROND EFF-1 | A A | - - | N N | 6 6 | EFF-1 |
| PB-206 | ENDF/B-5 ENDF/B-6 | N/A* A | CSEWG | Y | 6 | |
| PB-207 | ENDF/B-5 ENDF/B-6 | N/A* A | CSEWG | Y | 6 | |
| PB-208 | ENDF/B-5 ENDF/B-6 | N/A* A | CSEWG | Y | 6 | |
| Bi-209 | EFF-1 ENDF/B-6 | N/A END 89 | | | | |

* - generally not available but exists in "review kit"
EVALUATOR - review was done by evaluator

Graphs of intercomparison of evaluated cross section data from files presented for FENDL and EXFOR-data will be published as internal document of Nuclear Data Section.

4.3 Activation Subgroup

Participants: R. Forrest, J. Kopecky, F. Mann, and V. Pronyaev.

By mid-summer 1989, ECN Petten, Harwell, Hanford and Obninsk will send to the IAEA a list of about 200 reactions which are the most important as determined through calculations by Cheng and Forrest.

NDS will request from all interested parties (including, but not limited to, BROND, EFF, ENDF/B, JENDL) that evaluations for these reactions be sent to the IAEA by November.

Two months prior to the next FENDL meeting in 1990, the IAEA will distribute plots to interested parties showing the submitted evaluations and experimental data.

At the next FENDL meeting in 1990, a subgroup will review the submitted evaluations and will recommend evaluations for incorporation into the FENDL-1 Activation Library.

4.4 List of Reactions important for Fusion.
R. Forrest (Harwell, UK).

| <u>Number</u> | <u>Reaction</u> | <u>Target</u> | <u>Source</u> |
|---------------|-------------------------|---------------|---------------|
| 1 | $^{11}\text{B}(n,d)$ | S | 5 |
| 2 | $^{13}\text{C}(n,g)$ | S | 1,4,5 |
| 3 | $^{13}\text{C}(n,a)$ | S | 1,5 |
| 4 | $^{14}\text{C}(n,na)$ | 5730y | 1 |
| 5 | $^{14}\text{N}(n,p)$ | S | 2,3 |
| 6 | $^{14}\text{N}(n,d)$ | S | 5 |
| 7 | $^{14}\text{N}(n,np)$ | S | 5 |
| 8 | $^{16}\text{O}(n,a)$ | S | 1 |
| 9 | $^{17}\text{O}(n,a)$ | S | 1,5 |
| 10 | $^{17}\text{O}(n,na)$ | S | 1 |
| 11 | $^{20}\text{Ne}(n,a)$ | S | 1,5 |
| 12 | $^{23}\text{Na}(n,a)$ | S | 1,5 |
| 13 | $^{24}\text{Mg}(n,p)&$ | S | 4 |
| 14 | $^{24}\text{Mg}(n,na)$ | S | 1,5 |
| 15 | $^{26}\text{Mg}(n,g)$ | S | 1 |
| 16 | $^{27}\text{Al}(n,2n)&$ | S | 1,3,5 |
| 17 | $^{27}\text{Al}(n,a)&$ | S | 5 |
| 18 | $^{27}\text{Al}(n,na)$ | S | 5 |
| 19 | $^{28}\text{Si}(n,na)$ | S | 1 |
| 20 | $^{28}\text{Si}(n,np)$ | S | 1,5 |
| 21 | $^{28}\text{Si}(n,d)$ | S | 1,5 |
| 22 | $^{30}\text{Si}(n,g)$ | S | 1,4,5 |
| 23 | $^{31}\text{Si}(n,g)$ | 2.6h | 1,5 |
| 24 | $^{31}\text{P}(n,g)$ | S | 1,5 |
| 25 | $^{32}\text{P}(n,p)$ | 14.3d | 1,5 |
| 26 | $^{34}\text{S}(n,g)$ | S | 4 |
| 27 | $^{34}\text{S}(n,a)$ | S | 4 |
| 28 | $^{35}\text{Cl}(n,a)$ | S | 4 |
| 29 | $^{35}\text{Cl}(n,p)$ | S | 4 |
| 30 | $^{37}\text{Ar}(n,np)$ | 35d | 5 |
| 31 | $^{37}\text{Ar}(n,d)$ | 35d | 5 |
| 32 | $^{40}\text{Ar}(n,g)$ | S | 4 |
| 33 | $^{40}\text{Ar}(n,2n)$ | S | 1 |
| 34 | $^{39}\text{K}(n,p)$ | S | 3,5 |
| 35 | $^{39}\text{K}(n,a)$ | S | 5 |
| 36 | $^{41}\text{K}(n,p)$ | S | 4 |
| 37 | $^{40}\text{Ca}(n,a)$ | S | 5 |
| 38 | $^{40}\text{Ca}(n,2p)$ | S | 5 |
| 39 | $^{40}\text{Ca}(n,g)$ | S | 5 |
| 40 | $^{40}\text{Ca}(n,np)$ | S | 3,5 |
| 41 | $^{40}\text{Ca}(n,d)$ | S | 3,5 |
| 42 | $^{42}\text{Ca}(n,2n)$ | S | 1 |
| 43 | $^{42}\text{Ca}(n,a)$ | S | 1,3,5 |
| 44 | $^{43}\text{Ca}(n,2n)$ | S | 1 |
| 45 | $^{43}\text{Ca}(n,na)$ | S | 1 |

| <u>Number</u> | <u>Reaction</u> | <u>Target</u> | <u>Source</u> |
|---------------|--------------------------|---------------|---------------|
| 46 | $^{43}\text{Ca}(n,2p)$ | S | 5 |
| 47 | $^{44}\text{Ca}(n,2n)$ | S | 1 |
| 48 | $^{44}\text{Ca}(n,a)$ | S | 4 |
| 49 | $^{44}\text{Ca}(n,na)$ | S | 1 |
| 50 | $^{44}\text{Ca}(n,g)$ | S | 4 |
| 51 | $^{45}\text{Ca}(n,a)$ | 163d | 1,3,5 |
| 52 | $^{46}\text{Ca}(n,na)$ | S | 1,5 |
| 53 | $^{46}\text{Ca}(n,g)$ | S | 4 |
| 54 | $^{48}\text{Ca}(n,2n)$ | S | 4 |
| 55 | $^{45}\text{Sc}(n,a)$ | S | 1 |
| 56 | $^{45}\text{Sc}(n,p)$ | S | 1,4 |
| 57 | $^{45}\text{Sc}(n,g)$ & | S | 4 |
| 58 | $^{46}\text{Sc}(n,na)$ | 83d | 1 |
| 59 | $^{45}\text{Ti}(n,2n)$ | 3h | 5 |
| 60 | $^{46}\text{Ti}(n,a)$ | S | 1,5 |
| 61 | $^{46}\text{Ti}(n,np)$ & | S | 1 |
| 62 | $^{46}\text{Ti}(n,d)$ & | S | 1 |
| 63 | $^{46}\text{Ti}(n,2n)$ | S | 5 |
| 64 | $^{47}\text{Ti}(n,a)$ | S | 1 |
| 65 | $^{47}\text{Ti}(n,2n)$ | S | 1,5 |
| 66 | $^{48}\text{Ti}(n,a)$ | S | 1,3,5 |
| 67 | $^{49}\text{Ti}(n,a)$ | S | 1,5 |
| 68 | $^{49}\text{V}(n,a)$ & | 330d | 1 |
| 69 | $^{51}\text{V}(n,a)$ | S | 1,5 |
| 70 | $^{51}\text{V}(n,na)$ | S | 1 |
| 71 | $^{50}\text{Cr}(n,a)$ | S | 1,5 |
| 72 | $^{50}\text{Cr}(n,na)$ | S | 1,5 |
| 73 | $^{50}\text{Cr}(n,g)$ | S | 4 |
| 74 | $^{50}\text{Cr}(n,np)$ | S | 1 |
| 75 | $^{50}\text{Cr}(n,d)$ | S | 1 |
| 76 | $^{52}\text{Cr}(n,a)$ | S | 1,5 |
| 77 | $^{54}\text{Cr}(n,g)$ | S | 1 |
| 78 | $^{54}\text{Mn}(n,2n)$ | 312d | 1,5 |
| 79 | $^{55}\text{Mn}(n,2n)$ | S | 1,5 |
| 80 | $^{55}\text{Mn}(n,g)$ | S | 1,5 |
| 81 | $^{54}\text{Fe}(n,np)$ | S | 1,5 |
| 82 | $^{54}\text{Fe}(n,d)$ | S | 1,5 |
| 83 | $^{56}\text{Fe}(n,g)$ | S | 1,5 |
| 84 | $^{56}\text{Fe}(n,2n)$ | S | 5 |
| 85 | $^{57}\text{Fe}(n,g)$ | S | 1,5 |
| 86 | $^{58}\text{Fe}(n,g)$ | S | 1,5 |
| 87 | $^{59}\text{Fe}(n,g)$ | 45d | 1,4 |
| 88 | $^{58}\text{Co}(n,g)$ | 71d | 1 |
| 89 | $^{59}\text{Co}(n,g)$ & | S | 1,3,5 |
| 90 | $^{60}\text{Co}(n,p)$ | 5.3y | 1,2 |
| 91 | $^{60}\text{Co}(n,g)$ | 5.3y | 1,5 |
| 92 | $^{58}\text{Ni}(n,p)$ & | S | 1 |
| 93 | $^{58}\text{Ni}(n,g)$ | S | 1,2,3,5 |
| 94 | $^{58}\text{Ni}(n,2n)$ | S | 4 |
| 95 | $^{58}\text{Ni}(n,np)$ | S | 4 |
| 96 | $^{58}\text{Ni}(n,d)$ | S | 4 |
| 97 | $^{60}\text{Ni}(n,2n)$ | S | 1,2,3,5 |
| 98 | $^{60}\text{Ni}(n,p)$ & | S | 1,3,5 |

| <u>Number</u> | <u>Reaction</u> | <u>Target</u> | <u>Source</u> |
|---------------|-----------------------------|---------------|---------------|
| 99 | $^{60}\text{Ni}(n, np)$ | S | 1 |
| 100 | $^{60}\text{Ni}(n, d)$ | S | 1 |
| 101 | $^{61}\text{Ni}(n, g)$ | S | 1, 5 |
| 102 | $^{62}\text{Ni}(n, g)$ | S | 1, 2, 5 |
| 103 | $^{62}\text{Ni}(n, a)$ | S | 4 |
| 104 | $^{63}\text{Ni}(n, a)$ | 100y | 1 |
| 105 | $^{64}\text{Ni}(n, 2n)$ | S | 1, 2, 5 |
| 106 | $^{63}\text{Cu}(n, p)$ | S | 1, 2, 3, 5 |
| 107 | $^{63}\text{Cu}(n, g)$ | S | 4 |
| 108 | $^{63}\text{Cu}(n, a) \&$ | S | 1, 3, 5 |
| 109 | $^{64}\text{Zn}(n, 2n)$ | S | 1 |
| 110 | $^{64}\text{Zn}(n, p)$ | S | 1, 4 |
| 111 | $^{64}\text{Zn}(n, na)$ | S | 1 |
| 112 | $^{64}\text{Zn}(n, 2p)$ | S | 1 |
| 113 | $^{64}\text{Zn}(n, np)$ | S | 1 |
| 114 | $^{64}\text{Zn}(n, d)$ | S | 1 |
| 115 | $^{64}\text{Zn}(n, g)$ | S | 4 |
| 116 | $^{66}\text{Zn}(n, a)$ | S | 1 |
| 117 | $^{66}\text{Zn}(n, 2n)$ | S | 4 |
| 118 | $^{92}\text{Zr}(n, g)$ | S | 1, 5 |
| 119 | $^{93}\text{Zr}(n, a)$ | 1.5My | 1, 5 |
| 120 | $^{94}\text{Zr}(n, 2n)$ | S | 1, 2, 5 |
| 121 | $^{94}\text{Zr}(n, na)$ | S | 1, 5 |
| 122 | $^{94}\text{Zr}(n, g)$ | S | 1, 4, 5 |
| 123 | $^{96}\text{Zr}(n, 2n)$ | S | 1, 5 |
| 124 | $^{92}\text{Nb}(n, 2n) \&$ | 36My | 1 |
| 125 | $^{93}\text{Nb}(n, 2n) \&$ | S | 1, 2 |
| 126 | $^{93}\text{Nb}(n, p)$ | S | 1, 2 |
| 127 | $^{93}\text{Nb}(n, g) \&$ | S | 1, 2, 3, 5 |
| 128 | $^{95}\text{Nb}(n, 2n) \&$ | 35d | 1, 2, 5 |
| 129 | $^{92}\text{Mo}(n, 2n) \&$ | S | 1, 2, 5 |
| 130 | $^{92}\text{Mo}(n, g) \&$ | S | 1, 5 |
| 131 | $^{92}\text{Mo}(n, np) \&$ | S | 1, 5 |
| 132 | $^{92}\text{Mo}(n, d) \&$ | S | 1, 5 |
| 133 | $^{94}\text{Mo}(n, p) \&$ | S | 1, 2, 3, 5 |
| 134 | $^{94}\text{Mo}(n, 2n) \&$ | S | 3 |
| 135 | $^{95}\text{Mo}(n, np) \&$ | S | 1 |
| 136 | $^{95}\text{Mo}(n, d) \&$ | S | 1, 3 |
| 137 | $^{98}\text{Mo}(n, g)$ | S | 1, 2, 4, 5 |
| 138 | $^{100}\text{Mo}(n, 2n)$ | S | 1, 2, 5 |
| 139 | $^{103}\text{Rh}(n, g) \&$ | S | 1 |
| 140 | $^{103}\text{Rh}(n, na) \&$ | S | 1 |
| 141 | $^{104}\text{Pd}(n, g)$ | S | 1 |
| 142 | $^{105}\text{Pd}(n, g)$ | S | 1 |
| 143 | $^{106}\text{Pd}(n, g) \&$ | S | 1 |
| 144 | $^{107}\text{Pd}(n, g)$ | 6.5My | 1 |
| 145 | $^{108}\text{Pd}(n, g) \&$ | S | 1 |
| 146 | $^{107}\text{Ag}(n, g)^m$ | S | 1, 3, 5 |
| 147 | $^{107}\text{Ag}(n, p) \&$ | S | 1 |
| 148 | $^{107}\text{Ag}(n, 2n) \&$ | S | 1 |
| 149 | $^{109}\text{Ag}(n, 2n)^m$ | S | 1, 2, 3, 5 |
| 150 | $^{109}\text{Ag}(n, g)^m$ | S | 4, 5 |
| 151 | $^{110}\text{Cd}(n, g) \&$ | S | 5 |

| <u>Number</u> | <u>Reaction</u> | <u>Target</u> | <u>Source</u> |
|---------------|-----------------------------|---------------|---------------|
| 152 | $^{111}\text{Cd}(n, g)$ | S | 5 |
| 153 | $^{112}\text{Cd}(n, g)^m$ | S | 5 |
| 154 | $^{112}\text{Sn}(n, a)$ | S | 5 |
| 155 | $^{116}\text{Sn}(n, a)^m$ | S | 5 |
| 156 | $^{117}\text{Sn}(n, n')^m$ | S | 4 |
| 157 | $^{119}\text{Sn}(n, n')^m$ | S | 4 |
| 158 | $^{120}\text{Sn}(n, g)^m$ | S | 1, 4, 5 |
| 159 | $^{122}\text{Sn}(n, g)^m$ | S | 1, 4, 5 |
| 160 | $^{124}\text{Sn}(n, g)$ | S | 5 |
| 161 | $^{125}\text{Sn}(n, g)$ | S | 1, 5 |
| 162 | $^{121}\text{Sb}(n, p)^m$ | S | 1, 4 |
| 163 | $^{121}\text{Sb}(n, g)$ | S | 1 |
| 164 | $^{121}\text{Sb}(n, 2n)$ | S | 1 |
| 165 | $^{123}\text{Sb}(n, g) \&$ | S | 1 |
| 166 | $^{123}\text{Sb}(n, 2n) \&$ | S | 1 |
| 167 | $^{124}\text{Sb}(n, g)$ | 60d | 1, 5 |
| 168 | $^{125}\text{Sb}(n, p) \&$ | 2.7y | 1 |
| 169 | $^{126}\text{Sb}(n, p) \&$ | 12.4d | 1 |
| 170 | $^{122}\text{Te}(n, g)^m$ | S | 1 |
| 171 | $^{136}\text{Cs}(n, g)$ | 13d | 5 |
| 172 | $^{137}\text{Ba}(n, p)$ | S | 5 |
| 173 | $^{139}\text{La}(n, a) \&$ | S | 5 |
| 174 | $^{139}\text{La}(n, h)$ | S | 5 |
| 175 | $^{140}\text{Ce}(n, 2n) \&$ | S | 5 |
| 176 | $^{140}\text{Ce}(n, a) \&$ | S | 5 |
| 177 | $^{148}\text{Nd}(n, g)$ | S | 5 |
| 178 | $^{150}\text{Nd}(n, g)$ | S | 5 |
| 179 | $^{150}\text{Nd}(n, 2n)$ | S | 5 |
| 180 | $^{150}\text{Sm}(n, g)$ | S | 5 |
| 181 | $^{151}\text{Sm}(n, g)$ | 90y | 5 |
| 182 | $^{152}\text{Sm}(n, g)$ | S | 5 |
| 183 | $^{152}\text{Sm}(n, 2n)$ | S | 5 |
| 184 | $^{151}\text{Eu}(n, g) \&$ | S | 5 |
| 185 | $^{151}\text{Eu}(n, 2n)^m$ | S | 2, 3, 5 |
| 186 | $^{152}\text{Eu}(n, g)$ | 13.3y | 5 |
| 187 | $^{153}\text{Eu}(n, g) \&$ | S | 5 |
| 188 | $^{153}\text{Eu}(n, 2n)^g$ | S | 2, 5 |
| 189 | $^{154}\text{Eu}(n, g)$ | 8.6y | 5 |
| 190 | $^{158}\text{Gd}(n, g)$ | S | 3 |
| 191 | $^{160}\text{Gd}(n, 2n)$ | S | 3 |
| 192 | $^{159}\text{Tb}(n, 2n) \&$ | S | 3, 5 |
| 193 | $^{158}\text{Dy}(n, p) \&$ | S | 2 |
| 194 | $^{165}\text{Ho}(n, 2n) \&$ | S | 1 |
| 195 | $^{165}\text{Ho}(n, g)^m$ | S | 1, 2, 3, 5 |
| 196 | $^{166}\text{Ho}(n, n')^m$ | 1.1d | 3 |
| 197 | $^{164}\text{Er}(n, 2n)$ | S | 1 |
| 198 | $^{177}\text{Hf}(n, g)^n$ | S | 1, 3, 5 |
| 199 | $^{178}\text{Hf}(n, n')^n$ | S | 1, 3, 5 |
| 200 | $^{178}\text{Hf}(n, 2n) \&$ | S | 1 |
| 201 | $^{178}\text{Hf}(n, g)^n$ | S | 4 |
| 202 | $^{179}\text{Hf}(n, n')^n$ | S | 4 |
| 203 | $^{179}\text{Hf}(n, 2n)^n$ | S | 1, 2, 3, 5 |
| 204 | $^{180}\text{Hf}(n, 2n)^n$ | S | 4 |

| <u>Number</u> | <u>Reaction</u> | <u>Target</u> | <u>Source</u> |
|---------------|-----------------------------|---------------|---------------|
| 205 | $^{180}\text{Hf}(n, g)$ | S | 1 |
| 206 | $^{180}\text{Hf}(n, 3n)^n$ | S | 1 |
| 207 | $^{181}\text{Hf}(n, g) \&$ | 42.4d | 1, 5 |
| 208 | $^{179}\text{Ta}(n, 2n) \&$ | 1.8y | 1 |
| 209 | $^{181}\text{Ta}(n, na)^g$ | S | 1, 5 |
| 210 | $^{181}\text{Ta}(n, 2n)^m$ | S | 1 |
| 211 | $^{181}\text{Ta}(n, g) \&$ | S | 1, 4, 5 |
| 212 | $^{181}\text{Ta}(n, t)^n$ | S | 3 |
| 213 | $^{181}\text{Ta}(n, nd)^n$ | S | 3 |
| 214 | $^{182}\text{Ta}(n, p) \&$ | 115d | 1 |
| 215 | $^{182}\text{Ta}(n, g)$ | 115d | 1, 5 |
| 216 | $^{180}\text{W}(n, 2n) \&$ | S | 1, 3 |
| 217 | $^{182}\text{W}(n, a)^n$ | S | 3 |
| 218 | $^{182}\text{W}(n, na)^n$ | S | 1, 2, 3, 5 |
| 219 | $^{182}\text{W}(n, g) \&$ | S | 1, 5 |
| 220 | $^{183}\text{W}(n, g)$ | S | 1, 5 |
| 221 | $^{184}\text{W}(n, g) \&$ | S | 1, 3, 5 |
| 222 | $^{186}\text{W}(n, g)$ | S | 1, 3, 5 |
| 223 | $^{186}\text{W}(n, na) \&$ | S | 2 |
| 224 | $^{185}\text{Re}(n, g)^m$ | S | 1, 2, 3, 5 |
| 225 | $^{187}\text{Re}(n, 2n)^m$ | S | 1, 2, 3, 5 |
| 226 | $^{187}\text{Re}(n, g) \&$ | S | 1, 4 |
| 227 | $^{188}\text{Os}(n, g) \&$ | S | 1, 4, 5 |
| 228 | $^{188}\text{Os}(n, p) \&$ | S | 4 |
| 229 | $^{189}\text{Os}(n, g) \&$ | S | 1, 4, 5 |
| 230 | $^{190}\text{Os}(n, g) \&$ | S | 1, 3, 5 |
| 231 | $^{190}\text{Os}(n, a)$ | S | 1 |
| 232 | $^{192}\text{Os}(n, g)$ | S | 3 |
| 233 | $^{192}\text{Os}(n, 2n) \&$ | S | 3 |
| 234 | $^{191}\text{Ir}(n, g)^n$ | S | 1, 2, 3, 5 |
| 235 | $^{191}\text{Ir}(n, na)$ | S | 1 |
| 236 | $^{191}\text{Ir}(n, 2n) \&$ | S | 1 |
| 237 | $^{192}\text{Ir}(n, n')^n$ | 74d | 1, 5 |
| 238 | $^{193}\text{Ir}(n, 2n)^n$ | S | 1, 2, 3, 5 |
| 239 | $^{192}\text{Pt}(n, g) \&$ | S | 1, 4, 5 |
| 240 | $^{194}\text{Pt}(n, 2n) \&$ | S | 1, 4, 5 |
| 241 | $^{197}\text{Au}(n, a) \&$ | S | 1 |
| 242 | $^{197}\text{Au}(n, 2n) \&$ | S | 1 |
| 243 | $^{195m}\text{Hg}(n, 2n)$ | 1.7d | 1 |
| 244 | $^{196}\text{Hg}(n, 2n)^m$ | S | 1 |
| 245 | $^{203}\text{Tl}(n, 2n)$ | S | 4 |
| 246 | $^{204}\text{Pb}(n, p)$ | S | 4 |
| 247 | $^{204}\text{Pb}(n, t)$ | S | 4 |
| 248 | $^{204}\text{Pb}(n, 2n) \&$ | S | 4 |
| 249 | $^{204}\text{Pb}(n, n')^m$ | S | 4 |
| 250 | $^{206}\text{Pb}(n, 2n)$ | S | 1, 3, 5 |
| 251 | $^{206}\text{Pb}(n, a)$ | S | 4 |
| 252 | $^{208}\text{Pb}(n, g)$ | S | 1, 3, 5 |
| 253 | $^{208}\text{Bi}(n, 2n)$ | 0.37My | 1, 3, 5 |
| 254 | $^{209}\text{Bi}(n, 2n)$ | S | 1, 2, 3, 5 |
| 255 | $^{209}\text{Bi}(n, g)$ | S | 1, 3, 5 |
| 256 | $^{210}\text{Po}(n, 2n)$ | 138d | 1 |

Key

The Source of the reactions are:

- 1-R.A. Forrest and D.A.J. Endacott AERE R-13402
- 2-E. Cheng Private Communication (REAC2)
- 3-C. Ponti Long-Lived Products (see ECN-207)
- 4-C. Ponti Short-Lived Products (Priv. Comm.)
- 5-A. Khursheed PhD Thesis

Under the column Target S = Stable target, otherwise the half-life of the target is given.

Under the column Reaction & indicates the sum of cross sections forming all isomeric states. If particular isomeric products are required these are shown by:

^g ground state, ^m 1st isomer, ⁿ 2nd isomer.

For reference the half-lives of the isomers are shown below:

^{108m}Ag 127y
^{110m}Ag 250d
^{113m}Cd 14.1y
^{117m}Sn 14.0d
^{119m}Sn 293d
^{121m}Sn 50y
^{123m}Sn 40.1m
^{123m}Te 119.7d
^{150m}Eu 34.2y
^{152g}Eu 13.3y
^{166m}Ho 1200y
¹⁷⁸ⁿHf 31y
^{177g}Lu 6.7d
^{180m}Ta 8.1h
^{186m}Re 0.2My
¹⁹²ⁿIr 240y
^{195m}Hg 1.7d
^{204mp}Pb 1.1h

4.5 Dosimetry file

Following mainly the report of Prof. Vonach it was agreed that contributions to the IRDF-file will be collected by NDS and a review be made by IRK.

Actions

- all contributors to IRDF: send evaluated reaction cross sections to NDS;
- H. Vonach: check old IRK evaluations and re-evaluate if necessary and do evaluations of new reactions. The full list of reactions to be covered is as follows:

¹⁹F(n,2n), ²⁴Mg(n,p), ²⁷Al(n,α), ³¹P(n,p),
⁵⁸Ni(n,2n), ⁵⁹Co(n,2n), ⁵⁹Co(n,p), ⁶³Cu(n,2n),
⁶⁴Zn(n,2n), ⁹⁰Zr(n,2n), ⁹³Nb(n,n'), ¹⁰³Rh(n,n'),
¹⁹⁷Au(n,2n);

- V. Pronyaev: send to NDS the following evaluations together with covariances:
 Cl-37(n, γ), Mn-55(n, γ), Cu-63(n, γ), La-139(n, γ),
 W-186(n, γ);
- Z. Delin: prepare and send to NDS the following evaluations together with covariances:
 115-In(n,n')115m-In, 46-Ti(n,p), 48-Ti(n,p),
 109-Ag(n, γ)110m-Ag, 23-Na(n, γ), 45-Sc(n, γ),
 58-Fe(n, γ),59-Co(n, γ);
- D. Larson: prepare covariances for Mn-55(n,2n) and send them to JAERI for checking and to Vienna together with new evaluation for 32-S(n,p);
- NDS: take ENDF/B-VI dosimetry reactions from new ENDF/B-VI files upon availability, in particular standard reactions and fission and capture cross sections for actinides;
- Vonach: review the updated IRDF file before March 1990;
- NDS: issue the updated IRDF file by March 1990.

5. Report of Working Group II

Inter-Comparison of Benchmark Calculations

(K. Sumita, E.T. Cheng)

Participants: E.T. Cheng (secretary), U. Fischer, H. Gruppelaar, V. Goulo, H. Maekawa, F. Mann, D. Muir, S. Pelloni, V. Pronyaev, J.J. Schmidt, and K. Sumita (Chairman)

Presentations and Discussions:

The participants presented the results of their calculations and discussed the comparisons between calculations and experiments. The calculations were performed with nuclear data libraries processed from ENDF/B-IV, ENDF/B-V, EFF-1, BROND, and JENDL-3T files. The experimental results to be compared are those obtained from the Technical University Dresden integral experiments. Discussions on the inter-comparison between calculated results were also conducted. Appendix A gives the list of all reports submitted to this meeting relevant to Working Group II. Appendix B summarizes the results of all calculations. The results from the TUD-experiment are also given for comparison.

The participants also discussed future benchmark problems for the FENDL library and identified candidate integral experiments.

5.1 Conclusions and Recommendations

The following conclusions and recommendations were made by the participants regarding the benchmark comparison for lead evaluations and future FENDL libraries:

1. The participants found that all calculated results are very close to each other. The total neutron leakage multiplication factors calculated from all evaluations with Monte Carlo transport codes are within less than 1 %, while the discrete ordinates transport codes give results varying by up to 5 %.
2. The calculated total neutron leakage multiplication factor is about 10 % lower than the TUD experiment. However, it is within the experimented error of the TUD experiment. In order to derive a more meaningful conclusion about the comparison between calculated and measured neutron multiplication factors, it appears that more accurate integral experimental data (5 % or less) will be needed.
3. The most important energy region of the leakage spectrum appears to be that below 5 MeV. It contributes more than 90% to the total neutron multiplication factor. There are some discrepancies in the calculated neutron populations in energy regions from 0 to 1 MeV, 1 to 5 MeV, and 10 to 15 MeV.
4. Calculated dosimetry reaction and fission reaction rates within the lead sphere show large discrepancies compared with the TUD experiment. However, due to the lack of detailed information regarding the TUD experiment, particularly on the energy and angular distributions of the source neutrons, the participants were unable to present a conclusive statement about the comparison with experiment.

5. Small discrepancies were found in the tritium breeding ratios in the $Ll17Pb83$ blanket calculated with EFF-1 based nuclear data libraries processed using files 4 and 5 (MF4,5), and file 6 (MF6). The discrepancies occurred at energies below 10 keV when the neutron spectra were compared. The reason for these discrepancies was not well understood by the participants. Further work is needed to clarify them.
6. The participants believe that more accurate benchmark measurements for lead should be performed to have better comparisons for neutron multiplication factors and leakage spectra. The following recent integral experiments were recommended: (1) the JAERI experiments on lead slabs of 5, 20 and 40 cm thickness, (2) the Kurchatov integral experiment on the 22.5-cm TUD lead sphere, and (3) the OKTAVIAN 10-cm lead sphere experiment.
7. Beryllium is recommended as the next element for the benchmark inter-comparison. The available integral experiments that are recommended for the benchmark problems are (1) the JAERI beryllium slab experiment [5 and 15 cm thick, paper published in Nuclear Science and Engineering, 97 (1987) 220] and (2) the Kurchatov beryllium integral experiments with 1.5, 3 and 8 cm beryllium spheres. The neutron leakage spectrum from the 8-cm sphere experiment is highly recommended, if available. The following on-going and planned integral beryllium sphere experiments are also suggested as future benchmark problems: (1) SWINPC(PRC) experiment (14.85 cm), (2) EG&G/Idaho (U.S.) (20 cm), (3) KfK (FRG) (5 and 17 cm), and (4) OKTAVIAN (Japan) (14.85 cm) experiment.
8. It is recommended that the Agency sponsors a meeting in 1990 to discuss the neutron multiplication processes from beryllium and lead. The topics to be investigated should include measurements of $(n,2n)$ cross sections, evaluations of cross sections at energies above the $(n,2n)$ threshold, integral experiments, and benchmark calculations.

Actions

1. Professor Sumita: visit Professors Seeliger and Seidel of TUD at Dresden and discuss with them the detailed information needed for the benchmark comparison.
2. Maekawa: prepare the specifications and relevant experimental results for the JAERI lead and beryllium benchmark problems.
3. Goulo and Cheng: contact Markovskij of Kurchatov Institute in Moscow regarding the details of the recent 22.5 cm lead experiment and the specifications of the future beryllium benchmark problem.
4. Professor Sumita: prepare the specifications and relevant experimental results for the OKTAVIAN lead benchmark problems.
5. Maekawa: try to clean up the discrepancy in the results of S_n calculations, which is assumed to be due to differences in the calculational models or in the processing codes.
6. Cheng: prepare specifications of the standard ANISN code input data for future intercomparison between calculations.

H. Vonach's comments to report of Working Group II

- 1) The agreement of the total multiplication calculations (M) of the lead sphere using different libraries is $\sim \pm 1\%$. This is in agreement with the differences in the (n, 2n) and inelastic scattering cross-sections between the different files and the sensitivity of M to these cross-sections.

The present accuracy of the measurement of M can thus not improve our knowledge of cross-sections, but only check the measuring systems.

- 2) The situation is different for the shape of the leakage spectrum. BROND predicts a considerably harder leakage spectrum than ENDF/V, EFF being somewhere in the middle. For example BROND predicts 0.74 neutrons/source neutron in the 1-5 MeV range, ENDF/B-V only about 0.53; these differences can be checked experimentally by careful neutron spectrum measurements. Thus in addition to the Dresden measurement there should be some additional spectrum measurements.
- 3) The agreement between the results of different transport codes using the same cross-section evaluations is very unsatisfactory, especially in two respects:
 - a) Calculation of the total multiplication M. Although this quantity is determined to about $\pm 1\%$ by the accuracy of presently used cross-sections, differences up to 5% result from the use of different transport codes, that is the calculation of e.g. breeding ratios may have much larger errors due to the code specifications than due to the cross-section uncertainties.
 - b) There are very large discrepancies between different calculations of the attenuation of the primary neutrons in the lead sphere. Values for transmission of the primary 14 MeV neutrons (group 10-15 MeV in WGII Appendix) differ by up to 30%. This could have serious consequences especially for shielding calculations for steel/water shields where the deep-shield transmission is determined by the transmission of the source neutrons.

Thus it appears as an urgent problem to identify the reasons for the described discrepancies between the results of different codes and to eliminate the present deficiencies.

5.2. Summary of Calculated Results for Neutron Leakage Multiplication from the 22.5-cm TUD Lead Sphere

| <u>Calculations</u> | <u>0-15 MeV</u> | <u>0-1 MeV</u> | <u>1-5 MeV</u> | <u>5-10 MeV</u> | <u>10-15 MeV</u> |
|---------------------|-----------------|----------------|----------------|-----------------|------------------|
| <u>ENDF/B-IV</u> | | | | | |
| BLANK (IAE) | 1.796 | 1.093 | 0.549 | 0.017 | 0.137 |
| MCNP (Sofia) | 1.740 | 1.063 | 0.529 | 0.0195 | 0.126 |
| ANISN (Sofia) | 1.760 | 1.060 | 0.520 | 0.0178 | 0.161 |
| ANISN (JAERI) | 1.858 | 1.197 | 0.512 | 0.0198 | 0.129 |
| ANISN (KfK) | 1.78 | 1.12 | 0.52 | 0.02 | 0.12 |
| MCNP (KfK) | 1.78 | 1.08 | 0.54 | 0.02 | 0.14 |

| <u>Calculations</u> | <u>0-15 MeV</u> | <u>0-1 MeV</u> | <u>1-5 MeV</u> | <u>5-10 MeV</u> | <u>10-15 MeV</u> |
|---------------------|-----------------|----------------|----------------|-----------------|------------------|
| <u>ENDF/B-V</u> | | | | | |
| TART (LLNL) | 1.75 | 1.10 | 0.51 | 0.02 | 0.12 |
| MCNP (GA) | 1.746 | 1.060 | 0.5354 | 0.02163 | 0.1290 |
| MCNP (UCLA) | 1.749 | 1.045 | 0.549 | 0.021 | 0.134 |
| <u>BROND</u> | | | | | |
| BLANK (IAE) | 1.763 | 0.877 | 0.739 | 0.019 | 0.128 |
| <u>JENDL-3T</u> | | | | | |
| ANISN (JAERI) | 1.766 | 0.952 | 0.662 | 0.0243 | 0.128 |
| BERMUDA (JAERI) | 1.788 | 0.971 | 0.687 | 0.0224 | 0.108 |
| <u>EFF</u> | | | | | |
| ANISN (JAERI) | 1.804 | 1.079 | 0.571 | 0.0253 | 0.129 |
| BERMUDA (JAERI) | 1.822 | 1.024 | 0.667 | 0.0208 | 0.110 |
| ONEDANT (PSI) | | | | | |
| (MF4,5) | 1.756 | 0.973 | 0.633 | 0.023 | 0.127 |
| (MF6) | 1.761 | 0.971 | 0.636 | 0.026 | 0.128 |
| ANTRAI (KfK) | 1.76 | 0.98 | 0.61 | 0.03 | 0.14 |
| BLANK (IAE) | 1.743 | 0.977 | 0.605 | 0.023 | 0.138 |
| ANISN (Sofia) | 1.75 | 1.02 | 0.600 | 0.0219 | 0.128 |
| Pb99S | | | | | |
| ANISN (Sofia) | 1.803 | 1.111 | 0.600 | 0.0167 | 0.075 |
| Pb175F6 | | | | | |
| MORSE (Sofia) | 1.750 | 1.001 | 0.595 | 0.0189 | 0.135 |
| Pb99S | | | | | |
| <u>Experiment</u> | | | | | |
| TUD | 1.944 | 1.105 | 0.676 | 0.019 | 0.144 |
| | (±12 %) | | | | |

6. Processing FENDL-1 into Libraries for Applications (D. Muir)

1. It has been decided that files available and selected for FENDL will be processed into both a multigroup library (GENDF) for discrete ordinate codes and a library (ACE) for Monte Carlo codes (MCNP).
2. A pointwise data library in the NJOY PENDF format will be prepared by NDS and kept for further processing.
3. Action on NDS: request the version of MCNP from RSIC that handles MF=6 files and is compatible with NJOY version 87.1.
4. Recommended specifications for PENDF files
 - Pointwise resonance reconstruction at 0° K and subsequently broadened numerically to 300 K, 900 K, and 1500 K. 0° data to be saved in the file for He, N, Ti, Cu, Sn, and Nb;
 - Reconstruction accuracy of 0.2 %;
 - Total (energy-balance) KERMA, which assume neutron and γ -ray transport, and damage-energy production;
 - Thermal upscatter for Be in Be metal, C in graphite, and H in water.
5. Recommended specifications for GENDF files
 - Neutron group structure should be the Vitamin-J 175 group structure (having a single thermal-neutron group below 0.414 eV)
 - Gamma group structure should have approx. 40 groups (to be determined in detail by NDS) for both gamma-ray production and transport;
 - Legendre expansion to P_6 , for subsequent transport correction to P_5 ;
 - Background cross section (σ_0) values should be 1, 10, 100, 1000, and 10 000 barns, plus infinite dilution;
 - Weight function should be as in Vitamin-E.
6. Recommended specifications for ACE-format (MCNP) library
 - Should treat thermal upscatter;
 - Otherwise follow specifications of distributed MCNP libraries.
7. Contributions to this processing effort by laboratories participating in the FENDL effort is strongly encouraged.

7.Reports of participants

TABLE
EVALUATIONS FOR ENDF/B-VI

| <u>Material</u> | <u>Evaluator</u> | <u>Due Date</u> | <u>Phase I Review Status</u> | <u>Covariance Eval. Status</u> |
|-------------------|------------------|-----------------|------------------------------|--------------------------------|
| ¹ H | Dodder (LANL) | C | A | Y |
| ³ He | Hale (LANL) | 11/89 | 11/89 | N |
| ⁶ Li | Hale (LANL) | 04/89 | A | P |
| ⁷ Li | Young (LANL) | C | A | Y |
| ⁹ Be | Perkins (LLNL) | 04/89 | A | N |
| ¹⁰ B | Hale (LANL) | 04/89 | CA | P |
| ¹¹ B | Young (LANL) | C | A | P |
| C | Fu (ORNL) | 04/89 | A | Y |
| Si | Seeliger (GRD) | C | NA | Y(V5) |
| V | Smith (ANL) | ? | CA | Y |
| ⁵⁰ Cr | Hetrick (ORNL) | 04/89 | A | Y |
| ⁵² Cr | Hetrick (ORNL) | 04/89 | A | Y |
| ⁵³ Cr | Hetrick (ORNL) | 04/89 | A | Y |
| ⁵⁴ Cr | Hetrick (ORNL) | 04/89 | A | Y |
| ⁵⁵ Mn | Shibata (JAERI) | 11/89 | CA | Y |
| ⁵⁴ Fe | Fu (ORNL) | C | A | Y |
| ⁵⁶ Fe | Fu (ORNL) | C | A | Y |
| ⁵⁷ Fe | Fu (ORNL) | C | A | Y |
| ⁵⁸ Fe | Fu (ORNL) | C | A | Y |
| ⁵⁹ Co | Smith (ANL) | 04/89 | A | Y |
| ⁵⁸ Ni | Hetrick (ORNL) | C | A | Y |
| ⁵⁹ Ni | Mann (HEDL) | C | A | N |
| ⁶⁰ Ni | Hetrick (ORNL) | C | A | Y |
| ⁶¹ Ni | Hetrick (ORNL) | C | A | Y |
| ⁶² Ni | Hetrick (ORNL) | C | A | Y |
| ⁶⁴ Ni | Hetrick (ORNL) | C | A | Y |
| ⁶³ Cu | Hetrick (ORNL) | C | A | Y |
| ⁶⁵ Cu | Hetrick (ORNL) | C | A | Y |
| ⁸⁹ Y | Smith (ANL) | C | A | Y |
| Nb | Smith (ANL) | 11/89 | 11/89 | Y |
| ¹³⁴ Cs | Wright (ORNL) | C | A | N |
| ¹³⁴ Ba | Wright (ORNL) | C | A | N |
| ¹³⁵ Ba | Wright (ORNL) | C | A | N |

TABLE (Continued)
EVALUATIONS FOR ENDF/B-VI

| <u>Material</u> | <u>Evaluator</u> | <u>Due Date</u> | <u>Phase I Review Status</u> | <u>Covariance Eval. Status</u> |
|-----------------|------------------|-----------------|------------------------------|--------------------------------|
| 136Ba | Wright (ORNL) | C | A | N |
| 147Nd | Wright (ORNL) | C | A | N |
| 147Pr | Wright (ORNL) | 04/89 | A | N |
| 147Sm | Wright (ORNL) | 04/89 | A | N |
| 151Sm | Wright (ORNL) | 04/89 | A | N |
| 151Eu | Young (LANL) | 11/89 | CA | N |
| 152Eu | Wright (ORNL) | C | A | N |
| 153Eu | Young (LANL) | 11/89 | CA | N |
| 154Eu | Wright (ORNL) | C | A | N |
| 155Eu | Wright (ORNL) | C | A | N |
| 165Ho | Young (LANL) | 11/89 | CA | N |
| 166Er | Wright (ORNL) | C | A | N |
| 167Er | Wright (ORNL) | C | A | N |
| W | Muir (LANL) | 11/89 | CA | Y |
| 197Au | Young (LANL) | 11/89 | CA | P |
| 206Pb | Fu (ORNL) | 04/89 | A | Y |
| 207Pb | Fu (ORNL) | 04/89 | A | Y |
| 208Pb | Fu (ORNL) | 04/89 | A | Y |
| Bi | Smith (ANL) | 11/89 | 11/89 | ? |
| 185Re | Weston (ORNL) | 11/89 | 11/89 | N |
| 187Re | Weston (ORNL) | 11/89 | 11/89 | N |
| 235U | Weston (ORNL) | 04/89 | A | P |
| 236U | Schenter (HEDL) | 11/89 | 11/89 | P |
| 238U | Weston (ORNL) | 04/89 | A | P |
| 239Np | Wright (ORNL) | C | A | N |
| 239Pu | Young (LANL) | 04/89 | A | P |
| 240Pu | Weston (ORNL) | C | A | Y |
| 241Pu | Weston (ORNL) | C | A | Y |
| 241Am | Zhou (China) | 11/89 | CA | N |
| 243Am | Weston (ORNL) | C | A | N |
| 249Bk | Zhou (China) | C | A | N |
| 249Cf | Zhou (China) | C | A | N |

TABLE EXPLANATION

1. Due Date

C = complete

2. Phase 1 Review Status

A = approved

CA = conditionally approved, subject to a further Phase 1 review after suggested revisions.

NA = not approved

11/89 = will be reviewed at November 1989 CSEWG meeting.

3. Covariance Evaluation Status

Y = new evaluation will be complete for October 1989 review

P = partial evaluation will be complete for October 1989 review

N = no new evaluation planned for Version VI

(Contribution to the IAEA Specialists' Mtg. on the "Fusion Evaluated Nuclear Data Library (FENDL) and Benchmark Calculations", Vienna, 8-11 May, 1989)

H. Gruppelaar

Netherlands Energy Research Foundation ECN, P.O. Box 1, 1755ZG Petten
The Netherlands

The status of the European Fusion File Project and the plans for the future have been presented at the 1988 Mito Conference.*

Shortly after the Mito conference an EFF Users' Meeting was organised to assess the needs of the NET team for the coming three years. This has led to an adjustment of the programme. Meanwhile, a new three-years programme has been defined for the period 1989 to 1991.

The new programme contains the existing programme as given in App. A1, with, however, important changes in priority and with extensions to meet the specific needs of the NET team. The previous programme was mainly directed towards a better prediction of the tritium breeding ratio, i.e. emphasis on the cross-sections for tritium breeding materials (Li-6,7), including ceramics (with Al, Si) and neutron multipliers (Be, Pb). In the new 3-years programme there is much more emphasis on supporting the design of the basic NET machine for which EFF will be the standard data base.

In the new programme ("Neutronics data base for shielding") first of all any remaining deficiencies (e.g. kerma factors) or incompletenesses (e.g. Monte Carlo libraries, covariance data) in the data files derived from EFF-1 should be corrected for. Secondly, the cross-sections for the major shielding materials (Fe, Cr, Ni) should be known as accurately as possible, including covariance data. Finally, the quality of the library with respect to photon-production, double-differential neutron emission cross-sections (DDX) and kerma factors should be improved and the original programme (App. A1) should be completed. This includes the extension of the library with more materials and the development of an activation file (EAF-2) consistent with EFF-2. In addition, a separate European project has been defined to support the Low Activation Materials (LAM) research programme with activation and decay libraries.

The second point of the programme is both urgent and difficult. It is related to the fact that the uncertainty in the thickness of the inboard shield of the superconducting magnets is difficult to assess, as long as reliable covariance data are lacking. Even if these data are given, they are only given for the "1-dimensional" cross-sections. To assess the effect of uncertainties in the energy-angle distributions the data and tools are usually lacking. Therefore the new programme includes a subtask to calculate the sensitivity of the shielding parameters for errors in the double differential cross-sections and a subtask to develop tools to process DDX and covariance data.

* H. Gruppelaar "Status of the European Fusion File" Nuclear Data for Science and Technology (1988) Mito, Proc. of the Int. Conf. p.455-463, JAERI.

Guide to JENDL-3

(JAERI/Nuclear Data Center)

May 8, 1989

1. Compilation of numerical data for general purpose file of JENDL-3 was almost (99%) finished. Comment files (File 1) will be made by the end of this August. Before this deadline, minor errors like clerical error will be mended.
2. Compilation of the data for FP nuclides will be completed also before the above-mentioned deadline.
3. Formal procedure for open release will be made after this August. Approval for the open release will hopefully be achieved by the end of this year.
4. Before achieving the formal approval, JENDL-3 is a restricted data library which is distributed only for the domestic use. Review work for FENDL is considered as an extension of domestic one, if Japanese members willingly take part in the working.
5. General purpose file of JENDL-3 includes the data of 175 nuclides, 53 of which have the photon production data. The data for 172 nuclides are going to be compiled as the FP nuclear data file of JENDL-3.

Nuclides in both files are shown in Attachments 1 and 2, respectively.

Attachment 1

Nuclides to be included in the General Purpose File of JENDL-3

| Z | Nuclide | Z | Nuclide |
|----|--------------------------------------|-----|---|
| 1 | H-1, -2 | 40 | Zr-0, -90, -91, -92, -94, -96 |
| 2 | He-3, -4 | 41 | Nb-93 |
| 3 | Li-6, -7 | 42 | Mo-0, -92, -94, -95, -96, -97, -98, -100 |
| 4 | Be-9 | | |
| 5 | B-10, -11 | 47 | Ag-0, -107, -109 |
| 6 | C-12 | 48 | Cd-0 |
| 7 | N-14, 15 | 51 | Sb-0, -121, -123 |
| 8 | O-16 | 63 | Eu-0, -151, -153 |
| 9 | F-19 | 72 | Hf-0, -174, -176, -177, -178 -179, -180 |
| 11 | Na-23 | | |
| 12 | Mg-0, -24, -25, -26 | 73 | Ta-181 |
| 13 | Al-27 | 74 | W-0, -182, -183, -184, -186 |
| 14 | Si-0, -28, -29, -30 | 82 | Pb-0, -204, -206, -207, -208 |
| 15 | P-31 | 83 | Bi-209 |
| 16 | S-0, -32, -33, -34, -36 | 88 | Ra-223, -224, -225, -226 |
| 17 | Cl-0, -35, -37 | 89 | Ac-225, -226, -227 |
| 18 | Ar-40 | 90 | Th-227, -228, -229, -230, -232, -233, -234 |
| 19 | K-0, -39, -40, -41 | | |
| 20 | Ca-0, -40, -42, -43, -44, -46, 48 | 91 | Pa-231, -232, -233 |
| 21 | Sc-45 | 92 | U-232, -233, -234, -235, -236, -238 |
| 22 | Ti-0, -46, -47, -48, -49, -50 | 93 | Np-237, -239 |
| 23 | V-51 | 94 | Pu-236, -238, -239, -240, -241, -242 |
| 24 | Cr-0, -50, -52, -53, -54 | 95 | Am-241, -242g, -242m, -243, -244g, -244m |
| 25 | Mn-55 | | |
| 26 | Fe-0, -54, -56, -57, -58 | 96 | Cm-241, -242, -243, -244, -245, -246, -247, -248, -249, -250 |
| 27 | Co-59 | | |
| 28 | Ni-0, -58, -60, -61, -62, -64 | 97 | Bk-249, -250 |
| 29 | Cu-0, -63, -65 | 98 | Cf-249, -250, -251, -252, -254 |
| | | 99 | Es-254, -255 |
| | | 100 | Fm-255 |

*) The nuclide with 0 stands for a natural element.

Nuclides to be included in the Fission Product File of JENDL-3

| Z | Nuclide | Z | Nuclide |
|----|--|----|---|
| 33 | As-75 | 51 | Sb-121, -123, -124, -125 |
| 34 | Se-74, -76, -77, -78, -79, -80, -82 | 52 | Te-120, -122, -123, -124, -125, -126, -127m, -128, -129m, -130 |
| 35 | Br-79, -81 | 53 | I-127, -129, 131 |
| 36 | Kr-78, -80, -82, -83, -84, -85, -86 | 54 | Xe-124, -126, -128, -129, -130, -131, -132, -133, -134, -135, -136 |
| 37 | Rb-85, -87 | 55 | Cs-133, -134, -135, -136, -137 |
| 38 | Sr-86, -87, -88, -89, -90 | 56 | Ba-130, -132, -134, -135, -136, -137, -138, -140 |
| 39 | Y-89, -91 | | |
| 40 | Zr-90, -91, -92, -93, -94, -95, -96 | 57 | La-138, -139 |
| 41 | Nb-93, -94, -95 | 58 | Ce-140, -141, -142, -144 |
| 42 | Mo-92, -94, -95, -96, -97, -98, -99, -100 | 59 | Pr-141, -143 |
| 43 | Tc-99 | 60 | Nd-142, -143, -144, -145, -146, -147, -148, -150 |
| 44 | Ru-96, -98, -99, -100, -101, -102, -103, -104, -106 | 61 | Pm-147, -148g, -148m, -149 |
| 45 | Rh-103, -105 | 62 | Sm-144, -147, -148, -149, -150, -151, -152, -153, -154 |
| 46 | Pd-102, -104, -105, -106, -107, -108, -110 | 63 | Eu-151, -152, -153, -154, -155, -156 |
| 47 | Ag-107, -109, -110m | 64 | Gd-152, -154, -155, -156, -157, -158, -160 |
| 48 | Cd-106, -108, -110, -111, -112, -113, -114, -116 | 65 | Tb-159 |
| 49 | In-113, -115 | | |
| 50 | Sn-112, -114, -115, -116, -117, -118, -119, -120, -122, -123, -124, -126 | | |

Pronyaev V.G., Blokhin A.I., Golubev V.I.,
Ignatyuk A.V., Tsibulya A.M.

The new version (CJD-2) of the evaluated neutron cross-section files for natural chromium, iron and nickel is based mainly on the experimental data published before 1983 and physical models for interpolation and extrapolation of the cross-sections. Main attention was paid to the energy region of the fast reactor neutron spectra ($E_n=1$ keV - 4 MeV), although in many cases, the cross-section presentation for neutrons with higher energy is quite satisfactorily. The methods of the evaluation and used experimental data base have been discussed in previous publications [2,3]. The results of macro experiments at fast critical assemblies with a large quantity of chromium, nickel, and stainless steel in core and hard neutron spectra [4] were used for testing of the evaluated neutron cross-section files.

This paper presents the specific features of the evaluated data files important for their application in neutronics calculations of the fast neutron and fusion reactors.

RESOLVED RESONANCE REGION.

To take into account the cross-section structure, the presentation of the cross-sections by the resolved resonances was used up to the highest possible energies. Because the upper boundaries of the resolved resonance regions for s-, p- and d-waves are different for the same isotope the method of the pseudo isotopes was realized. The cross-sections for natural iron file were presented through ^{56}Fe s-resonances in the energy region from 10^{-5} eV to 850 keV, and through p- and d-resonances in the energy region from 10^{-5} eV to 500 keV. The potential scattering radius energy dependence becomes noticeable for a wide energy region. Because the format does not allow to represent such energy dependence, a lattice of remote resonances was used to model it. The number and neutron widths of these resonances have been chosen taking into account the description of the average cross-sections for the whole resolved resonance region.

This approach has given the possibility to describe realistically the resonance structure and self-shielding factors for the total cross-section up to 850 keV and for the capture cross-section up to 350 keV. It is important, that the deviations from the format due to the pseudo isotope presentation are of no importance and require no changes in the programs.

It is recommended to use the Reich-Moore formalism for the point-wise reconstruction of the cross-sections for the even-even isotopes of $^{54,56}\text{Fe}$, $^{50,52}\text{Cr}$ and $^{58,60}\text{Ni}$ in s-wave resolved resonance region. Because the use of Reich-Moore formalism was not allowed in ENDF-V format, the Reich-Moore parameters have been written in the format of the multi-level Breit-Wigner formalism and GRUKON code [5] was used for the point-wise cross-section reconstruction in the Reich-Moore formalism. Then the main drawback of the existing CJD-2 files for structural materials is that they not always can be processed by the standard programs. This problem was overcome for the ^{nat}Fe file by converting it to ENDF-VI format.

UNRESOLVED RESONANCE REGION.

The upper boundary for the unresolved resonance region of even-even isotopes was taken below the inelastic scattering threshold. The average resonance parameters for cross-section calculations in the unresolved resonance region have been evaluated in first approximation by averaging of the parameters in the resolved resonance region and then by EVPAR code [6] with taking into account the simple physical considerations for dependence of average level spacing and widths from spin, parity and energy and by comparison with available experimental data on average neutron capture cross-sections. The possible contribution from f-wave was taken into account effectively by some increase of radiative widths for d-wave.

The deficiency of the CJD-2 evaluated data files for structural materials is that in case of natural mixture of isotopes the high number of resonances for separate isotopes is taken into consideration and it leads to time consuming calculations of point-wise presentation of data for this energy region.

SMOOTH CROSS-SECTION ENERGY REGION.
ENERGY AND ANGULAR DISTRIBUTIONS OF THE SECONDARY PARTICLES.

Neutron energy region above the inelastic scattering threshold on structural materials is the most important for fusion reactors. The evaluation of the levels excitation functions with energy up to 4 - 4.5 MeV as well as elastic scattering cross-sections was done in the framework of the optical-statistical approach with account of direct processes. Because the total number of discrete levels was higher than that limited by the format the part of levels was combined in the groups of pseudo levels.

The angular distributions are given for all levels of ^{nat}Fe and many of them have nonsymmetric around 90° angular distributions (direct reaction contribution). For ^{nat}Cr and ^{nat}Ni files the angular distributions are given isotropic in C.M.S..

The shape of angular distributions for neutron elastic scattering on ^{nat}Fe was taken from ENDF/B-IV evaluation for iron and based on interpolation for $E_n < 1$ MeV and $E_n > 14$ MeV. For energy region $1 \text{ MeV} \leq E_n \leq 14 \text{ MeV}$ the evaluation of angular distributions was done in the framework of phenomenological approach, when cross-sections obtained in optical model were corrected with account of recent experimental data. The data obtained in [7] were taken as evaluated elastic scattering angular distributions for ^{nat}Ni .

The evaluation of (n,2n) reaction cross-section as well as other threshold reactions was obtained from evaluations of this reaction cross-sections for separate isotopes of BOSPOR library [8] (^{nat}Fe) or from statistical model calculations with description of level density in the framework of generalized superfluid model [9] with consideration of pre-equilibrium processes (Cr, Ni isotopes).

An evaluation of neutron inelastic scattering spectra in the energy region of continuum levels was done for natural iron with phenomenological consideration of the direct processes contribution and temperature description of compound nucleus processes.

The obtained neutron emission spectra are consistent with neutron emission spectra measured for $E_n = 7, 9, 14$ and 26 MeV.

The temperature presentation of secondary neutron spectra was used in ^{nat}Cr and ^{nat}Ni files. This presentation allows to reproduce the emission spectra for neutrons with initial energy up

to (n,2n) reaction threshold but it leads to softening of the spectrum for higher energies.

Summing up, the main shortcomings of the secondary neutron spectra description are the following:

1. Double-differential cross-sections are isotropic for continuum part of spectrum (^{nat}Fe , ^{nat}Cr , ^{nat}Ni), as well as in region of discrete levels (^{nat}Cr , ^{nat}Ni).

2. Temperature presentation of spectra (^{nat}Cr , ^{nat}Ni) although is satisfactory for fast brider neutron spectrum, is needed improvement for fusion reactor neutron spectrum.

3. The data on secondary γ -rays production are absent in ^{nat}Fe files. ^{nat}Cr and ^{nat}Ni files include this data taken from ENDF/B-IV library.

FILES TESTING IN INTEGRAL AND MACROSCOPIC EXPERIMENTS.

Up to now this data testing was done for critical assemblies with neutron spectra similar to the spectrum of fast reactor [4]. As was shown by comparison of calculations with experiments for seven uranium assemblies with different content of iron, chromium and nickel and different neutron spectra, the deviations in k_{∞} in the 26-group constant system generated from CJD-2 evaluation files are from -0.8% to +2.3%, for BNAB-78 constants [10]- from -1% to -5% and for ENDF/B-IV - from -2.5% to -8% (Fig.1).

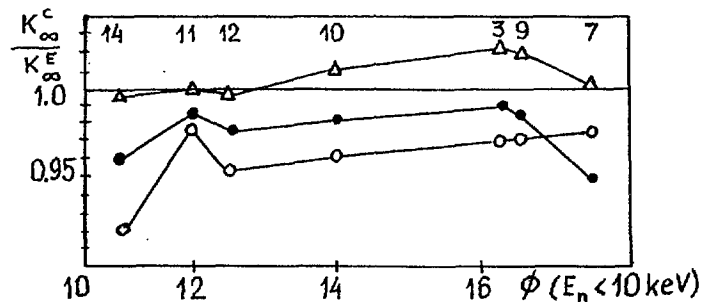


Fig.1 Ratio of calculated value of k_{∞} obtained from different system of constants (points - BNAB-78, open circles - ENDF/B-IV, triangles - CJD-2) to the experimental one for different critical assemblies [4] (critical assemblies with number 3,9,10,11,12 contain the stainless steel, 14 - chromium and 7 nickel). A part of neutron spectra with energy below 10 keV shown on the abscess axis.

The largest deviations in the prediction of k_{∞} were obtained for iron assemblies with soft neutron spectrum. Authors [4] have

noted that the increase of capture cross-section for ^{nat}Fe of CJD-2 evaluation in the energy group 4.65-10 keV from 15.6 mB to 23 mB (ENDF/B-IV value) without any changes of other quantities led to the 1% accuracy. However at present there are no grounds for revision of cross-section of the ^{nat}Fe CJD-2 evaluation, because the main contribution to the capture cross-section in this energy region is determined by the first ^{54}Fe resonances, the capture areas of which are measured with rather high accuracy [11].

A lack of these data in time of ENDF/B-IV, BNAB-78 and JENDL-2 evaluation work led to increase of the cross-section in these group on 35-50%.

Comparison of the ^{238}U fission subthreshold withdrawal cross-section averaged on ^{235}U fission spectrum induced by thermal neutrons for files of ^{nat}Cr , ^{nat}Fe and ^{nat}Ni (Table 1) shows that within the error limits the theoretical results agree with existing experimental data.

Table 1. Comparison of the ^{238}U subthreshold fission neutron withdrawal cross-section for the thermal neutron induced ^{235}U fission spectrum.

| MATERIAL | EXPERIMENT [12],B | CALCULATIONS,B | | |
|-----------------|-------------------|----------------|-----------|-------|
| | | BNAB-78 | ENDF/B-IV | CJD-2 |
| Fe | 0.70 ± 0.02 | 0.66 | 0.70 | 0.66 |
| Cr | 0.66 ± 0.02 | 0.67 | 0.67 | 0.67 |
| Ni | 0.74 ± 0.02 | 0.81 | 0.75 | 0.76 |
| Stainless steel | 0.69 ± 0.02 | 0.68 | 0.70 | 0.67 |

The next step of CJD-2 evaluation files testing for structural materials will be inter comparison of the calculation results and experimental data on 14 MeV neutron transmission through the spherical layers. There is BRAND-code [13] for neutron fields calculation by means of Monte-Carlo method and the

experiments on neutron leakage measurements are in progress now [14]. However the preliminary revision of ^{nat}Cr , ^{nat}Fe and ^{nat}Ni files is needed.

THE FIRST PRIORITY REVISION OF THE STRUCTURAL MATERIALS FILES OF CJD-2 EVALUATION.

The existing plans of the revision of structural material files include the following actions:

1. Conversion of the files into ENDF-VI format and in particular the use of Reich-Moor presentation in the resolved resonance region of s-wave for even-even isotopes.

2. The improvement of the neutron spectra presentation for ^{nat}Cr and ^{nat}Ni files.

3. To add the files by secondary γ -ray spectra, needed for energy release and shielding calculations.

The work on revision of the secondary neutron energy-angular distributions and γ -spectra for ^{93}Nb file of BROND library is in progress now.

REFERENCES.

1. BROND, USSR Recommended Evaluated Neutron Data Library, INDC(CCP)-283, IAEA, Vienna, 1988.
2. Belanova T.S. et al., INDC(NDS)-152/L, 1984.
3. Pronyaev V.G., Ignatyuk A.V., in: Problems of Atomic Science and Technology. Ser. Nuclear Constants, No 3, 1986, p.13;
Pronyaev V.G. Ignatyuk A.V., ibid, No 4, 1986, p.51.
4. Nikolaev M.N. et al., "Neutron Data Testing for Cr, Fe and Ni on Integral and Macroscopic Experiment", paper presented at 1988 Intern. Conf. on Nucl. Data for Sci and Technol., Mito, Japan.
5. Sinitza V.V., Report INDC(CCP)-228/GL, IAEA, Vienna, 1984.
6. Manturov G.N., Preprint FEI-666, Obninsk, 1976 (in Russian).
7. Guenther P. et al., Report ANL/NDM-11, 1975.
8. Bychkov V.M. et al. "Threshold Reaction Cross-Sections Induced by Neutrons", M., Energoatomizdat, 1982 (in Russian).
9. Blokhin A.I. et al., Izv. AN SSSR, ser fiz., 1985, v.49(5), p.962
10. Abagyan L.P. et al "Group Constants for Reactor and Shielding Calculations", M., Energoatomizdat, 1981. (in Russian).

11. Gayther D.B. et al., paper presented at Geel 79 Meeting;
Brusegun A. et al., in: Proc. Int. Conf. on Nuclear Cross-Sections for Sci. and Technol. (Antwerp.,1982), Holland,1983,p.127.
12. Dulin V.A. et al., Atomnaya Energia,1985,v.59,p.116 (in Russian).
13. Androsenko A.A.,Androsenko L.A., in: Problem of Atomic Science and Technol.,ser.Phys. and Tech. of Atom. React., 1985, ,p.33.
14. Androsenko A.A. et al., "Measurements and Comparisons with Calculation of Neutron Leakage Spectra from U, Pb and Be Assemblies with 14-MeV Neutron Source in a Centre", paper presented at Specialist Meeting on the Problem of the Experimental Fusion Reactors, Varna, Bulgaria, March 1987.

Work on Fusion Activation at Harwell

R.A. Forrest - Harwell Laboratory, England

Effort in: > Cross section data
> Decay data
> Inventory code
> Applications of code
> Experiments

Additional effort: > Biological hazard data
[NRPB + Culham]

Collaboration: > ECN Petten
> KfK Karlsruhe

Cross Section Data Library

The data library UKACT1 has been described at the meeting held here last year. This is now the primary source for UK calculations.

Work currently in hand to update this:

- > More targets ($T_{1/2} > 0.5$ day)
- > Better (n,gamma) data
- > Better isomer ratios
- > More evaluated files
- > New calculations

Rather than produce UKACT2, results are input to ECN Petten to form the European Activation File (EAF)

Decay Data Library

All nuclides in cross section library and decay products require decay data.

For UKACT1 data for 1314 nuclides required.

- > UKDECAY2

For EAF data for about 1356 nuclides required.

- > UKDECAY3

To construct UKDECAY3 use has been made of evaluated files from ENSDF. Problem that some files contain unnormalised data.

There remain about 68 nuclides with data extracted by hand from standard handbooks [No gamma spectrum].

Nuclides with estimated data

⁸Be
³¹Al, ³²Al
³³Si
³⁰P
⁴¹Cl, ⁴²Cl
⁶³Fe
⁶⁵Co, ⁶⁶Co
⁶⁸Ni, ⁶⁹Ni
⁹⁶nY(2.3m)
^{90m}Nb(18.8s)
^{100m}Rh(4.7m)
^{113m}Pd(1.48m)
^{131m}Sb(16.7m)
¹²⁹Ba, ^{129m}Ba(2.17h)
^{132m}La(24.3m)
¹³³Ce
¹⁵²ⁿPm(15m)
¹⁴⁸Gd
^{151m}Tb(25s), ^{156m}Tb(5.3h)
¹⁵⁴Dy
¹⁵⁸Ho, ^{158m}Ho(21.3m), ¹⁵⁸ⁿHo(27m), ¹⁶⁰Ho,
^{160m}Ho(5.02h), ¹⁶⁰ⁿHo(3s), ¹⁷¹Ho, ¹⁷²Ho
¹⁷⁹Yb
¹⁸²Lu
¹⁷¹Hf, ¹⁸⁵Hf
¹⁸⁰Ta, ¹⁸⁷Ta, ¹⁸⁸Ta
¹⁸⁹W, ¹⁹¹W
¹⁷⁹Re, ¹⁹¹Re, ¹⁹²Re, ¹⁹³Re, ¹⁹⁴Re
¹⁸¹Os, ¹⁹⁵Os, ¹⁹⁶Os, ¹⁹⁷Os
¹⁸⁵Ir, ¹⁸⁷Ir, ¹⁹¹ⁿIr(5.5s), ^{196m}Ir(1.4h), ¹⁹⁷Ir,
^{197m}Ir(8.9m), ¹⁹⁸Ir, ¹⁹⁹Ir, ²⁰⁰Ir
¹⁸⁷Pt, ¹⁸⁸Pt, ¹⁹³Pt, ²⁰¹Pt
^{192m}Au(0.17s), ^{194m}Au(0.6s), ²⁰³Au
¹⁹³Hg
^{199m}Pb(12.2m), ^{201m}Pb(1.02m)

Inventory Code FISPACT

Version 1.3 of FISPACT fully documented. Available from NEA Data Bank.

Version 1.4 has been completed and is currently being documented. Additional features include:

- > Calculation of pathways
- > Use of A₂ numbers for transport
- > More flexible graphics
- > Improved output, bugs removed

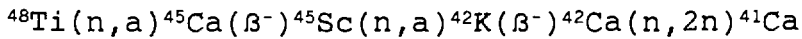
In addition the code has been implemented on personal computers e.g. 80386 based PC with FTN77/386 compiler.

Pathway Analysis

Calculation of inventories by FISPACT involves no knowledge of the method of formation of the daughter.

Useful to know which are the dominant pathways.

Example in DEMO 1st wall spectrum (5 MW m⁻², 2.5 y):



This pathway contributing 99.1% of all ⁴¹Ca formed from ⁴⁸Ti. Contains 5 links (2 decays + 3 reactions).

- > Linear path
- > All nuclides different - No loops

FISPACT will search for all possible pathways from parent to daughter (maximum 6 links) and give %.

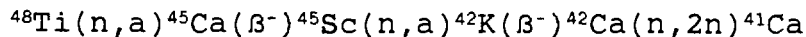
Scaling of Pathways

Nuclide production via pathways can be estimated analytically. Each nuclide in pathway is short- or long-lived (S or L) in relation to irradiation time and connected by a reaction or decay (r or d). With each nuclide associate a factor:

| | |
|-------|---------------|
| L_r | $\emptyset T$ |
| S_r | \emptyset |
| L_d | T |
| S_d | 1 |

Then form the product = F. This tells you how the amount of the daughter scales if the flux (\emptyset) or irradiation time (T) is varied.

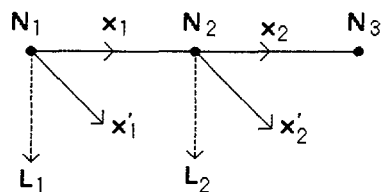
Example in DEMO 1st wall spectrum (5 MW m⁻², 2.5 y):



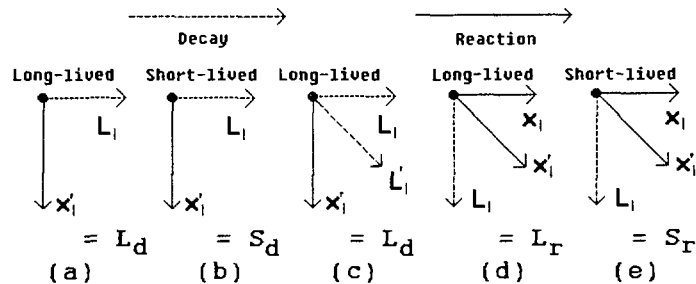
This pathway has a scaling factor of $\emptyset^3 T^3$.

Pathways

A typical pathway is:
[x_i = cross sections, L_i = decay constants]



If both N_1 and N_2 are long lived then this is a $L_r L_r$ case.



Use of scaling factors for each nuclide gives the final factor F for any pathway.

Applications of code FISPACT

FISPACT in use by Harwell, Culham, Imperial College, and KfK. In order to give results of calculations of relevance to designers, metallurgists etc the following report produced:

**"Activation data for some elements
 relevant to fusion reactors"**
AERE R 13402

For 30 elements activities, dose rates, heating and biological hazard data are tabulated or given as graphs. Also information on which natural isotopes produce which long-lived nuclide:

Important long-lived nuclides

^{53}Mn (3.697 10^6 y), ^{60}Fe (2.998 10^5 y), ^{60}Co (5.268 y), ^{59}Ni (7.495 10^4 y), ^{63}Ni (100.03 y)

Percentage of nuclide from natural abundance of isotope

| | ^{54}Fe | ^{56}Fe | ^{57}Fe | ^{58}Fe |
|------------------|------------------|------------------|----------------------|----------------------|
| ^{53}Mn | 99.93 | 0.07 | $1.22 \cdot 10^{-5}$ | $8.08 \cdot 10^{-6}$ |
| ^{60}Fe | 0 | 0.08 | 1.83 | 98.09 |
| ^{60}Co | 0 | 0.05 | 1.44 | 98.50 |
| ^{59}Ni | 0 | 0.02 | 0.87 | 99.11 |
| ^{63}Ni | 0 | 0.01 | 0.71 | 99.28 |

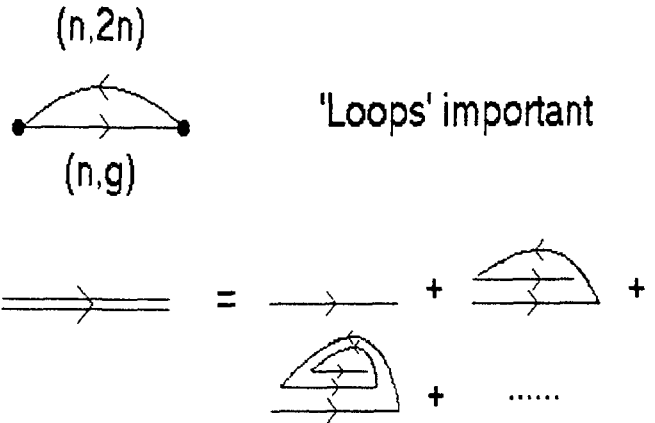
And information on dominant pathways to produce long-lived nuclides:

| ^{53}Mn | Reaction | % | F |
|--|----------|------|-------------------|
| $^{54}\text{Fe}(n,d)^{53}\text{Mn}$ | | 98.9 | $\emptyset T$ |
| $^{56}\text{Fe}(n,2n)^{55}\text{Fe}(n,2n)^{54}\text{Fe}(n,d)^{53}\text{Mn}$ | | 40.9 | $\emptyset^3 T^3$ |
| $^{56}\text{Fe}(n,2n)^{55}\text{Fe}(n,t)^{53}\text{Mn}$ | | 22.2 | $\emptyset^2 T^2$ |
| $^{56}\text{Fe}(n,d)^{55}\text{Mn}(n,2n)^{54}\text{Mn}(n,2n)^{53}\text{Mn}$ | | 15.1 | $\emptyset^3 T^2$ |
| $^{57}\text{Fe}(n,2n)^{56}\text{Fe}(n,2n)^{55}\text{Fe}(n,2n)^{54}\text{Fe}(n,d)^{53}\text{Mn}$ | | 31.0 | $\emptyset^4 T^4$ |
| $^{57}\text{Fe}(n,2n)^{56}\text{Fe}(n,2n)^{55}\text{Fe}(n,t)^{53}\text{Mn}$ | | 23.1 | $\emptyset^3 T^3$ |
| $^{57}\text{Fe}(n,t)^{55}\text{Mn}(n,2n)^{54}\text{Mn}(n,2n)^{53}\text{Mn}$ | | 15.9 | $\emptyset^3 T^2$ |
| $^{58}\text{Fe}(n,a)^{55}\text{Cr}(\beta^-)^{55}\text{Mn}(n,2n)^{54}\text{Mn}(n,2n)^{53}\text{Mn}$ | | 99.8 | $\emptyset^3 T^2$ |

Future Work

FISPACT

- > Include gas production e.g. tritium
- > Allow 'loops' in pathways
- > Improved search - longer (n,g) paths
- > Add gamma dose rate < 0.1 MeV



Decay data

- > Include more evaluated files

Cross sections

- > Include effects of secondary charged particle reactions
- > Include errors in library

Reactions (p,n), (a,n) could be important. Charged particles produced in (n,p), (n,a) reactions.

⁵⁶Co production from irradiation of Fe could be increased by factor of ~ 1000.

Applications

- > Repeat compilation for 83 elements using new data and gas production in FISPACT.

J. Kopecky

Netherlands Energy Research Foundation ECN P.O.Box 1,
1755 ZG Petten, The Netherlands

1. INTRODUCTION

The EAF-project is part of the European Fusion Technology Programme of the European Community. The two following laboratories are involved:
ECN (Petten) - new evaluations, assembling and maintenance of the pointwise activation library EAF, using REAC-ECN-3 as a starter, as well as processing into a multigroup library.

AERE (Harwell) - assembling and maintenance of the decay library, based on UKDECAY1 and improvements and maintenance of the inventory code FISPACT.

The ultimate goal of these activities is to create a general inventory code and data libraries (consistent with JEF and EFF) for calculation of activation and transmutations in materials used in fusion reactor technology. The recent interest in low-activation materials (the LAM-project of EC), in view of recycling or simple waste disposal and production of low activation materials for NET and DEMO, has accelerated the need to have a high quality and complete activation file.

The requirements of the European Activation File are:

- a) A complete data base for all stable isotopes ($A < 210$) and isotopes (including isomers) with half lives longer than 1/2 day.
- b) An improvement of low energy data (in particular (n, γ) and $(n, n'\gamma)$ cross-sections).
- c) An inclusion of uncertainty estimates for the whole energy range of 0-20 MeV.
- d) Detailed evaluations for the most important activation reactions.

2. PRESENT STATUS

REAC-ECN-3 and UKACT-1

Important steps in the direction of the EAF have been made at ECN-Petten and AERE-Harwell during 1988. The results were presented in two contributions to the Mito conference /1,2/. In a collaborative effort the two labo-

ratories have made libraries that are based upon the REAC-2 data file of Mann et al./3/, with many extensions and renormalizations at 14.5 MeV to experimental data or results from systematics. In particular with respect to the systematics of cross-sections /4/ and of isomer ratios /5/ important progress has been made. As a by-product uncertainty estimates are available for all reactions that have been renormalized to the systematics at 14.5 MeV. The REAC-ECN-3 data file /6/ contains about 8500 reactions with cross-sections between 0 and 20 MeV. There are 51 reactions that were re-evaluated to obtain reliable predictions of long-lived products, including uncertainty information. This work was supported by the JRC Ispra and the file was applied in the activation studies of Ponti /7/. The data file has been processed into a multigroup library of 100 groups (GAM-structure) and 175 groups (VITAMIN-J structure, consistent with GEF-1). The UK library is based upon REAC-ECN-2 and because of intense cooperation between ECN and AERE both data libraries are very similar.

REAC-ECN-4 (EAF-0)

Recently the preliminary starter of the EAF has been assembled by means of the code SYMPAL (the new ECN code for processing and maintenance of the activation library). It contains the following improvements:

1. The REAC-ECN-3 library has been extended by the addition of reactions on 142 targets (many of them isomers) and further improved by applying proper effective thresholds for isomeric states. This version contains now all stable targets and isotopes (including isomers) with $T_{1/2} > 1$ day, with 10787 reactions.

2. The neutron emission cross-sections, in particular $(n, n'\gamma)$ cross-sections have been improved to compensate for the shortcomings of the code THRES:

- 2.1 The $(n, n'\gamma)$ isomeric cross-sections have been derived by applying the branching ratio systematics for one-step reactions /5,6/ and by adding a constant component based on the systematics of Vonach /8/ at 14.5 MeV.

- 2.2 For 19 target nuclides with the $(n, 3n)$ threshold below 14 MeV energy, the overestimated steep rise of the excitation function was decreased, in order to get the competing $(n, 2n)$ cross section to agree with the systematics or experimental data.

3. All renormalisations based on the experimental information are being checked carefully against the recent data. This action has been completed and thus the REAC-ECN-4 is at present probably the best data base for activation calculations of the first wall and inner blanket.

The main emphasis of the next version (EAF-1), which shall be completed and released for benchmark testing at the end of 1989, will be in the completeness and quality of the radiative capture data. The (n,γ) reaction, together with $(n,n'\gamma)$, is important at relatively low energies and therefore also the thermal and resonance ranges will be considered. This is of importance in "thermal" blankets and in the NET water-cooled blanket.

The re-evaluation of radiative capture data is done in two steps. Firstly all available evaluations from general purpose files (in particular JEF 1.1) will replace the old data. Further the existing experimental information concerning the isomer branch (based on thermal cross sections or resonance integrals) shall be used in connection with systematics accepted at 14.5 MeV.

For targets with no evaluation or experimental information (especially the radioactive targets) a simplified statistical code MASGAM, with $1/v$ and direct-semidirect components, has been developed at the ECN. The input is prepared from minimal information such as Z and A, entirely from global systematics. The data will be checked and renormalised at three energies, $E_n =$ thermal, 30 keV and 14.5 MeV. Also the resonance integral will be considered. The existing information on uncertainties will be included in a more systematic way.

3. CONCLUSION

The work on the first version of the European Activation File is in good progress. By means of recent improvements of the low energy data, EAF-1 will become a general activation file, applicable in fission and fusion reactor technology. Further international cooperation is required to meet the increasing demands for high-quality data for important targets or reactions supplied with covariance information.

REFERENCES

1. J.Kopecky and H.Gruppelaar, Proc.Int.Conf. on Nuclear Data for Science and Technology, May 30-June 3, 1988, Mito (Saikon Publ. Comp. Ltd., Tokyo, 1988), p. 245.
2. R.A.Forrest et al., *ibid*, p. 1061.

3. F.M.Mann et al., Proc.Int.Conf. on Nuclear Data for Basic and Applied Science, May 13-17,1985, Santa Fe (Gordin and Breach Sci. Publ.,New Yorh, 1986), p. 207.
4. R.A.Forrest, AERE-R-12419 (1986).
5. J.Kopecky and H.Gruppelaar, ECN-200 (1987).
6. H.Gruppelaar et al., ECN-207 (1988).
7. C.Ponti, Fusion Technology 13(1988) 157.
8. H.Vonach, Proc. IAEA Adv. Group Meeting on Nuclear Data for Fusion Reactor Technology, December 1-5, 1986, Gaussig, GDR.

Motoharu Mizumoto
Japan Atomic Energy Research Institute

An evaluation of data for neutron induced reactions on lead isotopes and natural lead have been carried out for JENDL-3. The evaluation was mainly based on model calculations which reproduced the experimental data. Evaluated data were given for neutron cross sections, angular and energy distributions of secondary neutrons. The calculations were first carried out for each isotope and then the data were summed to produce the cross sections for ^{nat}Pb . The data (called as JENDL-3T) are stored in the ENDF/B-V format. The major improvements compared with JENDL-2 are the evaluations to include direct reaction process and multi-step statistical mode calculations. The gamma-ray production cross section and energy spectra have been newly evaluated.

The total, elastic scattering and capture cross sections below 480 keV were evaluated with the Multi-level Breit-Wigner formula using the newly observed resonance parameters from Oak Ridge¹⁾ and Geel²⁾. Above 480 keV, the statistical mode code CASTHY³⁾ was used to calculate the total cross section, the elastic scattering cross section and its angular distribution with adjusted optical potential parameters (similar to JENDL-2) and new level density parameters. The present level density parameters were obtained from the new resonance experiments compiled in BNL-325⁴⁾. The total cross section for ^{nat}Pb in the unresolved resonance region were evaluated on the basis of the experimental data of Schwartz⁵⁾. The giant resonance structure of the capture cross section above 10 MeV was reproduced by the experimental data for ^{208}Pb and ^{nat}Pb .

The inelastic scattering cross sections and angular distributions to the discrete levels were calculated with CASTHY³⁾. The additional direct reaction components to these inelastic levels were added by using the DWBA code DWUCK⁶⁾. The deformation parameters for the calculation were adopted from the experimental results⁷⁾. The neutron induced reaction cross sections such as (n,2n), (n,3n), gamma-ray production cross section were calculated with the multi-step statistical model calculation code GNASH⁸⁾. Other charged particle cross sections (n,p), (n,alpha), which are much smaller in the lead isotopes, were also obtained with GNASH and adjusted to reproduce the experimental data.

The (n,2n) cross sections were carefully compared with the data by Frehaut⁹⁾ et al. and other published data^{10,11)} at 14 MeV. A small adjustment of the calculated (n,2n) cross section values had to be made at 14 MeV to fit the experimental data. A comparison of the experimental data and the present adapted values for ^{nat}Pb at 14 MeV is shown in Table 1. The angular distribution of the continuum part of neutrons, which was claimed to be slightly unisotropic, was not taken into account in the present evaluation.

Further improvements

After the completion of the JENDL-3T works, some problems were still found to remain in the evaluated neutron emission spectra. Considerable discrepancy particularly between the present result and OKTAVIAN DDX data¹²⁾ in the 2-6 MeV region were pointed out. The cause seems to come mainly from the conventional level density formula used in the present evaluations. In the case of the Pb isotope, the conventional composite formula proposed by Gilbert Cameron could not reproduce the neutron spectra. The revision is being carried out to solve this problem by taking into account the new level density formula proposed by Ignatyuk et al.¹³⁾ The test calculation has been made by ignoring the effect of the discrete levels¹⁴⁾. Fig. 1. showed the test calculation. The modification of the GNASH code to include the Ignatyuk level density formula is being carried out. The work has not been completed yet and the revised results will be included in the file.

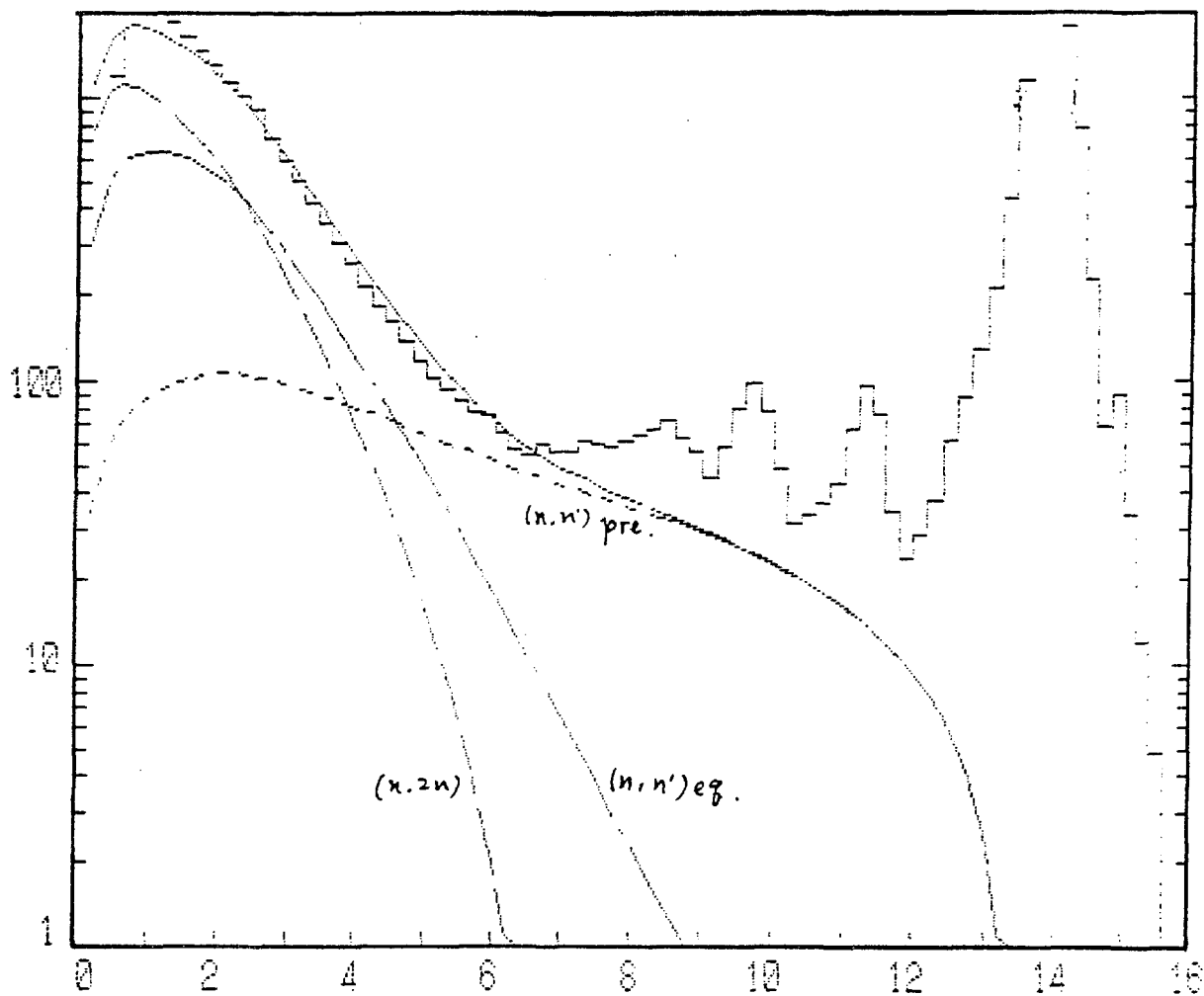
References

- 1) D.J. Horen et al., Phys. Rev. C29(1984) 2126
D.J. Horen et al., Phys. Rev. C24(1981) 1961
D.J. Horen et al., Phys. Rev. C34(1986) 429
- 2) R. Koehler et al., Phys Rev. C35(1987) 1646
- 3) S. Igarasi, J. Nucl. Sci. Technol., 12, 67 (1975).
- 4) S.F. Mughabghab, Neutron Cross Section Vol.1 Part B, Academic Press, Upton New York, 1984
- 5) R.B. Schwartz et al.: NBS-Mono-138 (1974), Data in EXFOR (1974)
- 6) P.D. Kunz, Univ Colorado (1974)
- 7) C.M. Lederer and V.S. Shirley, Table of isotopes, 7th edition
- 8) P.G. Young and E.D. Arthur, LA-6974(1977)
- 9) J. Frehaut et al., BNL-NCS-51245 Vol 1 p399 (1980)

- 10) S. Iwasaki et al., Proc. Santa Fe Conf. p191 (1985)
- 11) A. Takahashi et al., ibid p59
- 12) A. Takahashi et al., j. Nucl. Sci. Technol., 25(1988) 215
- 13) A.V. Ignatyuk, Sov. J. Nucl. Phys. 21(1976) 255
- 14) N. Watanabe, Private communication (1988)

Table (n,2n) cross section at 14 MeV

| Author/ Library | σ (n,2n) (barn) |
|--------------------|---------------------------|
| Frehaut | 1.95 ± 0.15 |
| Iwasaki | 2.13 ± 0.25 |
| Yanagi | 2.33 ± 0.16 |
| Vonach | 2.103 ± 0.065 |
| Takahashi | 2.43 ± 0.10 |
| Weighted average | 2.184 ± 0.048 |
| ENDF/B-4 | 2.167 |
| ENDL-82 | 2.15 |
| JENDL-2 | 1.921 |
| BROND | 2.26 |
| EFF | 2.0958 |
| JENDL-3T | 2.037 |



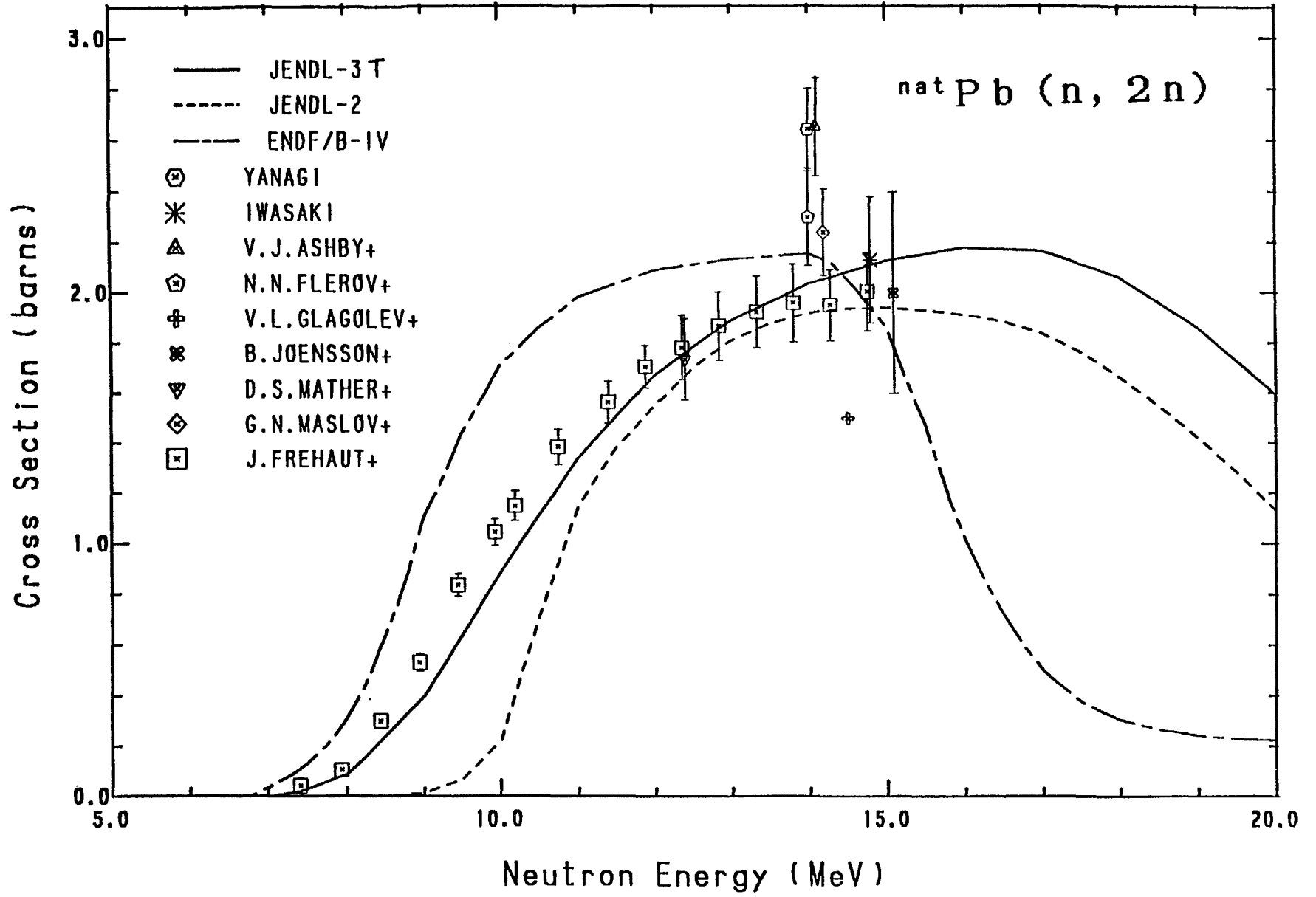
- $Na^{23}Pb(n, xn)$ 14.1 MeV

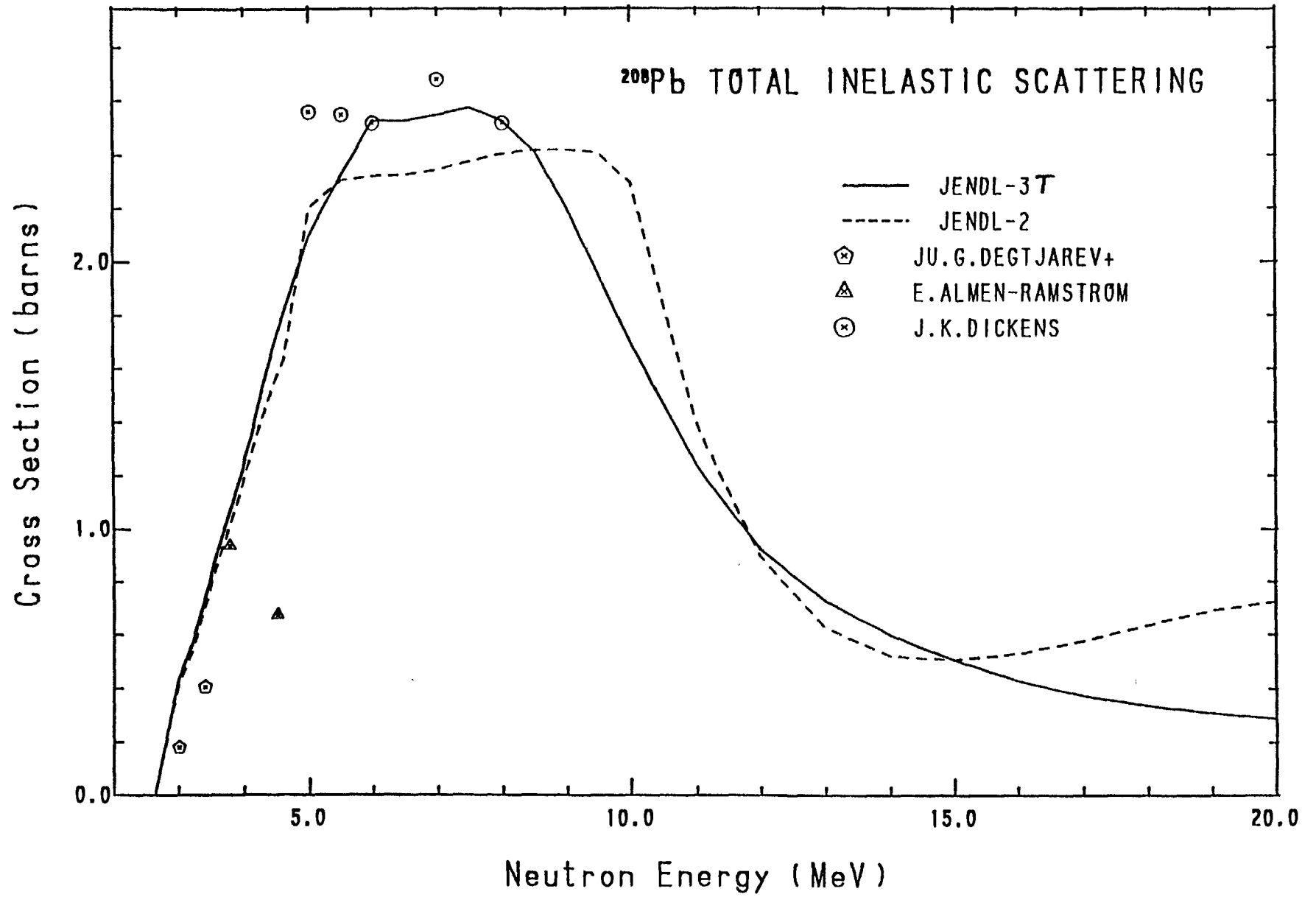
$Q(U)$: Ignitynk a \bar{n} izh

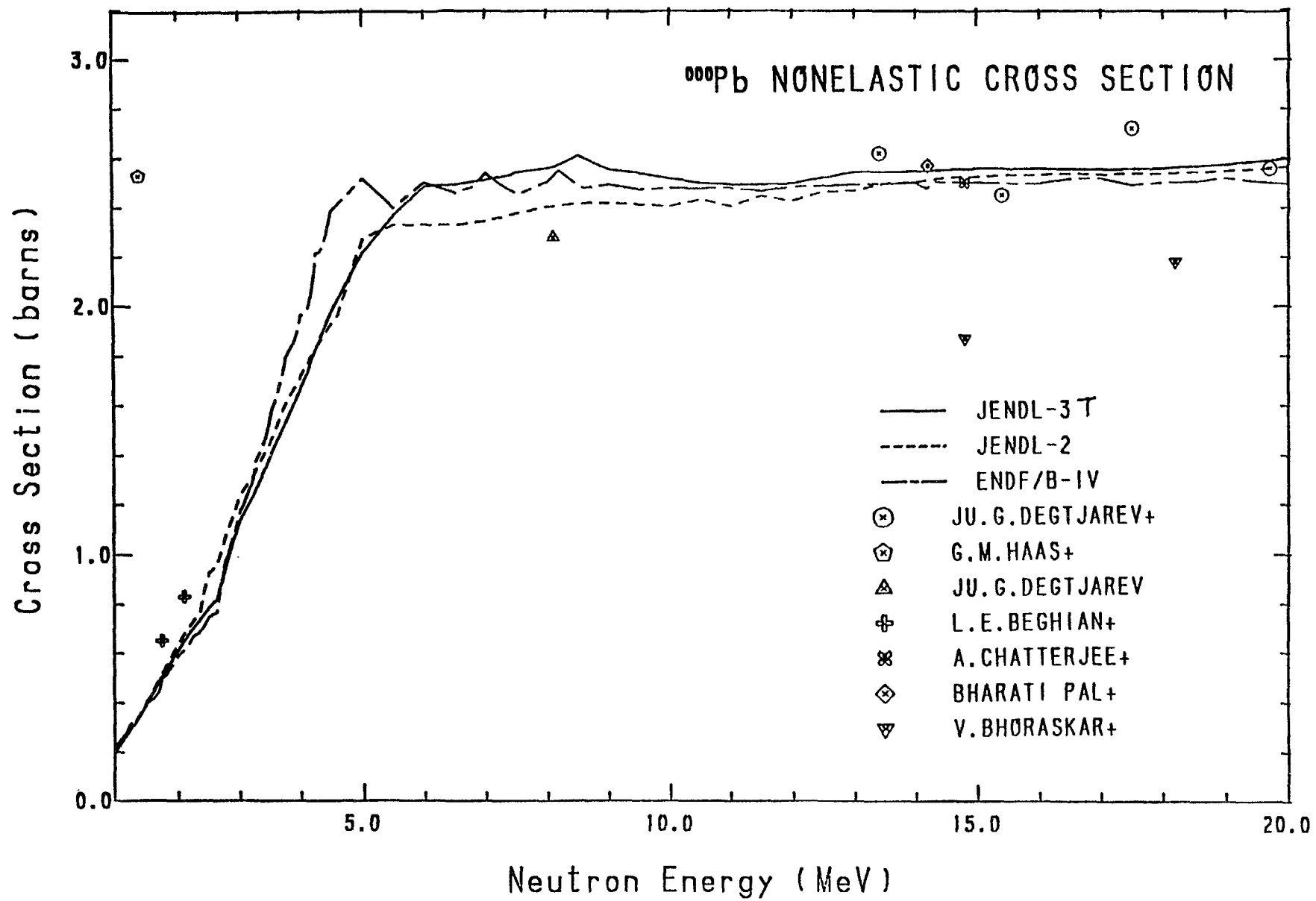
$Q(B_0 - \Delta) = Q_{mp.}$

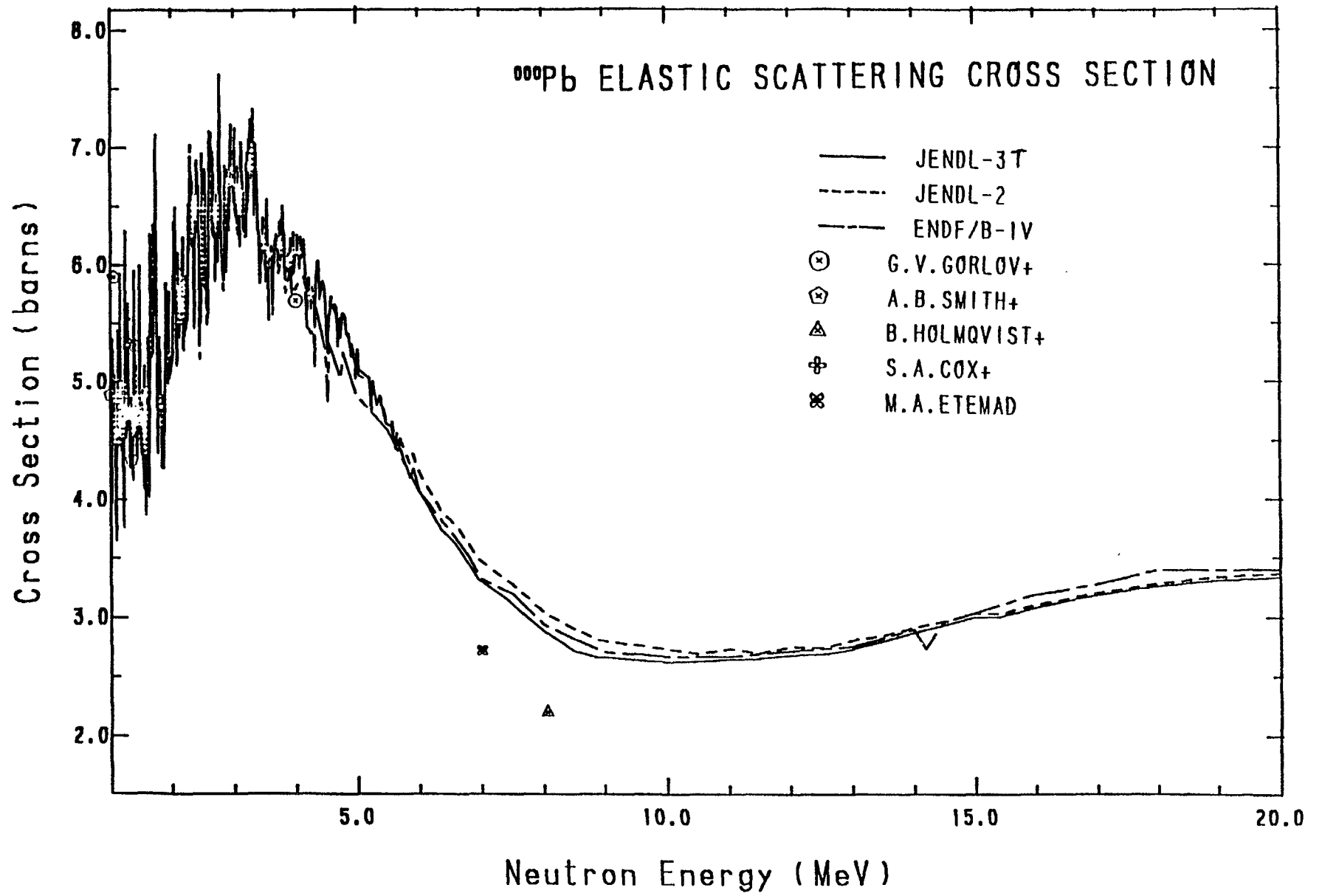
$k = 660 \text{ MeV}^2 (550 \times 1.2)$

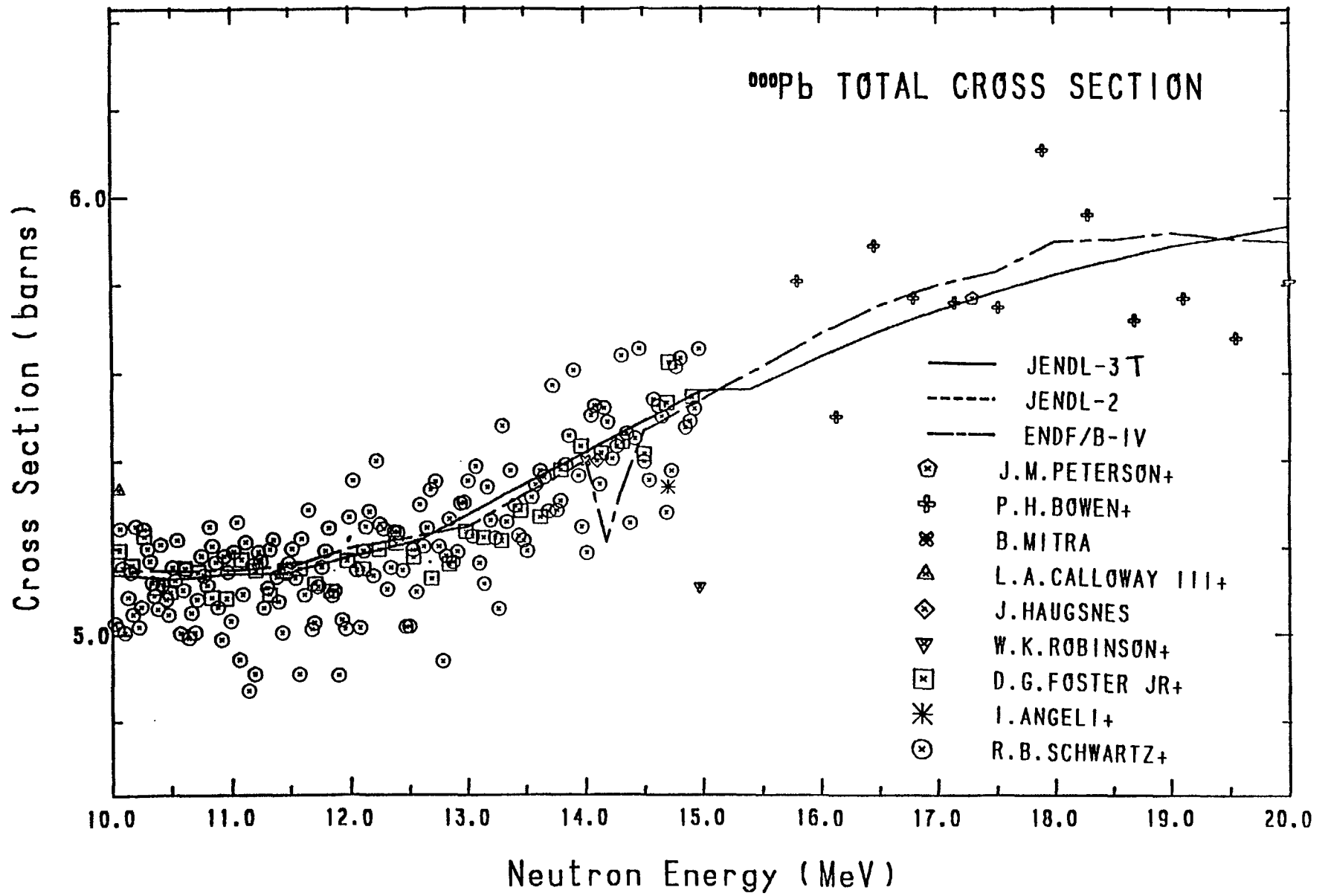
Fig. 1









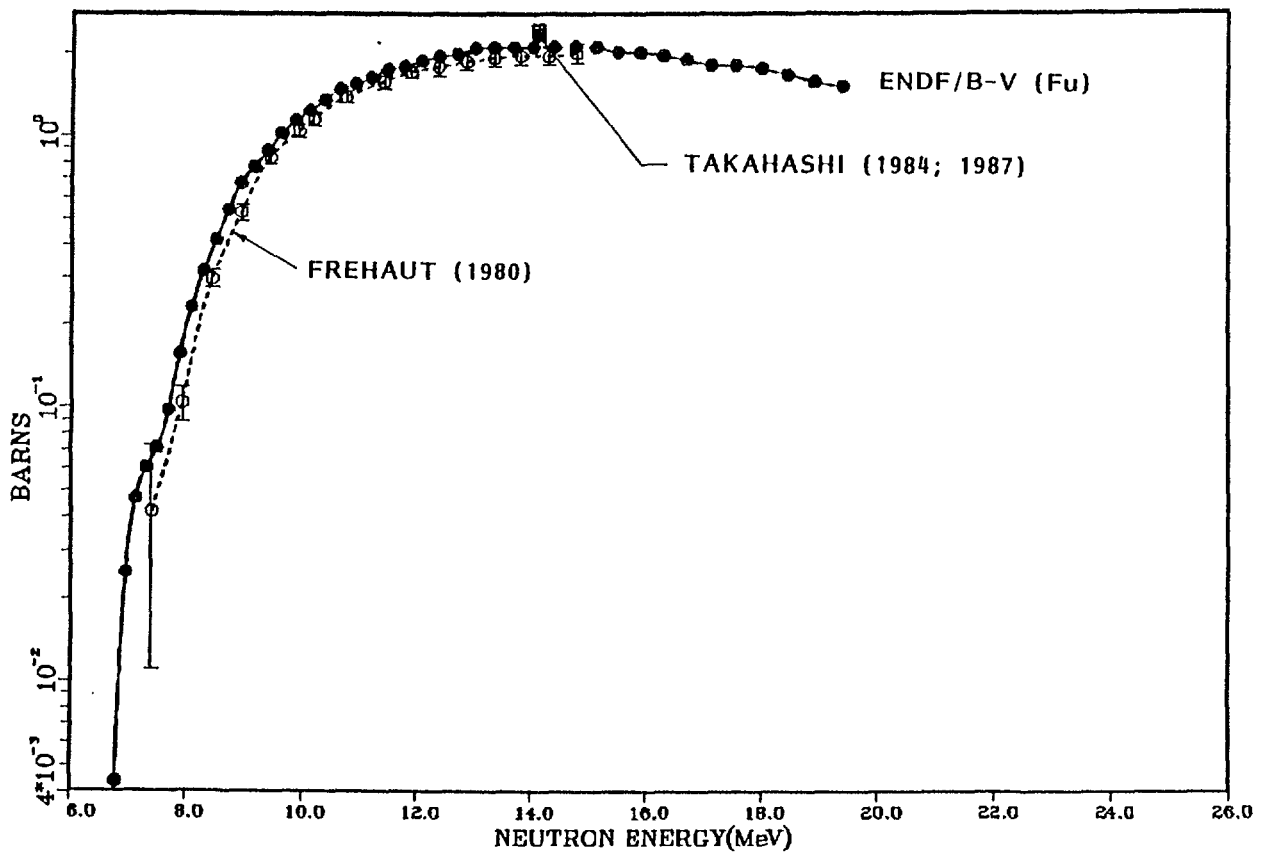


E.T. CHENG
 GENERAL ATOMICS
 SAN DIEGO, CALIFORNIA
 (619)455-4221

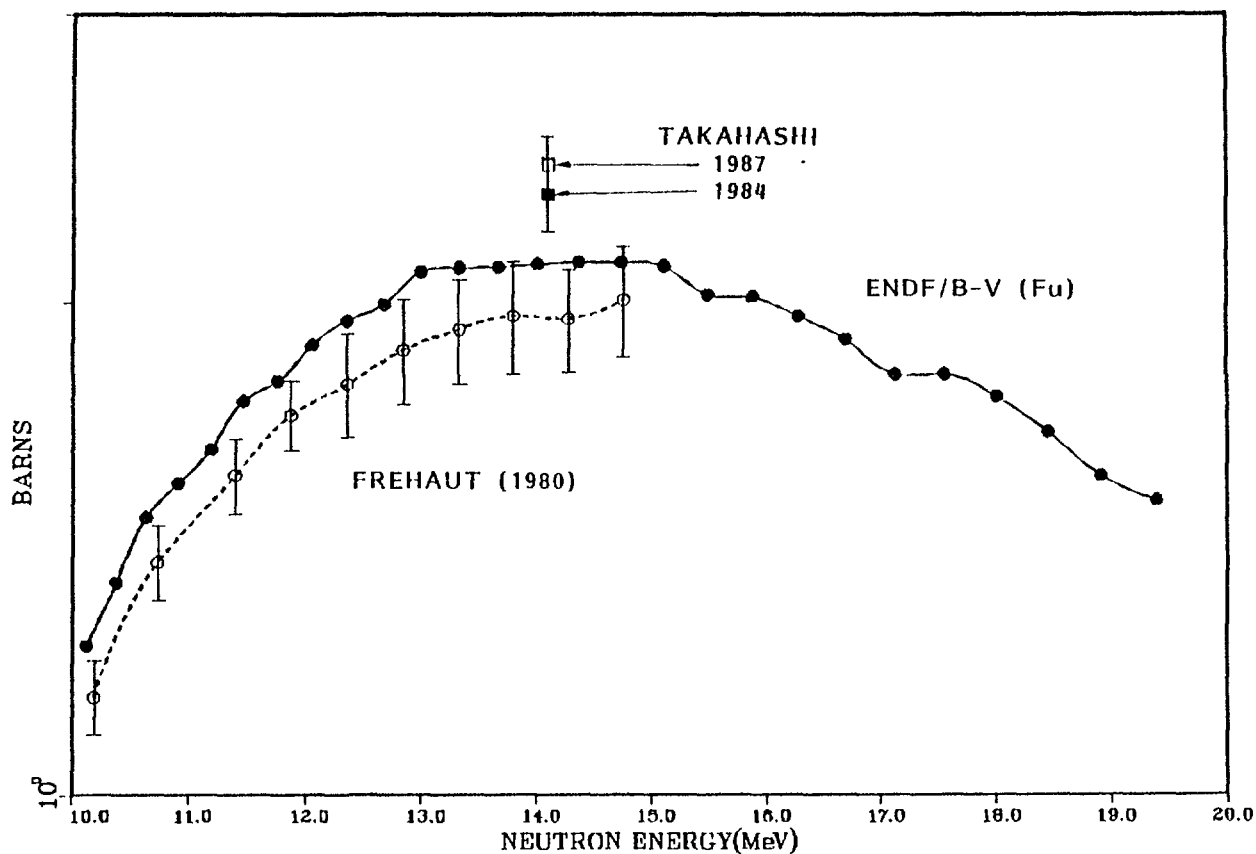
Pb ($n,2n$) CROSS-SECTIONS at 14.1 MeV

| Evaluation/Experiment | Cross-Section (b) | Ratio to ENDF/B-V |
|-----------------------|-------------------|-------------------|
| ENDF/B-V | 2.14 | 1.00 |
| ENDF/B-IV | 2.15 | 1.00 |
| EFF-1 | 2.10 | 0.98 |
| OKTAVIAN (1984) | 2.33 (5.2%) | 1.09 |
| OKTAVIAN (1987) | 2.43 (4.1%) | 1.14 |
| Frehaut (1980) | 1.95 (7%) | 0.91 |

LEAD N,2N CROSS SECTIONS

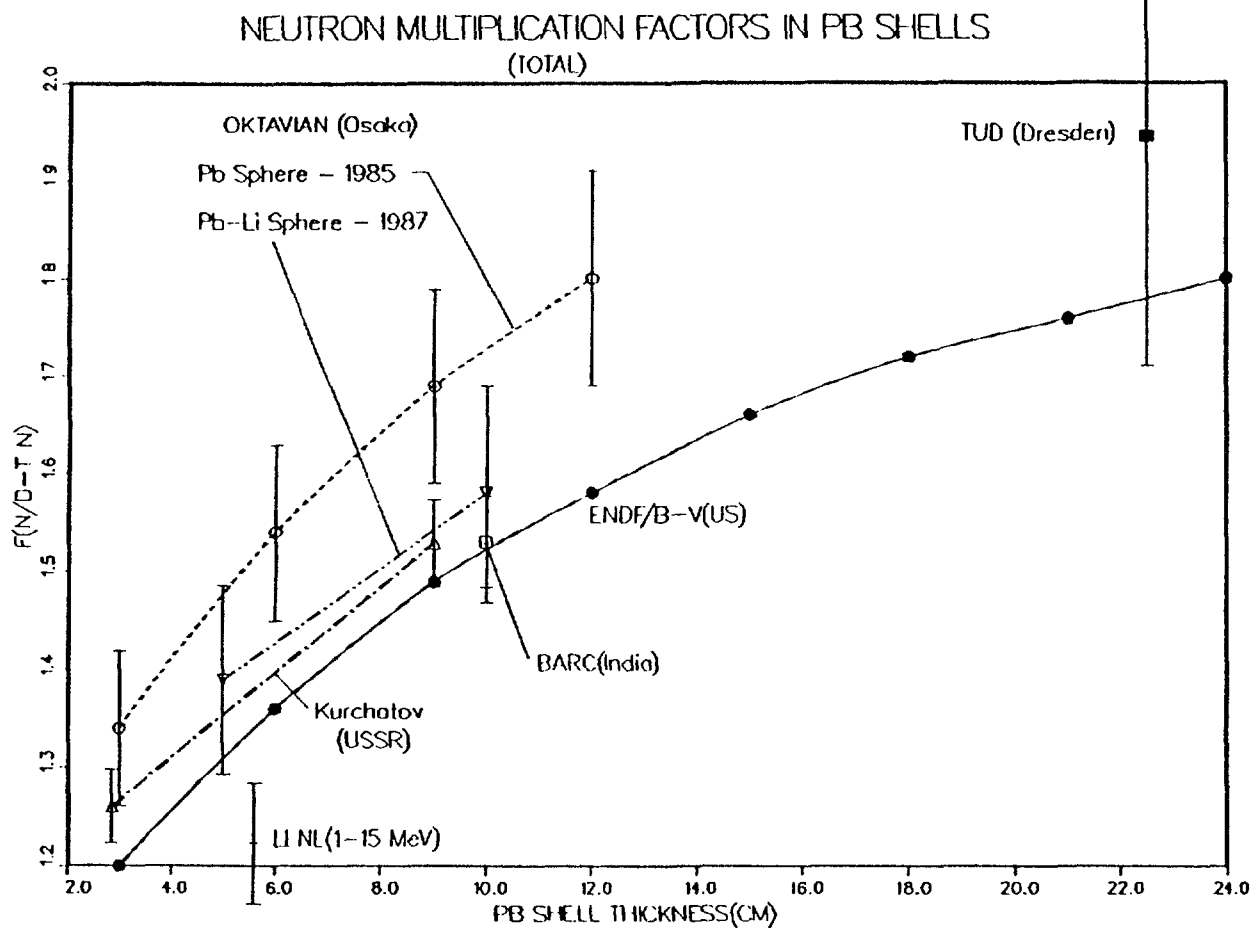


LEAD N,2N CROSS SECTIONS



COMPARISON OF INTEGRAL RESULTS ON LEAD NEUTRON MULTIPLICATION FACTOR

| Thickness (cm) | ENDF/B-V | OKTAVIAN Experiment | Dresden Experiment | BARC Experiment | Kurchatov Experiment |
|-------------------|----------|------------------------|-----------------------|--------------------|-------------------------|
| 2.85 | 1.19 | — | — | — | 1.26 (2.9%) |
| 5 | 1.31 | 1.39 (7%) | — | — | — |
| 9 | 1.49 | — | — | — | 1.53 (2.9%) |
| 10 | 1.52 | 1.58 (7%) | — | 1.53 (3%) | — |
| 22.5 | 1.78 | — | 1.94 (12%) | — | — |



STATUS OF LEAD CROSS SECTIONS AND BENCHMARK CALCULATIONS CALCULATIONAL METHODS

- * ONE-DIMENSIONAL SPHERICAL GEOMETRY MODEL
 - 14.1 MeV NEUTRON SOURCE
 - UNIFORM DISTRIBUTION IN THE TARGET REGION
- * MCNP MONTE CARLO CODE
 - 60,000 PARTICLES
 - SD - TOTAL (0.3%); ENERGY BIN (10% MAX.)
- * ENDF/B-V BASED NUCLEAR DATA LIBRARY
 - CONTINUOUS ENERGY
 - SIMILAR TO ENDF/B-VI

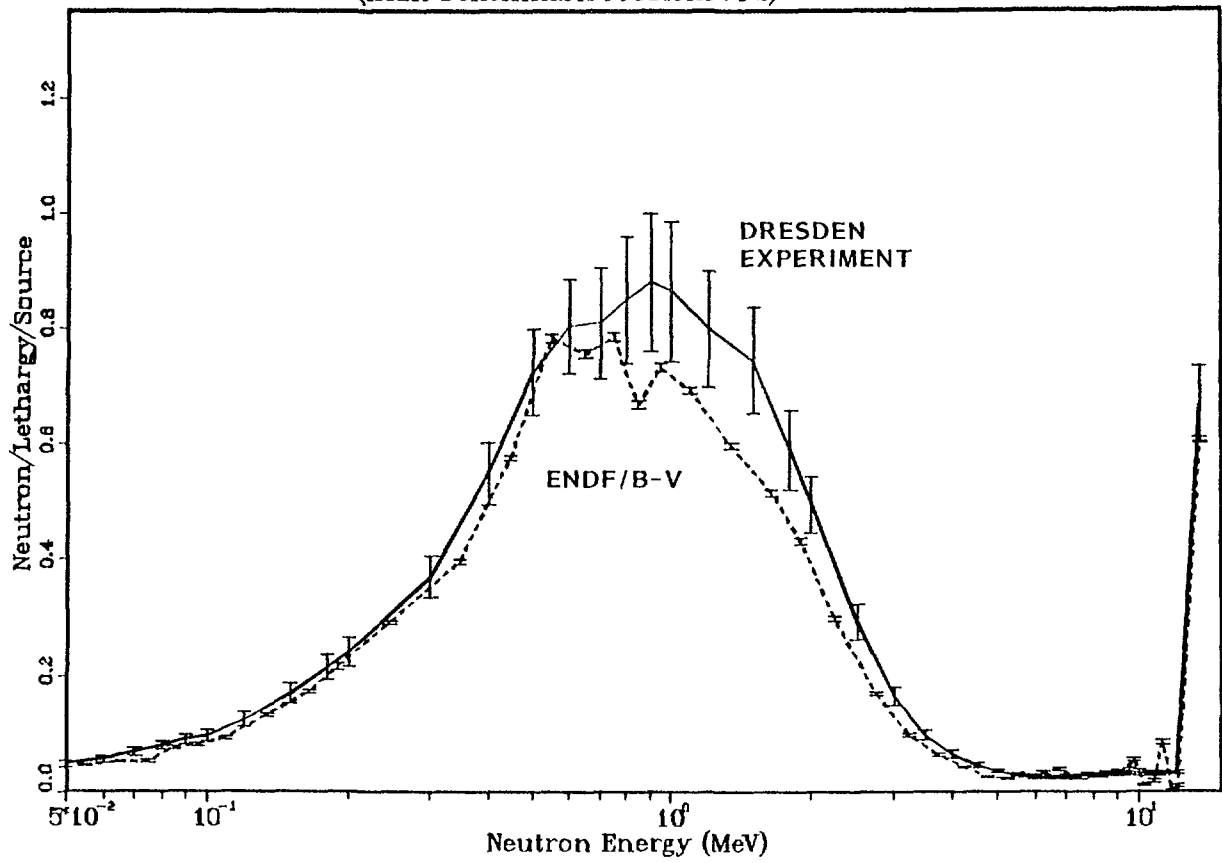
DOSIMETRY AND FISSION CROSS SECTIONS

| <u>Isotope/Reaction</u> | <u>Source Library</u> |
|----------------------------|-----------------------|
| $^{103}\text{Rh}(n,n')$ | ACTL |
| $^{115}\text{In}(n,n')$ | ENDF/B-V |
| $^{58}\text{Ni}(n,p)$ | ENDF/B-V |
| $^{64}\text{Zn}(n,p)$ | ACTL |
| $^{27}\text{Al}(n,\alpha)$ | ENDF/B-V |
| $^{203}\text{Tl}(n,2n)$ | ACTL |
| $^{65}\text{Cu}(n,2n)$ | ENDF/B-V |
| ^{235}U fission | ENDF/B-V |
| ^{238}U fission | ENDF/B-V |
| ^{237}Np fission | LANL(T2) |
| ^{232}Th fission | ENDF/B-V |
| ^{239}Pu fission | LANL(T2) |

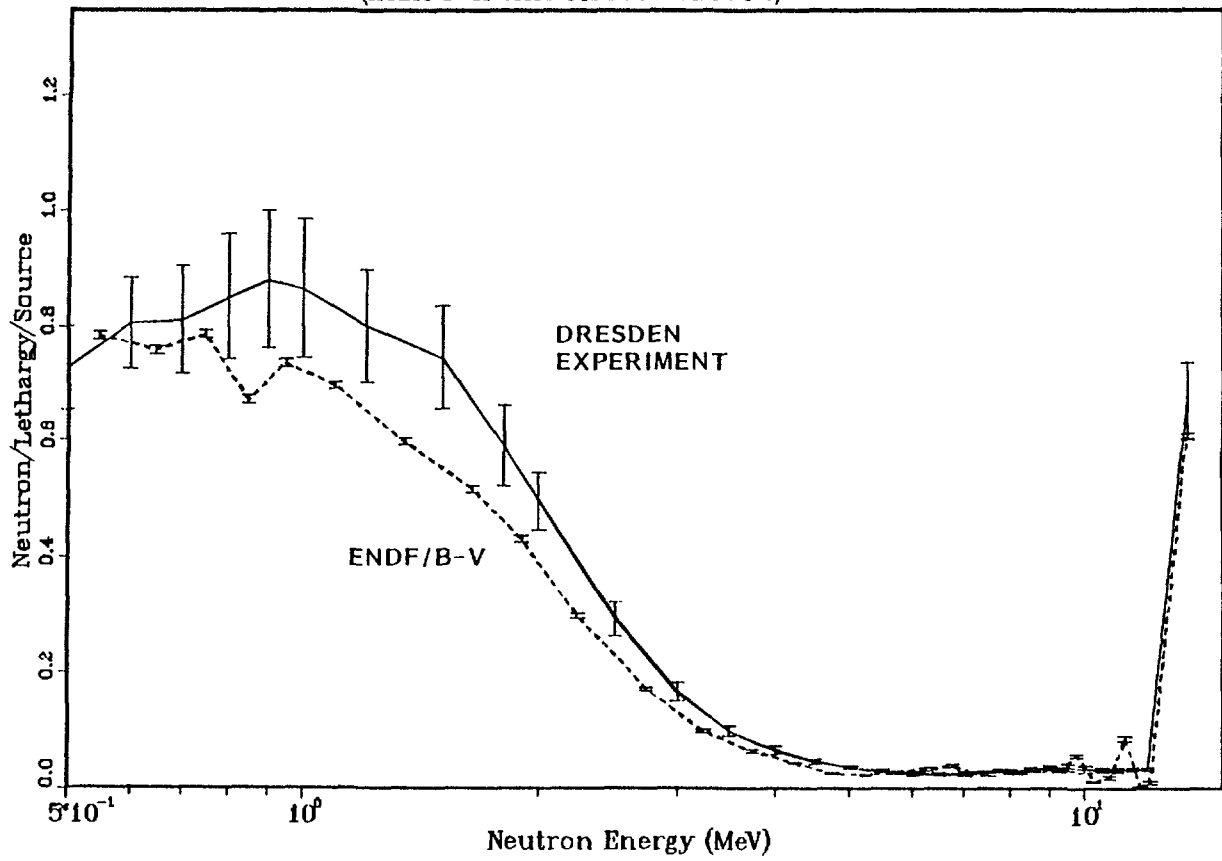
Summary of Leakage Neutrons

| Energy Range (MeV) | Calculated (ENDF/B-V) | Measured (Dresden) | Difference | <u>Difference Measured (Total)</u> |
|--------------------|-----------------------|--------------------|------------|------------------------------------|
| 0-1 | 1.0600 | 1.105 | 0.045 | 2.3% |
| 1-5 | 0.5354 | 0.676 | 0.1406 | 7.2% |
| 5-10 | 0.02163 | 0.0190 | -0.00263 | -0.14% |
| 10-15 | 0.1290 | 0.144 | 0.015 | 0.77% |
| Total | 1.746 (0.08%) | 1.944 (12%) | 0.198 | 10.2% |

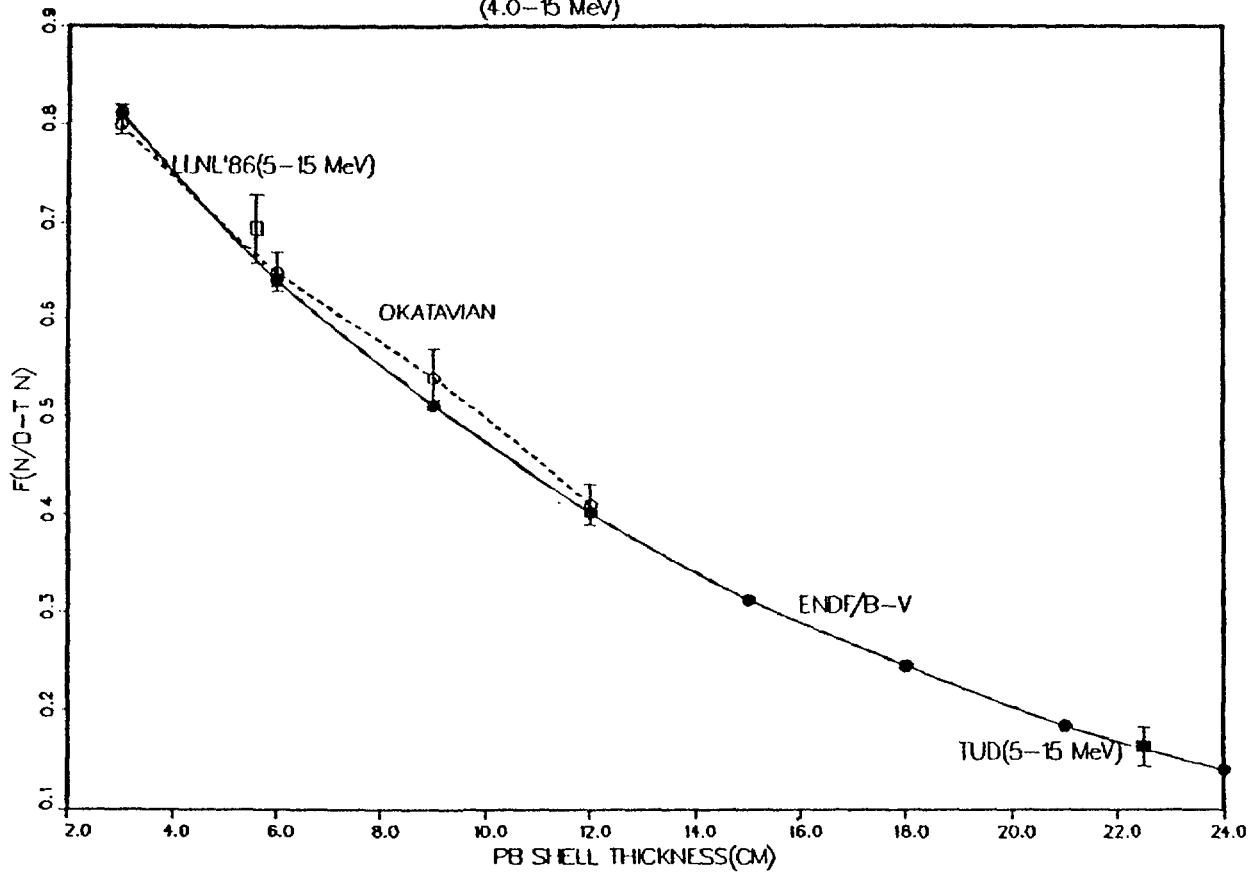
Comparison of leakage spectra from lead
(IAEA Benchmark Problem : Pb)



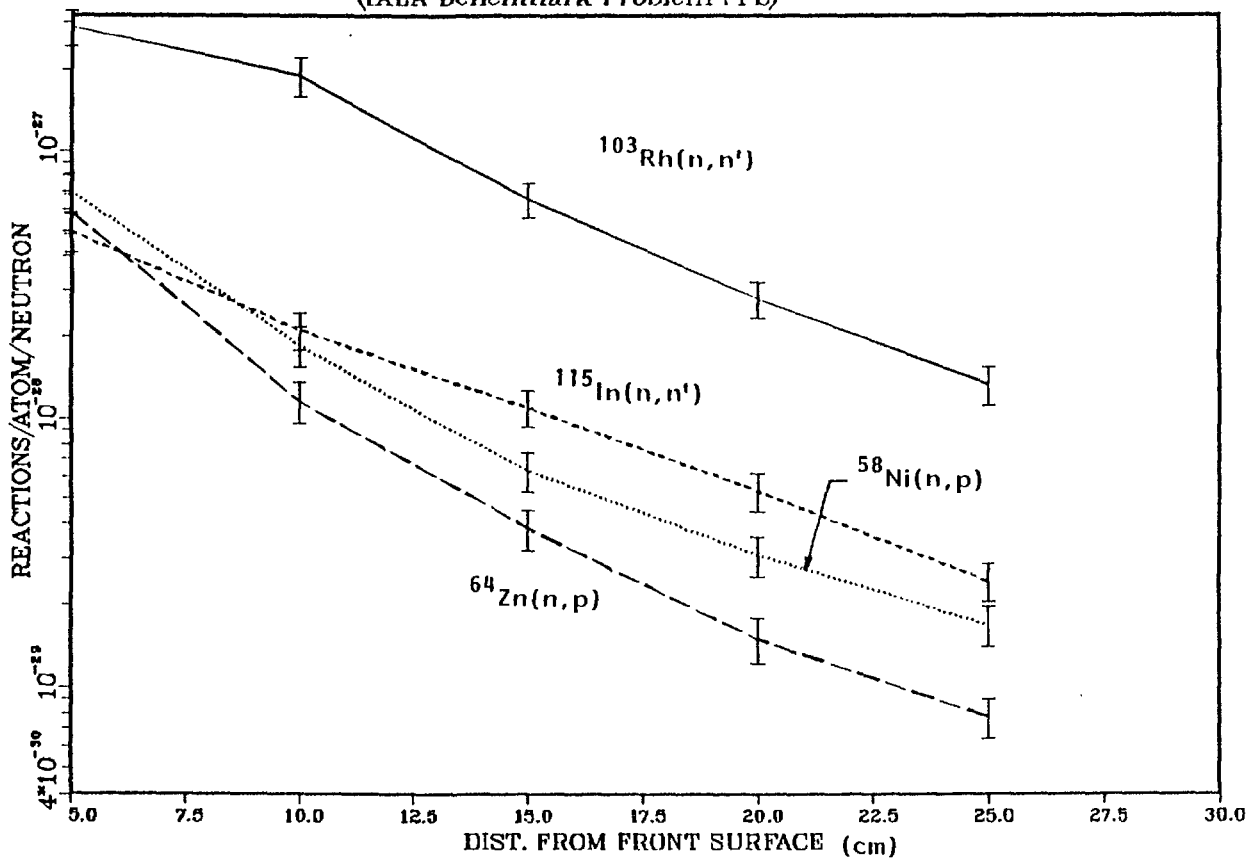
Comparison of leakage spectra from lead
(IAEA Benchmark Problem : Pb)



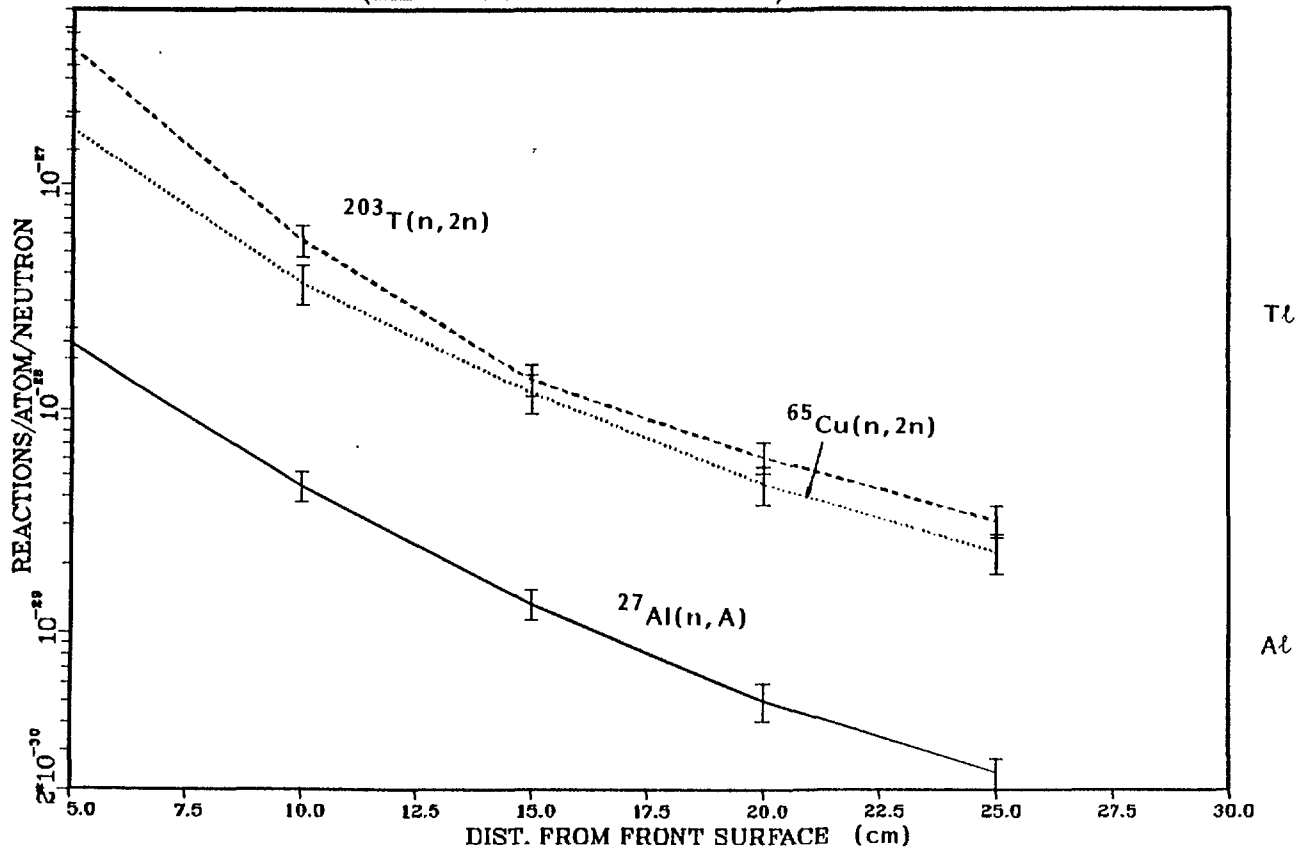
NEUTRON MULTIPLICATION FACTORS IN PB SHELLS
(4.0-15 MeV)



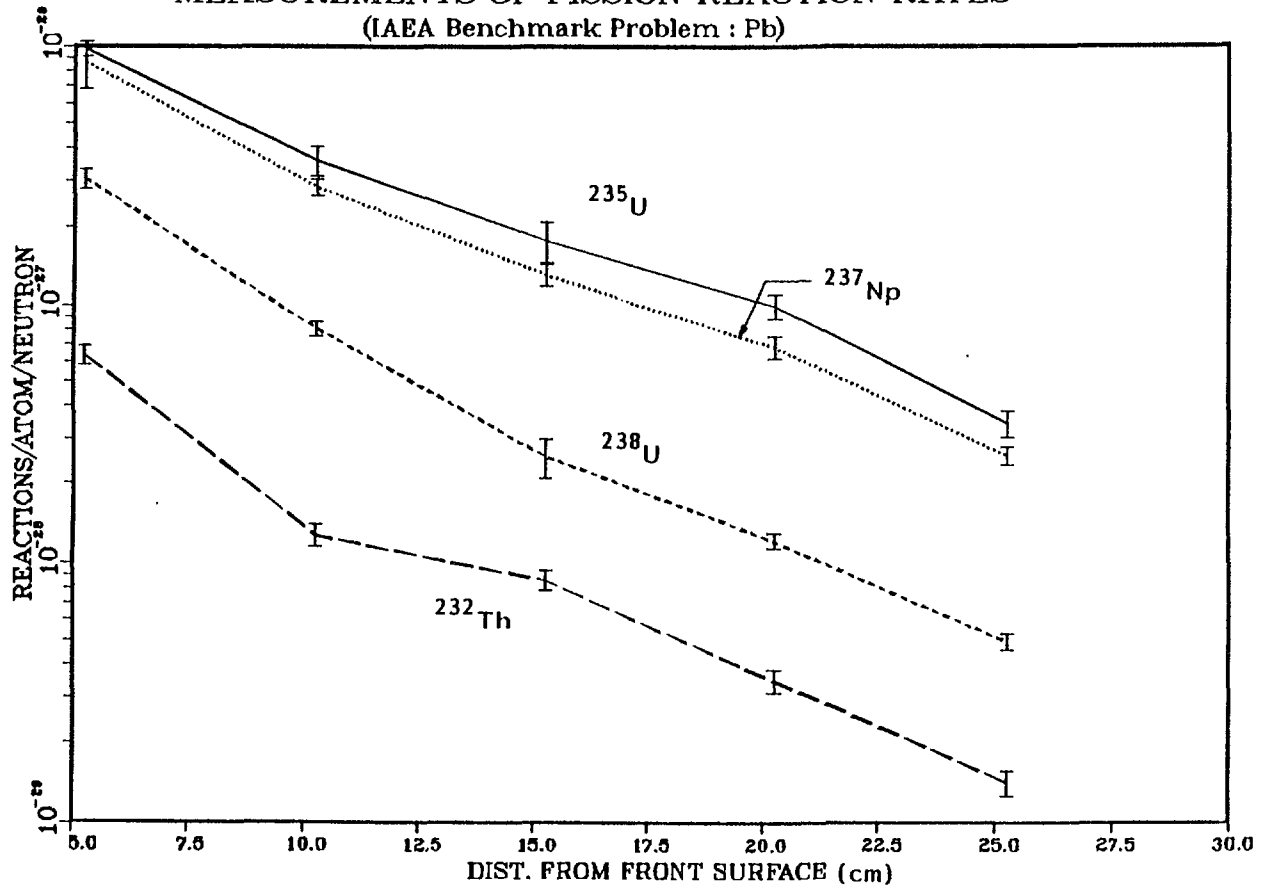
MEASUREMENTS OF ACTIVATION RATES : N,N' AND N,P
(IAEA Benchmark Problem : Pb)



MEASUREMENTS OF ACTIVATION RATES : N,A AND N,2N
(IAEA Benchmark Problem : Pb)



MEASUREMENTS OF FISSION REACTION RATES
(IAEA Benchmark Problem : Pb)



Comparison with Dresden Experiment
(Activation Rates)

| | Position (cm) | | | | |
|-----------------------------|---------------|-----------|------------|------------|------------|
| | 5 | 10 | 15 | 20 | 25 |
| $^{103}\text{Rh}(n, n')$ | 1.46(16%) | 1.56(16%) | 1.30(15%) | 1.48(16%) | 1.01(16%) |
| $^{115}\text{In}(n, n')$ | 1.74(16%) | 1.50(16%) | 1.35(16%) | 1.30(16%) | 0.939(16%) |
| $^{58}\text{Ni}(n, p)$ | 2.05(17%) | 1.58(17%) | 1.58(17%) | 1.27(17%) | 0.858(17%) |
| $^{64}\text{Zn}(n, p)$ | 1.13(17%) | 1.11(17%) | 1.10(17%) | 1.09(19%) | 0.788(17%) |
| $^{27}\text{Al}(n, \alpha)$ | 1.69(15%) | 1.25(15%) | 1.24(15%) | 1.21(19%) | 1.02(15%) |
| $^{203}\text{Tl}(n, 2n)$ | 1.39(16%) | 1.70(16%) | 2.07(16%) | 1.70(16%) | 1.31(16%) |
| $^{65}\text{Cu}(n, 2n)$ | 1.24(20%) | 1.01(20%) | 0.892(20%) | 0.834(20%) | 0.668(20%) |

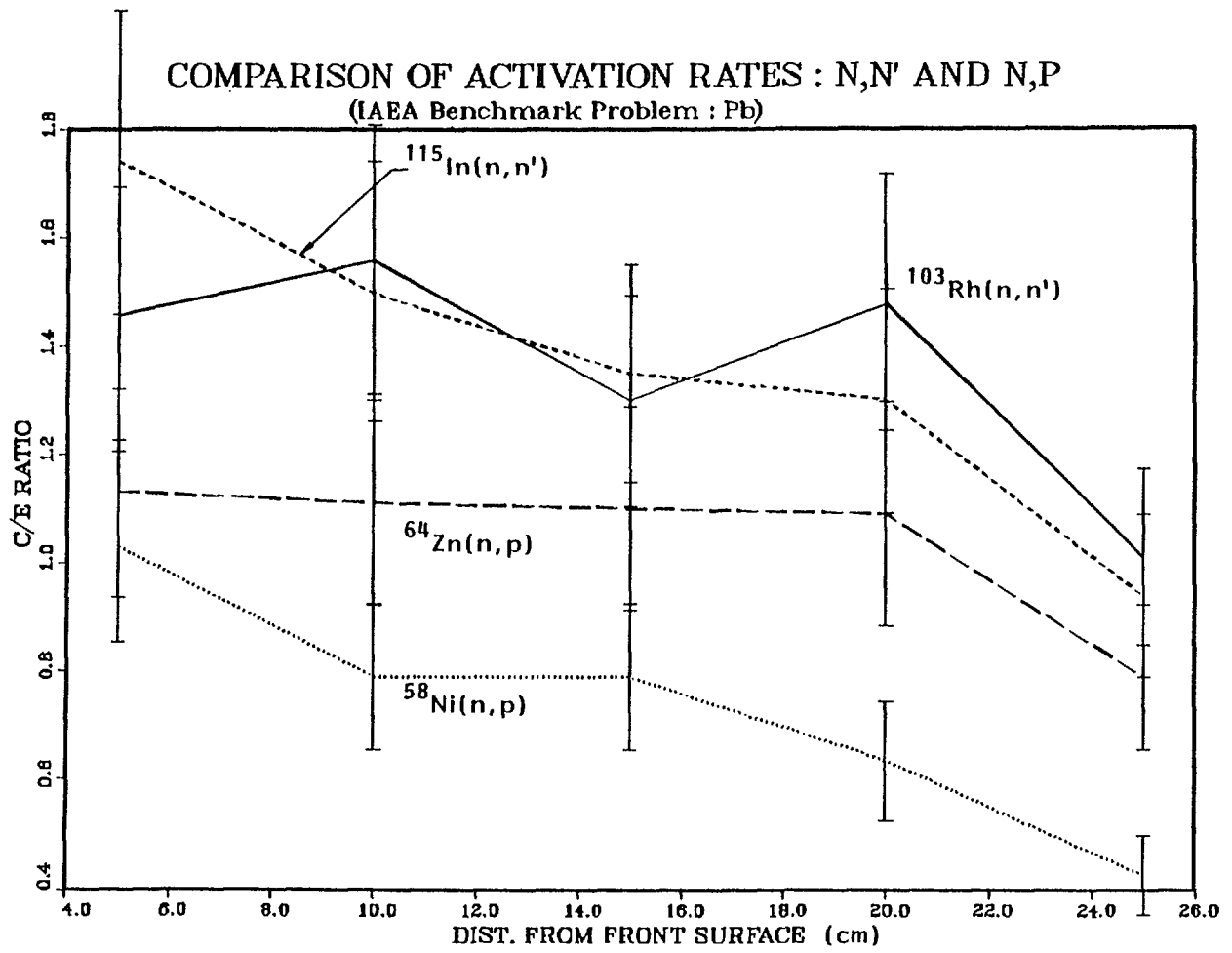
* Experimental errors are given in parentheses.

Comparison with Dresden Experiment
(Fission Rates)

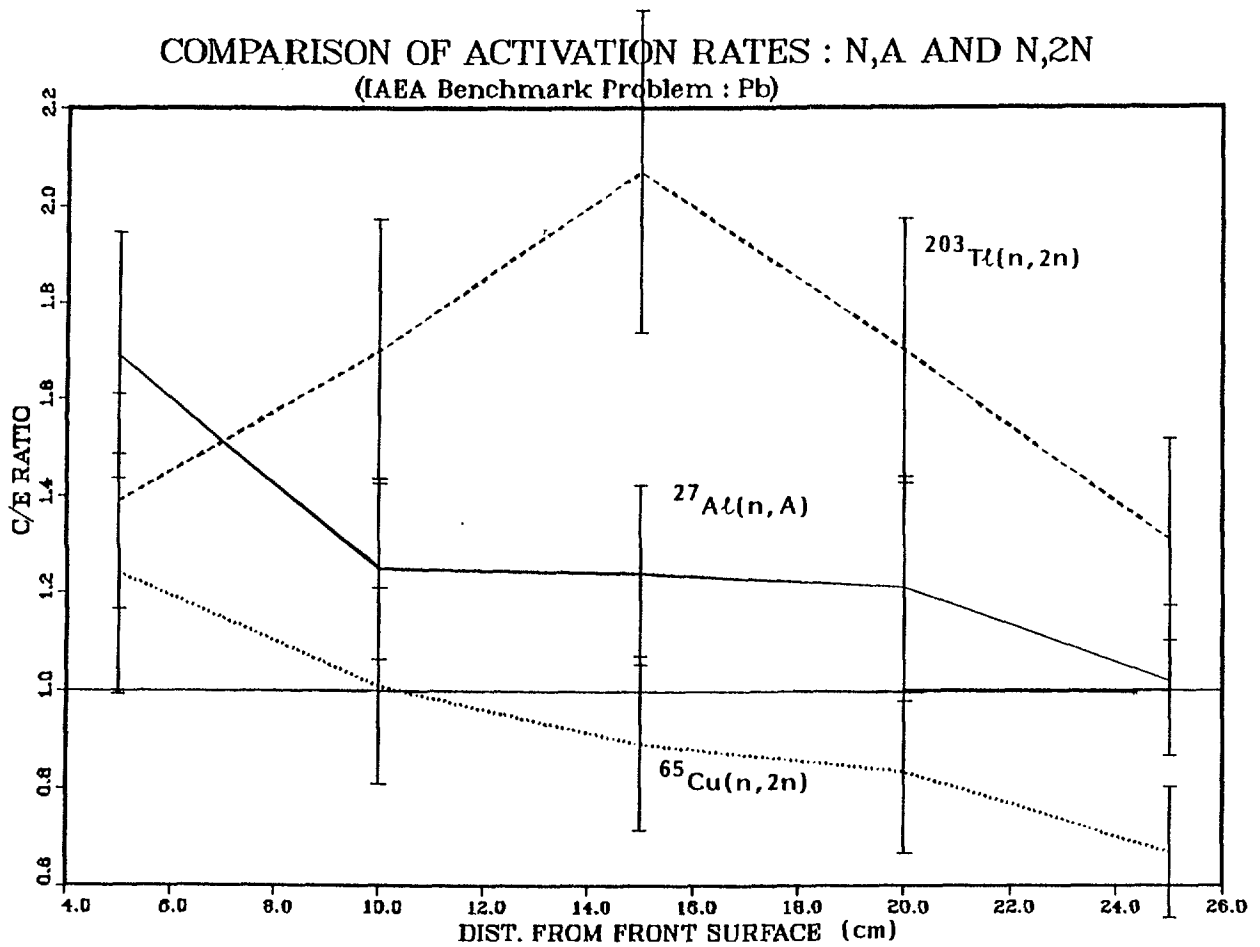
| | Position (cm) | | | | |
|-------------------|---------------|------------|------------|-------------|------------|
| | 5.25 | 10.25 | 15.25 | 20.25 | 25.25 |
| ^{235}U | 1.43(6.5%) | 1.57(13%) | 1.63(18%) | 1.41(11%) | 1.20(12%) |
| ^{238}U | 1.20(8.9%) | 1.10(6.7%) | 1.35(18%) | 1.20(6.6%) | 1.03(7.1%) |
| ^{237}Np | 1.41(21%) | 1.46(7.7%) | 1.49(9.9%) | 1.36(10.1%) | 1.20(8.2%) |
| ^{232}Th | 1.67(8.5%) | 1.93(9.4%) | 1.06(8.6%) | 1.09(10%) | 0.944(11%) |
| ^{239}Pu | | | | | 0.973(12%) |

* Experimental errors are given in parentheses.

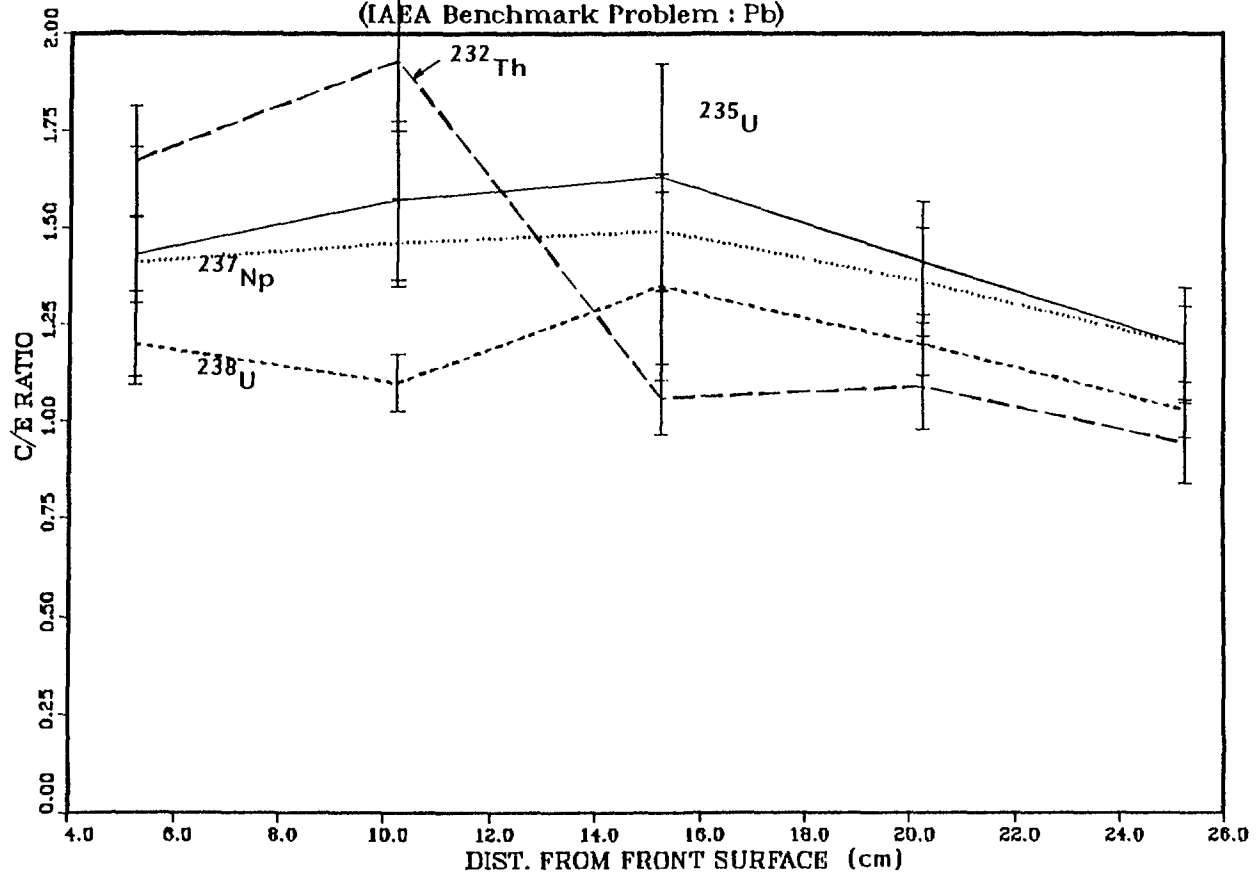
COMPARISON OF ACTIVATION RATES : N,N' AND N,P
(IAEA Benchmark Problem : Pb)



COMPARISON OF ACTIVATION RATES : N,A AND N,2N
(IAEA Benchmark Problem : Pb)



COMPARISON OF FISSION REACTION RATES (IAEA Benchmark Problem : Pb)



STATUS OF LEAD CROSS SECTIONS AND BENCHMARK CALCULATIONS SUMMARY

★ FUSION APPLICATIONS

RECENT SAFETY ANALYSIS INDICATES UNDESIRABLE FEATURES OF LEAD AS BLANKET MATERIAL FOR FUSION REACTORS

PO-210 (α EMITTER; 138 DAYS HALF-LIFE) IS PRODUCED IN LEAD

★ STATUS OF LEAD (n,2n) CROSS SECTIONS

EVALUATIONS ARE CONVERGING (ENDF/B-VI AND EFF)

MEASUREMENTS VARY BY UP TO 25% : FREHAUT(1980) - 1.95 b (7%); TAKAHASHI(1987) - 2.43 b (4.1%)

★ BENCHMARK CALCULATIONS

ENDF/B-V RESULT (1.74) IS WITHIN THE EXPERIMENTAL ERROR OF DRESDEN EXPERIMENT (1.94, 12% ERROR)

MAIN DISCREPANCY OCCURS AT ENERGIES FROM 0.5 TO 5 MeV FOR SECONDARY NEUTRONS

ENDF/B-VI WILL IMPROVE THE SPECTRUM COMPARISON BECAUSE OF MORE ANISOTROPIC IN ANGULAR DISTRIBUTION OF SECONDARY NEUTRONS

DISCREPANCIES IN COMPARISON OF DOSIMETRY AND FISSION RATES NEED TO BE RESOLVED

Analytical Results on IAEA Benchmark Problem
Based on TUD Pb Sphere Experiment

Hiroshi MAEKAWA Kazuaki KOSAKO
Tomoo SUZUKI Akira HASEGAWA
Japan Atomic Energy Research Institute

Case I ANISN

Transport Code : ANISN-JR

Cross Section Set :

Number of group : 125
Weight function : 1/E except thermal
Maxwell for thermal
Process code : MACS-N system

Nuclear Data Library : JENDL-3T
ENDF/B-IV
EFF

*Nuclear data of ENDF/B-IV were used for
H, N, O, Cu in all calculation.

Conditions of Transport Calculation :

Geometry : 1D Sphere
Legendre order : P-5
Angular quadrature : S-16
Source : Isotropic distribution
13.5 - 14.92 MeV
uniform distribution
normalized to unity (1.0)

Used Resource :

Computer : FACOM M-760
CPU time : 1'20"
I/O times : 3700

Neutron Multiplication

| Energy | | ENDF/B-IV | EFF | JENDL-3T | Expr. |
|---------|---------|-----------|----------|----------|--------|
| 1 - 5 | A | 0.512 | 0.571 | 0.662 | 0.676 |
| | (C/E) A | (0.757) | (0.845) | (0.979) | |
| (C/E) B | B | | 0.667 | 0.687 | 0.676 |
| | (C/E) B | | (0.987) | (1.016) | |
| 5 - 10 | A | 0.0198 | 0.0253 | 0.0243 | 0.0190 |
| | (C/E) A | (1.042) | (1.332) | (1.279) | |
| (C/E) B | B | | 0.0208 | 0.0224 | 0.0190 |
| | (C/E) B | | (1.0947) | (1.179) | |
| 10 - 15 | A | 0.129 | 0.129 | 0.128 | 0.144 |
| | (C/E) A | (0.896) | (0.896) | (0.889) | |
| (C/E) B | B | | 0.110 | 0.108 | 0.144 |
| | (C/E) B | | (0.764) | (0.750) | |
| Total | A | 1.858 | 1.804 | 1.766 | 1.944 |
| | (C/E) A | (0.956) | (0.928) | (0.908) | |
| (C/E) B | B | | 1.822 | 1.788 | 1.944 |
| | (C/E) B | | (0.937) | (0.920) | |

A : ANISN B : BERMUDA

Observation

Leakage Spectrum

- 1) Calculated spectra based on EFF & ENDF/B-IV agreed fairly well with measured one.
- 2) All calculated results underestimate the spectrum around 1 MeV.
- 3) The leakage spectrum calculated by BERMUDA agrees well with that by ANISN except 5 - 10 MeV.

Neutron Multiplication

- 1) All calculations underestimate the neutron multiplication factor by 4-9 %.
- 2) The measured results of neutron multiplication seem to be a little inconsistent with those of reactor rates.

Reaction Rates & Fission Rates

- 1) Most of C/E values within 10 cm are over 1.2.
Effect of target assembly ?
Neutron yield monitor ?
- 2) In the case of ANISN, C/E values decrease with the distance from the target.
- 3) C/E curves of BERMUDA are rather flat comparing with those of ANISN.

Case I I BERMUDA

Transport Code : BERMUDA-1DN
1D, Sphere

Cross Section Set :
Number of group : 125 (Structure is same as library for ANISN.)

Nuclear Data Library : JENDL-3T/R0
EFF

Common data : H(B-V), O(J-3PR2),
N(B=IV), Cu(B-IV)

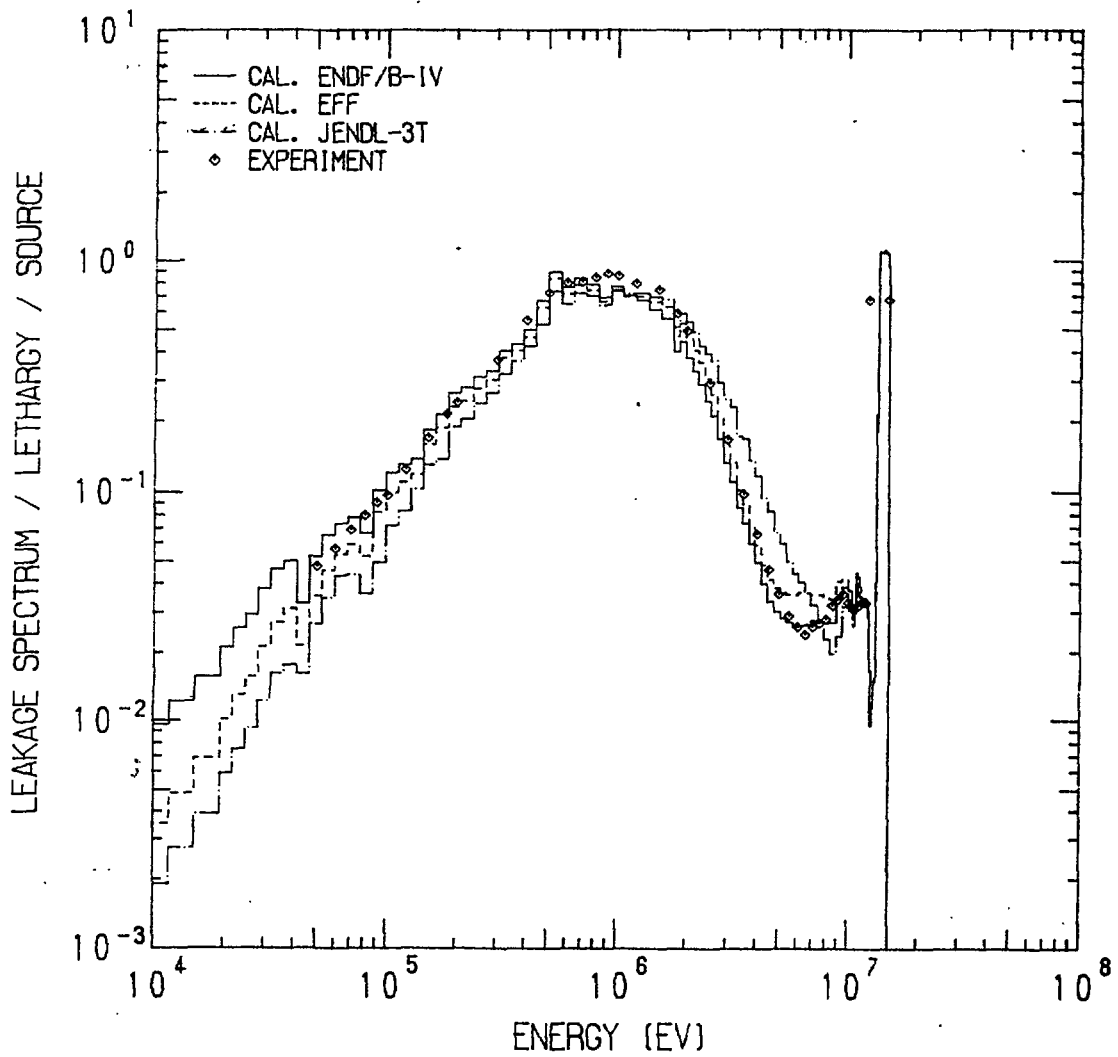
Source : Isotropic volume source
13.5 - 14.92 MeV
uniform distribution in lethargy
normalized to unity (1.0)

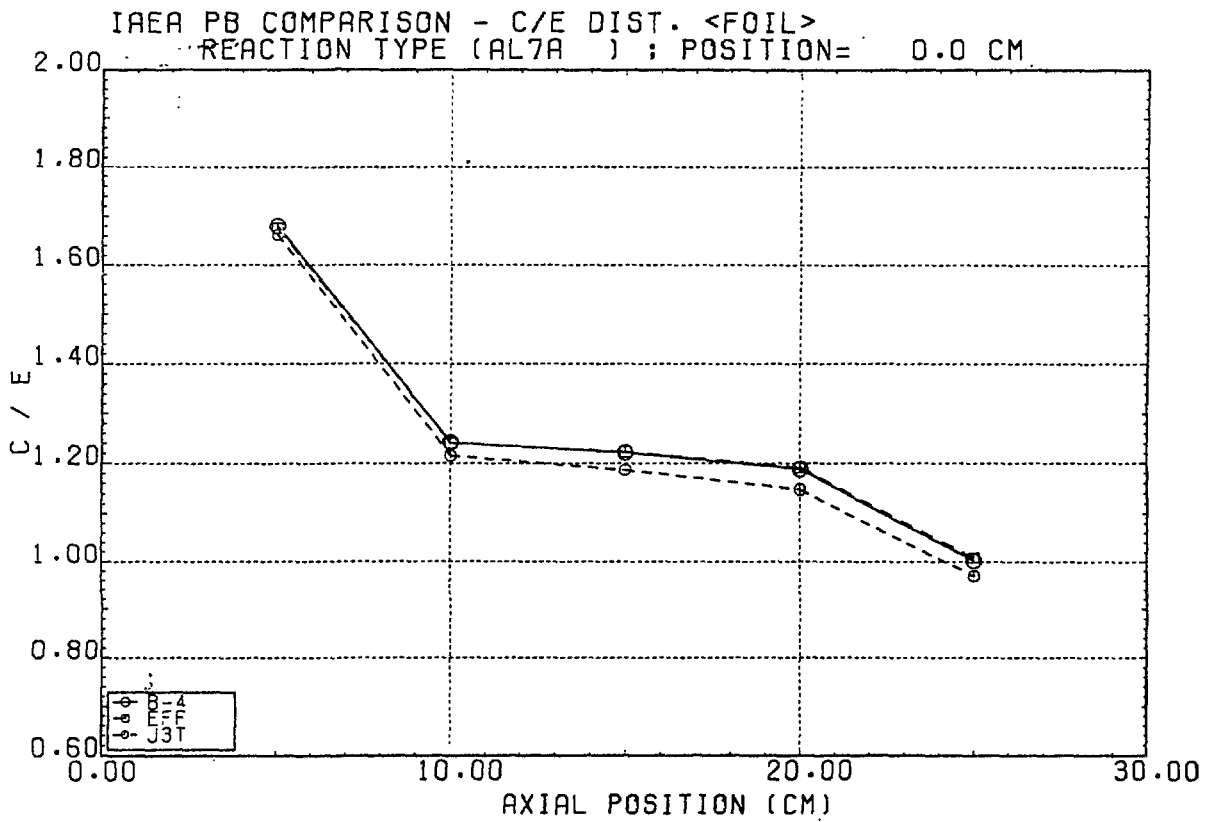
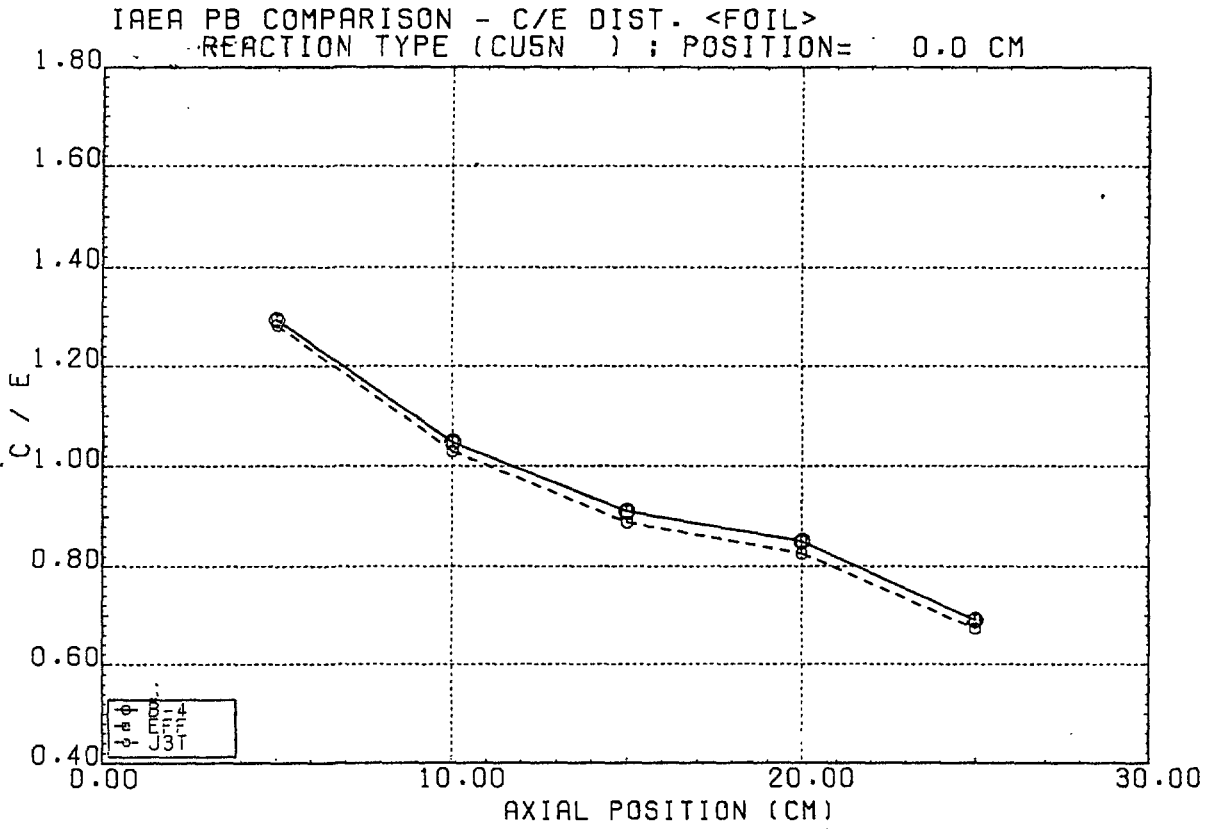
Used Resource :
Computer : FACOM VP-100 (Vector Machine)
CPU time : 1'50"
I/O times : 881

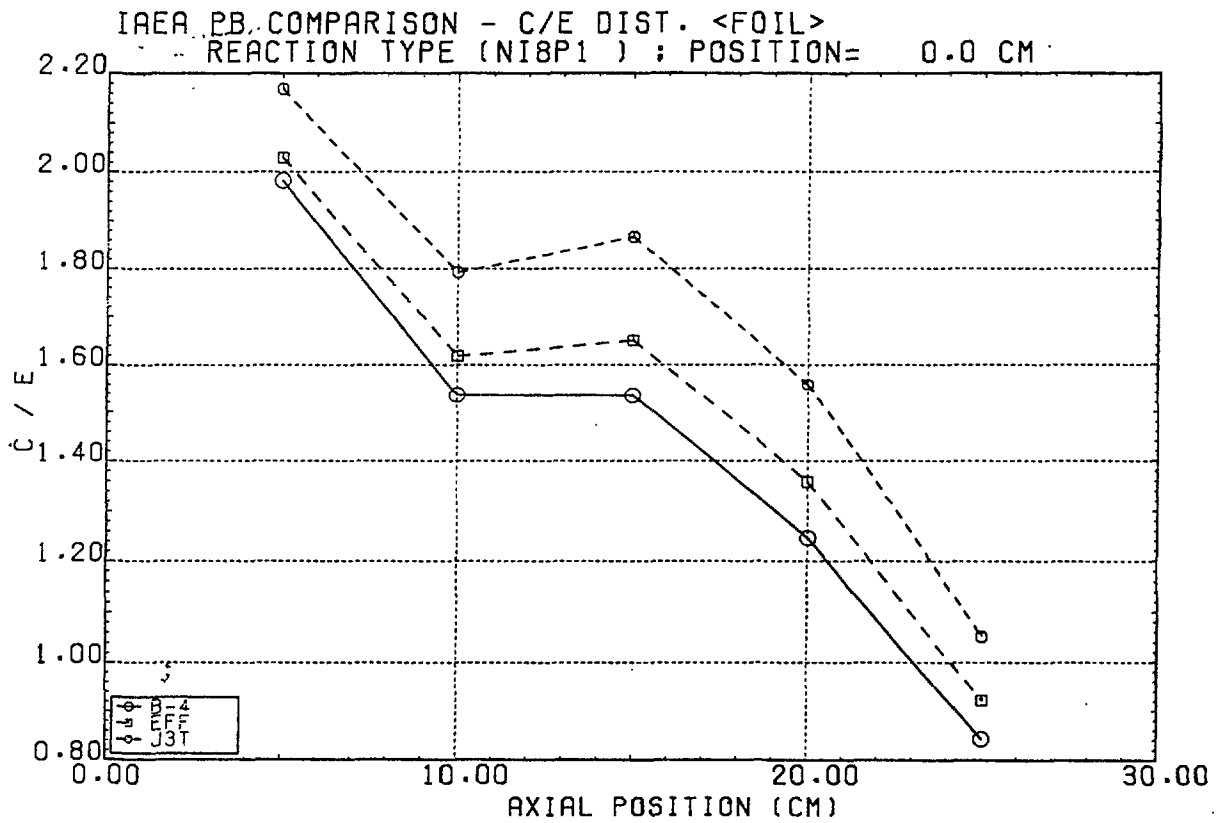
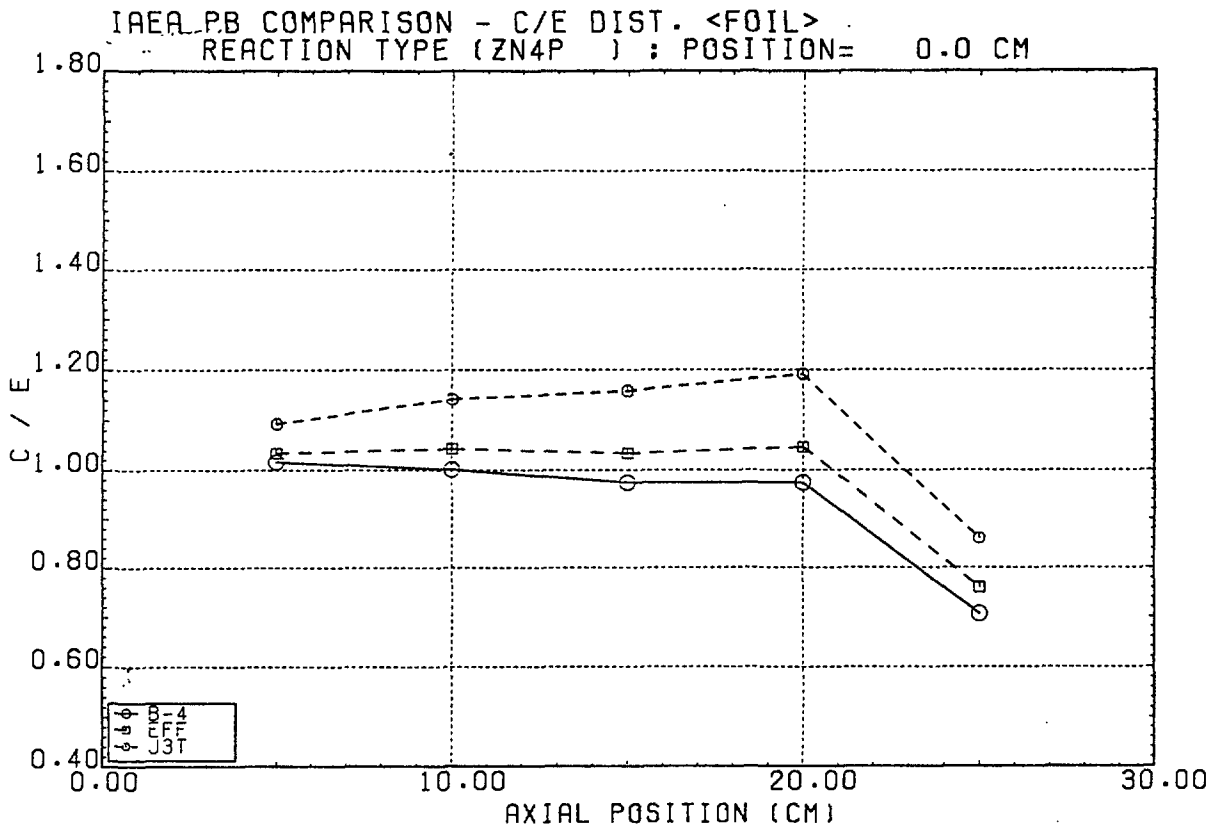
| Number of Mesh | | Radius | Region |
|----------------|-------|--------|-----------------|
| BERMUDA | ANISN | (cm) | |
| (2) | (5) | 0.0 | Source |
| (8) | (10) | 0.5 | |
| | (20) | 2.5 | Target Assembly |
| (40) | (44) | 7.5 | |
| | | 25.0 | Pb (Lead) |
| | (3) | 28.0 | |
| (40) | (25) | 498.0 | Air |
| | (2) | 500.0 | |
| (90) | (109) | | |

Calculational Model

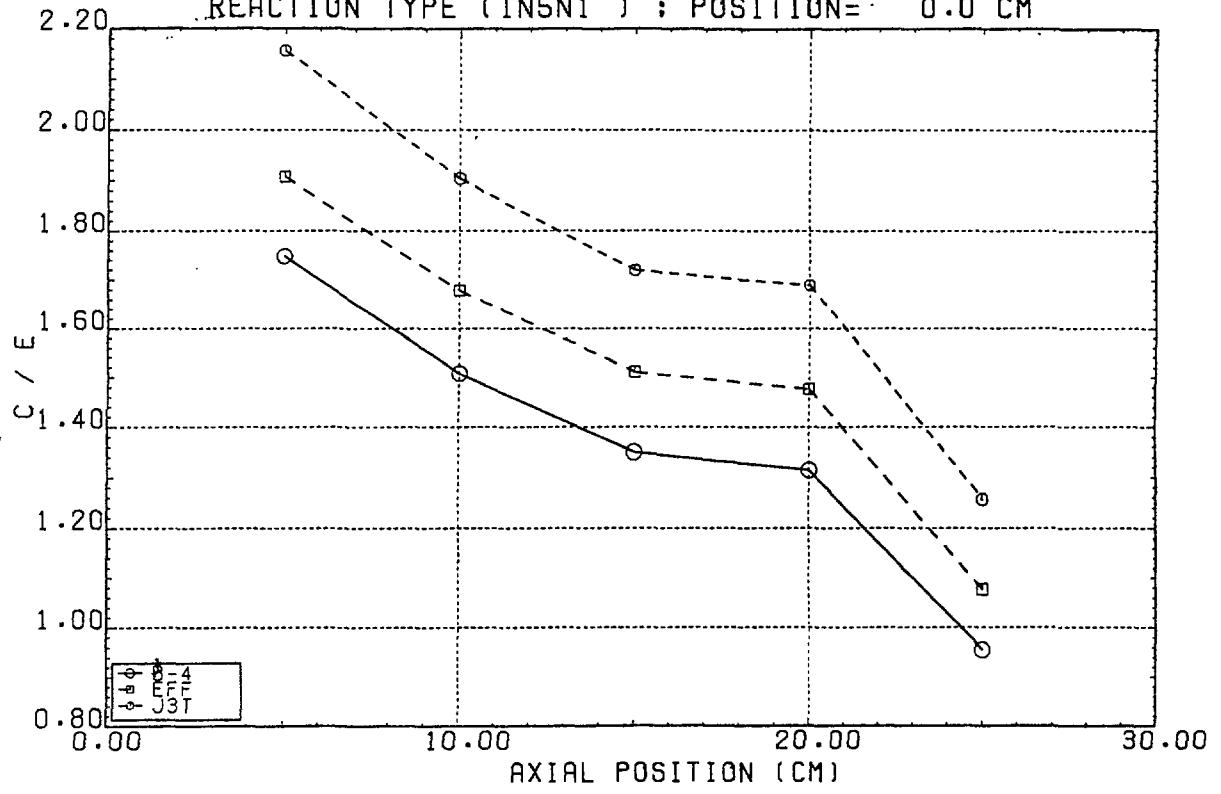
PB SPHERE LEAKAGE SPECTRUM







IAEA PB COMPARISON - C/E DIST. <FOIL>
REACTION TYPE (IN5N1) ; POSITION= 0.0 CM



Preliminary Result of Time-of-Flight Experiment
on Lead Slabs

Hiroshi MAEKAWA, Yukio OYAMA and Seiya YAMAGUCHI

Japan Atomic Energy Research Institute

Background

- *Pb is a promising candidate as neutron multiplier.
- * $\text{Li}_{17}\text{Pb}_{83}$ is one of hopeful blanket breeder material.
- *Measured neutron multiplication factors are deviated each other.
- *IAEA benchmark problem
TUD Pb sphere experiment
- *Systematic measurements of angular neutron flux spectra at FNS/JAERI
Li, Li_2O , C, Be

Purpose

- *To provide benchmark data.
- *To check nuclear data of Pb.
- *Integral evaluation of JENDL-3T.

Experiment

Assembly : Pb cylindrical slab
Material : Pb block (purity : 99.998 %)
Radius : 315 mm
Thickness : 50.6, 203, 205 mm
Angle : 0°, 12.2°, 24.9°, 41.8°, 66.8°

Condition of Accelerator

Pulse width : 2 ns
Period : 4 μ s
Peak current : 30 mA
Beam energy : 350 kV

Analysis

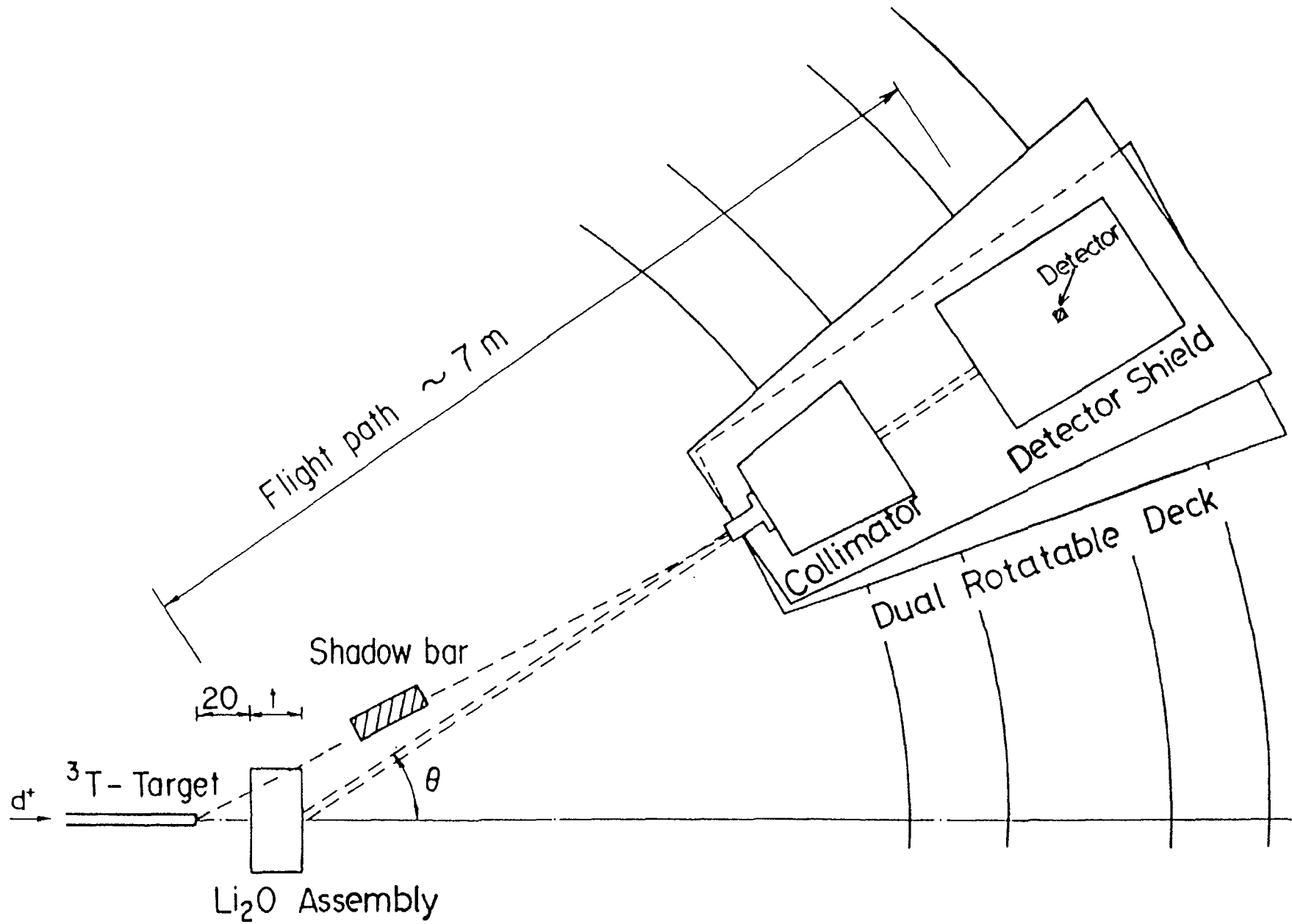
Transport code : DOT3.5
with first collision source
calculated by GRTUNCL
Approximation : P₅-S₁₆
Number of group : 125
Nuclear data : JENDL-3T/RO
ENDF/B-IV
EFF

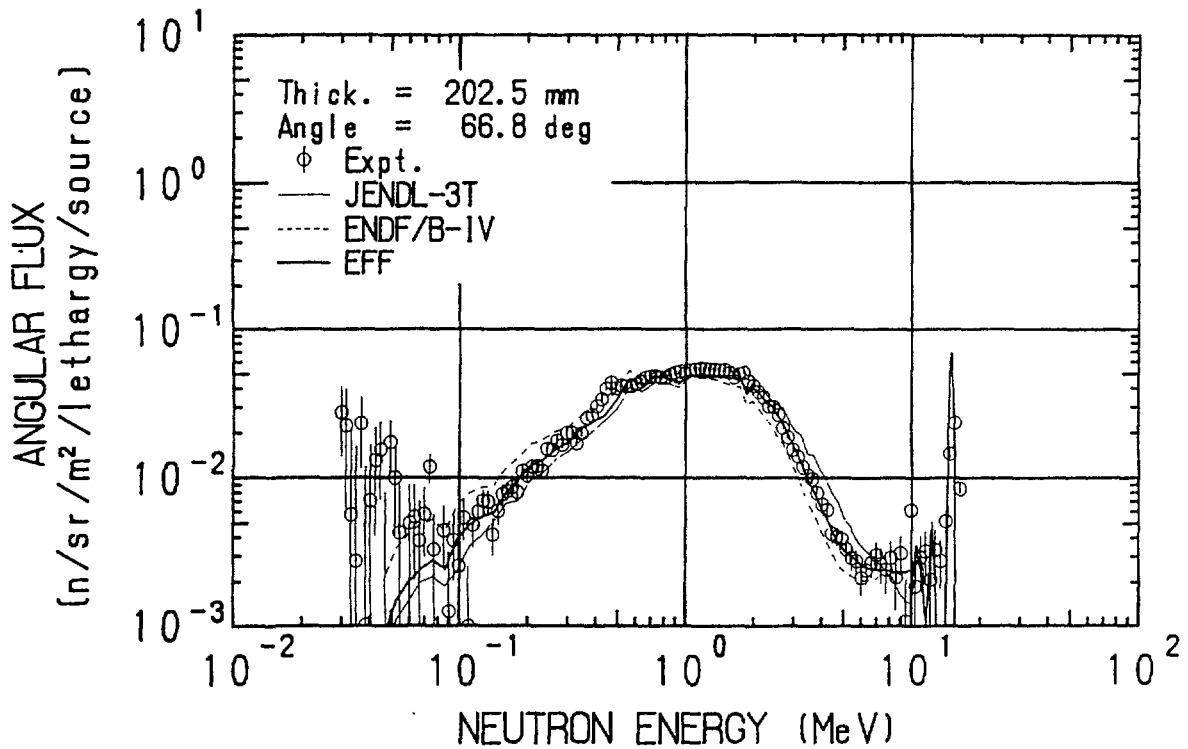
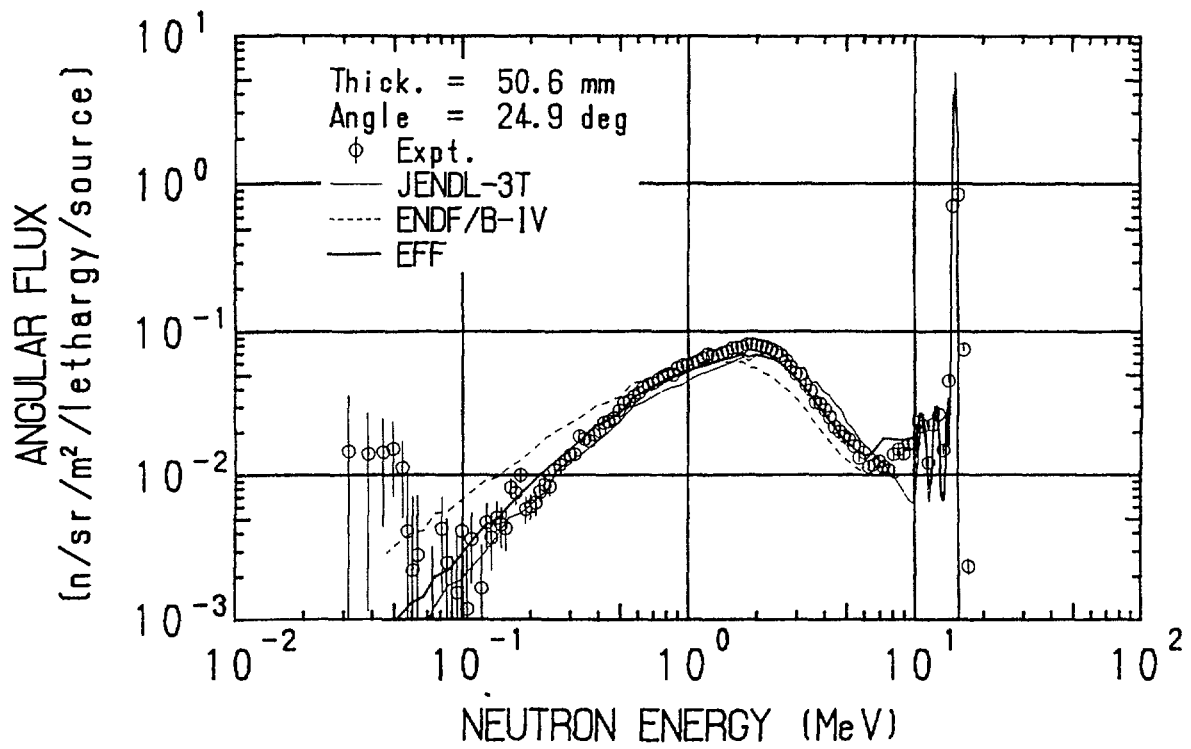
Summary

- 1) Angular neutron flux spectra from Pb slabs have been obtained as benchmark data for integral test.
- 2) Calculated spectra based on EFF agree well with measured ones as the whole.
overestimation at low angle and 4 - 12 MeV
underestimation at 2 - 4 MeV
- 3) Calculated spectra based on JENDL-3T/RO agree fairly well with measured ones as the whole.
overestimation at 2 - 4 MeV
underestimation at below 1 MeV
- 4) Following modifications are desirable for the nuclear data of Pb in JENDL-3T/RO ;
cross section of (n,2n) :
a little increase
DDX, especially energy distribution :
minor change

Future Work

- 1) To examine the deviation between experiment and calculation at the elastic scattering region.
* To be analyzed by,
Monte Carlo code (MCNP, MORSE-DD)
DDX code (BERMUDA, DOT-DD)
- 2) To perform the integral test of JENDL-3.





d. Neutron source

(i)Energy distribution

| No. | Energy(MeV) | $\phi(E)dE$ |
|-----|---------------|-------------|
| 1 | 16.487-16.231 | 1.000E-9 |
| 2 | 16.231-15.980 | 0.0 |
| 3 | 15.980-15.732 | 0.0 |
| 4 | 15.732-15.488 | 0.0 |
| 5 | 15.488-15.248 | 0.0 |
| 6 | 15.248-15.012 | 0.0 |
| 7 | 15.012-14.779 | 9.930E-2 |
| 8 | 14.779-14.550 | 1.613E-1 |
| 9 | 14.550-14.324 | 1.592E-1 |
| 10 | 14.324-14.102 | 1.563E-1 |
| 11 | 14.102-13.883 | 1.542E-1 |
| 12 | 13.883-13.668 | 1.514E-1 |
| 13 | 13.668-13.456 | 1.183E-1 |
| 14 | 13.456-13.248 | 0.0 |

(ii) Position the first radial interval (R_1)

(iii) Isoropy (case I): Isotropic volume source ($S(R_1, E)$)

(case II): Shell source ($S(R_1, S_{17}, E)$)

2. Results and Comparision with TUD Experimental Data

(1) Partial and total neutron multiplications (Fig. 1)

⇒ C/E values of partial and total neutron multiplications.

Calculations were done with three evaluated nuclear data files of ENDF/B- IV, EFF and JENDL-3I(R)

(2) Neutron leakage spectra from the TUD lead sphere. (Fig. 2, 3 and 4)

⇒ The measured spectrum is compared with the calculated one with

ENDF/B-IV in Fig. 2, EFF in Fig. 3 and FENDL-3I(R) in Fig. 4, respectively.

(3) Activation rates (Fig. 5 to 8)

⇒ Figure 5 shows the excitation functions for $^{27}\text{Al}(n, \alpha)$, $^{58}\text{Ni}(n, p)$ and $^{115}\text{In}(n, n')$. The activation rates were calculated for the three reactions using ENDF/B-IV, EFF and FENDL-3T. Only three kinds of reactions were adopted but they were enough to investigate the tendency of C/E values for the activation rates in the TUD lead sphere. Because $^{27}\text{Al}(n, \alpha)$ reaction covers the high energy region over 6 MeV as shown in Fig. 5 and $^{58}\text{Ni}(n, p)$ reaction covers between 2 to 10 MeV. $^{115}\text{In}(n, n')$ reaction covers the lower energy region than those of $^{58}\text{Ni}(n, p)$. 500 KeV was almost the measurable lowest energy in the leakage spectrum, so that the activation rates, which are sensitive to the neutron energy more than 500 KeV, are applicable to check the consistency between the C/E values for the leakage spectrum and the activation rates.

⇒ Figures 6, 7 and 8 show the C/E values of activation rates.

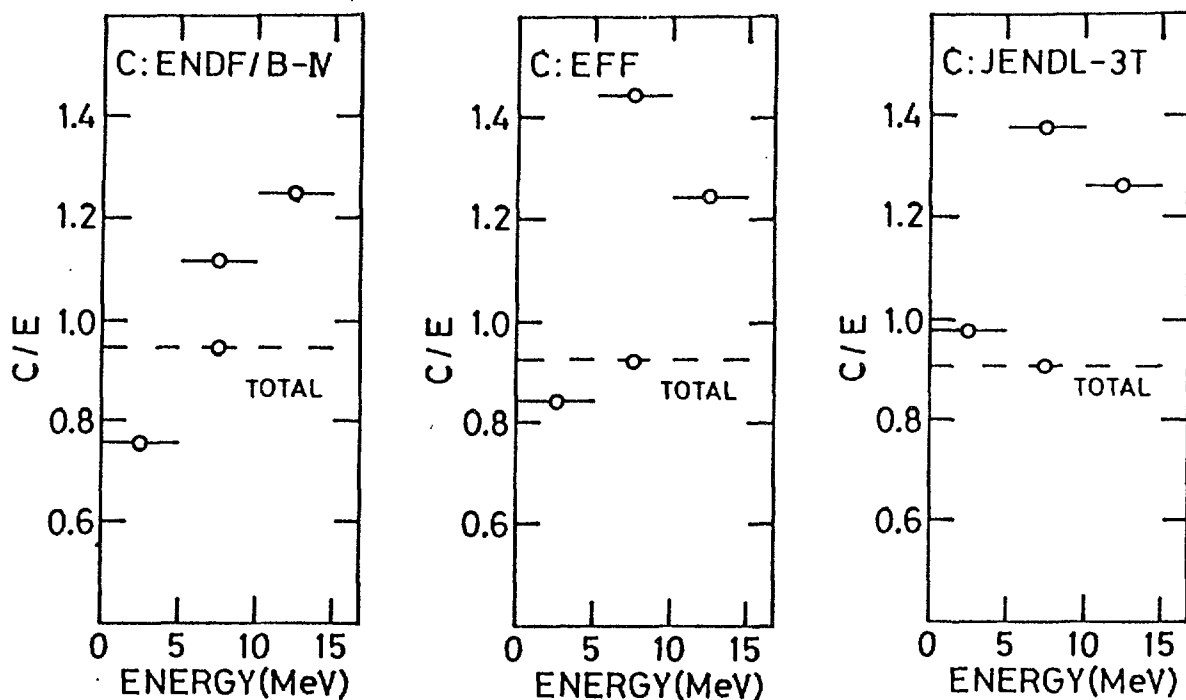
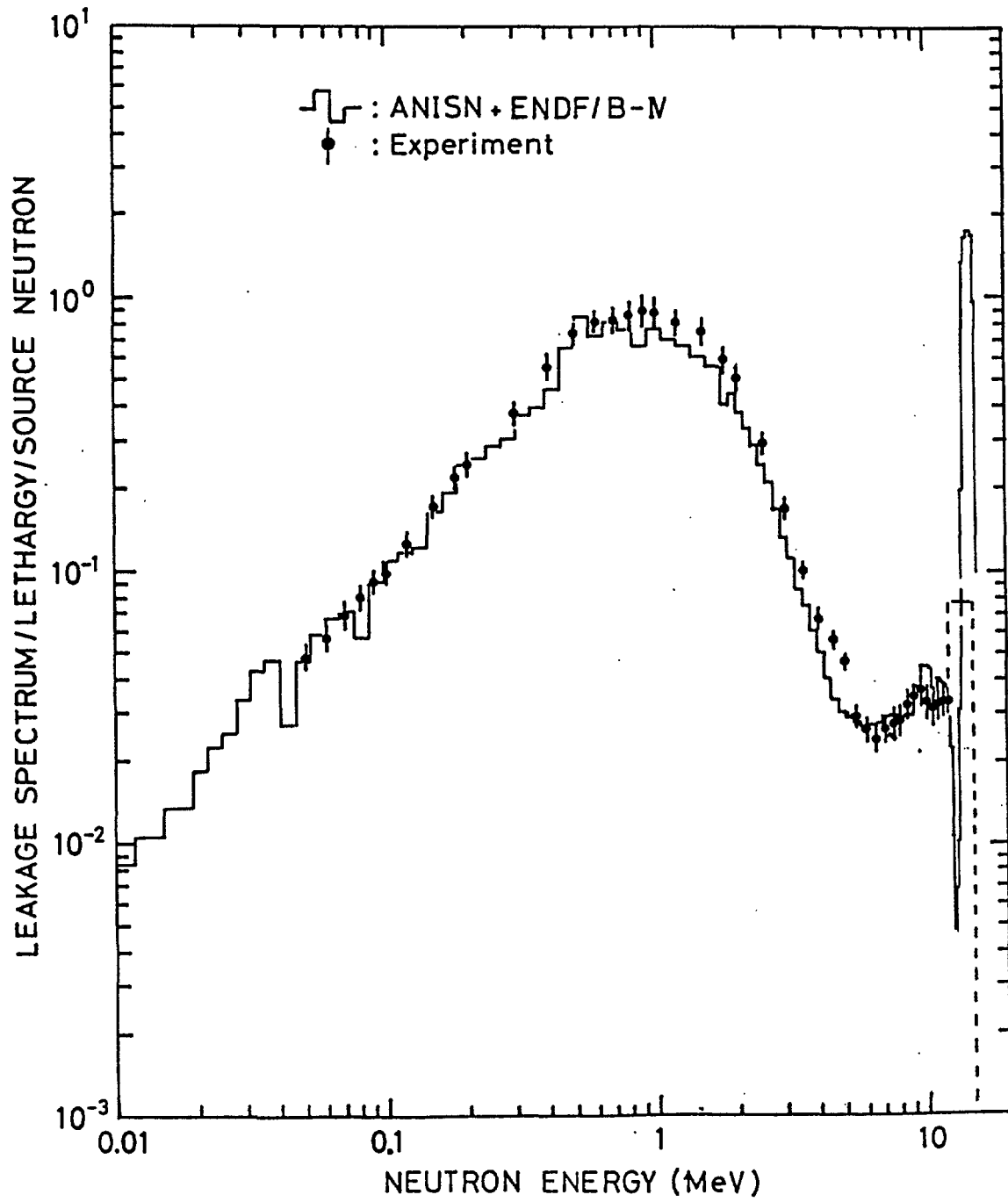
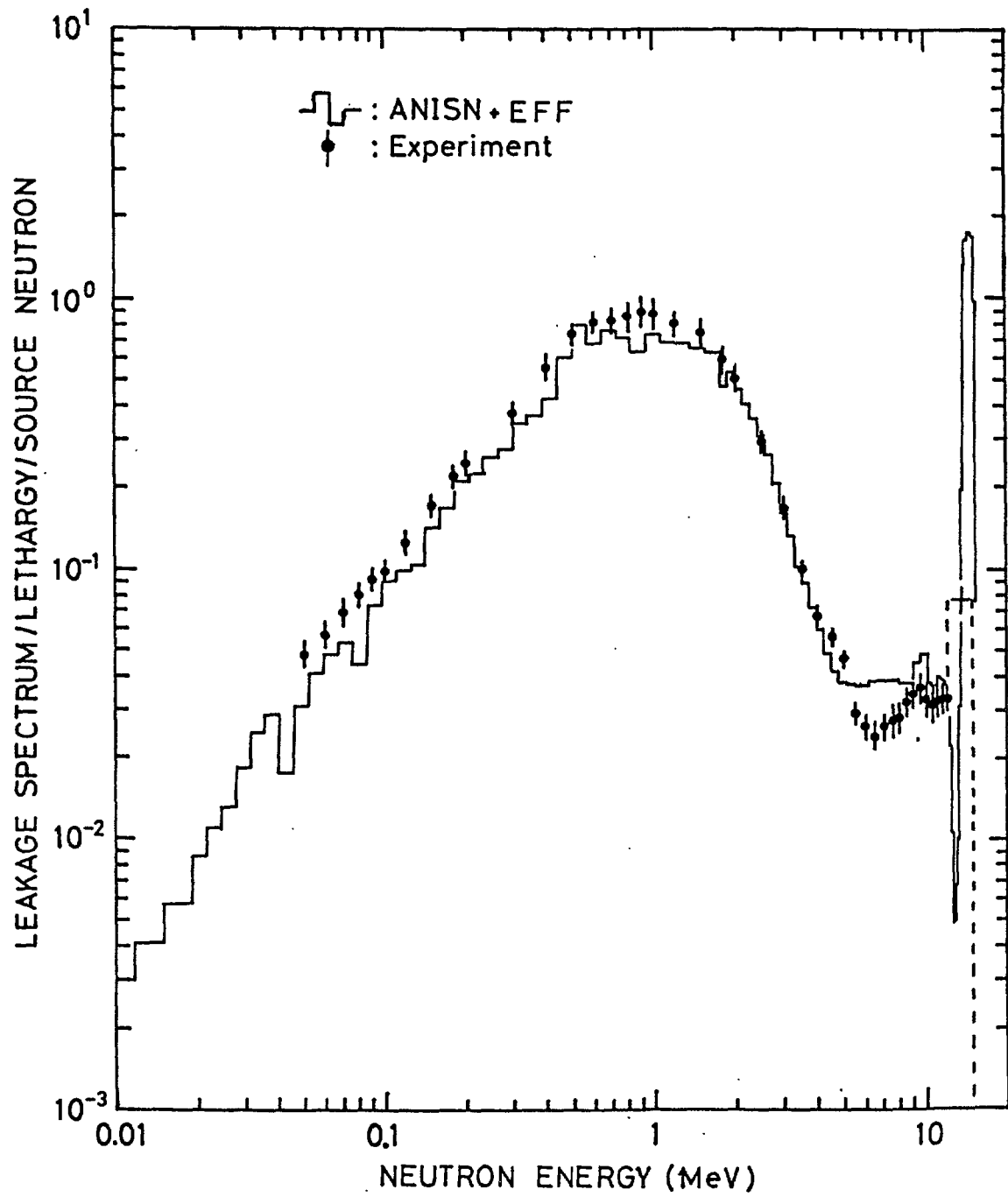


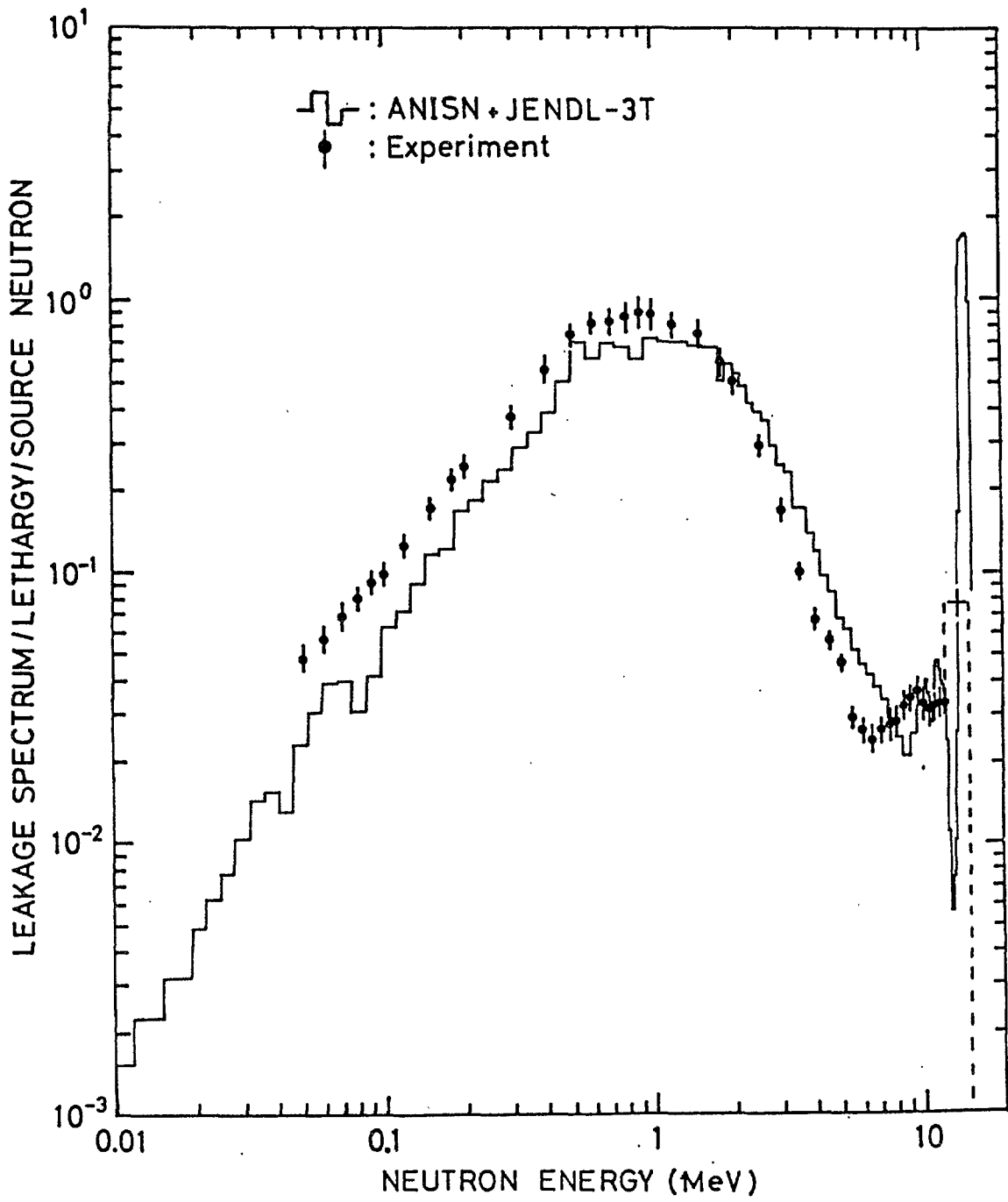
Fig. 1



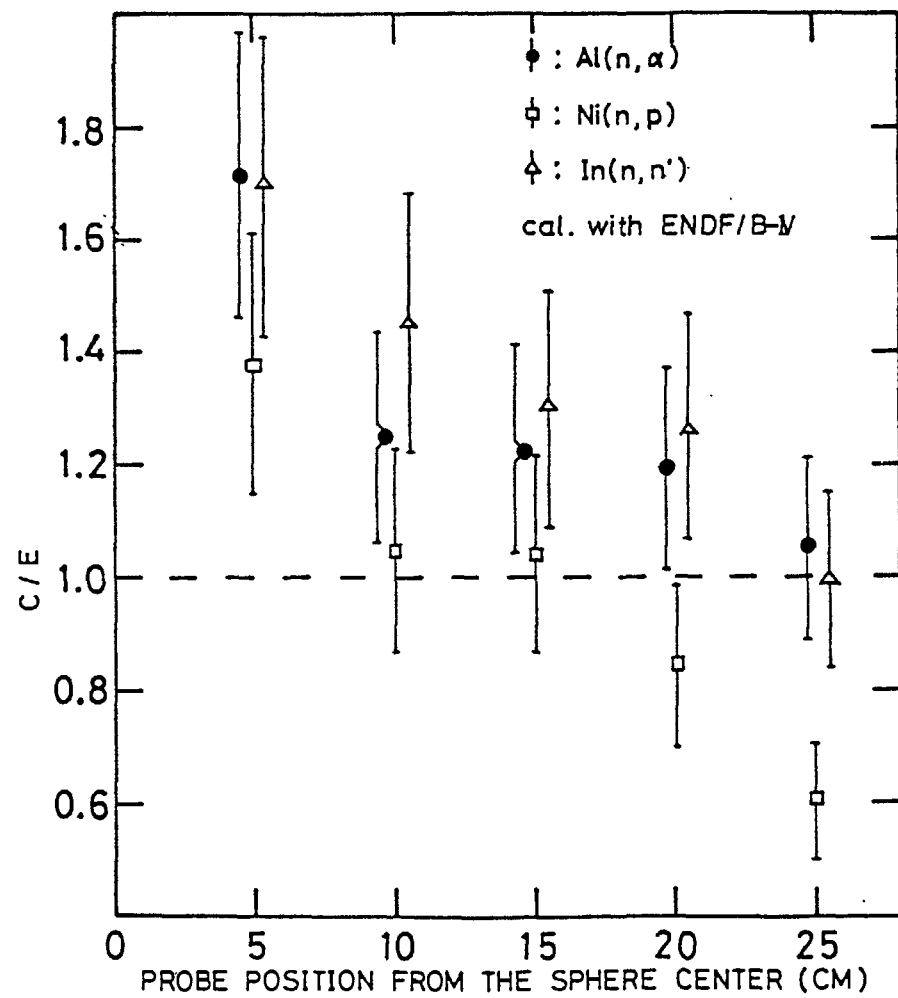
F i g . 2



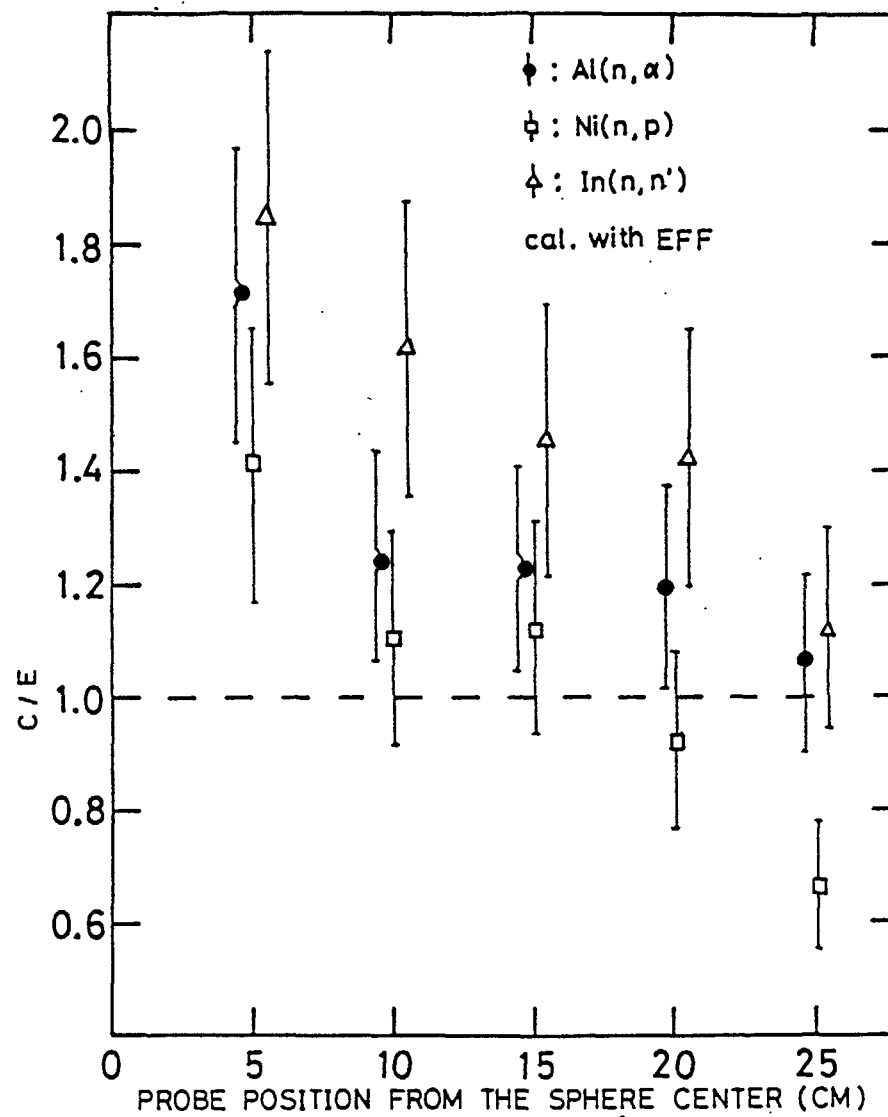
F i g . 3



F i g . 4



F i g . 6



F i g . 7

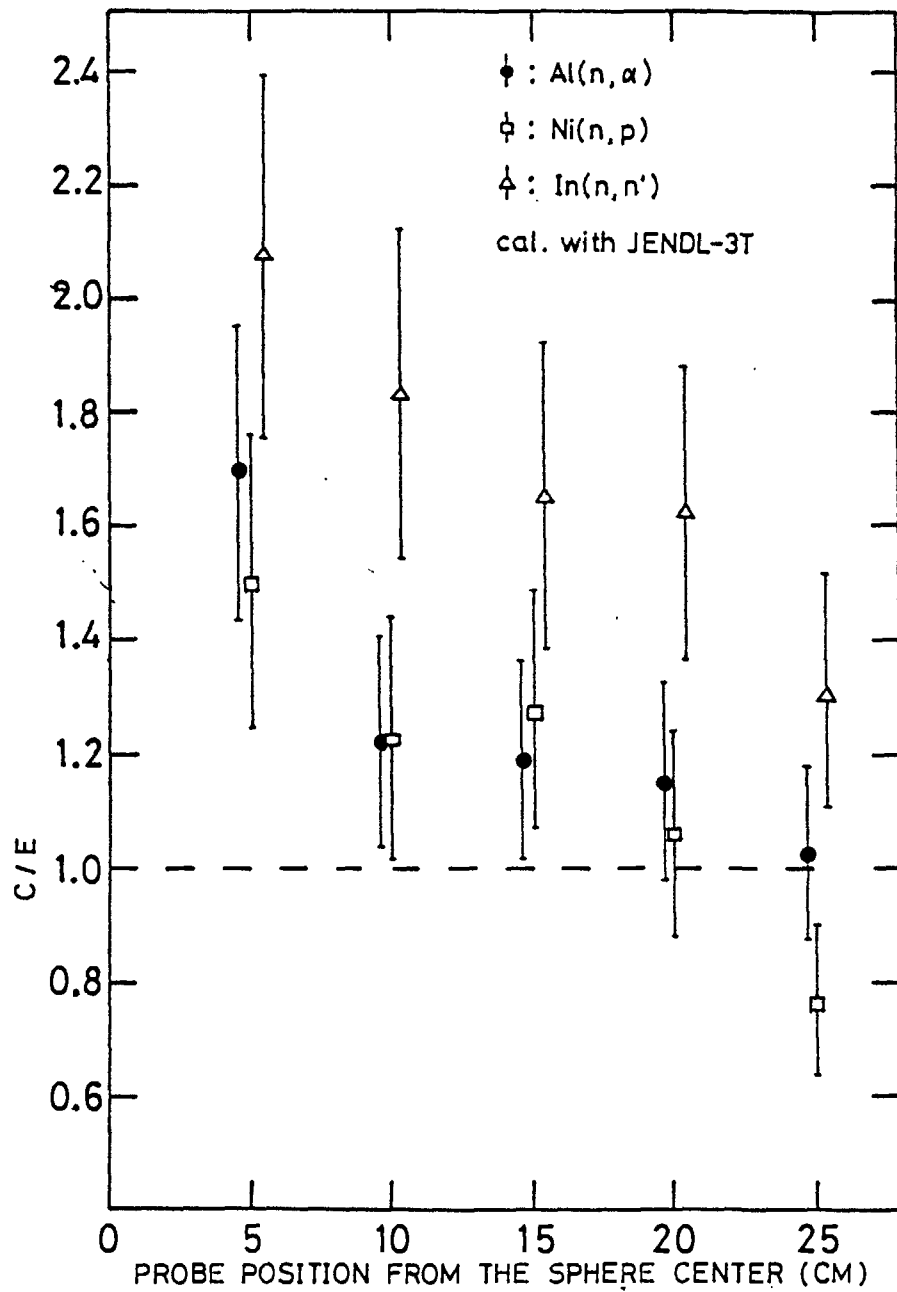


Fig. 8

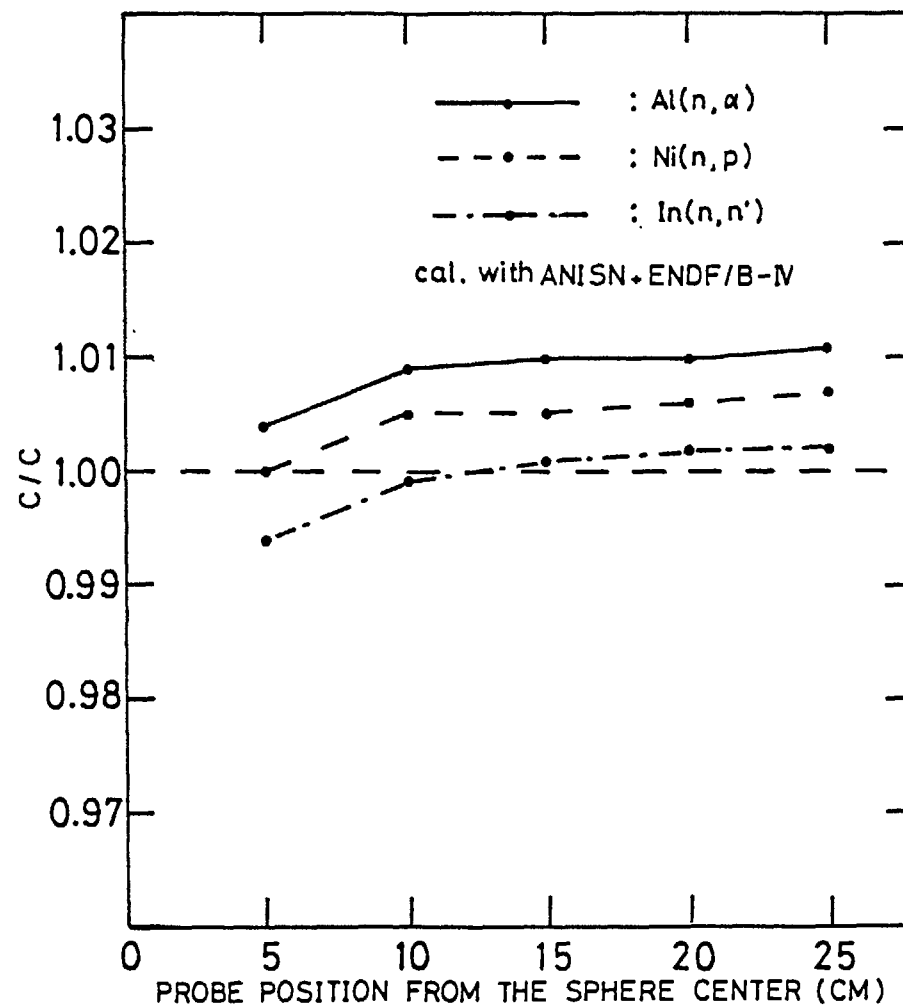
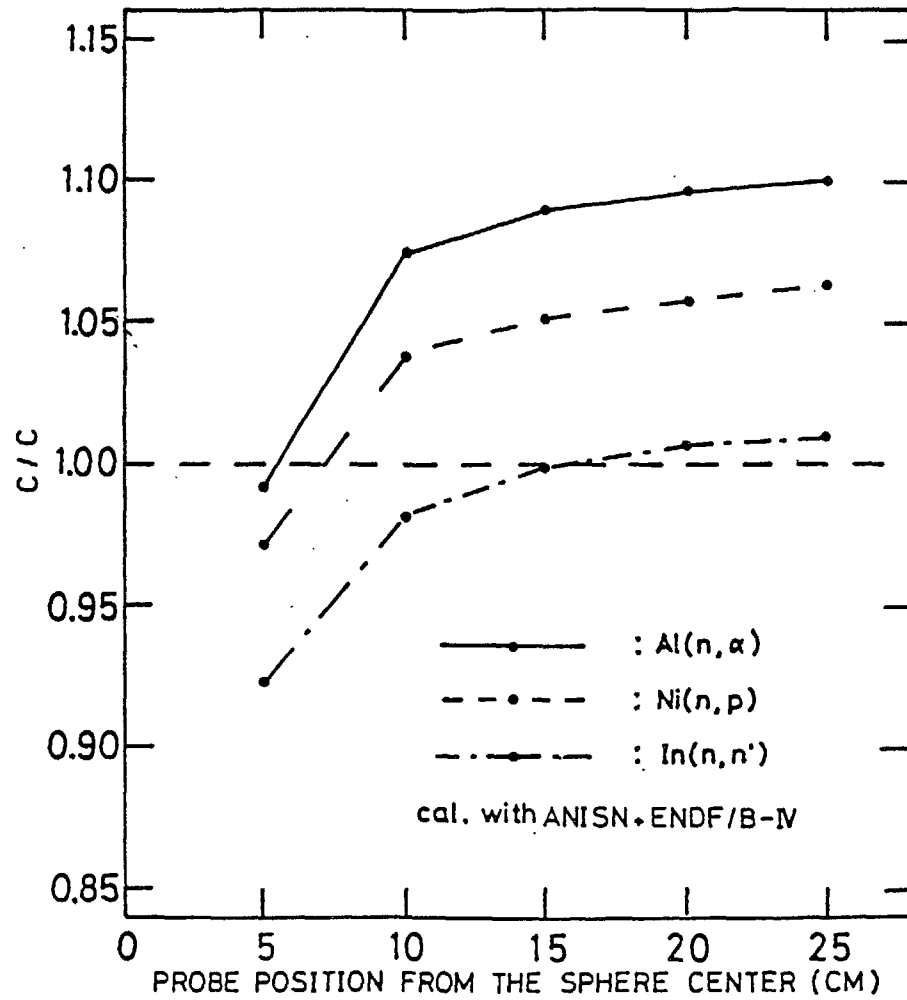
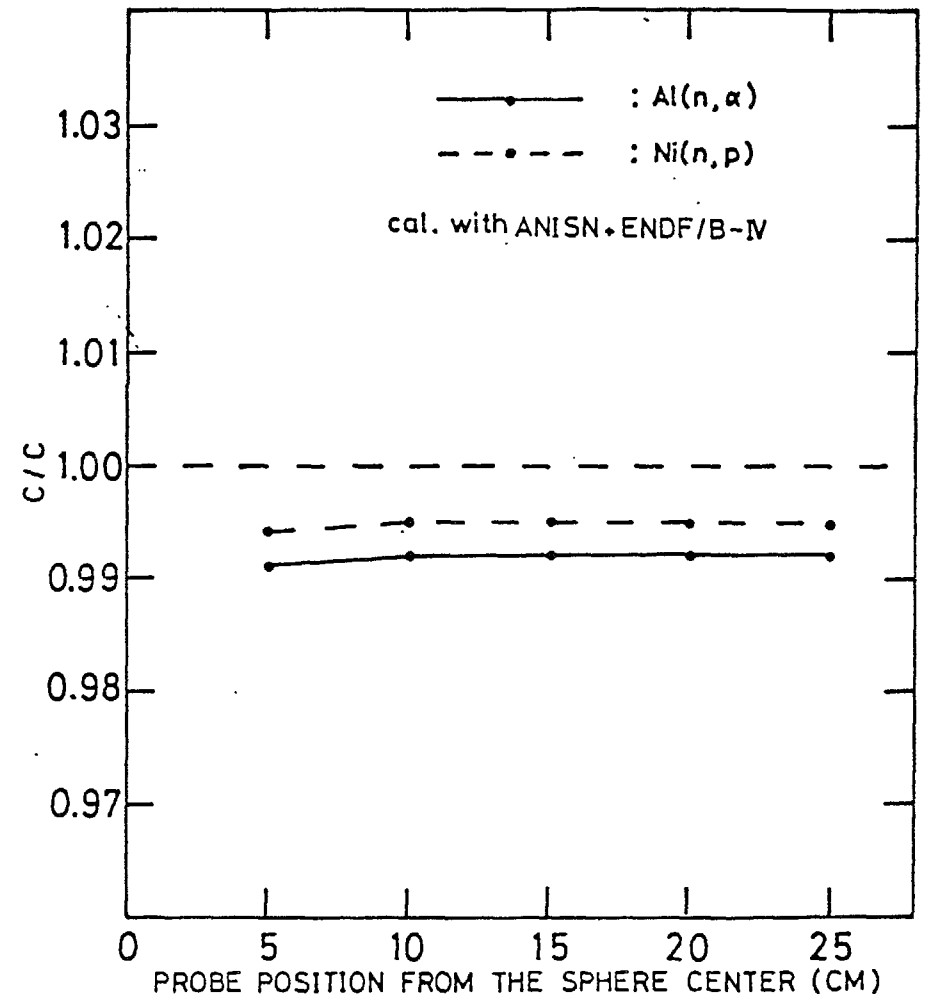


Fig. 9



F i g . 1 0



F i g . 1 1

Lead Sphere Benchmark Calculations

U. Fischer, A. Schwenk-Ferrero,
E. Wiegner

kfk, Karlsruhe, Federal Republic of Germany

Objective: Check of methods and data

Procedures: Id Sn-procedure

- conventional Pe-approximation
(ONETRAN)
- rigorous method using angle-dependent scattering
matrices (ANTRAL)

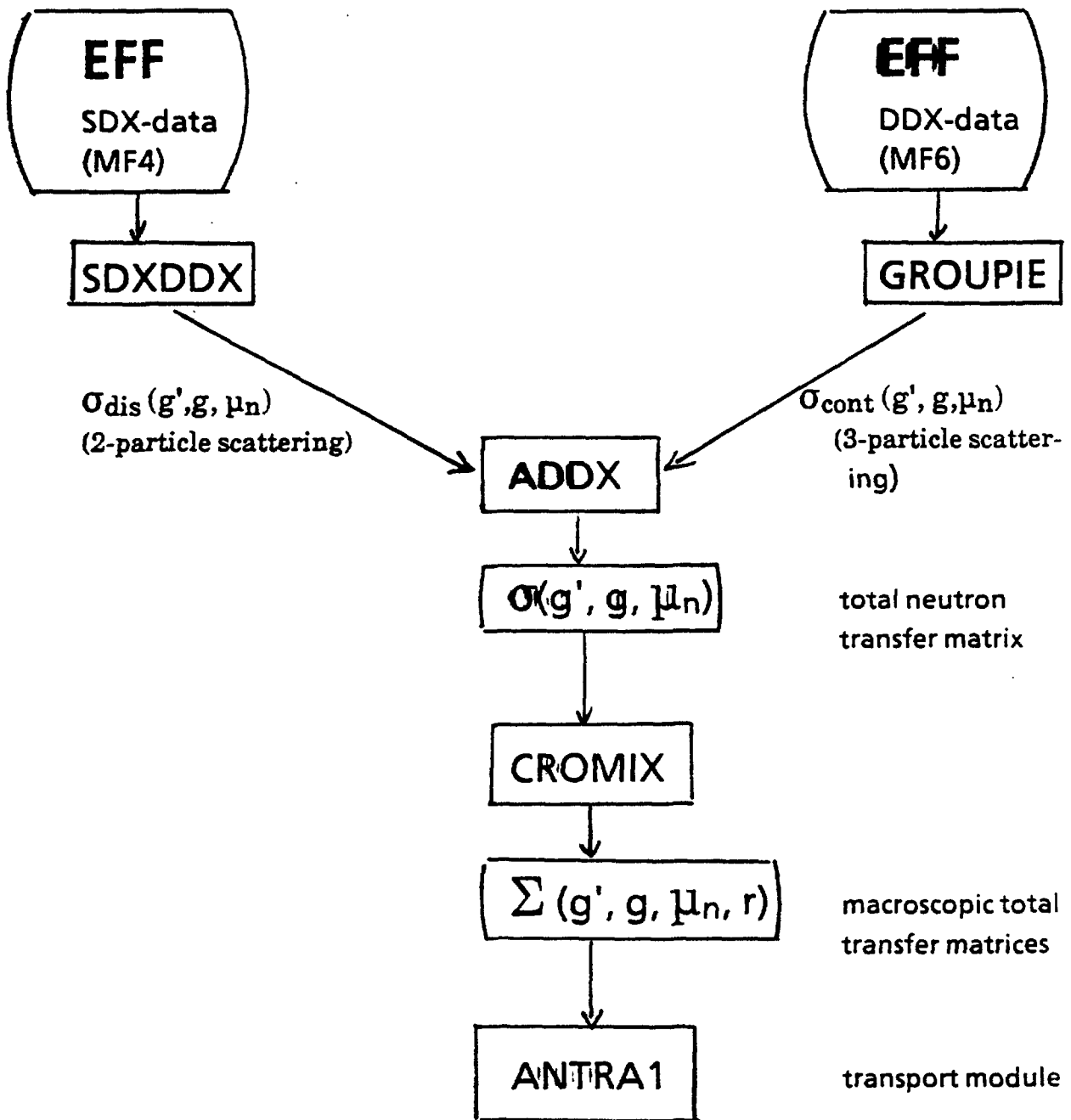
Monte Carlo Method (MCNP)

Data: EFF. 1 (DDX-data)

ENDF/B-VI (V), ENDL 85

Experiments: Dresden lead sphere experiment
Osaka lead sphere experiment

"Neutron Multiplication in Lead", Int. Symp. Fusion Nucl. Techn., Tokyo,
10-15 April, 1988.



DDX - processing system DOUBLE
and use in transport code ANTRA1

| Data Base | EFF-1 | | ENDF/B-IV | | | ENBF/B-V | ENDL85 | Experiment /6/ |
|-----------------|---------------------|-----------------------|-----------------------|------|------------|--------------------|--------|-------------------|
| Transport Code | ANTR1 ^{a)} | ONETRAN ^{b)} | ONETRAN ^{c)} | MCNP | NITRAN/17/ | MCNP ^{d)} | MCNP | |
| shell thickness | | | | | | | | |
| 3 cm | 1.20 | 1.19 | 1.20 | 1.20 | 1.20 | 1.20 | 1.20 | 1.34±0.08 |
| 6 cm | 1.35 | 1.35 | 1.37 | 1.36 | 1.36 | 1.36 | 1.37 | 1.54±0.09 |
| 9 cm | 1.48 | 1.47 | 1.49 | 1.49 | 1.49 | 1.49 | 1.50 | 1.69±0.10 |
| 12 cm | 1.57 | 1.57 | 1.59 | 1.58 | 1.58 | 1.58 | 1.60 | 1.80±0.11 |

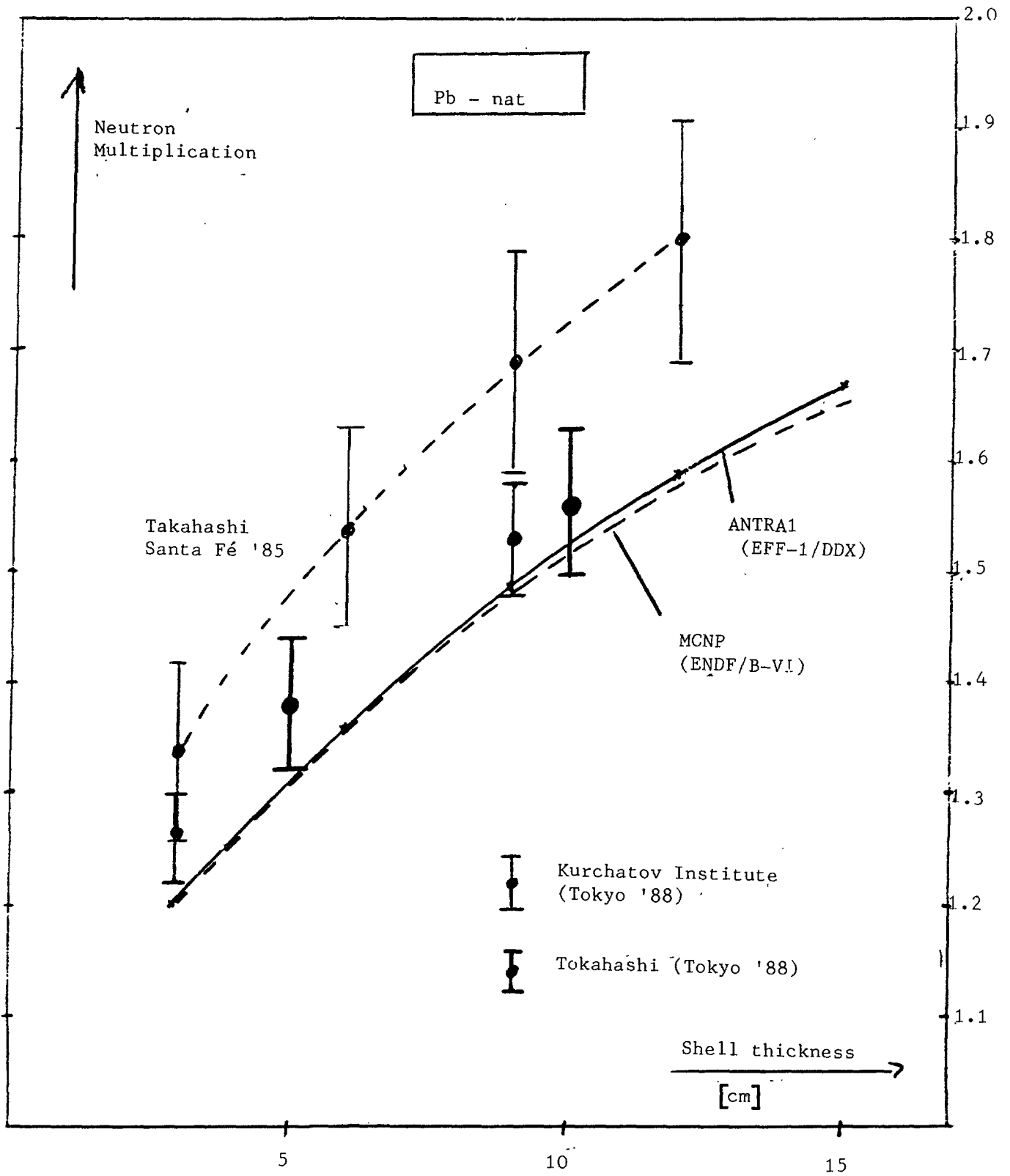
Table I: Osaka lead sphere experiment: Comparison of the total neutron multiplication obtained with different methods and data evaluations.

a) rigorous method (30 energy groups/ S_8 -segmentation)

b) P_4 -approximation (30/ S_8)

c) P_3 -approximation (25/ S_8)

d) performed by E.T. Cheng (cited in /6/)



Multiplication of 14 MeV neutrons in spherical lead shells.

(Status 5188)

| Data Base | Transport Code | M_{tot} | Partial Multiplication | | |
|------------------------------|--------------------|-------------------------|-------------------------|-------------------------|-------------------------|
| | | | (1-5 MeV) | (5-10)MeV | (10-15)MeV |
| ENDF/B-IV | ANISN/5/ | 1.78 | 0.52 | 0.02 | 0.12 |
| ENDF/B-IV | MCNP | 1.78 | 0.54 | 0.02 | 0.14 |
| ENDF/B-V | TART ^{a)} | 1.85 1.75 | 0.57 0.51 | 0.01 0.02 | 0.14 0.12 |
| ENDL85 | MCNP | 1.79 | 0.53 | 0.02 | 0.14 |
| EFF-1 | ANTRA1 | 1.76 | 0.61 | 0.03 | 0.14 |
| ⇒ $\sigma_{n,2n} + 10\%$ | | | | | |
| Experiment ^{b)} /5/ | | 1.94 | 0.68 | 0.02 | 0.14 |
| TOF | | -- | 0.653 | 0.019 | 0.144 |
| PRS | | 2.031 | 0.701 | 0.023 | 0.143 |

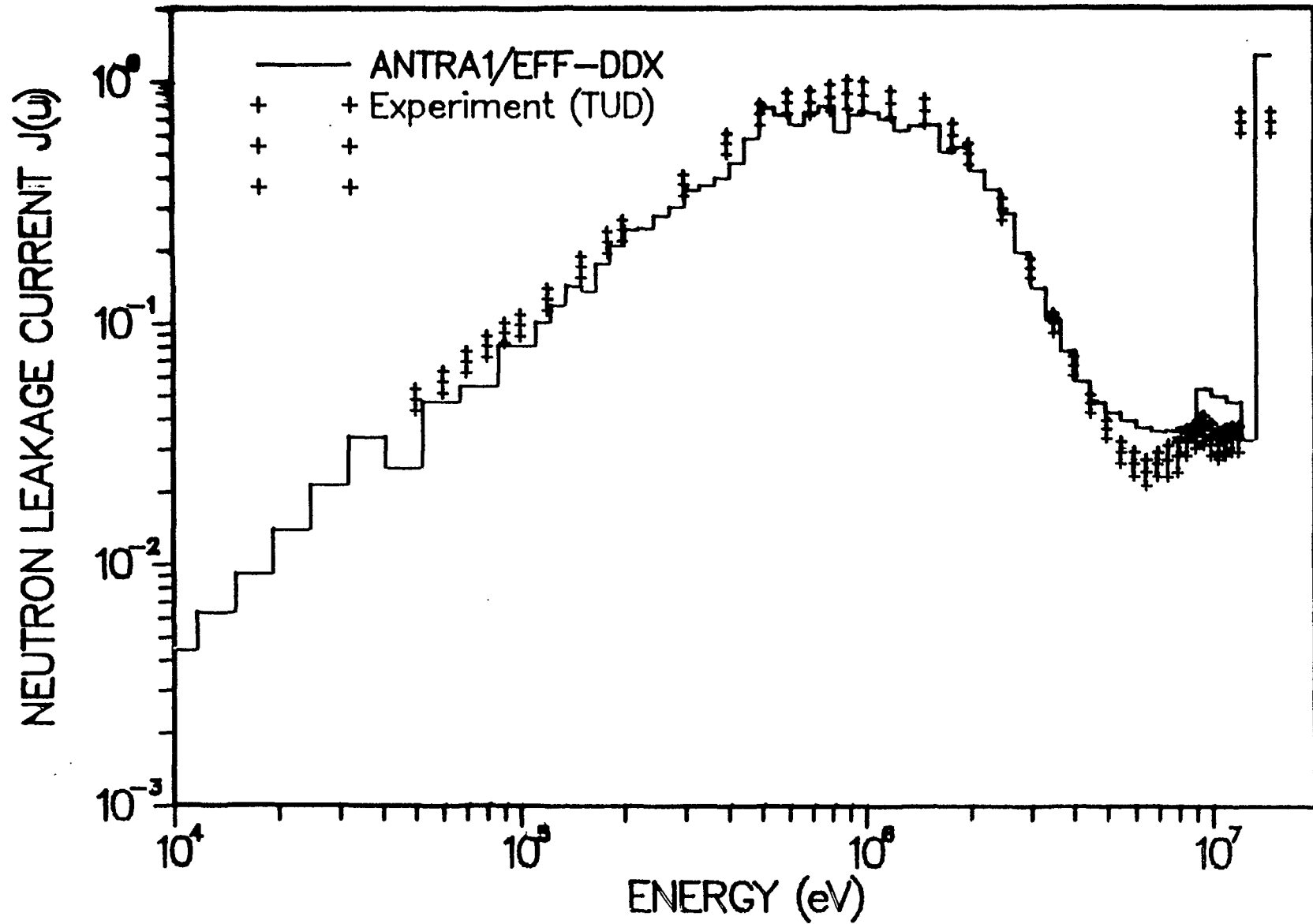
Table II: Dresden lead sphere experiment^{c)}: Comparison of the neutron multiplication obtained with different methods and data.

a) performed by L.F. Hansen, Livermore (cited in /5/)

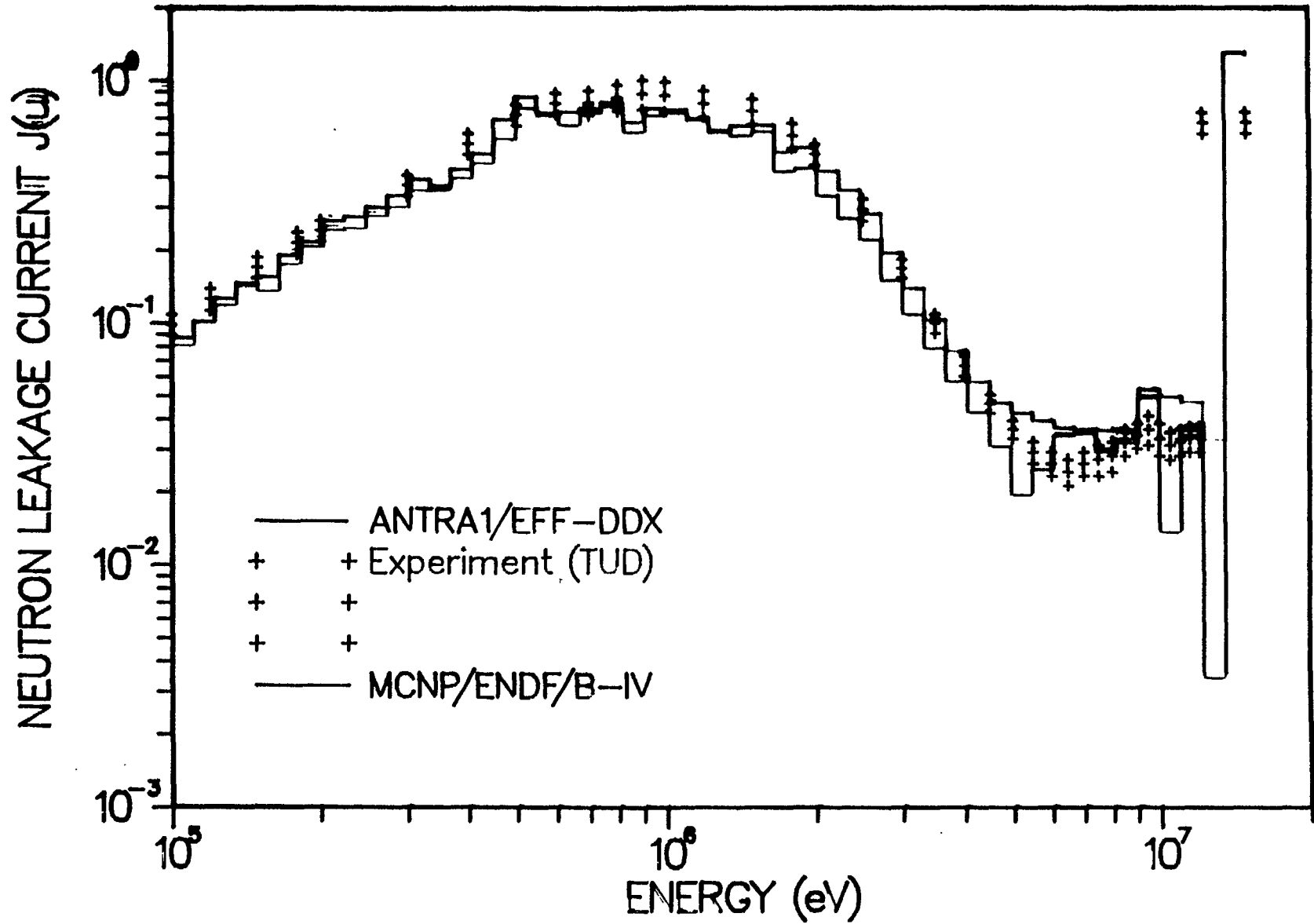
b) TOF: Time-of-Flight measurement, PRS: Proton recoil spectra measurement; the recommended experimental values are a combination of both measurements (see /5/)

c) The thickness of the lead shell is 22.5 cm

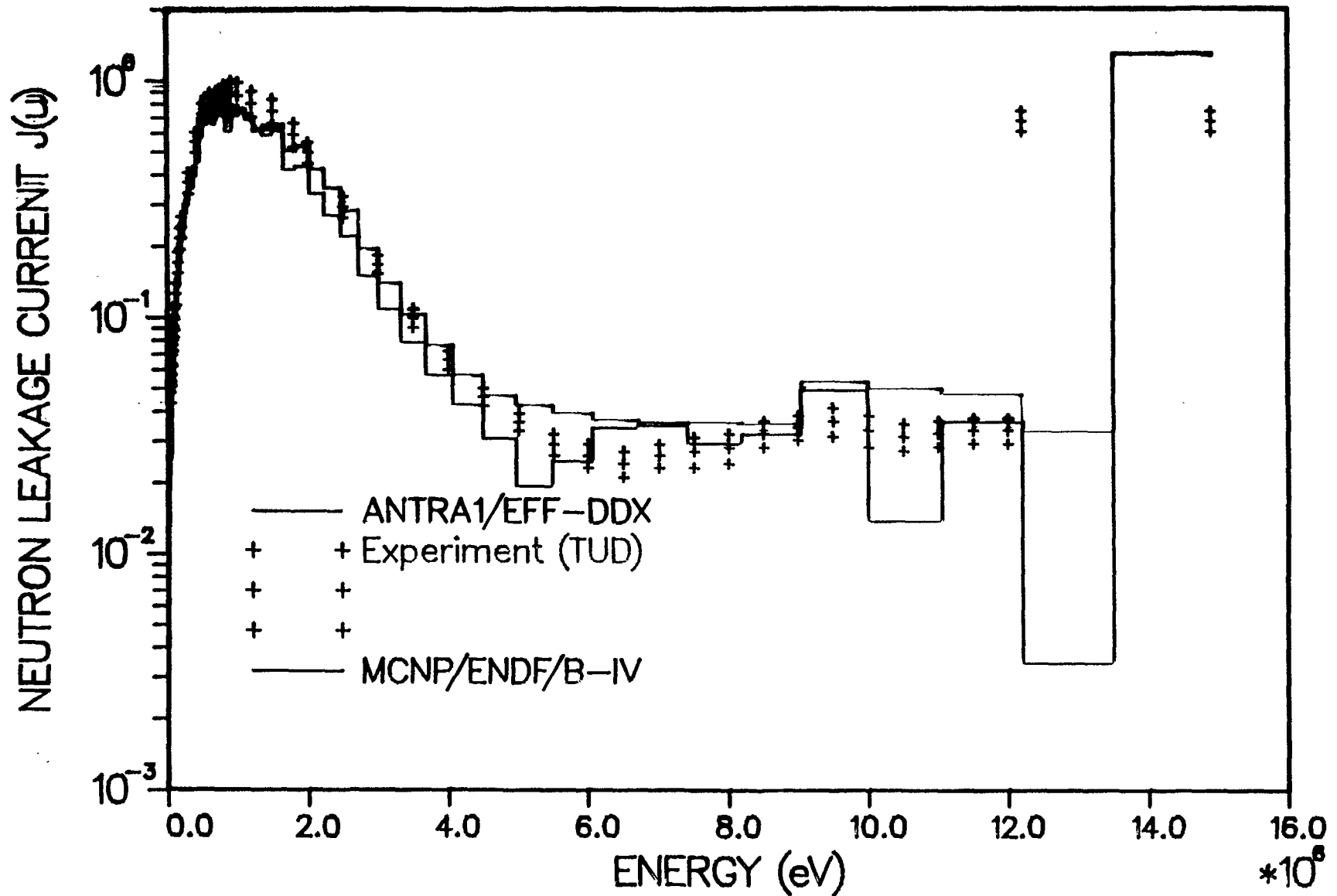
TUD LEAD SPHERE BENCHMARK



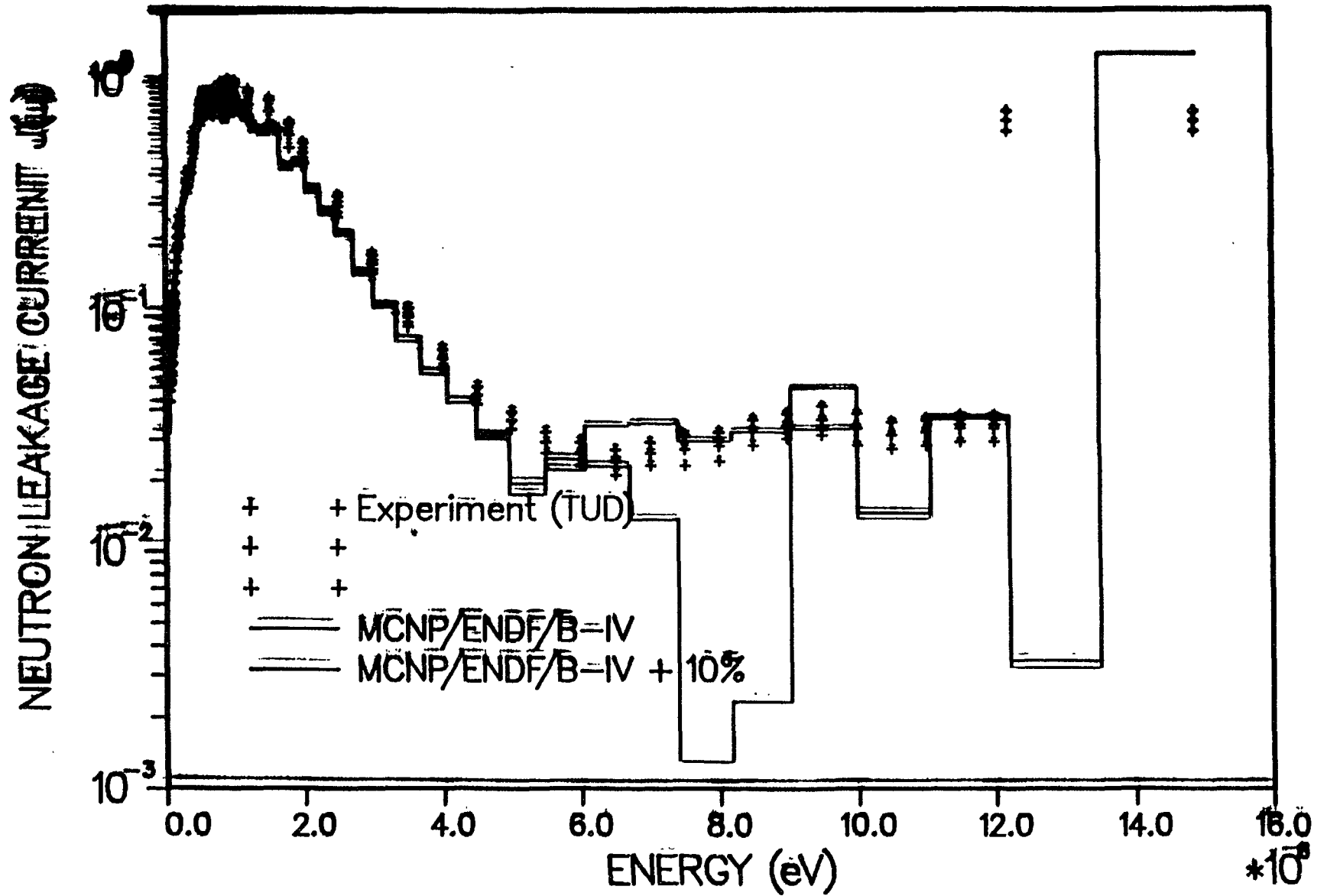
TUD LEAD SPHERE BENCHMARK



TUD LEAD SPHERE BENCHMARK



TUD LEAD SPHERE BENCHMARK



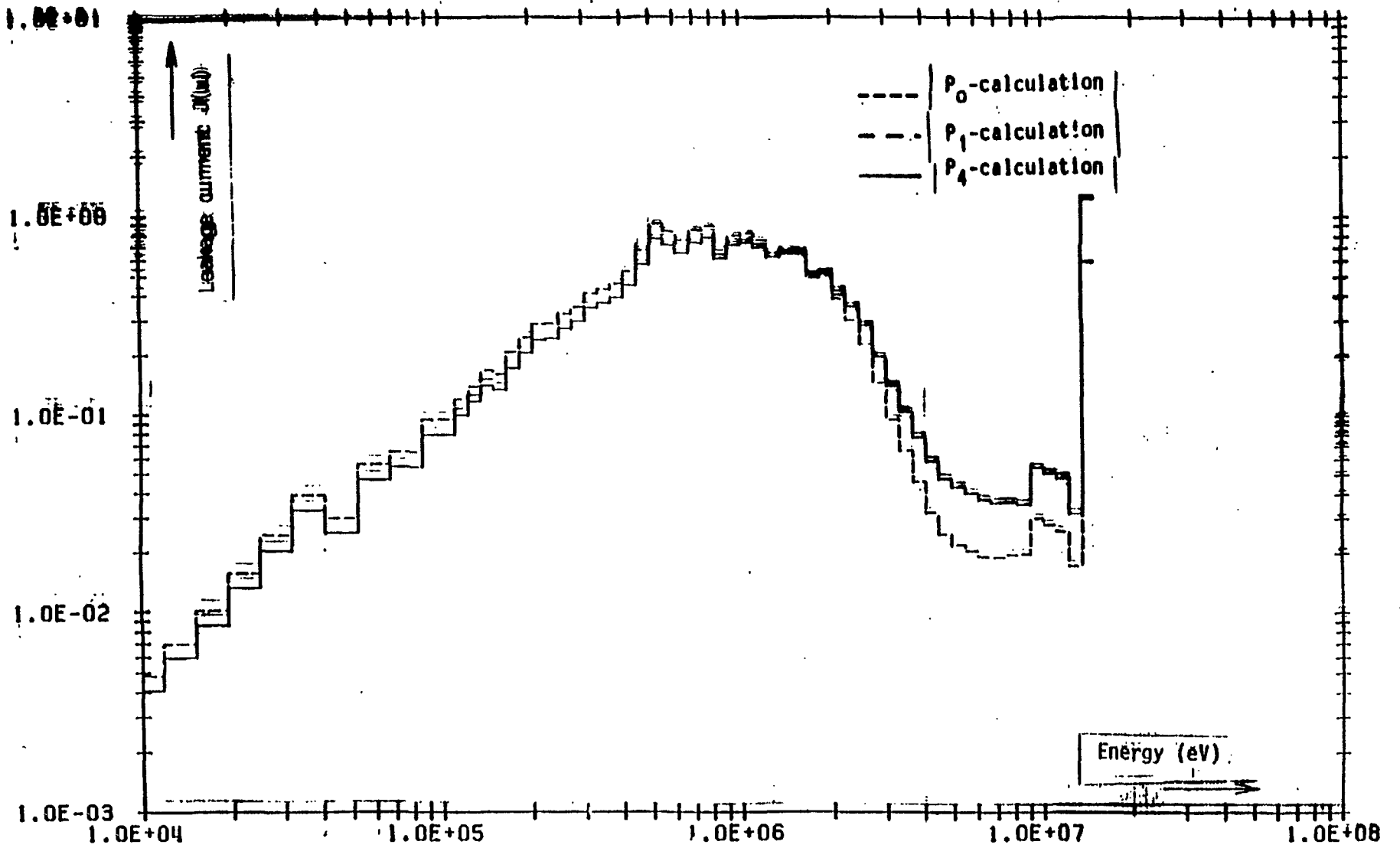


Fig 1

Conclusions

Integral data

- . Agreement for neutron multiplication calculated with different evaluations.
- . Agreement between calculated neutron multiplication and recent experiments.
- . Calculated energy spectrum of testing neutrons correct with EFF-1/DDX -data

Differential data

- . $\sigma_{n,2n}$ to be incorrect in EFF-1 (2.10b \rightarrow 2.193b at 14 MeV, already revised)
- . Energy-angle correlation correct in EFF-1

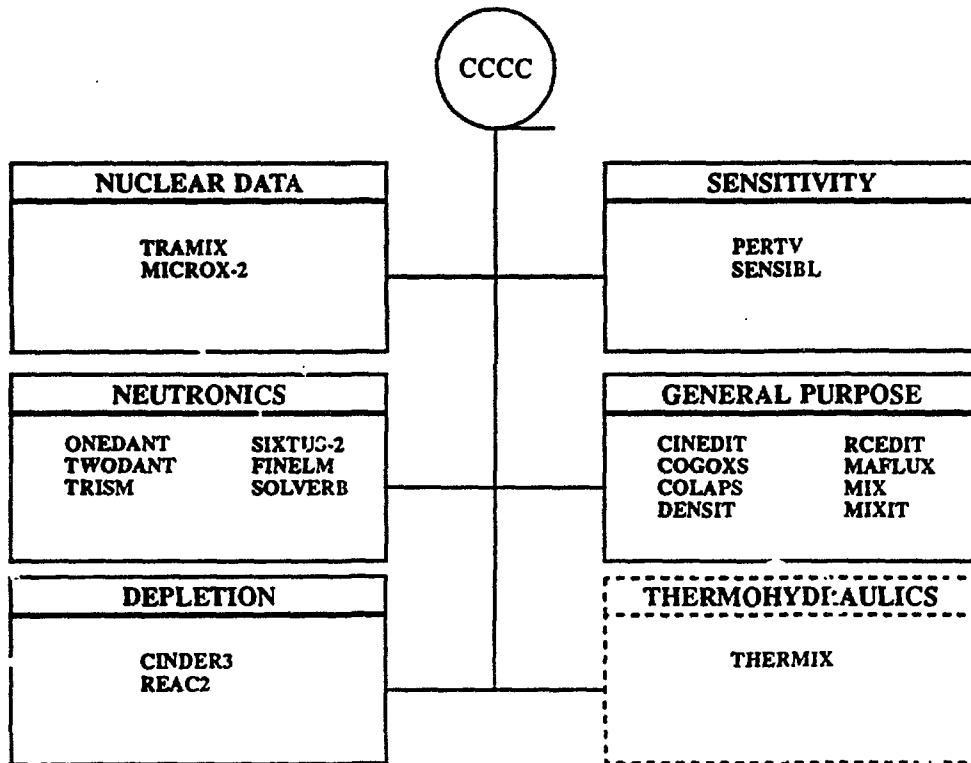
Methodology

- . Conventional S_n/P_1 - approximation sufficient
- . Neutron transport in lead only weakly anisotropic:
 P_1 - approximation sufficient

Effect of Double-Differential Lead Cross Sections
in the Performance Parameters
of Lead Spheres and Fusion Blankets

S. Pelloni

Swiss Federal Institute for Reactor Research (EIR),
Wuerenlingen, Switzerland



Block Diagram of the AARE System

Vitamin-J Coupled 175 Neutron-, 42 Photon Group Library

- Purpose : Coupled Neutron-Photon Analysis of Shields, Fusion Blankets, etc
- Contains Data for 59 Isotopes of 37 Elements from EFF-1 and JEF-1
- 11 Thermal Energy Groups
- Weighting Spectra : Vitamin-E for Neutrons i.e. (Thermal)-(1/E)-(Fission)-(1/E)-(Fusion)-(1/E)
Constant Weighting Spectrum for Photons
- P6 Legendre Ordre of Scattering both for Neutrons and Photons
- Temperatures : 296 600 900 (1200) K
- 6 σ_0 Background Cross Section Values : 10^{10} 10^4 10^3 100
10 1 (0.1) barn

Table 1: Vitamin-J Structure Coupled 175 Neutron-,42 Photon Group Library
List of Isotopes ; a := 296 600 900 K

| Isotope | Temperatures Kelvin | No. of σ_0 | Thermal Scattering Treatment | Photon Prod. |
|-----------------------|------------------------|----------------------|---------------------------------|-----------------|
| ¹ H | 293.6 473.6 623.6 | 1 | incl H in H ₂ O | yes |
| ² H | 293.6 473.6 573.6 | 1 | incl D in D ₂ O | yes |
| ³ H | a | 1 | - | no |
| ³ He | a | 1 | - | no |
| ⁴ He | a | 1 | - | no |
| ⁶ Li | a | 1 | - | yes |
| ⁷ Li | a | 1 | - | yes |
| ⁷ Li(EFF) | a | 1 | - | yes |
| ⁹ Be | 296 600 1000 | 1 | coh,inch Be and BeO | yes |
| ⁹ Be(EFF) | a | 1 | - | yes |
| ¹⁰ B | a | 1 | - | yes |
| ¹¹ B | a | 1 | - | no |
| C(nat) | 293.6 500 800 1200 | 1 | coh,inch graphite | yes |
| ¹⁴ N | a | 1 | - | yes |
| ¹⁶ O | 296 600 1200 | 1 | incl O in UO ₂ | yes |
| ¹⁹ F | a | 1 | - | yes |
| ²³ Na | a | 1 | - | no |
| Mg(nat) | a | 1 | - | yes |
| ²⁷ Al | a | 6 | - | yes |
| Si(nat) | a | 6 | - | yes |
| Cl(nat) | a | 6 | - | yes |
| K(nat) | a | 6 | - | yes |
| Ca(nat) | a | 6 | - | yes |
| Ti(nat) | a | 6 | - | yes |
| V(nat) | a | 6 | - | yes |
| Cr(nat) | a | 6 | - | yes |
| ⁵⁵ Mn | a | 6 | - | yes |
| Fe(nat) | 296 600 1200 | 7 | - | yes |
| ⁵⁹ Co | a | 6 | - | yes |
| Ni(nat) | a | 6 | - | yes |
| ⁷⁰ Zn(nat) | a | 6 | - | yes |
| Zr(nat) | a | 6 | - | yes |
| ⁹³ Nb | a | 6 | - | yes |
| Mo(nat) | a | 6 | - | yes |
| ¹⁰⁷ Ag | 296 | 6 | no free gas | no |
| ¹⁰⁹ Ag | 296 | 6 | no free gas | no |
| Cd(nat) | a | 6 | - | no |

Table 1: Vitamin-J Structure Coupled 175 Neutron-,42 Photon Group Library
List of Isotopes ; a := 296 600 900 ,b := 296 600 900 1200 K

| Isotope | Temperatures Kelvin | No. of σ_0 | Thermal Scattering Treatment | Photon Prod. |
|-------------------|------------------------|----------------------|---------------------------------|-----------------|
| ¹¹⁴ Sn | 296 | 6 | no free gas | no |
| ¹¹⁵ Sn | 296 | 6 | no free gas | no |
| ¹¹⁶ Sn | 296 | 6 | no free gas | no |
| ¹¹⁷ Sn | 296 | 6 | no free gas | no |
| ¹¹⁸ Sn | 296 | 6 | no free gas | no |
| ¹¹⁹ Sn | 296 | 6 | no free gas | no |
| ¹²⁰ Sn | 296 | 6 | no free gas | no |
| ¹²² Sn | 296 | 6 | no free gas | no |
| ¹²⁴ Sn | 296 | 6 | no free gas | no |
| ¹³³ Cs | 296 | 6 | - | no |
| Hf(nat) | a | 6 | - | no |
| ¹⁸¹ Ta | a | 6 | - | yes |
| ¹⁸² W | 296 | 6 | no free gas | yes |
| ¹⁸³ W | 296 | 6 | no free gas | yes |
| ¹⁸⁴ W | 296 | 6 | no free gas | yes |
| ¹⁸⁶ W | 296 | 6 | no free gas | yes |
| Pb(nat) | a | 6 | - | yes |
| Pb(EFF) | a | 6 | - | yes |

Table 1: Vitamin-J Structure Coupled 175 Neutron-,42 Photon Group Library
List of Isotopes ; b := 296 600 900 1200 K

| Isotope | Temperatures Kelvin | No. of σ_0 | Thermal Scattering Treatment | Photon Prod. |
|-----------------------|------------------------|----------------------|---------------------------------|-----------------|
| ²³² Th | b | 6 | - | no |
| ²³³ U | b | 6 | - | no |
| ²³⁴ U | b | 6 | - | no |
| ²³⁵ U | b | 6 | - | yes |
| ²³⁵ U | b | 6 | - | yes |
| ²³⁶ U | b | 6 | - | no |
| ²³⁸ U | b | 6 | - | no |
| ²³⁸ U(B4) | b | 6 | - | yes |
| ²³⁸ Pu | b | 6 | - | no |
| ²³⁹ Pu | b | 6 | - | no |
| ²³⁹ Pu(B4) | b | 6 | - | yes |
| ²⁴⁰ Pu | b | 6 | - | no |
| ²⁴¹ Pu | b | 6 | - | no |
| ²⁴² Pu | b | 6 | - | no |
| ²⁴¹ Am | b | 6 | - | no |

LEAD MF=6 (GROUPXS)

infinite dilute $\begin{array}{c} || \\ || \\ \vee \end{array}$ FIDO

ONEDANT

$\begin{array}{c} || \\ || \\ \vee \end{array}$

MACRXS (n,2n),(n,g) taken from

$\begin{array}{c} || \\ || \\ \vee \end{array}$

VITAMIN-J

COGOXS

$\begin{array}{c} || \\ || \\ \vee \end{array}$

WORKING LIBRARY
FOR TRANSPORT CALCULATIONS

Transport calculations performed with P S .
5 16

Table 1: Neutronics model for lithium-lead BCSS blanket (20 cm thick breeding blanket)

| Zone No. | Outer Radius (cm) | Component | Materials Composition |
|----------|-------------------|-------------|---|
| 1 | 49.0 | Plasma | Void |
| 2 | 60.0 | Vacuum | Void |
| 3 | 60.3 | First Wall | V15Cr5Ti |
| 4 | 80.3 | T. Breeding | 7.1% V15Cr5Ti + 73.7% Li ₁₇ Pb ₈₃ |
| 5 | 120.3 | Manifold | 10% V15Cr5Ti + 20% Li ₁₇ Pb ₈₃ + 70% Fe1422 |
| 6 | 122.3 | Gap | Void |
| 7 | 152.3 | Shield | 20% H ₂ O + 80% Fe1422 |

Table 2: Comparison of calculated reaction rates in lithium-lead BCSS blanket using EFF-1 and ENDF/B-V libraries (30% ^6Li in lithium)

| Breeding Zone Thickness (m) | 0.2 | 0.2 | 0.5 | 0.5 | 0.6 | 0.6 |
|-----------------------------|-------|----------|-------|----------|-------|----------|
| Library | EFF-1 | ENDF/B-V | EFF-1 | ENDF/B-V | EFF-1 | ENDF/B-V |
| T6 | 0.718 | 0.769 | 1.122 | 1.169 | 1.225 | 1.282 |
| T7 | 0.014 | 0.015 | 0.017 | 0.018 | 0.018 | 0.018 |
| TBR | 0.732 | 0.784 | 1.149 | 1.187 | 1.243 | 1.300 |
| Pb(n,2n) | 0.585 | 0.625 | 0.706 | 0.714 | 0.714 | 0.714 |
| Pb(n, γ) | 0.027 | 0.032 | 0.053 | 0.057 | 0.059 | 0.064 |

Table 3: Comparison of calculated reaction rates in lithium-lead BCSS blanket using EFF-1 and ENDF/B-V libraries (90% ^6Li in lithium)

| Breeding Zone Thickness (m) | 0.2 | 0.2 | 0.5 | 0.5 | 0.6 | 0.6 |
|-----------------------------|-------|----------|-------|----------|-------|----------|
| Library | EFF-1 | ENDF/B-V | EFF-1 | ENDF/B-V | EFF-1 | ENDF/B-V |
| T6 | 1.085 | 1.138 | 1.448 | 1.495 | 1.520 | 1.560 |
| T7 | 0.002 | 0.002 | 0.002 | 0.002 | 0.002 | 0.003 |
| TBR | 1.087 | 1.140 | 1.451 | 1.498 | 1.522 | 1.563 |
| Pb(n,2n) | 0.584 | 0.621 | 0.705 | 0.712 | 0.712 | 0.711 |
| Pb(n, γ) | 0.020 | 0.023 | 0.034 | 0.037 | 0.037 | 0.039 |

Dresden Sphere*

(VITAMIN-J MF4-5 versus MF6)

| Data base | M-tot | M ₁₋₅ | M ₅₋₁₀ | M ₁₀₋₁₅ |
|----------------------|--------|------------------|-------------------|--------------------|
| MF4-5 | 1.756 | 0.633 | 0.023 | 0.127 |
| MF6 | 1.761 | 0.636 | 0.026 | 0.128 |
| Exp | 1.94 | 0.68 | 0.02 | 0.14 |
| Reaction rates of Pb | (n,2n) | (n,γ) | | |
| MF4-5 | 0.766 | 0.0107 | | |
| MF6 | 0.768 | 0.0107 | | |

* Compares well with previously published results, and with ENDF/B-V

Oktavian sphere experiments

| Data base | MF4-5 | MF6 | Exp. |
|----------------------|-------------------------|-------|----------|
| Shell thickness (cm) | M _{tot} values | | |
| 3 | 1.238 | 1.239 | 1.34±.08 |
| 6 | / | 1.401 | 1.54±.09 |
| 9 | / | 1.521 | 1.69±.1 |
| 12 | 1.605 | 1.609 | 1.80±.11 |

M = leakage spectrum

Comparison of Pb MF4-5 and MF6 using a fusion blanket (30% Li-6 in Li)

| | | | | | | |
|----------------|-------|--------|-------|-------|-------|-------|
| Breeding Zone | 0.2 | 0.2 | 0.5 | 0.5 | 0.6 | 0.6 |
| Thickness (m) | MF4-5 | MF6 | MF4-5 | MF6 | MF4-J | MF6 |
| T ₆ | 0.753 | 0.727 | 1.153 | 1.083 | 1.254 | 1.169 |
| T ₇ | 0.014 | 0.014 | 0.017 | 0.017 | 0.018 | 0.018 |
| TBR | 0.767 | 0.0741 | 1.170 | 1.100 | 1.272 | 1.187 |
| Pb(n,2n) | 0.585 | 0.586 | 0.706 | 0.708 | 0.714 | 0.715 |
| Pb(n,γ) | 0.033 | 0.032 | 0.065 | 0.062 | 0.073 | 0.069 |

Comparison of Pb MF4-5 and MF6 using a fusion blanket (90% Li-6 in Li)*

| | | | | | | |
|----------------|-------|-------|-------|-------|-------|-------|
| Breeding Zone | 0.2 | 0.2 | 0.5 | 0.5 | 0.6 | 0.6 |
| Thickness (m) | MF4-5 | MF6 | MF4-5 | MF6 | MF4-J | MF6 |
| T ₆ | 1.112 | 1.102 | 1.469 | 1.443 | 1.536 | 1.509 |
| T ₇ | 0.002 | 0.002 | 0.002 | 0.002 | 0.003 | 0.003 |
| TBR | 1.114 | 1.104 | 1.471 | 1.445 | 1.539 | 1.511 |
| Pb(n,2n) | 0.584 | 0.585 | 0.705 | 0.706 | 0.712 | 0.714 |
| Pb(n,γ) | 0.023 | 0.023 | 0.039 | 0.038 | 0.042 | 0.041 |

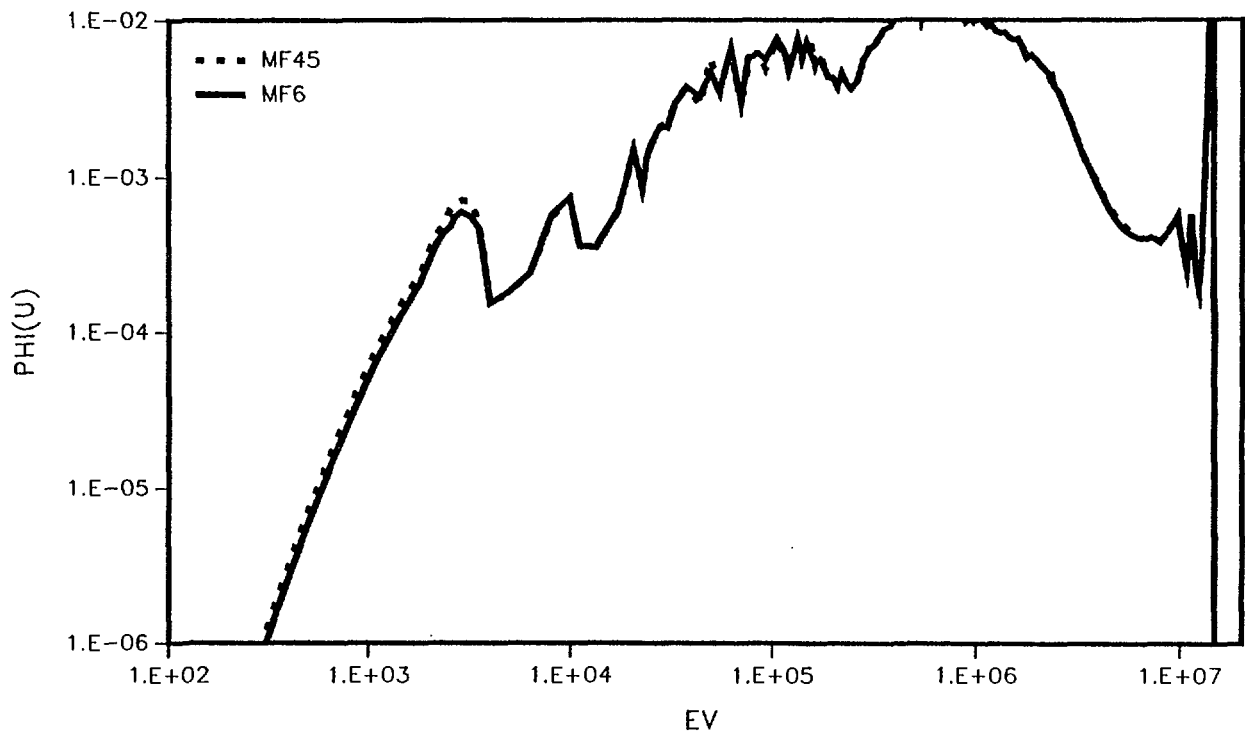
* Small differences from previous results due to a more accurate shielding procedure.

. Main differences:

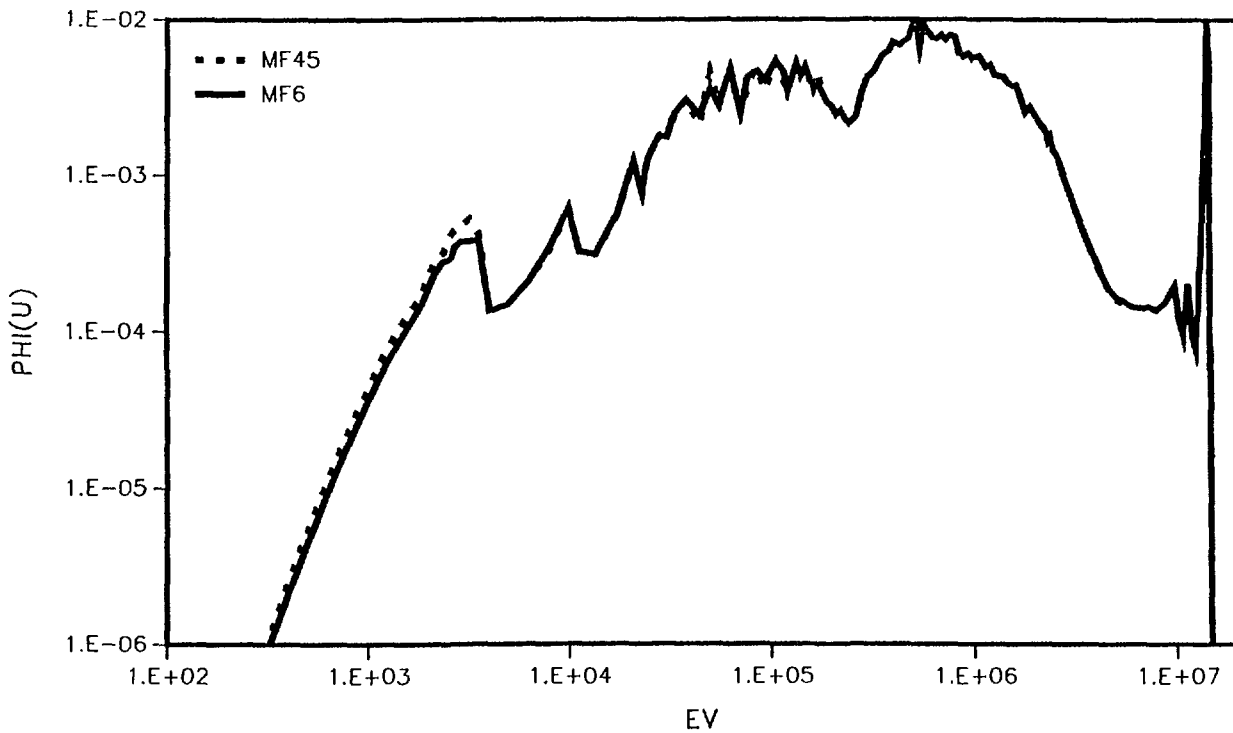
- (1) Energy range lower than 10 keV
- (2) Anisotropic scattering lower than 10 keV
- (3) From 10 keV up both data to compare very well

(resulting in good agreement between leakage spectra of pure spheres)

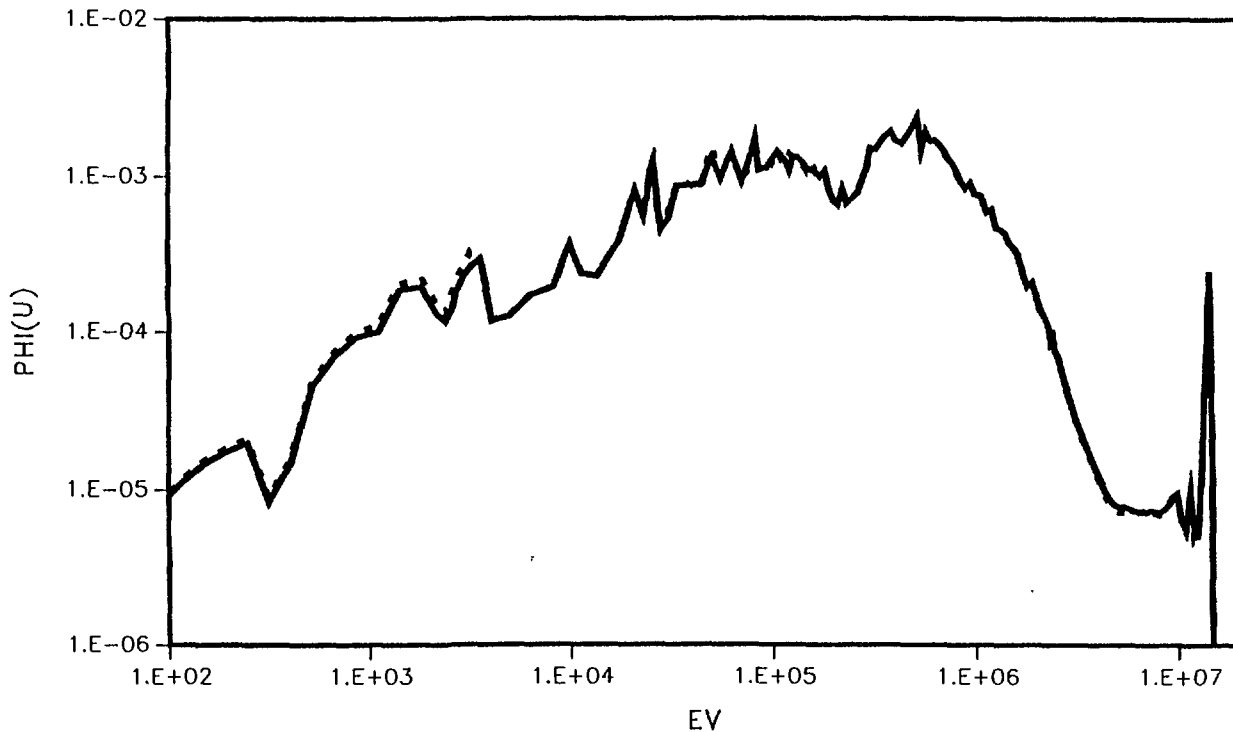
90% LI-6 60CM BREEDING LEFT POSITION (MF45 VERSUS MF6)



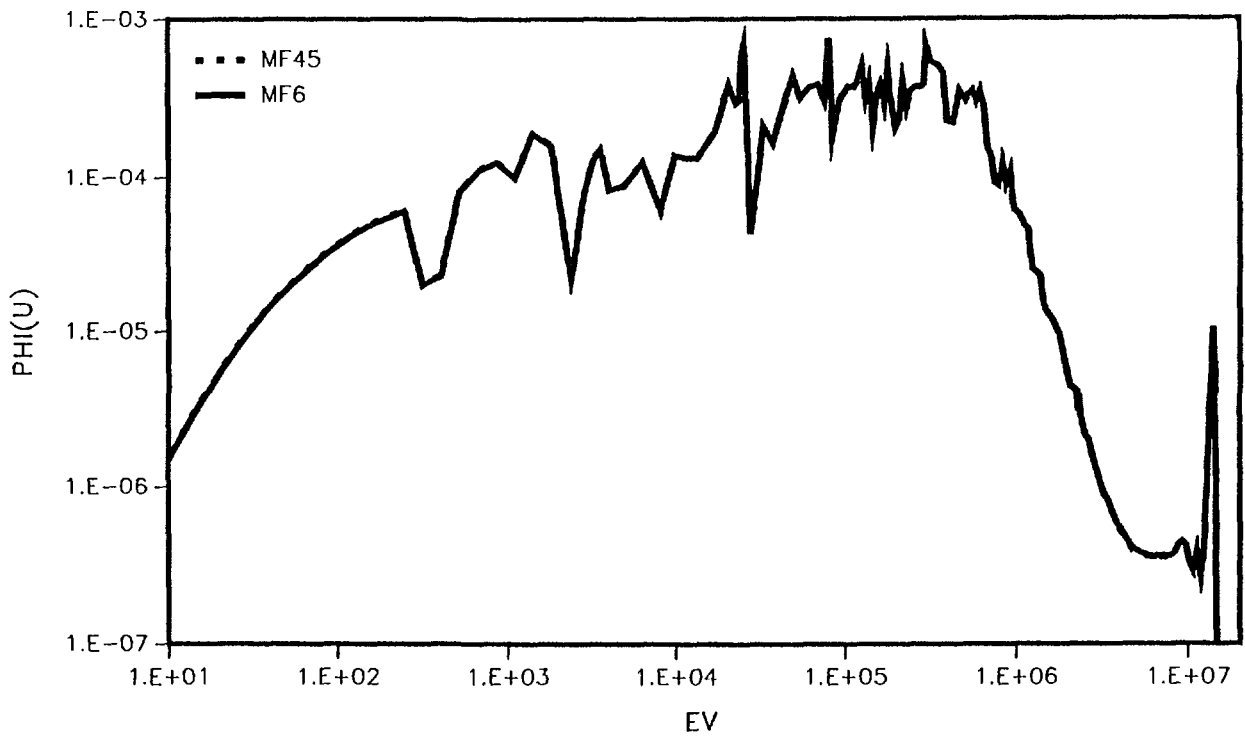
90% LI-6 60CM BREEDING MEDIUM POSITION (MF45 VERSUS MF6)



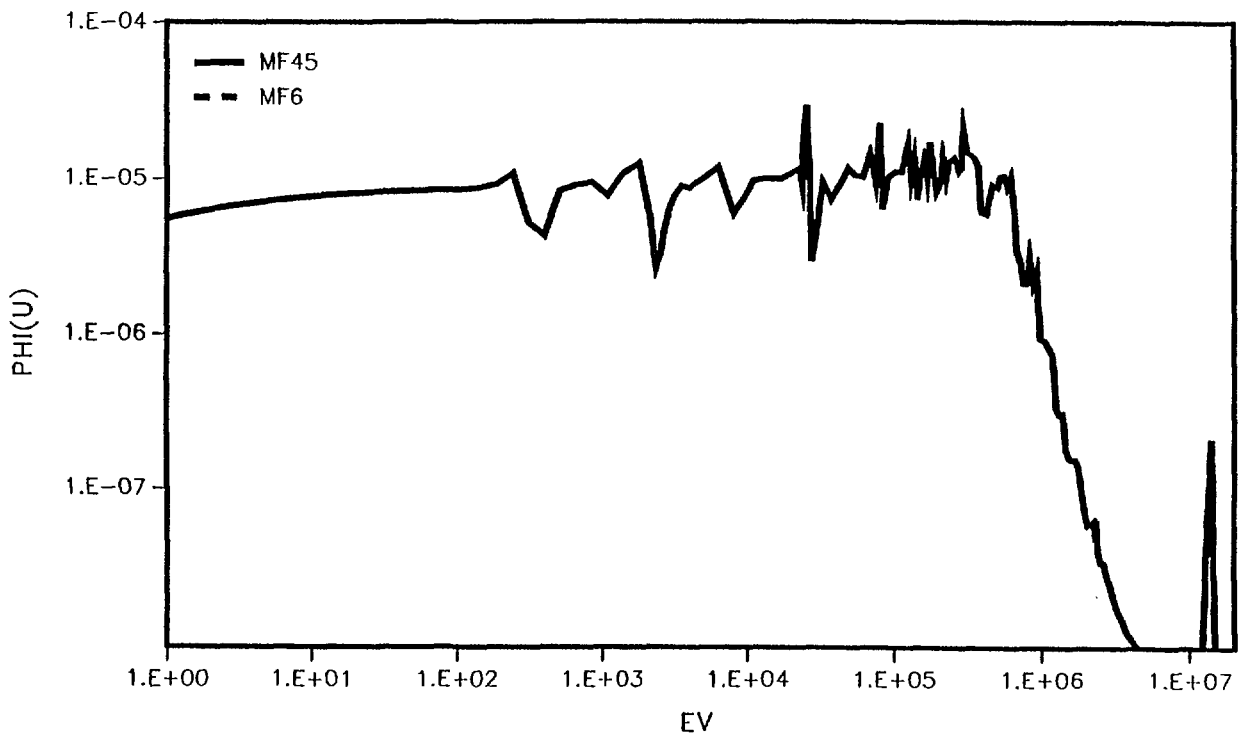
90% LI-6 60CM BREEDING RIGHT POSITION (MF45 VERSUS MF6)



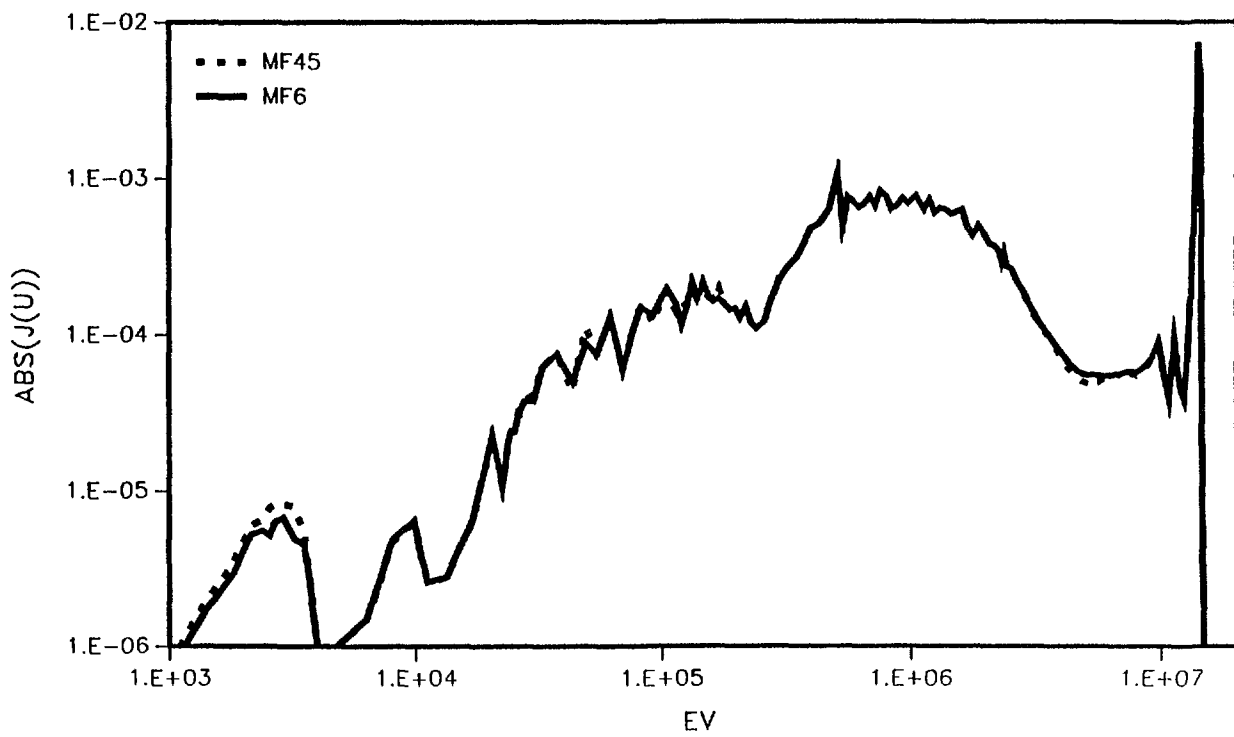
90% LI-6 60CM BREEDING MANIFOLD (MIDDLE) (MF45 VERSUS MF6)



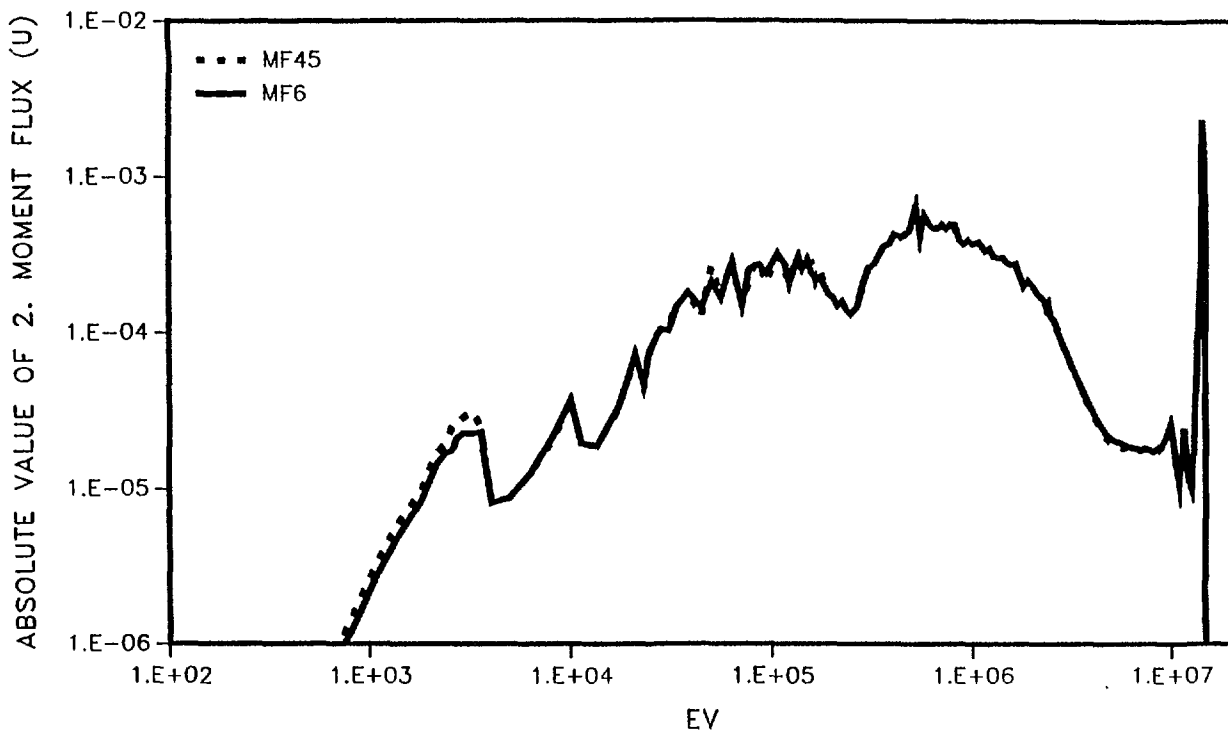
90% LI-6 60CM BREEDING SHIELD (MIDDLE) (MF45 VERSUS MF6)



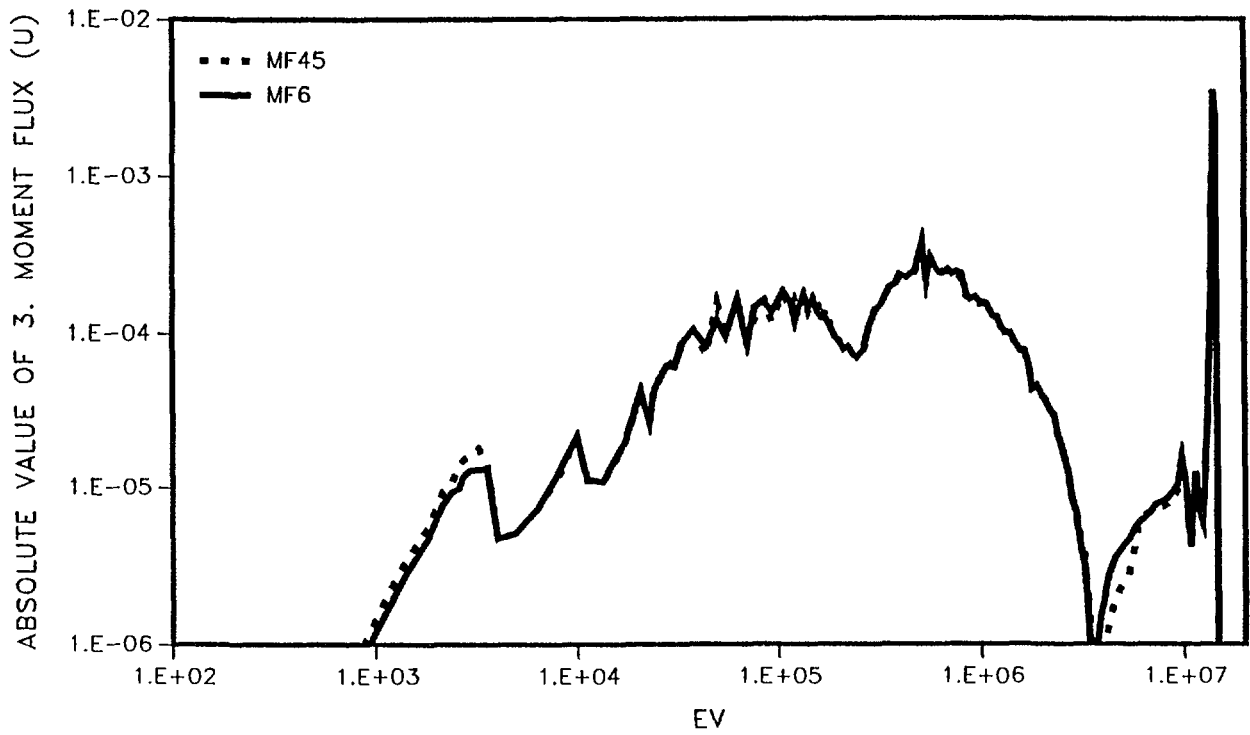
90% LI-6 BREEDING MEDIUM POSITION CURRENTS (MF45 VERSUS MF6)



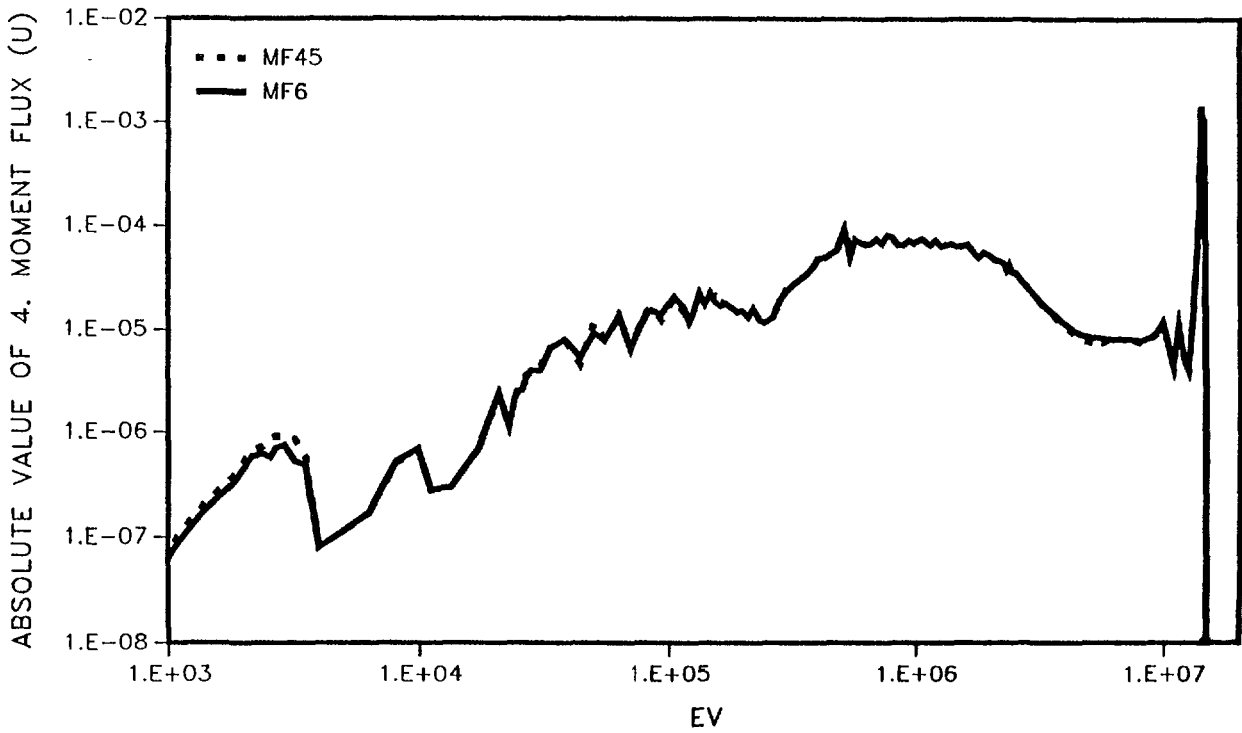
90% LI-6 MEDIUM POSITION 60 CM BREEDING PHI2 (MF45 VERSUS MF6)



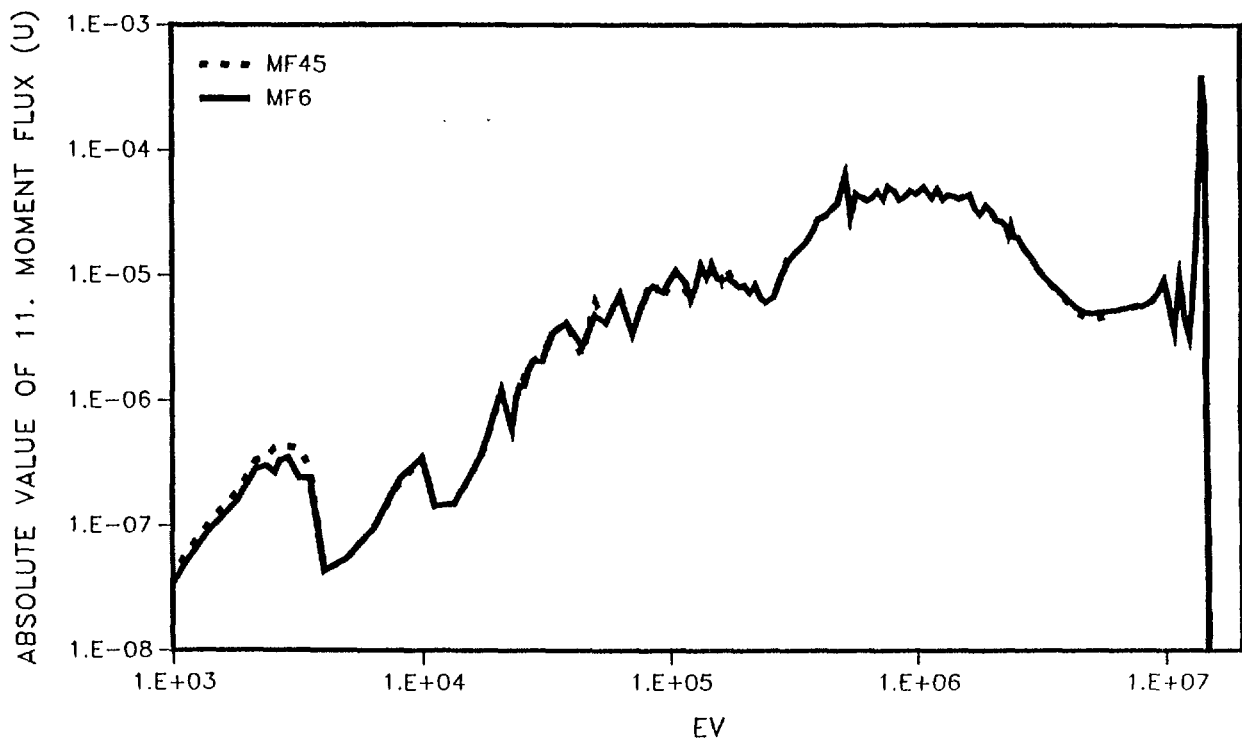
90% LI-6 MEDIUM POSITION 60 CM BREEDING PHI3 (MF45 VERSUS MF6)



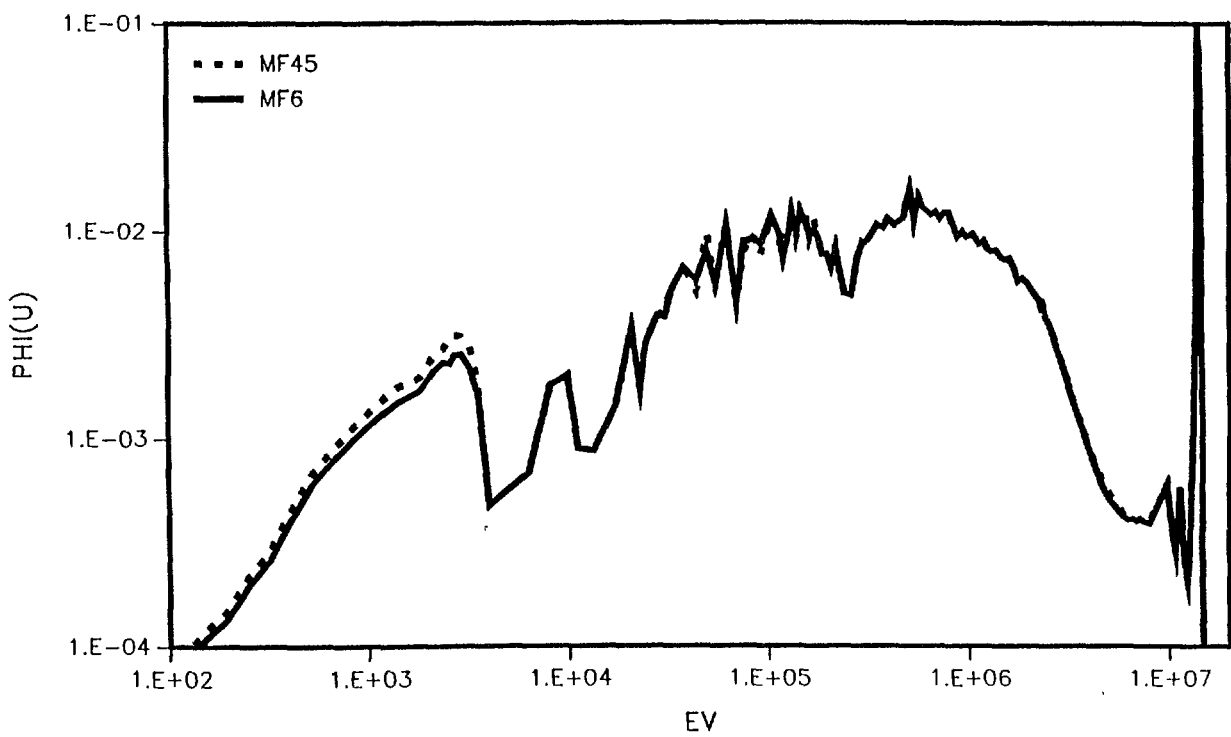
90% LI-6 MEDIUM POSITION 60 CM BREEDING PHI4 (MF45 VERSUS MF6)



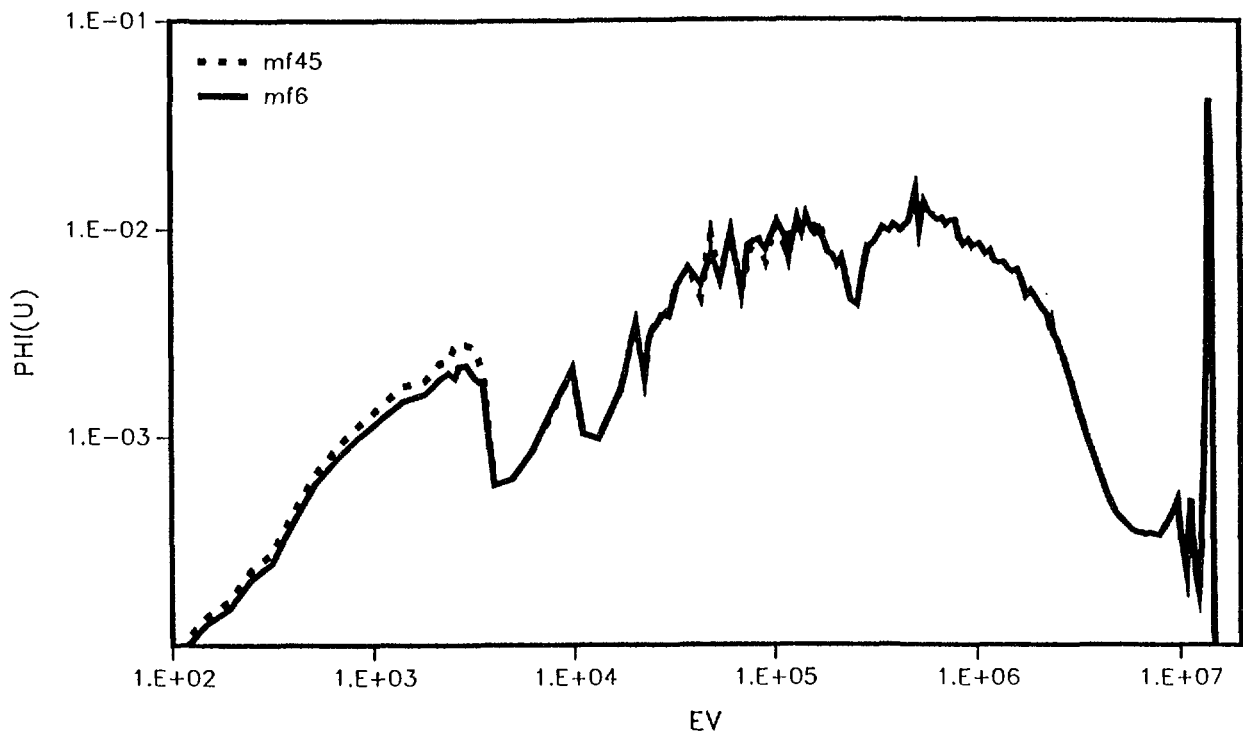
90% LI-6 MEDIUM POSITION 60 CM BREEDING PHI11 (MF45 VERSUS MF6)



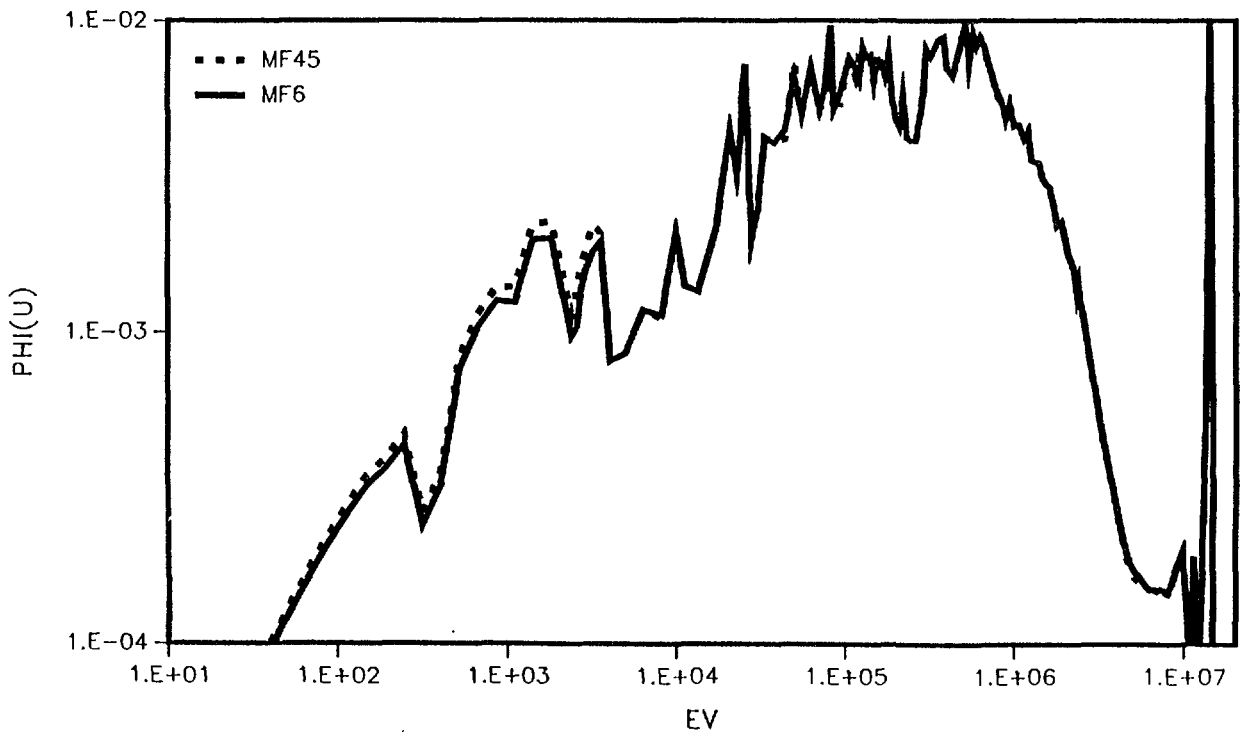
30% LI-6 20CM BREEDING LEFT POSITION (MF45 VERSUS MF6)



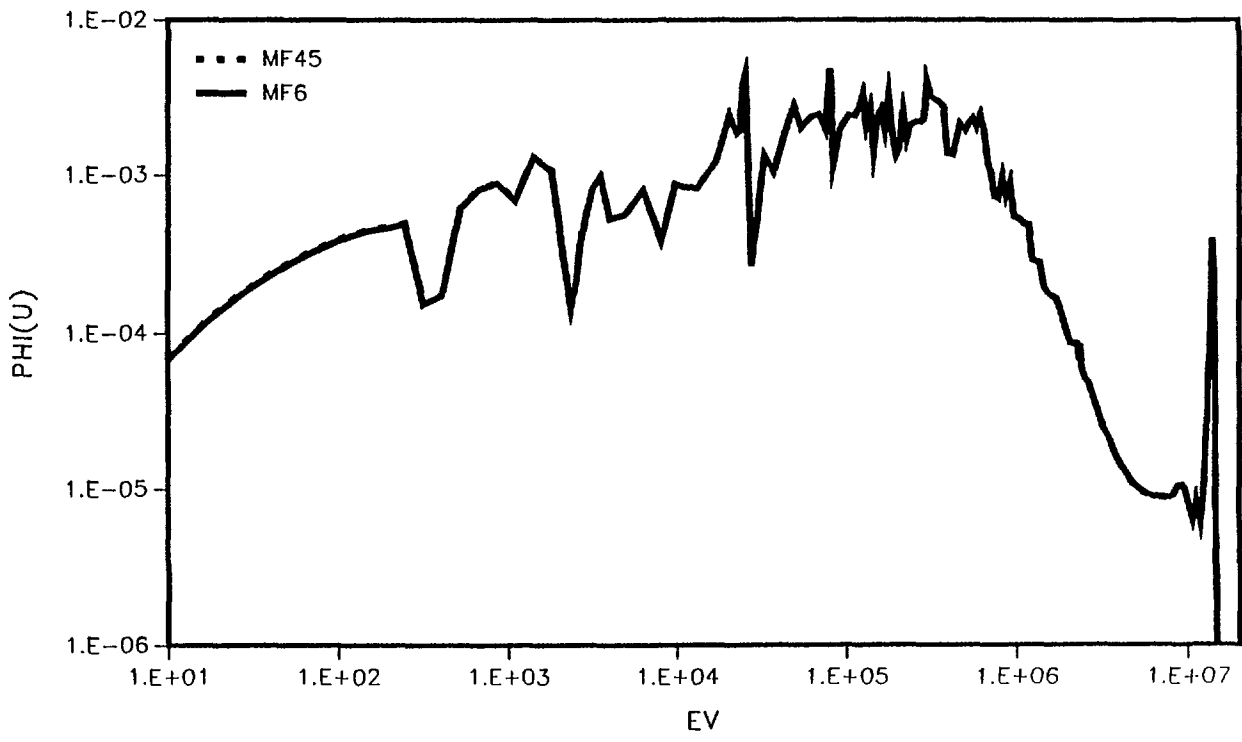
30% LI-6 20CM BREEDING MIDDLE POSITION (MF45 VERSUS MF6)



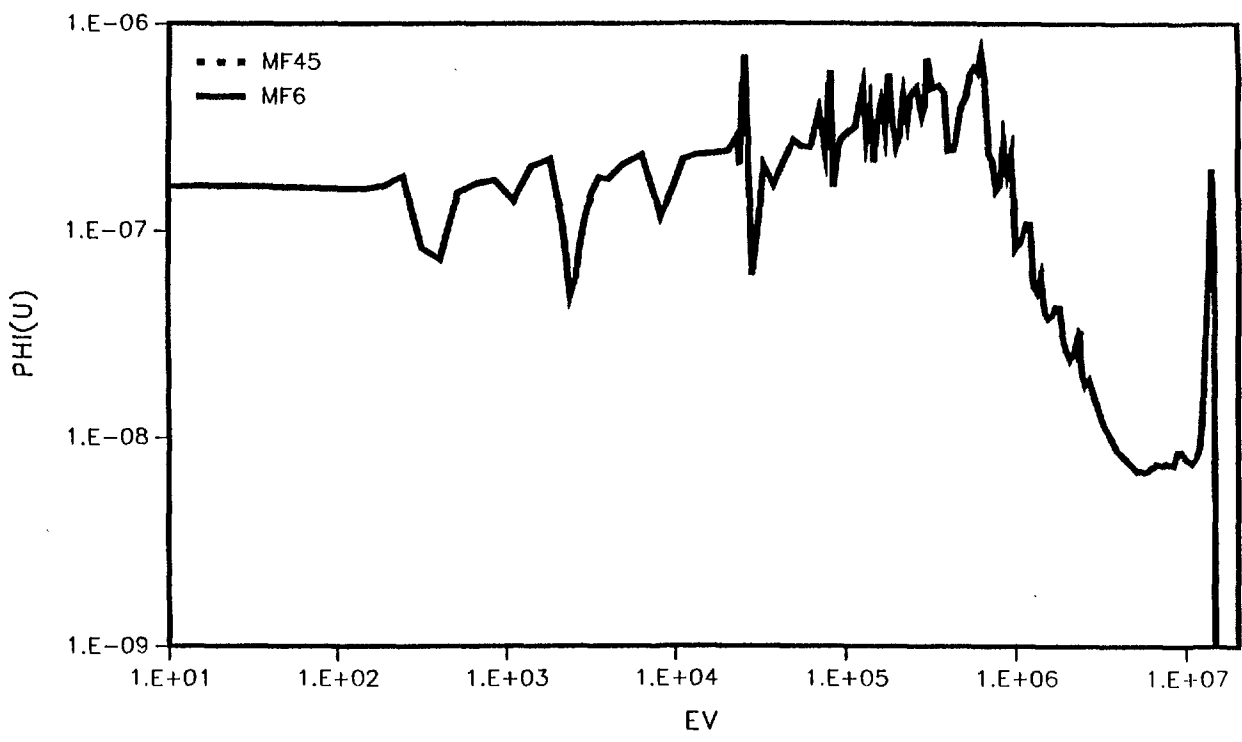
30% LI-6 20CM BREEDING RIGHT POSITION (MF45 VERSUS MF6)



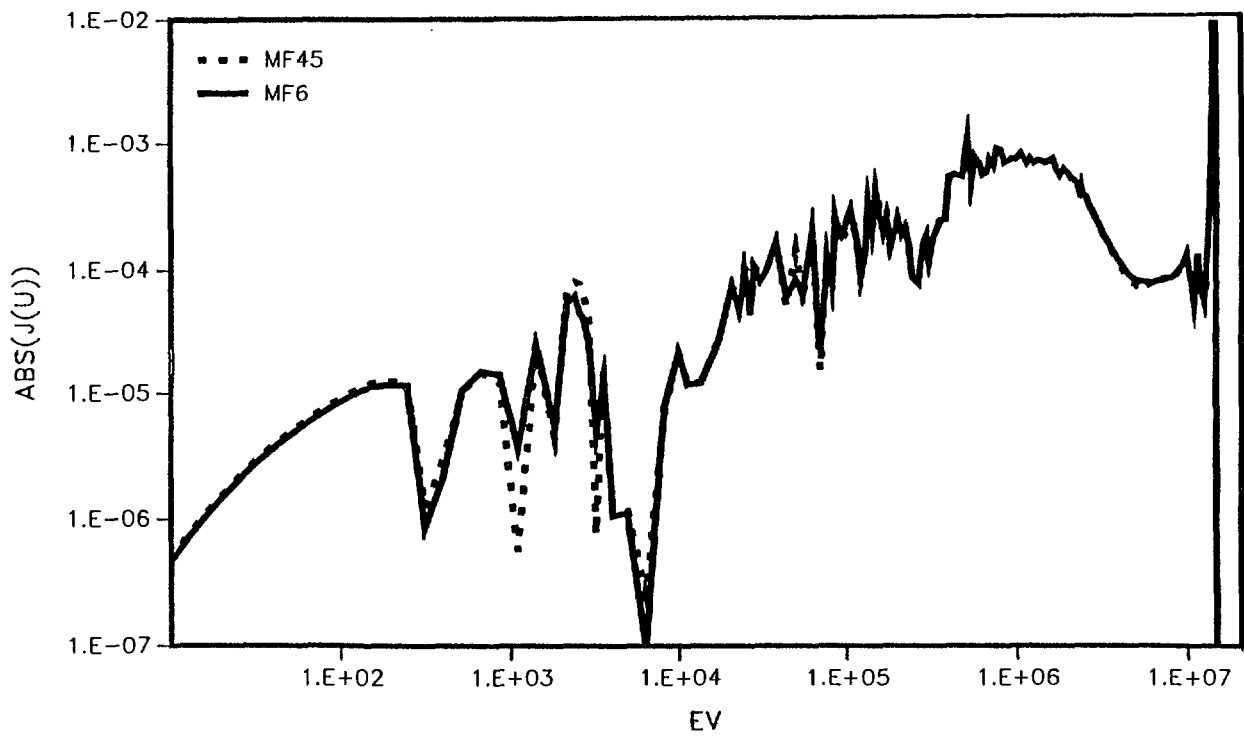
30% LI-6 20CM BREEDING MANIFOLD (MIDDLE) (MF45 VERSUS MF6)



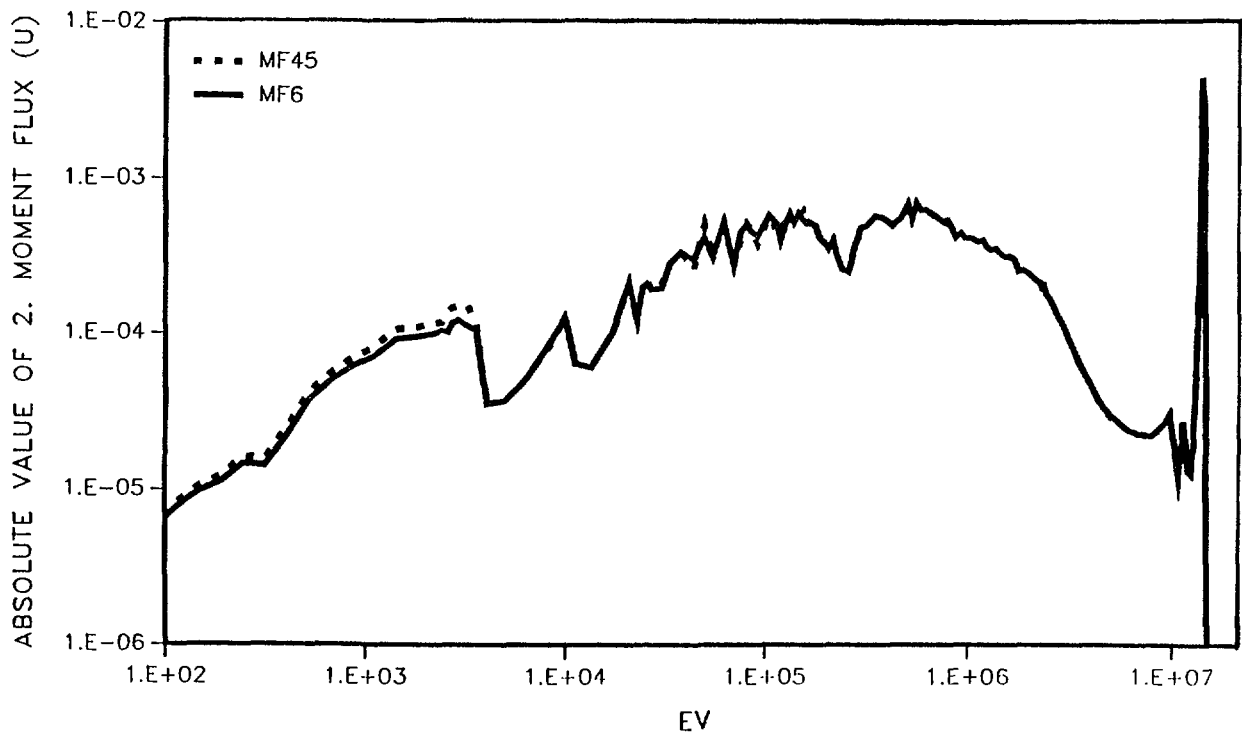
30% LI-6 20CM BREEDING SHIELD (RIGHT) (MF45 VERSUS MF6)



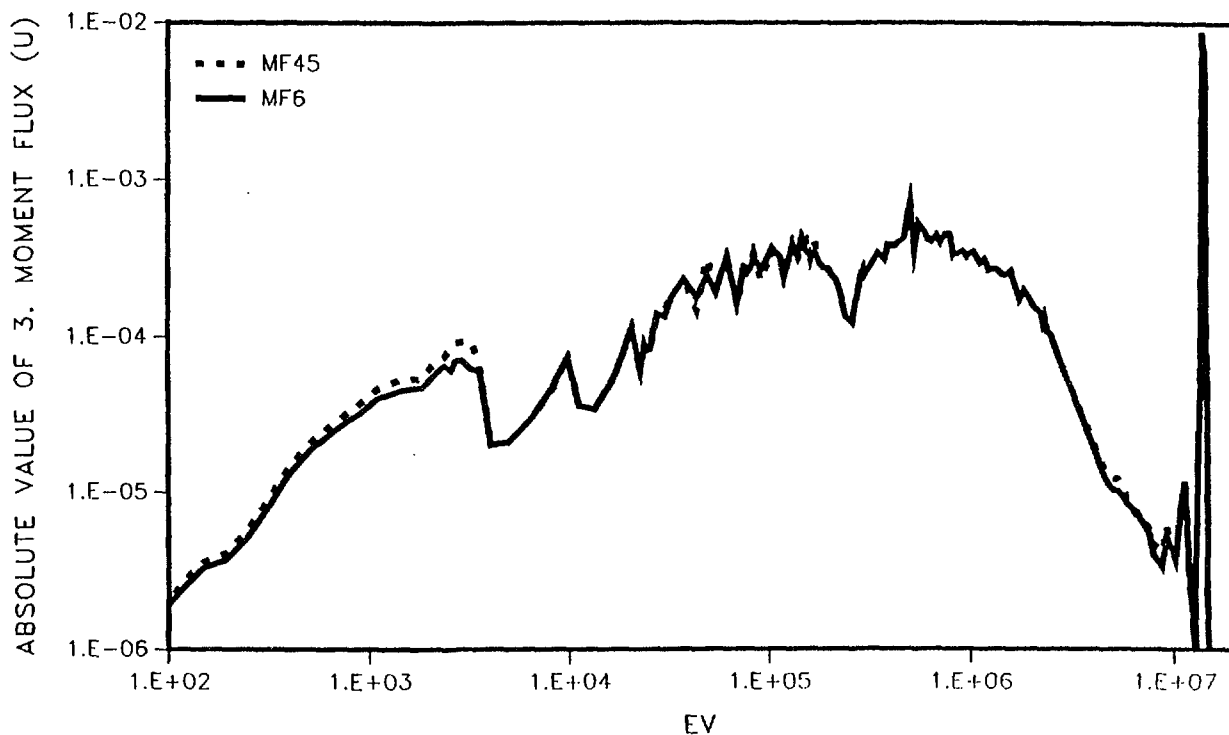
30% LI-6 BREEDING MEDIUM POSITION CURRENTS (MF45 VERSUS MF6)



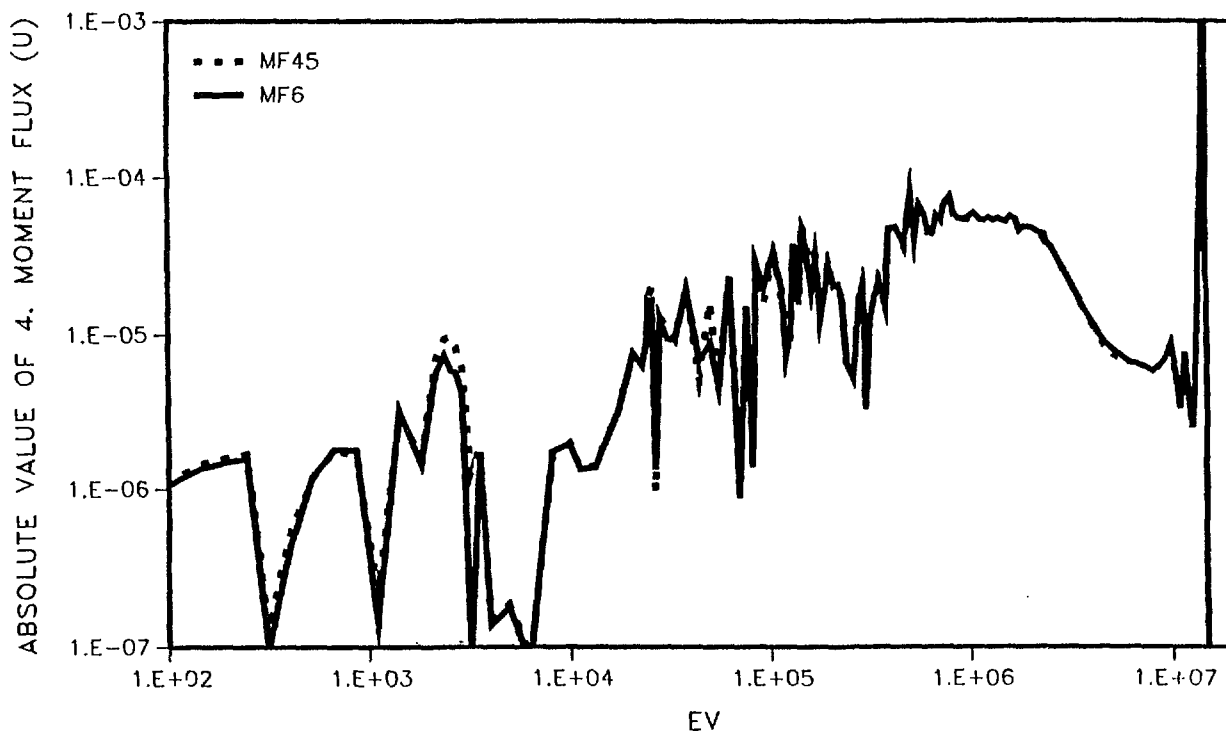
30% LI-6 MEDIUM POSITION 20 CM BREEDING PHI2 (MF45 VERSUS MF6)



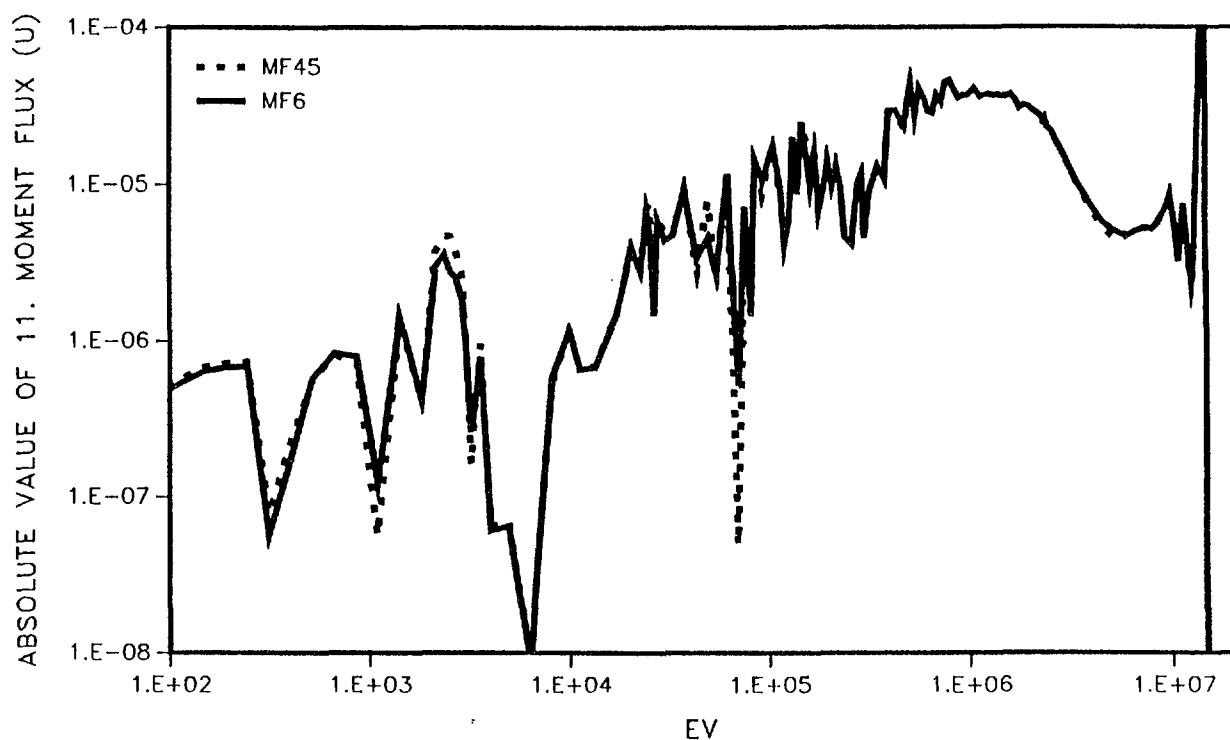
30% LI-6 MEDIUM POSITION 20 CM BREEDING PHI3 (MF45 VERSUS MF6)



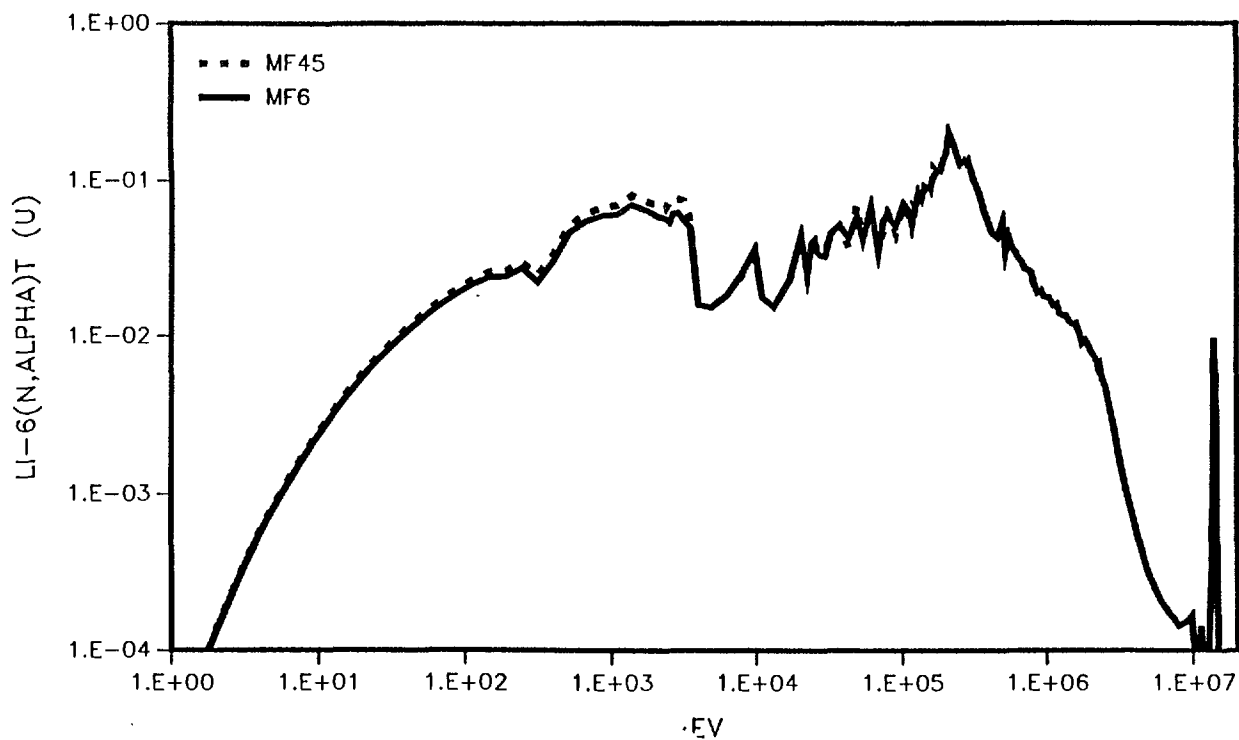
30% LI-6 MEDIUM POSITION 20 CM BREEDING PHI4 (MF45 VERSUS MF6)



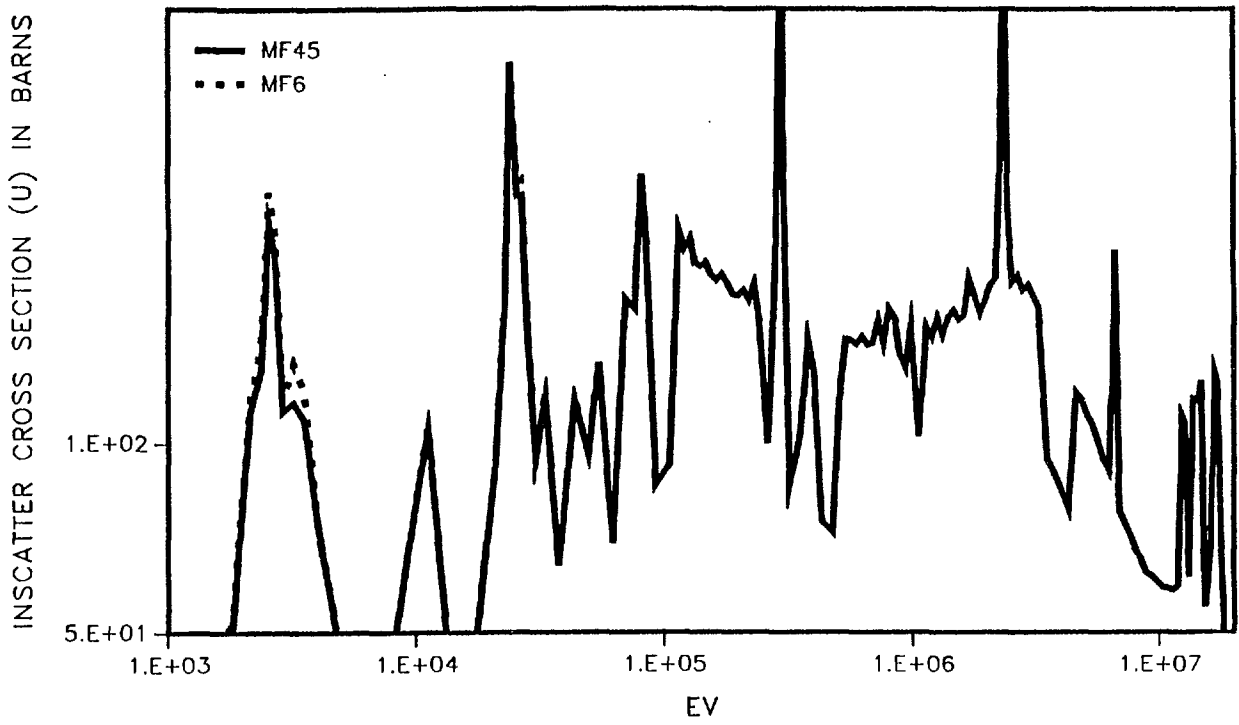
30% LI-6 MEDIUM POSITION 20 CM BREEDING PHI11 (MF45 VERSUS MF6)



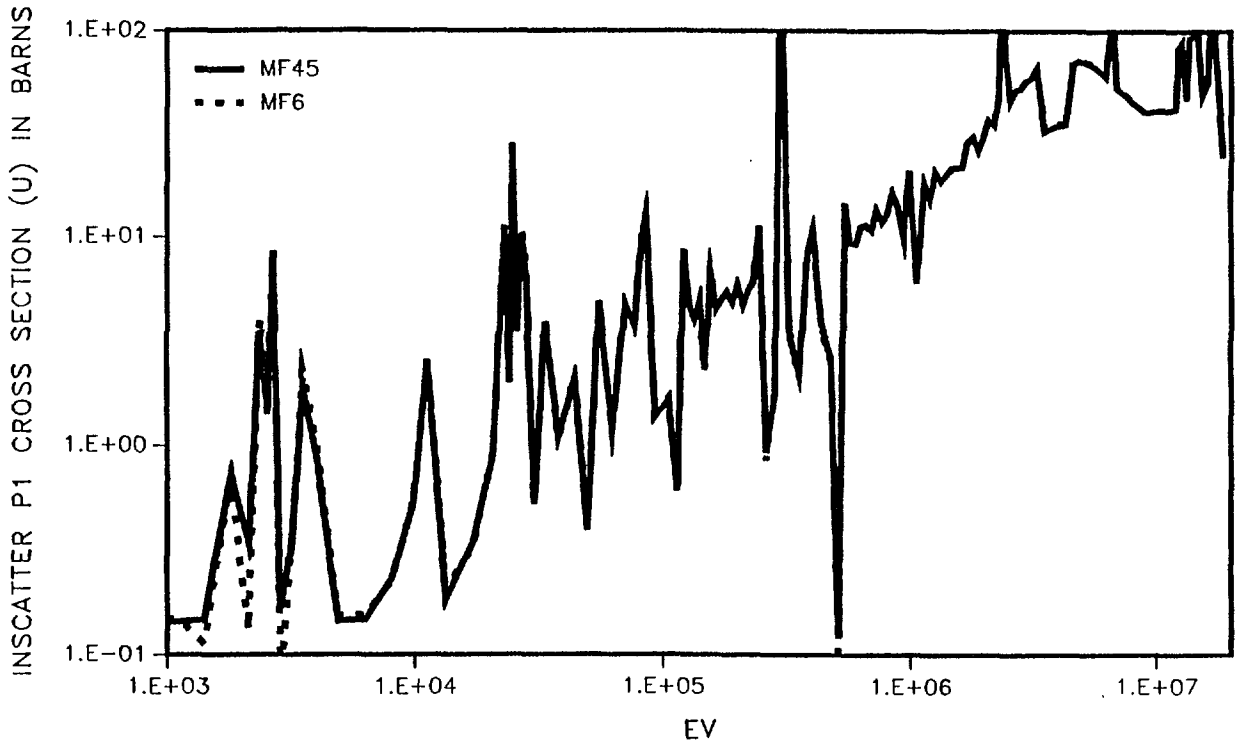
LI-6(N,ALPHA)T REACTION RATE RATIO IN 20CM BREEDING BLANKET (30% LI-6 IN LI)



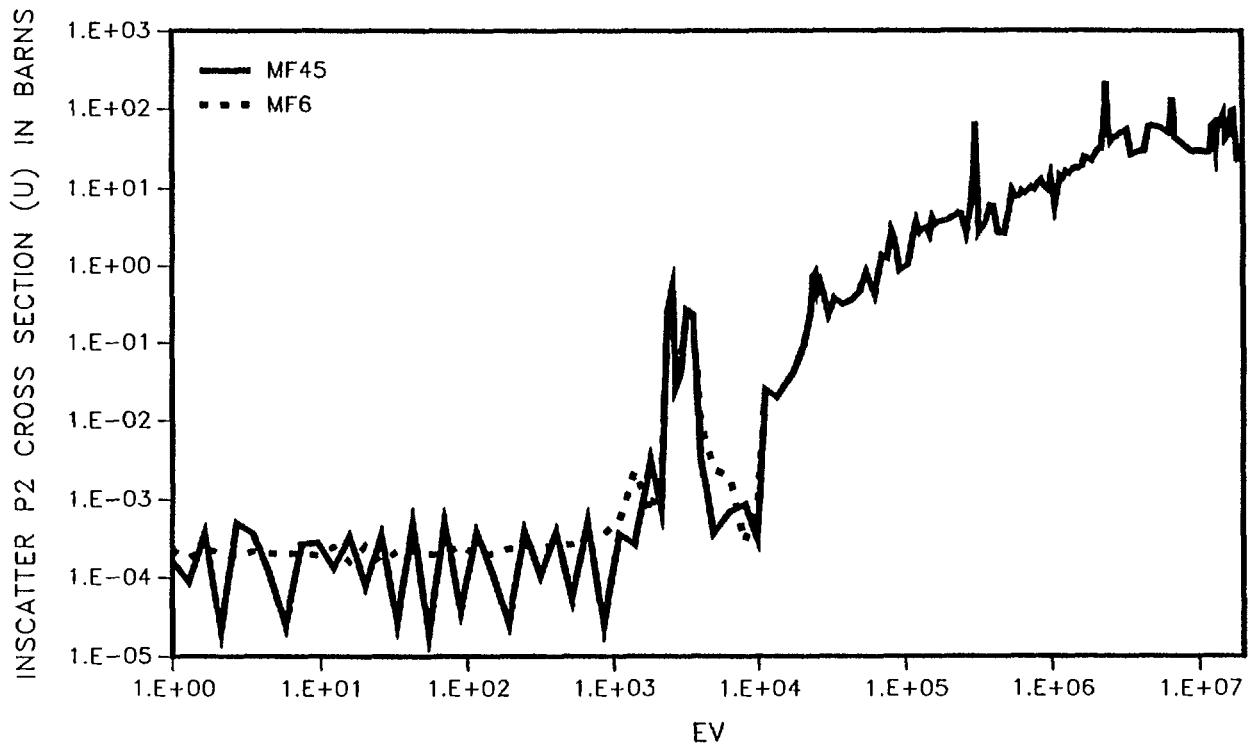
INSCATTER CROSS SECTIONS OF LEAD



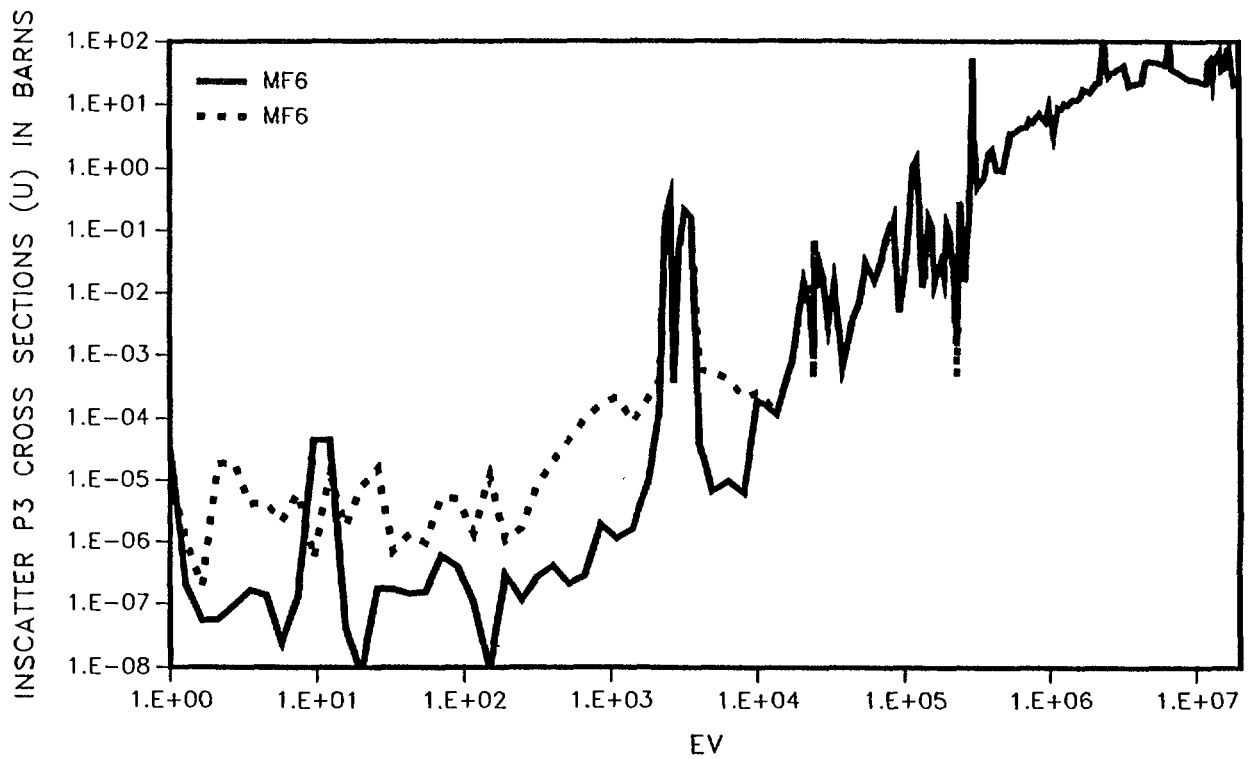
LEAD P1 INSCATTER CROSS SECTIONS



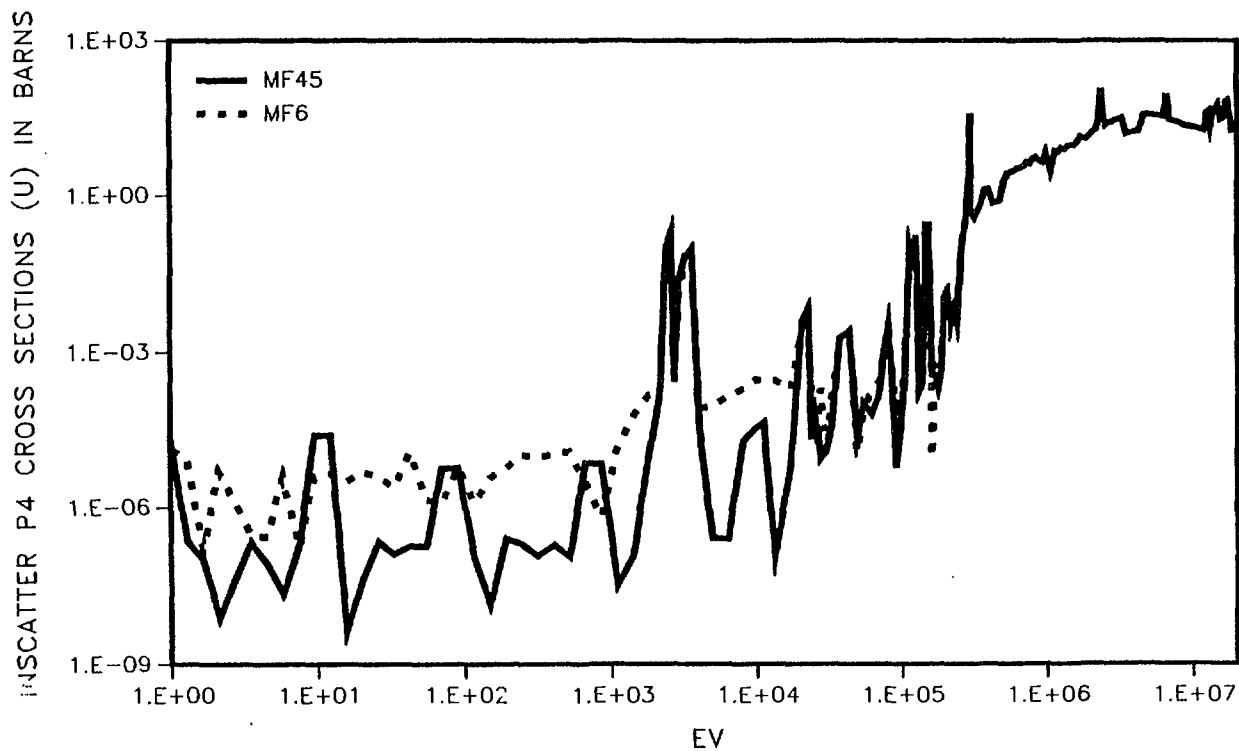
LEAD P2 INSCATTER CROSS SECTIONS



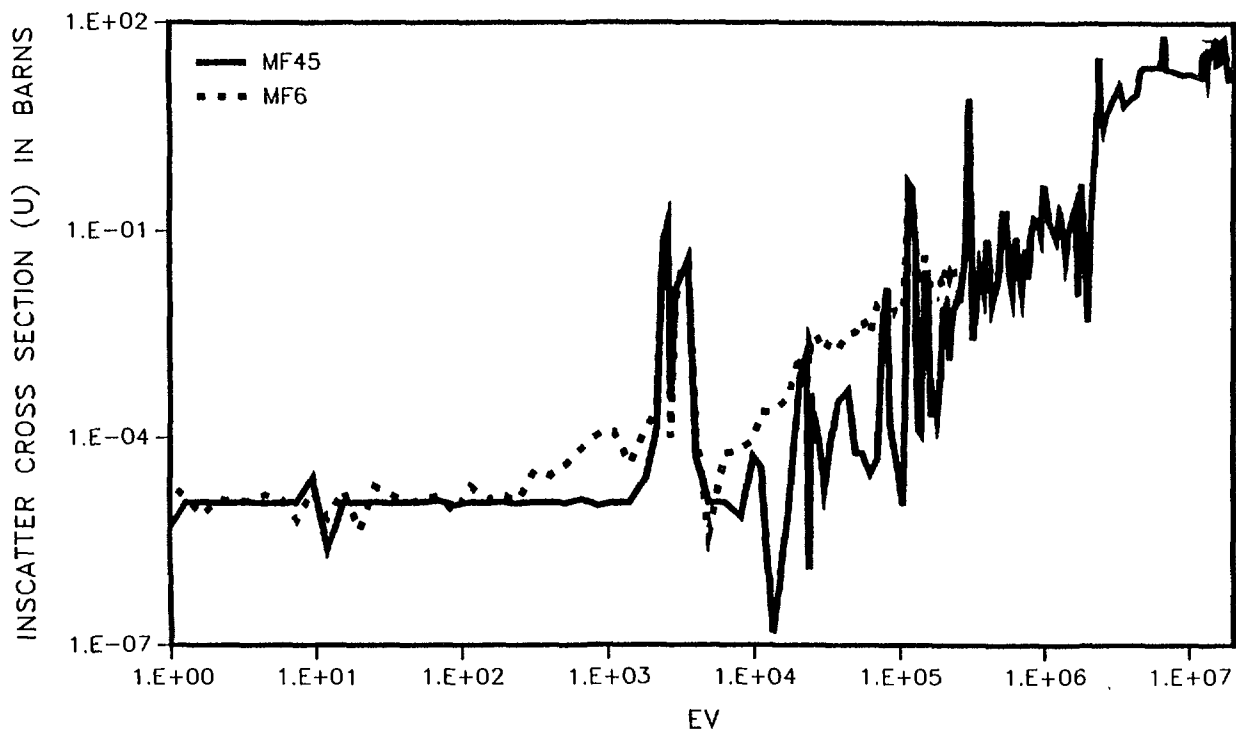
LEAD P3 INSCATTER CROSS SECTIONS (ABSOLUTE VALUES)



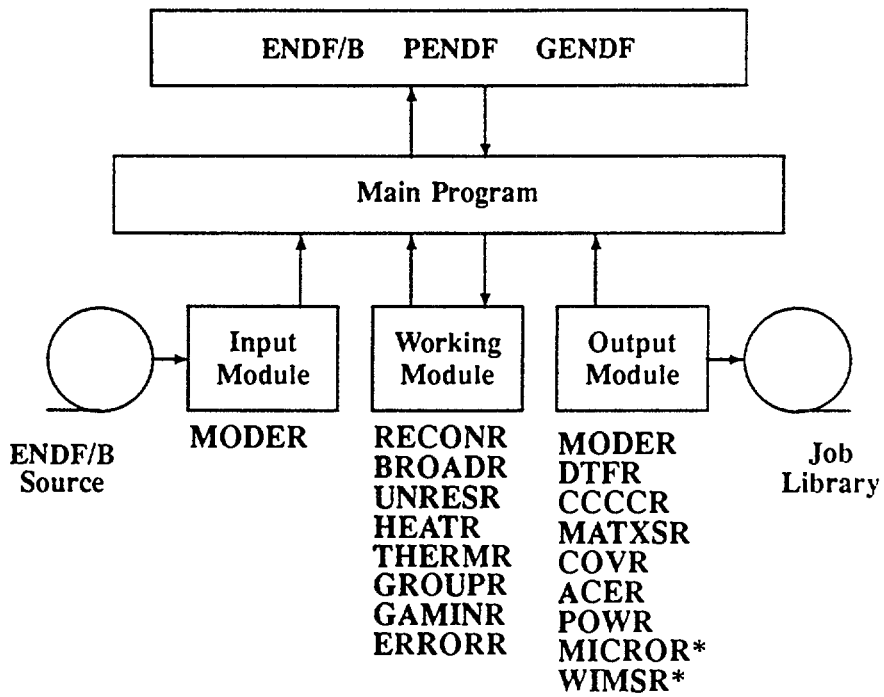
LEAD P4 INSCATTER CROSS SECTIONS (ABSOLUTE VALUES)



LEAD P5 INSCATTER CROSS SECTIONS (ABSOLUTE VALUES)



NJOY



* PSI Implementations

7.14 NEUTRON MULTIPLICATION IN LEAD IN THE EXPERIMENTS
WITH NEUTRON GENERATORS

D.V.Markovskij

I.V.Kurchatov Institute of Atomic Energy, Moscow, USSR

INTRODUCTION

A tendency to achieve a maximal production of useful products (tritium, fissile fuel) in the fusion reactor blanket results in the use of neutron-multiplicating materials in the first blanket layers. Lead is one of the promising multipliers in "pure" reactors [1] and in hybrid ones [2]. This can explain a noticeable interest in the study and precision of its neutron data in differential and integral experiments [4-7], in data evaluation [8] and its testing in calculations.

A calculational analysis of experimental data on neutron multiplication in lead spheres with a neutron generator as a neutron source shows that the calculation with various neutron data in all the cases [4-7] underestimates the multiplication and a discrepancy increases with increase in the lead layer thickness, reaching ~ 0.2 at $\Delta = 22.5$ cm [6]. An increase in the cross-section of $(n, 2n)$ - reaction and in the energy of secondary neutrons in inelastic reactions [4,6] has been proposed as a technique for data corrections to eliminate the discrepancy.

A calculational analysis of neutron multiplication in lead, including the estimates of multiplication limits for the standard ENDF/BIV data set and the effects of various changes in the data themselves, is done in a

given paper. The calculations have been done with the BLANK-code [9] realizing the Monte-Carlo method in the whole energy range.

In the range of energies higher than 0.1MeV the 52 Group constants prepared from the files of evaluated data have been used. Below 0.1 MeV the 13-Group constants have been used for the calculation in the P_4 -approximation [10].

Multiplication limit in the calculation with the ENDF/BIV data file

Experimental data on neutron multiplication in lead spheres of different thickness are given in Fig.1. In the experiments on OKTAVIAN [4] the neutron leakage measurements by the time-of-flight technique in the energy range 17 keV - 15 MeV with the spheres 3,6,9,12 cm thick, ha-

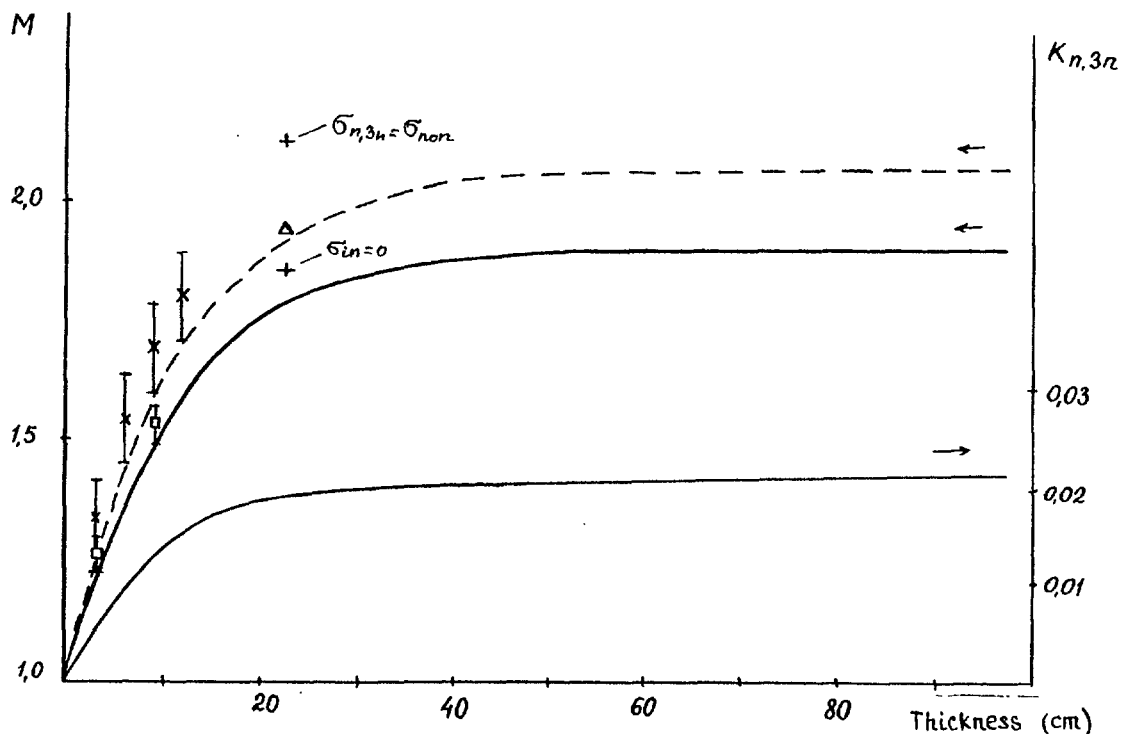


Fig.1. Neutron multiplication vs. spherical lead layer thickness.
 — Calculation with ENDF/BIV data, -- calculation with the changed data.
 Experiments: * [4], Δ [6], □ [7].

ving an internal radius 10 cm, were done. The multiplication within the spheres 6 and 9 cm thick, internal radii 3 cm and 6 cm, was measured by the total absorption (boron tank) technique at the I.V.Kurchatov Institute of Atomic Energy. In the joint experiment done by Dresden Technical University, the Central Institute of Nuclear Researches, GDR, and by the I.V.Kurchatov Institute of Atomic Energy [6] the neutron leakage from the sphere with the radius 25 cm was measured by the time-of-flight technique in the range 1-14 MeV together with the measurements with a hydrogen chamber in the range 0.05-1 MeV and with a stilbene scintillator in the range 0.75-14 MeV. The calculated curve of multiplication dependence on thickness for a lead sphere with the internal radius 2.5 cm is given in Fig.1 for comparison. The calculations have been done for the isotropic source with uniform neutron energy distribution in the range 13.5-14.92 MeV. One can see that the curve is saturated, when the lead layer is about 50cm thick, and an asymptotic value of multiplication in lead for the data file ENDF/BIV is 1.9. For the lead layer 22.5 cm thick in the experiment [6] the calculated multiplication is about 1.78, i.e. close to the calculations with other data for lead (see Table 4 [6]) and noticeably lower than the experimentally-measured value 1.94. The calculation underestimates the multiplication at other experimental points at Fig.1 too.

The calculated dependences of multiplication on the energy of neutrons within the range 13.5-14.92 MeV for a layer 22.5 cm thick and for an infinitely - thick one are given in Fig.2. Horizontal lines correspond to the multi-

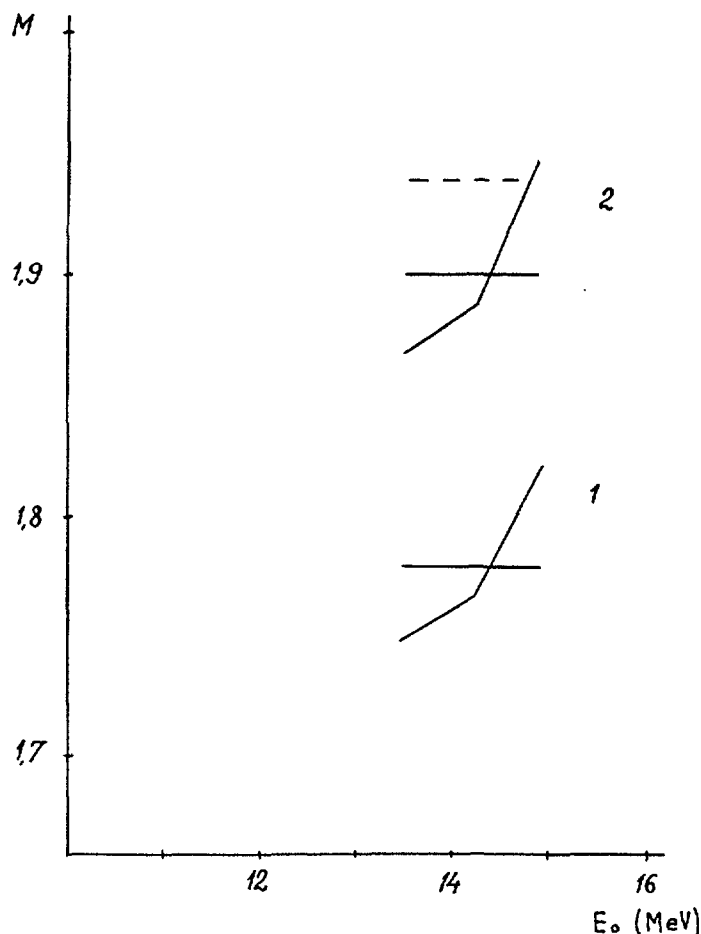


Fig.2. Multiplication vs. neutron source energy.
 1 - $\delta_{Pb} = 22.5$ cm, 2 - $\delta_{Pb} \rightarrow \infty$

plication at an uniform source energy distribution in the range 13.5-14.92 MeV. One can see that the slope of the curves increases above the (n,3n) - reaction threshold (14.18 MeV). However, a value of total multiplication does not reach the experimental one for the thickness 22.5 cm even at an infinitely - thick layer and at a maximum-possible source energy. Thus, in the calculation with the data from the ENDF/BIV Library for lead it is impossible, in principle, to obtain the multiplication factor 1.94 measured in [6] .

Multiplication dependence on data variations

In connection with a considerable discrepancy between calculations and experiments, it is of interest to analyze the opportunities for an increase in multiplication in the calculations by a change in some limits for various data in the initial file for lead. Such an analysis can be formally done to estimate the scales of corresponding effects, i.e. without discussions about whether it is admissible or not.

An increase in multiplication, in principle, can be related with the possibility of $(n, 2n)$ branching process due to increase in the energy of secondary neutrons in the data file and due to reduction in the effective threshold of this reaction, by increase in the $(n, 2n)$ -reaction cross-section in the range of source energies and by increase in the $(n, 3n)$ -reaction threshold.

The calculations of corresponding effects have been done for a sphere 22.5 cm thick, for which the neutron leakage from a source is small and the multiplication by the $(n, 2n)$ -channel is close to saturation. The most of changes in data have been done directly in the working group constants for lead processed from the ENDF/BIV file.

In order to estimate an effect of secondary multiplication in the $(n, 2n)$ -reaction a number of calculations, where neutrons were marked by a type of inelastic interaction (inelastic scattering or $n, 2n$) from their birth up to the end of their history (leakage or absorption), has been done. From these calculations it follows that about 96% of the $(n, 2n)$ -reactions occur under neutrons without their preliminary inelastic scattering for the un-

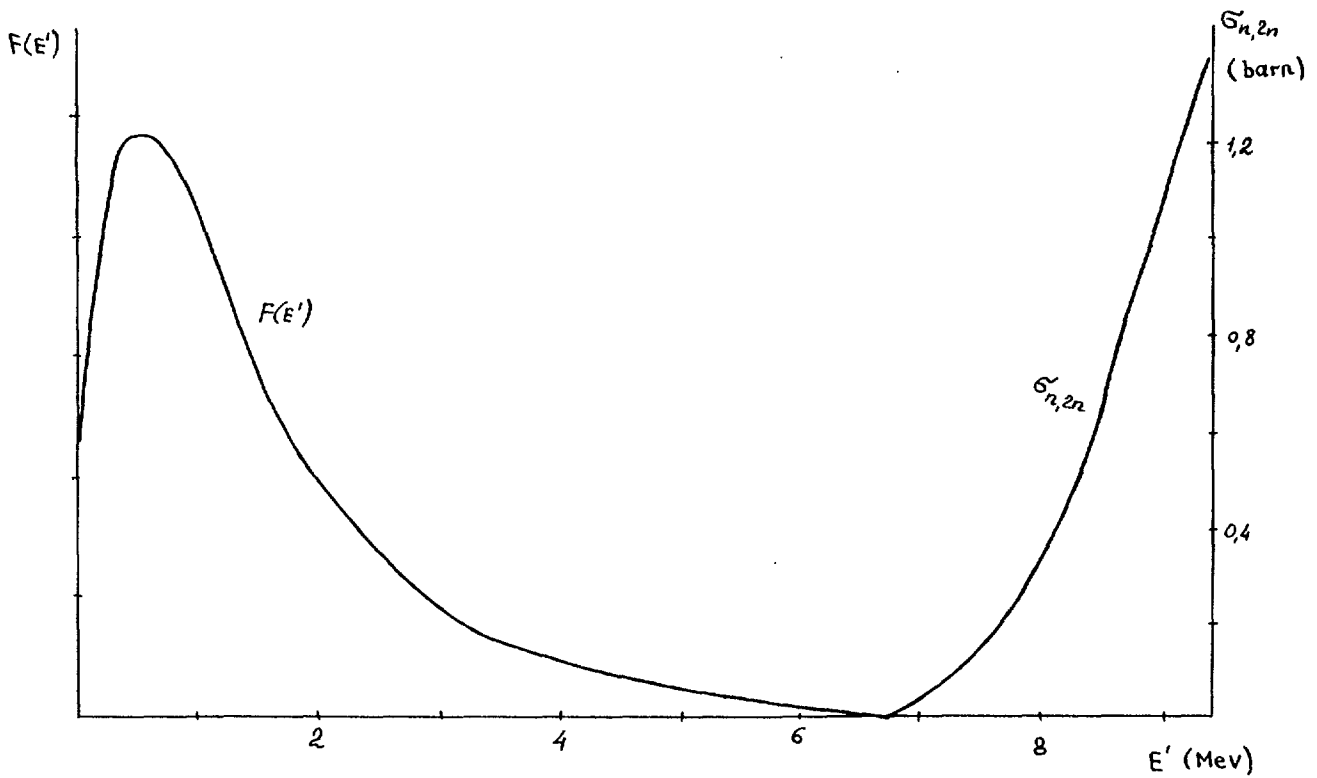


Fig.3. Spectrum of secondary neutrons from (n,2n) - reaction.

perturbed data file and about 4% of them are produced by the neutron after one inelastic scattering, the contribution of the (n,2n)-reactions after two inelastic scatterings being negligible ($\sim 0.03\%$). The secondary multiplication of neutrons by the (n,2n)-reaction in the calculation with the ENDF/BIV-data is absent, since the maximal energy of secondary neutrons from the (n,2n)-reaction equal to 6 MeV is lower than the reaction threshold 6.766 MeV (Fig.3). The calculations with the secondary neutron spectrum having distribution "tail" extended up to $E \approx E_0 - E_{\text{threshold}} = 7.3$ MeV have shown that the fraction of secondary (n,2n)-reactions is small (about 0.03%). It is evident that the secondary neutrons of successive (n,2n)-generations have the energy much lower than the threshold and further breeding is impossible. A change in the shape of (n,2n)-cross-section curve in the vicinity to the threshold in the calculation with the changed spectrum of secondary neutrons

also does not result in an essential multiplication growth. Thus, the secondary multiplication in the $(n,2n)$ -reaction in lead is absent or so small that it cannot explain the discrepancy between calculations and experiments.

As noted above, in a sphere 22.5 cm thick, the $(n,2n)$ - reaction rate is close to saturation and one can expect that an increase in the cross-section will have a low effect on the breeding growth. An estimate for the maximal multiplication growth due to the $(n,2n)$ -reaction has been done to verify this assumption. The probability of inelastic scattering in the range 13-14.18 MeV was put to be equal zero, and the probability of the $(n,2n)$ -reaction was equal to the total probability of inelastic interaction. The multiplication obtained in this calculation is equal to $M=1.846$ (as shown in Fig.1) and is much lower than that measured in the experiment [6] and confirms the assumption about a weak dependence of breeding in a thick sphere on the $(n,2n)$ -cross-section.

In experiments with neutron generators the neutron energy of a source is usually assumed to be uniformly distributed in the range 13.5-14.9 MeV; thus, at the energy higher than the threshold 14.18 MeV the neutron multiplication in the $(n,3n)$ -reaction takes place. The calculated dependence of this reaction rate on the lead layer thickness for the data file ENDF/BIV is given in Fig.1. For a large thickness of the layer the reaction rate is equal to 0.022 that corresponds to an average $(n,3n)$ -reaction probability in the range 14.18-14.9 MeV equal to 0.055.

In order to estimate the dependence of multiplication on the ratio of $(n,2n)$ - cross-section to $(n,3n)$ - one

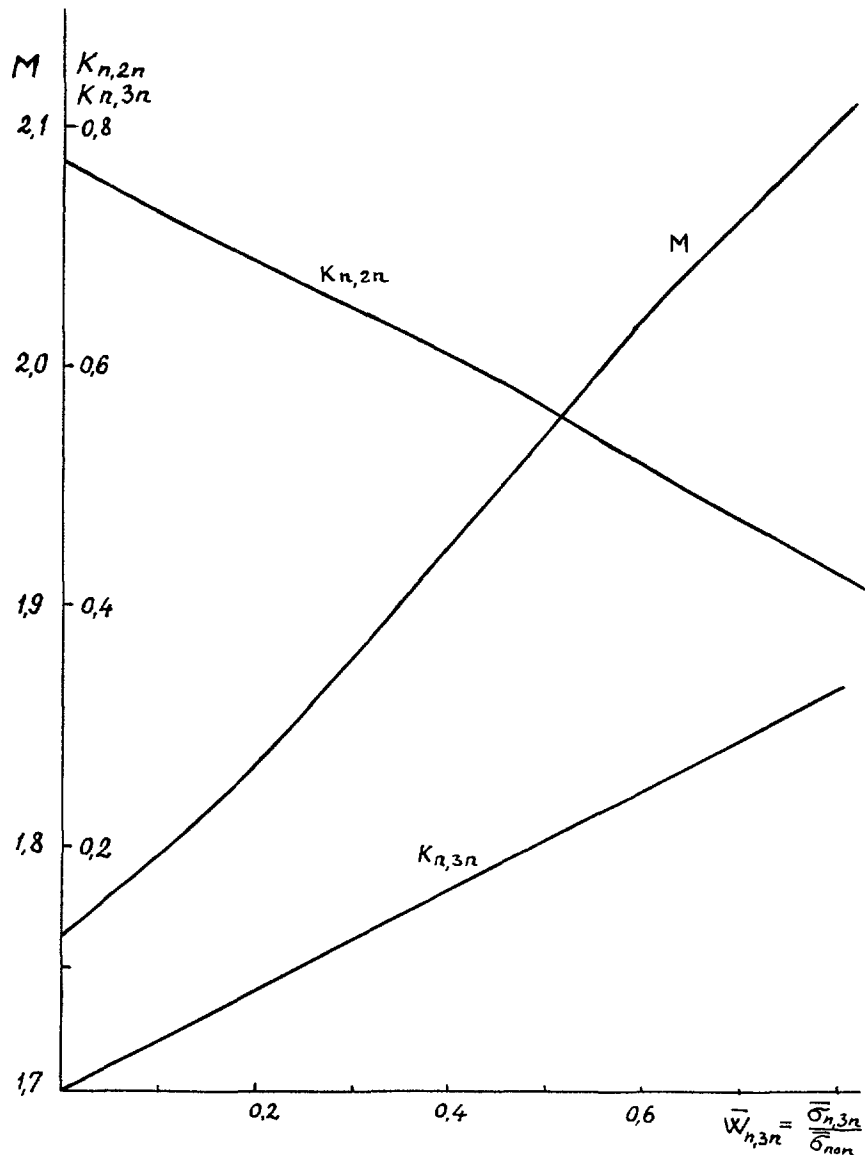


Fig.4. Multiplication in the sphere 22,5 cm thick vs. average probability of (n,3n) - reaction in the range 14.18-14.9 MeV.

in this energy range a number of calculations was done, where an average probability of the (n,3n)-reaction (up to the limit value 0.86) was varied with simultaneous variation in the (n,2n)-reaction probability at a fixed total inelastic and inelastic scattering cross-sections. The results of calculations are given in Fig.4. One can see that the experimental multiplication for a sphere 22.5cm thick can be obtained at an average (n,3n)-reaction probability equal to about 0.4 in the range 14.18-14.9 MeV. The

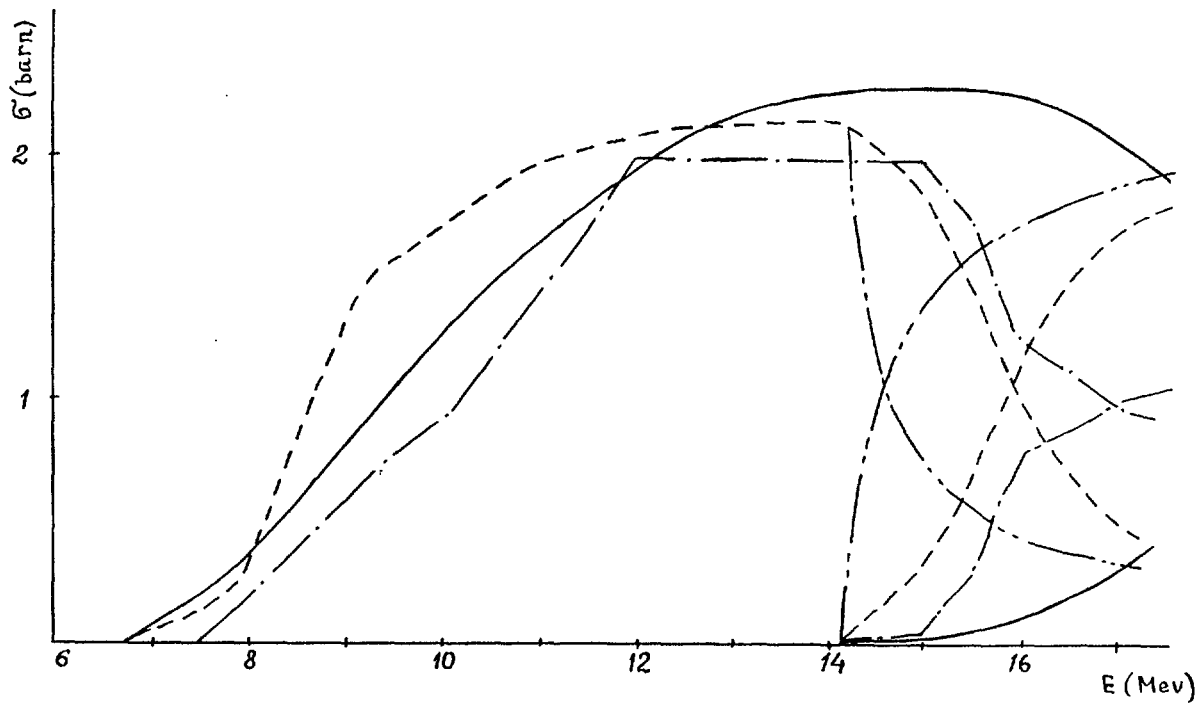


Fig.5. Cross-sections of neutron multiplication in lead

— BROND; --- ENDF/BIV; - - - ENDL-75; - · - · - changed $n,3n$

shapes of energy dependencies fit for the cross-sections of $(n,2n)$ and $(n,3n)$ - reactions are shown in Fig.5 in comparison with the corresponding curves from the ENDF/BIV files, ENDL-75, EFF-1. The calculated dependence of multiplication on the thickness of a sphere with these data introduced into the file of lead in ENDF/BIV are shown in Fig.1. One can see that this curve within its error bars is in agreement with experimental values.

Thus, a change in the cross-section for the $(n,3n)$ -reaction in the range 14.18-14.9 MeV by an effect on multiplication can serve as a means of eliminating the discrepancy between calculations and experiments. However, it should be noted that if the discrepancy in multiplication within lead between calculations and experiments is caused by an inaccuracy in the $(n,3n)$ -reaction cross-section, the very discrepancy belongs, to a great extent, to the calculations of the models with a neutron spectrum from a neu-

tron generator, where the neutron energy "smearing" reaches 13.5-14.9 MeV at the deuteron energy in the range 150-200 keV. Therefore, the experiments with different energies of deuterons, in principle, can give different results in breeding within the spheres of the same geometry observed in the comparison of experiments. In a D-T fusion reactor, where the ion energy is lower (~ 10 keV), an effect of the (n,3n)-reaction will be less significant. Therefore the compensation of discrepancy between the calculations and the experiments with neutron generators by a change in the (n,2n) cross-section or in some other data can result, in this case, in errors in the reactor calculations.

CONCLUSION

A calculational analysis of neutron multiplication in lead spheres for the experiments with neutron generators allows one to make the following conclusions:

1. Neutron breeding in the experiments with lead spheres in all the cases mentioned above is higher than that in the calculations with different versions of lead evaluated data.

2. This discrepancy is so great that in the calculations with the ENDF/BIV data for lead it cannot be eliminated by variation in the source energy and in the geometry of the model used in the calculation.

3. The analysis done for the dependence of multiplication in the sphere 22.5 cm thick on variations in different data for lead has shown that a discrepancy between the experiment and the calculation for this sphere cannot

be eliminated by an increase in the (n,2n)-reaction cross-section in the source energy range up to a value equal to the total inelastic cross-section. Variations in the spectrum of secondary neutrons and in the effective threshold of the (n,2n)-reaction give a negligible effect of multiplication by secondary neutrons in this reaction.

4. The maximal opportunity of formal multiplication growth can correspond to an increase in the (n,3n)-reaction cross-section in the range from a threshold to a maximum energy in the spectrum of a neutron generator (14.92 MeV is assumed in the calculations). The calculation with the chosen (in this range) ratio between the (n,2n) and (n,3n)-reactions corresponding to the average probability $W_{n,3n} = \frac{\sigma_{n,3n}}{\sigma_{n,2n}} \approx 0.4$, satisfactorily represents experimental results obtained for various lead layer thicknesses.

5. The analysis done for a formal scale estimation of the effects in neutron multiplication in lead cannot evidently replace the necessary qualified study of the problem from the viewpoint of theory. An experimental verification of the role of (n,3n)-reaction in breeding within lead is desirable. It can be done in differential experiments with the neutron energy higher than the reaction threshold, as well as in integral experiments with spheres in the measurements of leakage dependent on a polar angle.

REFERENCES

1. International Tokamak Reactor. Phase one. IAEA STI (PUB), 619 (1982), p. 450.
2. Orlov V.V. et al. Experimental fusion reactor (OTR). The fusion reactor first wall issues and neutron-physical studies. Proc. CMEA member countries expert meeting, April 26-29, 1983, Sukhumi, Moscow, TsNII Atominform, 1984.
3. Wong C. et al. Livermore Pulsed Sphere Program Summary Through July 1971. UCRL-5144 (1972).
4. Takahashi A. Integral measurements and analysis of nuclear data pertaining to fusion reactors. Proc. of Conf. on Neutr. Interact. with Nucl. Santa-fe, May 1985.
5. Hansen L.F. et al. The transport of 14 MeV neutrons through heavy materials $150 < A < 208$, NSE, 92 (1986), 382.
6. Elfrut T. et al. The neutron multiplication of lead at 14 MeV neutron incidence energy. Atomkernenergie-Kerutechnik 44 (1987), 121-125.
7. Novikov V.M. et al. Measurement of 14 MeV neutron multiplication factor in spherical lead and bismuth assemblies by the total absorption method. INDC (CCP)-264G. Translated from Russian by IAEA, 1987.
8. Hermsdorf D. Description of file 8201 for lead for library "BROND", IAEA, Vienna, Report IND (GDR)-039 (1986).
9. Marin S.V. et al. The BLANK code for one-dimensional neutron field calculation in the model with fast neutron source. Voprosy atomnoi nauki i tekhniki. Ser.:

Fizika i tekhnika yadernykh reaktorov, vyp. 9(22),
p. 26-31. Moscow, NIKIET, 1981.

10. Zakharova S.V. et al. Nuclear-physical constants for reactor calculations. The bulletin of the informational center on nuclear data 3, N 1 (1967), Atomizdat 1978.

7.15 CALCULATION OF SPHERICAL MODELS OF LEAD WITH A SOURCE OF 14 MeV- NEUTRONS

D.V.Markovskij, A.A.Borisov
I.V.Kurchatov Institute of
Atomic Energy, Moscow

Neutron transport calculations of the lead benchmark-models have been carried out in accordance with the ^{IAEA}sponsored "Advisory Group Meeting" on Nuclear Data for Fusion Reactors Technology, Dresden/Gaussig, 1-5 December, 1988.

The draft specification of the models has been prepared and spread by E.T.Cheng /1/. It includes:

1) A spherical ~~(shell) lead~~ with a density of 11.34 g/cm^3 . The outer shell radius is 25 cm and the inner radius is 25 cm. The point isotropic neutron source at the centre of sphere has a uniform energy distribution in the range 13,5-14,92 MeV. This model corresponds to the experiment carried out at the Technical University, Dresden (TUD) /2/.

2) Four spherical shells of lead with an inner radius 10 cm and outer radii 13,16,19,22 cm. A source is similar to that of the model 1. The dimensions follow that of the OSAKA (OKTAVIAN) experiments /3/.

The calculations have been done with the one-dimensional code BLANK /4/ realizing the direct Monte Carlo method in the whole range of neutron energies.

In the energy range 0.1-15 MeV the code uses the multigroup constants prepared from the evaluated data files by the SMOK-code which actually is the modified version of the NEDAM-code /5/. The probabilities of processes are preset on the 52-group energy scale, for the elastic scattering anisotropy the 16-group scale is used. The data of inelastic processes are presented on the energy scale individual for each material in accordance with the inelastic reactions given in the evaluated data file. The secondary neutron anisotropy of inelastic reactions, in the form of double-differen-

tial cross-sections in the MF6-file of the ENDF/BVI-format is also taken into account.

The 13-group constants in the P_1 -approximation /6/ are used below 0,1 MeV.

The calculations have been done with the data of lead prepared from the files EFF, BROND, ENDF/BIV.

The comparison with the experiment of total and partial neutron leakage from the model I (TUD) is shown in Table I. The spectra of neutron leakage from the sphere are given in Figs. 1-3, detector activation and fission rates are given in Figs. 4,5 and in Table 2.

Table I

NEUTRON MULTIPLICATION IN MODEL I

| File | Energy range, MeV | | | | | | | | Sum | C/E |
|----------|-------------------|-------|-------|-------|--------|-------|-------|-------|-------|-------|
| | 0 - 1 | C/E | 1 - 5 | C/E | 5 - 10 | C/E | 10-15 | C/E | | |
| BROND | 0.887 | 0.803 | 0.739 | 1.079 | 0.019 | 1.0 | 0.128 | 0.889 | 1.763 | 0.906 |
| ENDF/BIV | 1.093 | 0.989 | 0.549 | 0.812 | 0.017 | 0.895 | 0.137 | 0.951 | 1.796 | 0.924 |
| EFF-1 | 0.977 | 0.884 | 0.605 | 0.895 | 0.023 | 1.21 | 0.138 | 0.958 | 1.743 | 0.897 |
| Exp. | 1.105 | | 0.676 | | 0.019 | | 0.144 | | 1.944 | |

The neutron leakage spectra from the model 2 (OKTAVIAN) are given in Figs. 6-9, integrals of the spectra in the energy ranges 0.13-15, 4-15, 0.017-15 MeV are given in Table 3. The dependence of total leakage on the thickness of spheres is shown in Fig.10.

From the comparison between the calculation and the experiment one can make the following conclusions:

1. Total multiplication in the calculation of the model I for all the data files is practically the same (1,73-1,78) and considerably lower than that obtained in the experiment (1,944).

The calculation with the BROND-data more precisely represents the neutron leakage spectrum at the energy higher than 1 MeV. However, at the energy lower than 1 MeV, it underestimates the leakage by about 20%. The calculation with the ENDF/BV-data, on the contrary, provides the leakage close to the experiment at $E > 1$ MeV and underes-

Table 2

ACTIVATION AND FISSION RATES IN THE DETECTORS IN MODEL I (PER ONE SOURCE NEUTRON
AND THE DETECTOR NUCLEUS, $\times 10^{28}$)

| Detector | File | 5 cm | C/E | 10 cm | C/E | 15 cm | C/E | 20 cm | C/E | 25 cm | C/E |
|-------------------------|--------|-------|------|-------|------|-------|------|-------|------|--------|------|
| $^{115}\text{In}(n,n')$ | BROND | 8.86 | 1.79 | 3.31 | 1.56 | 1.59 | 1.44 | 0.787 | 1.48 | 0.3 | 1.22 |
| | ENDF-4 | 8.51 | 1.72 | 3.19 | 1.50 | 1.49 | 1.35 | 0.700 | 1.92 | 0.228 | 0.93 |
| $^{58}\text{Ni}(n,p)$ | BROND | 9.79 | 1.41 | 2.06 | 1.10 | 0.718 | 1.14 | 0.295 | 0.95 | 0.113 | 0.67 |
| | ENDF-4 | 9.84 | 1.41 | 2.07 | 1.10 | 0.706 | 1.12 | 0.281 | 0.91 | 0.101 | 0.6 |
| $^{64}\text{Zn}(n,p)$ | BROND | 6.70 | 1.15 | 1.32 | 1.14 | 0.437 | 1.13 | 0.173 | 1.15 | 0.067 | 0.85 |
| | ENDF-4 | 6.80 | 1.16 | 1.34 | 1.15 | 0.439 | 1.13 | 0.170 | 1.15 | 0.063 | 0.80 |
| $^{27}\text{Al}(n,p)$ | BROND | 3.22 | 1.63 | 0.541 | 1.20 | 0.158 | 1.17 | 0.057 | 1.12 | 0.0224 | 0.94 |
| | ENDF-4 | 3.33 | 1.68 | 0.577 | 1.28 | 0.171 | 1.27 | 0.063 | 1.24 | 0.0245 | 1.03 |
| $^{65}\text{Cu}(n,p)$ | BROND | 22.37 | 1.25 | 3.66 | 1.01 | 1.05 | 0.88 | 0.370 | 0.80 | 0.146 | 0.65 |
| | ENDF-4 | 23.12 | 1.30 | 3.91 | 1.08 | 1.14 | 0.85 | 0.411 | 0.90 | 0.163 | 0.72 |
| $^{235}\text{U}(n,f)$ | BROND | 118.7 | 1.21 | 44.22 | 1.23 | 22.31 | 1.26 | 11.25 | 1.12 | 3.82 | 1.11 |
| | ENDF-4 | 131.4 | 1.34 | 51.35 | 1.43 | 25.81 | 1.46 | 12.70 | 1.27 | 3.84 | 1.12 |
| $^{238}\text{U}(n,f)$ | BROND | 37.52 | 1.23 | 9.27 | 1.14 | 3.62 | 1.42 | 1.61 | 1.33 | 0.618 | 1.28 |
| | ENDF-4 | 37.58 | 1.23 | 9.20 | 1.14 | 3.50 | 1.37 | 1.49 | 1.23 | 0.517 | 1.05 |
| $^{237}\text{Np}(n,f)$ | BROND | 119.9 | 1.38 | 40.29 | 1.42 | 19.15 | 1.46 | 9.48 | 1.39 | 3.52 | 1.38 |
| | ENDF-4 | 125.4 | 1.45 | 43.09 | 1.51 | 20.09 | 1.53 | 9.60 | 1.41 | 3.15 | 1.23 |
| $^{232}\text{Th}(n,f)$ | BROND | 11.05 | 1.74 | 2.56 | 2.02 | 0.96 | 1.12 | 0.416 | 1.20 | 0.160 | 1.13 |
| | ENDF-4 | 11.14 | 1.75 | 2.57 | 2.02 | 0.84 | 1.10 | 0.391 | 1.13 | 0.139 | 0.98 |
| $^{239}\text{Pu}(n,f)$ | BROND | 176.5 | | 69.4 | | 34.9 | | 17.2 | | 5.21 | 1.08 |

Table III

NEUTRON MULTIPLICATION IN MODELS 2

| File | Layer thick- ness, cm | Energy ranges, MeV | | | | | |
|----------|--------------------------------|--------------------|-------|--------|-------|--------|-------|
| | | 0.017-15 | C/E | 0.3-15 | C/E | 4 - 15 | C/E |
| BROND | | 1.195 | 0.891 | 1.168 | 0.919 | 0.787 | 0.983 |
| ENDF/BIY | 3 | 1.189 | 0.887 | 1.143 | 0.9 | 0.781 | 0.976 |
| EFF-1 | | 1.178 | 0.879 | 1.146 | 0.902 | 0.787 | 0.983 |
| EXPER | | 1.34 | | 1.27 | | 0.8 | |
| BROND | | 1.352 | 0.878 | 1.299 | 0.921 | 0.615 | 0.946 |
| ENDF/BIY | 6 | 1.352 | 0.878 | 1.26 | 0.894 | 0.614 | 0.945 |
| EFF-1 | | 1.33 | 0.863 | 1.263 | 0.896 | 0.621 | 0.955 |
| EXPER | | 1.54 | | 1.41 | | 0.65 | |
| BROND | | 1.471 | 0.87 | 1.391 | 0.927 | 0.479 | 0.887 |
| ENDF/BIV | 9 | 1.473 | 0.872 | 1.335 | 0.89 | 0.482 | 0.892 |
| EFF-1 | | 1.449 | 0.857 | 1.345 | 0.897 | 0.491 | 0.915 |
| EXPER | | 1.69 | | 1.5 | | 0.54 | |
| BROND | | 1.588 | 0.866 | 1.479 | 0.936 | 0.377 | 0.919 |
| ENDF/BIY | 12 | 1.572 | 0.873 | 1.389 | 0.878 | 0.37 | 0.902 |
| EFF-1 | | 1.543 | 0.857 | 1.399 | 0.885 | 0.378 | 0.922 |
| EXPER | | 1.8 | | 1.58 | | 0.41 | |

timates it by about 15% at $E < 1$ MeV. In the calculation with the EFF-1 data the least multiplication and underestimation of neutron leakage in the ranges below 0,1 MeV and higher than 1 MeV have been obtained.

A somewhat steeper dependence on the radius of location, than that in the experiment corresponds to the calculated activation rates of threshold detectors. It can be provided by overestimated probability of inelastic interaction in the calculation. Overestimation of the calculated rates by 10-15% in comparison with the experiment can be provided by ignoring the energy-angle source correlation within the framework of one-dimensional calculations.

2. In the calculations of Model 2 the total multiplication is lower by 10-15% than that obtained in the experiments at the OKTAVIAN-stand.

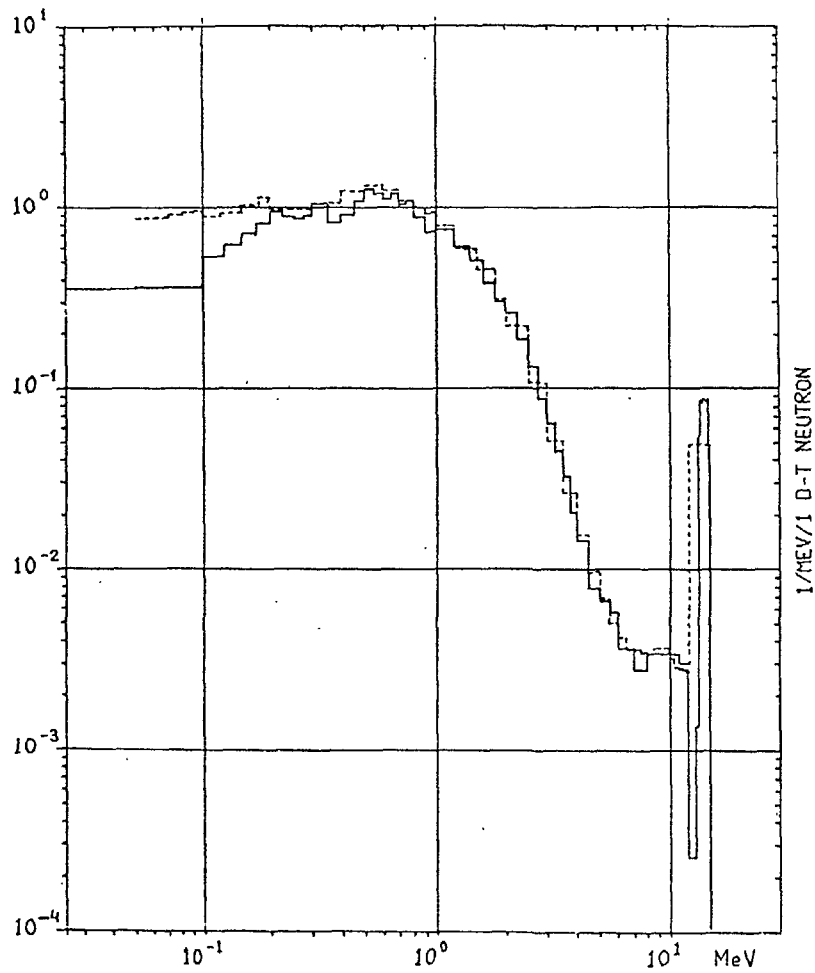


Fig. 1 Neutron leakage spectrum from PB sphere

$E_{source} = 13.5-14.92$ MeV

| | M_{TOT} | L_{TOT} | c/e | $L^{>0.05}$ | $L^{>1.00}$ | $L^{>5.00}$ | $L^{>10.00}$ |
|-------|-----------|-----------|-------|-------------|-------------|-------------|--------------|
| BROND | 1.773 | 1.763 | 0.907 | 1.750 | 0.876 | 0.147 | 0.128 |
| EXPER | | 1.944 | | 1.940 | 0.911 | 0.161 | 0.140 |

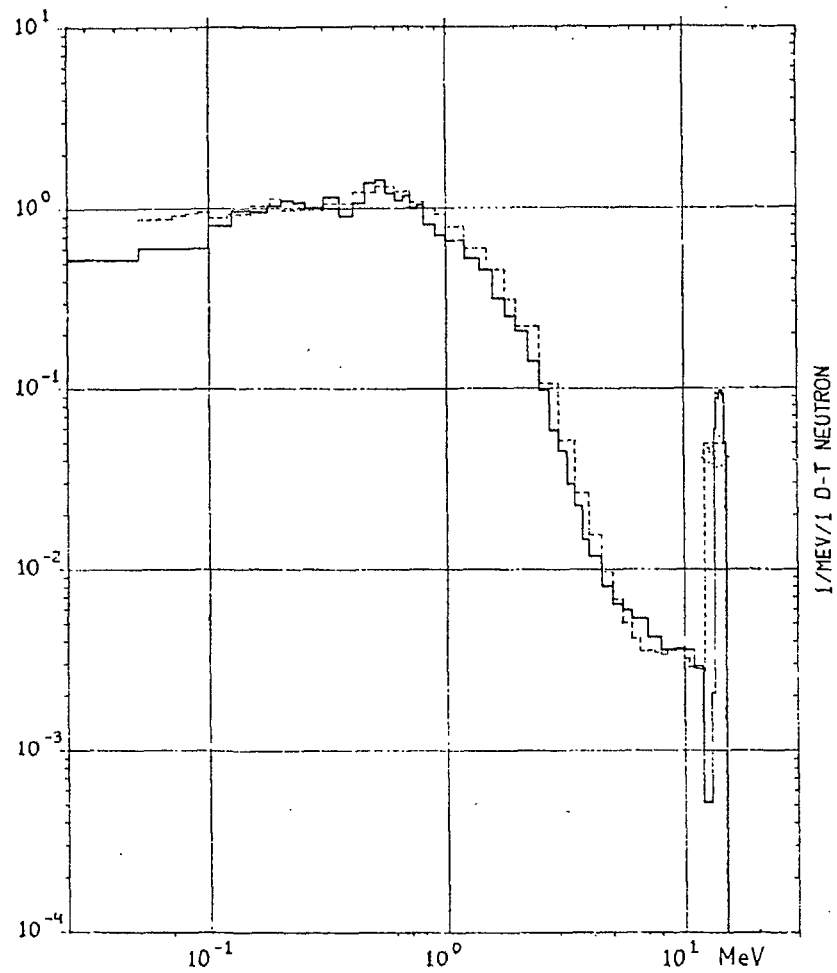


Fig. 2 Neutron leakage spectrum from PB sphere

$E_{source} = 13.5-14.92$ MeV

| | M_{TOT} | L_{TOT} | c/e | $L^{>0.05}$ | $L^{>1.00}$ | $L^{>5.00}$ | $L^{>10.00}$ |
|-------|-----------|-----------|-------|-------------|-------------|-------------|--------------|
| EFF | 1.755 | 1.744 | 0.897 | 1.721 | 0.766 | 0.161 | 0.138 |
| EXPER | | 1.944 | | 1.940 | 0.911 | 0.161 | 0.140 |

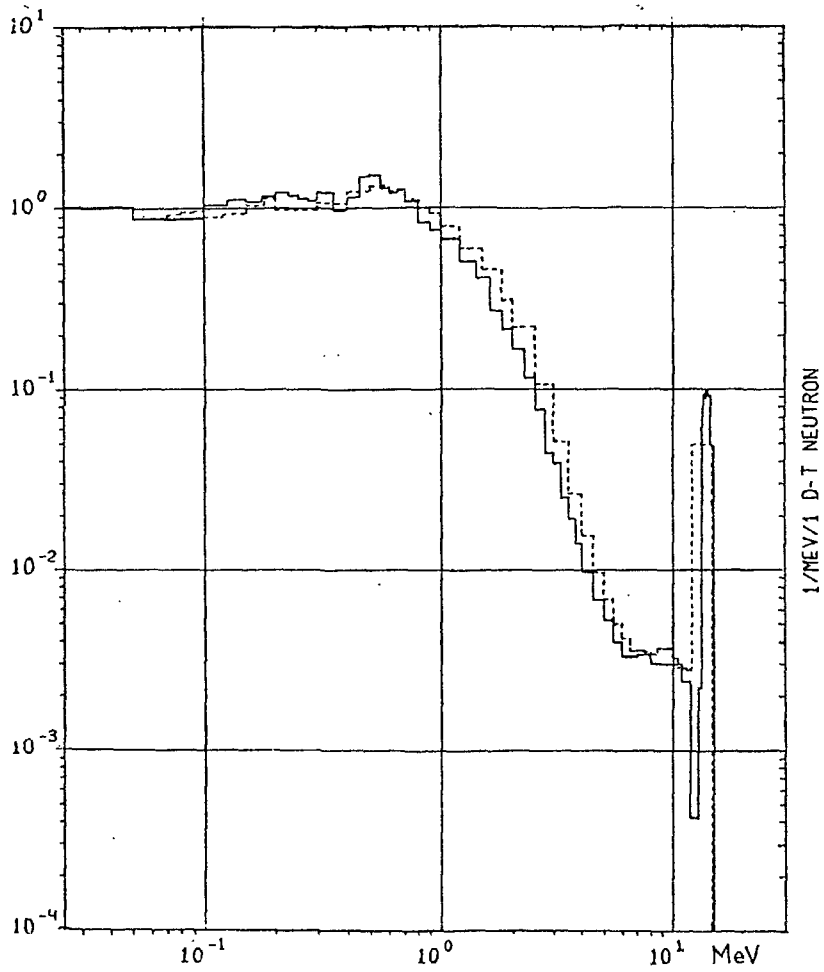


Fig. 3 Neutron Leakage spectrum from PB sphere

$E_{source} = 13.5-14.92$ MeV

| | M_{TOT} | L_{TOT} | c/e | $L^{>0.05}$ | $L^{>1.00}$ | $L^{>5.00}$ | $L^{>10.00}$ |
|--------|-----------|-----------|-------|-------------|-------------|-------------|--------------|
| ENDF-4 | 1.808 | 1.796 | 0.924 | 1.745 | 0.703 | 0.154 | 0.137 |
| EXPER | --- | 1.944 | --- | 1.940 | 0.911 | 0.161 | 0.140 |

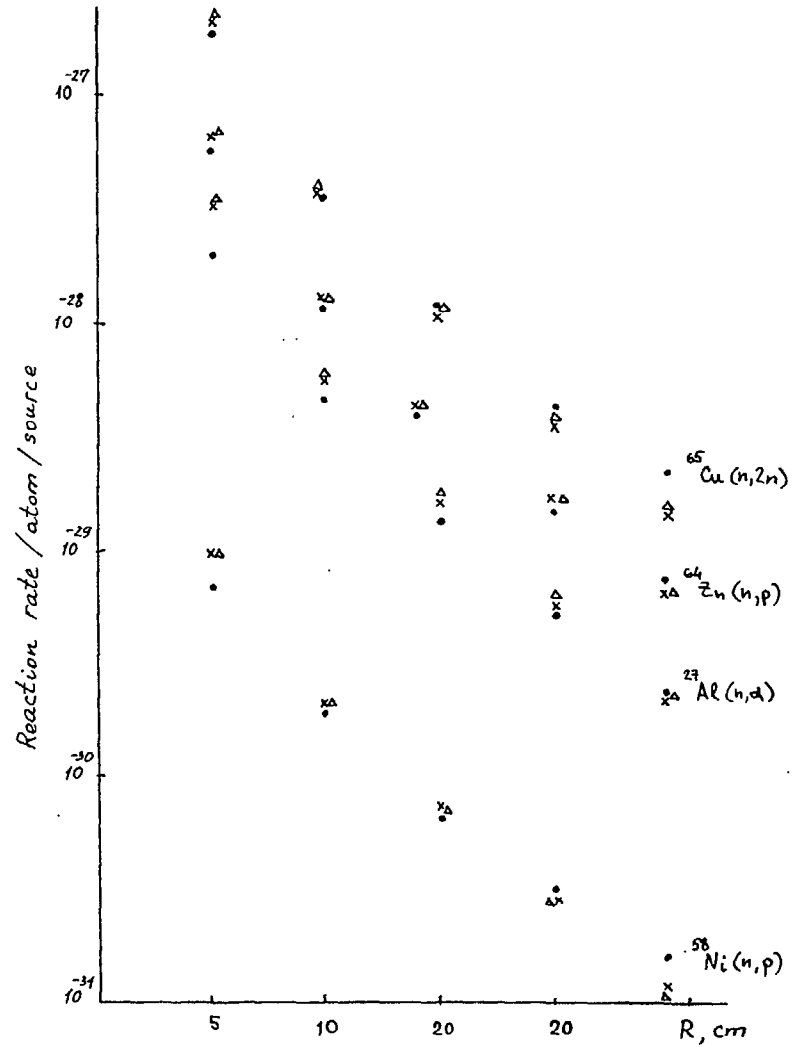


Fig. 4 Reaction rates in thick lead sphere.

x - BROND, Δ - ENDF/BIV
• Experiment [2]

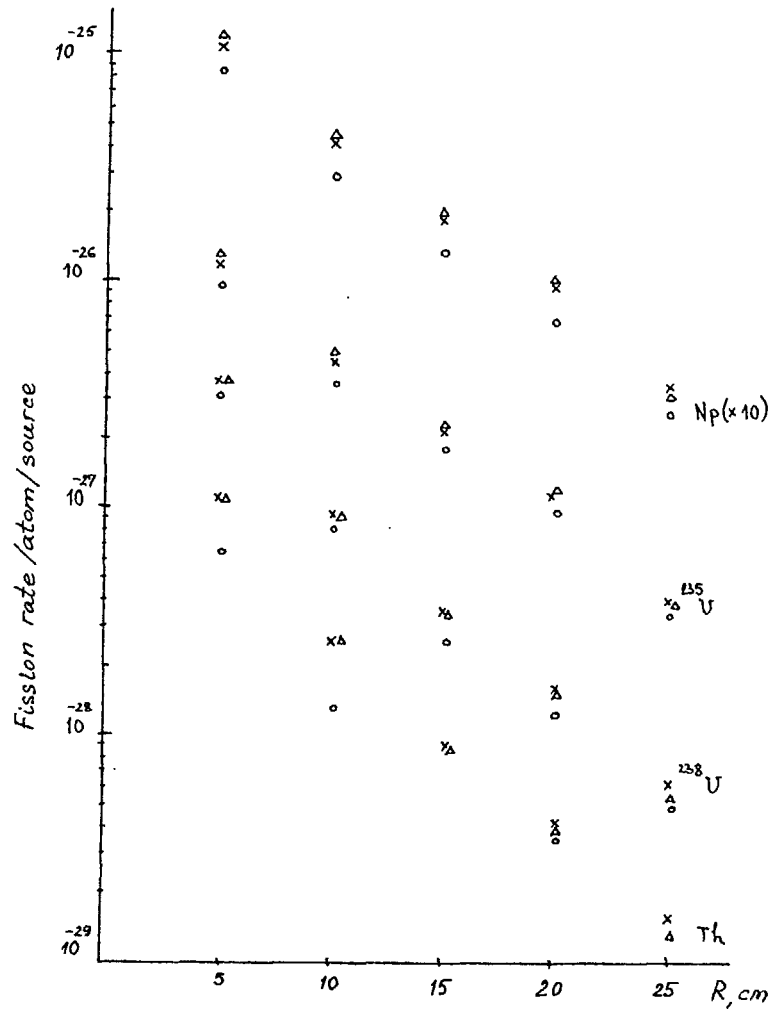


Fig. 5 Fission rates in thick lead sphere.

x-BROND, Δ - ENDF/BIV
Experiment o [2]

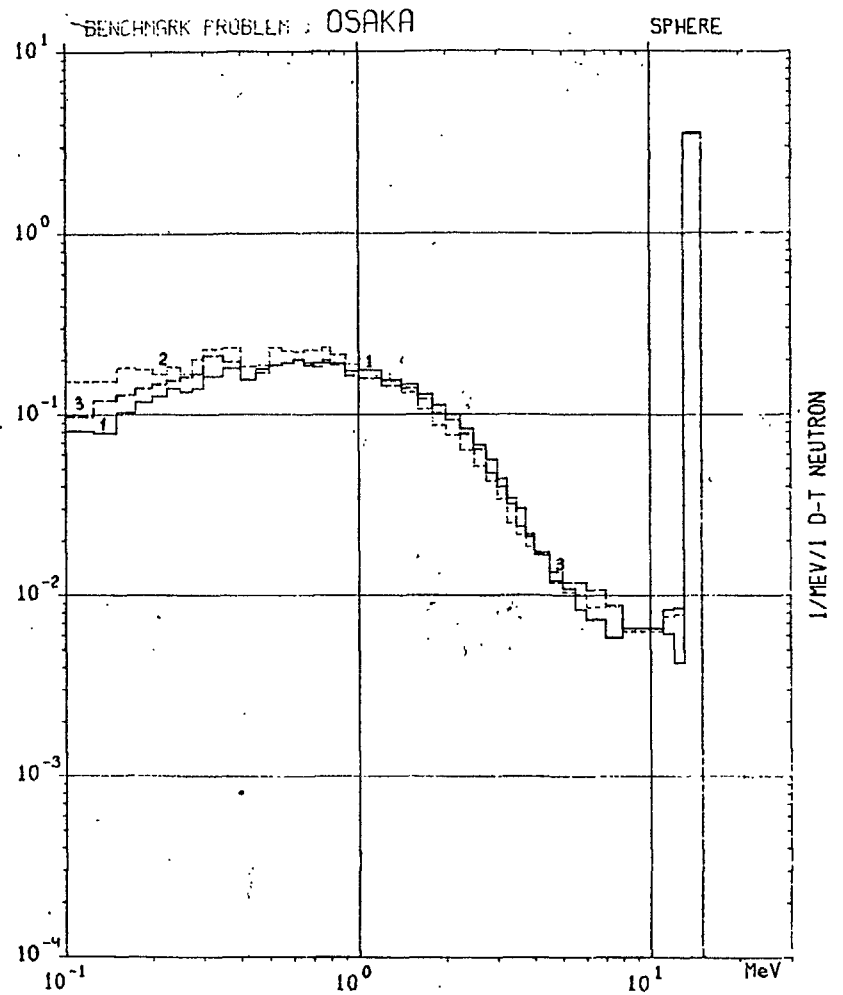


Fig. 6 Neutron leakage spectrum from PB sphere

$E = 13.5 - 14.92 \text{ MeV}$, thickness - 3.00 cm, BLANK - 1×10^5 histories

| source | M_{tot} | L_{tot} | c/\bar{e} | $L^{>0.0}$ | $L^{>0.02}$ | $L^{>0.1}$ | $L^{>0.05}$ |
|-----------------|------------------|------------------|-------------|------------|-------------|------------|-------------|
| BROND (1) — | 1.197 | 1.195 | 0.892 | 1.195 | 1.195 | 1.168 | 0.787 |
| ENDF-4 (2) --- | 1.200 | 1.192 | 0.889 | 1.192 | 1.189 | 1.143 | 0.781 |
| EFF-1 (3) - - - | 1.187 | 1.179 | 0.879 | 1.179 | 1.178 | 1.146 | 0.787 |
| EXPER | | 1.340 | | | 1.340 | 1.220 | 0.800 |

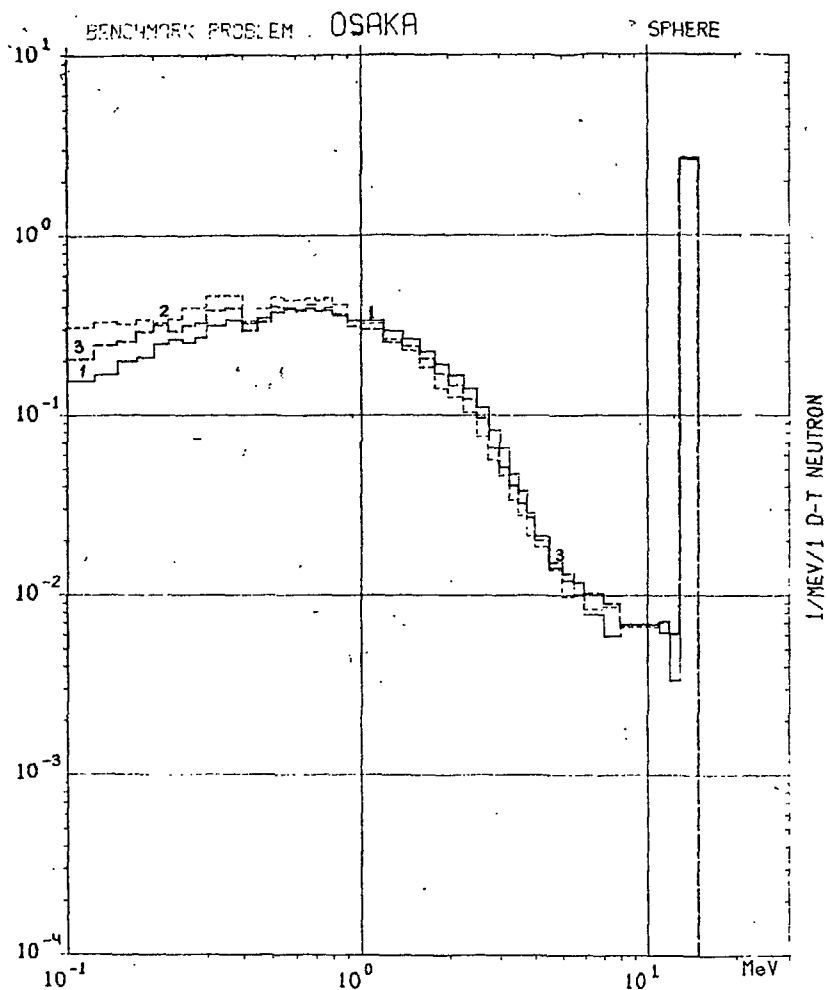


Fig. 7 Neutron leakage spectrum
from PB sphere

$E=13.5-14.92$ MeV, thickness-6.00 cm, BLANK -1×10^5 histories

| source | | M_{TOT} | L_{TOT} | c/e | $L^{>0.00}$ | $L^{>0.02}$ | $L^{>0.30}$ | $L^{>4.00}$ |
|--------|-----|-----------|-----------|-------|-------------|-------------|-------------|-------------|
| BRND | (1) | 1.354 | 1.352 | 0.878 | 1.352 | 1.352 | 1.299 | 0.615 |
| ENDF-4 | (2) | 1.363 | 1.356 | 0.881 | 1.356 | 1.352 | 1.260 | 0.614 |
| EFF-1 | (3) | 1.332 | 1.331 | 0.864 | 1.331 | 1.330 | 1.263 | 0.621 |
| EXPER | | | 1.540 | | 1.540 | | 1.410 | 0.650 |

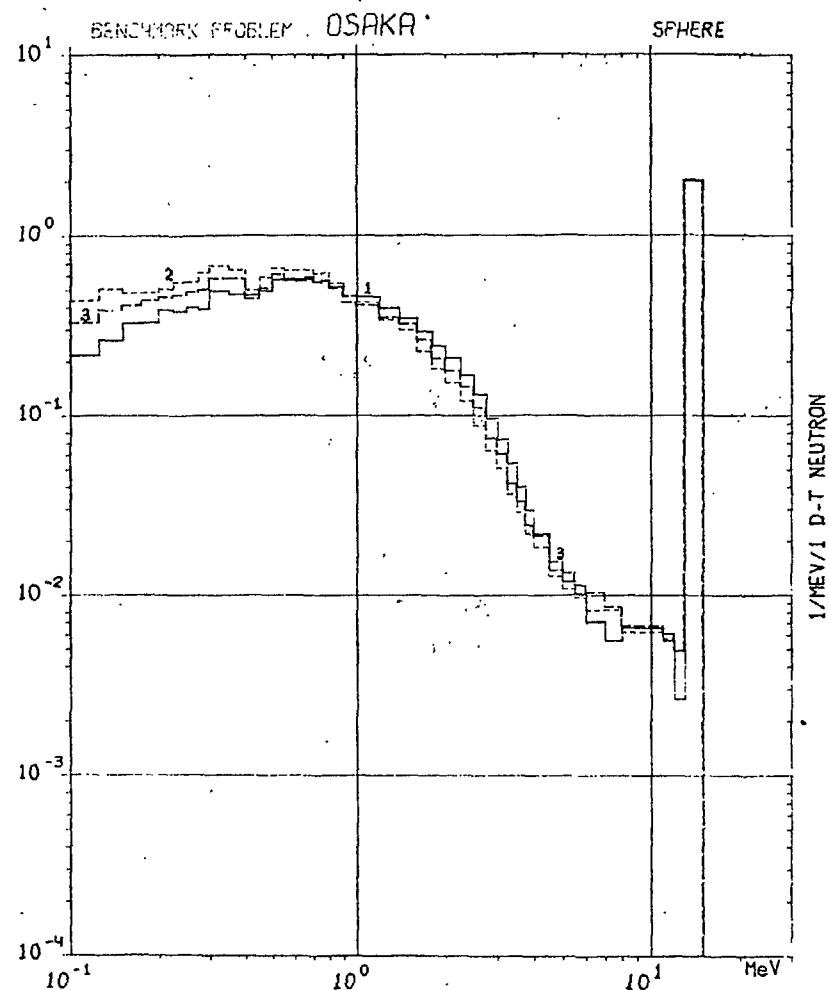


Fig. 8 Neutron leakage spectrum
from PB sphere

$E=13.5-14.92$ MeV, thickness-9.00 cm, BLANK -1×10^5 histories

| source | | M_{TOT} | L_{TOT} | c/e | $L^{>0.00}$ | $L^{>0.02}$ | $L^{>0.30}$ | $L^{>4.00}$ |
|--------|-----|-----------|-----------|-------|-------------|-------------|-------------|-------------|
| BRND | (1) | 1.475 | 1.471 | 0.870 | 1.471 | 1.471 | 1.391 | 0.479 |
| ENDF-4 | (2) | 1.487 | 1.480 | 0.876 | 1.480 | 1.473 | 1.335 | 0.482 |
| EFF-1 | (3) | 1.456 | 1.450 | 0.858 | 1.450 | 1.449 | 1.345 | 0.491 |
| EXPER | | | 1.690 | | 1.690 | | 1.590 | 0.540 |

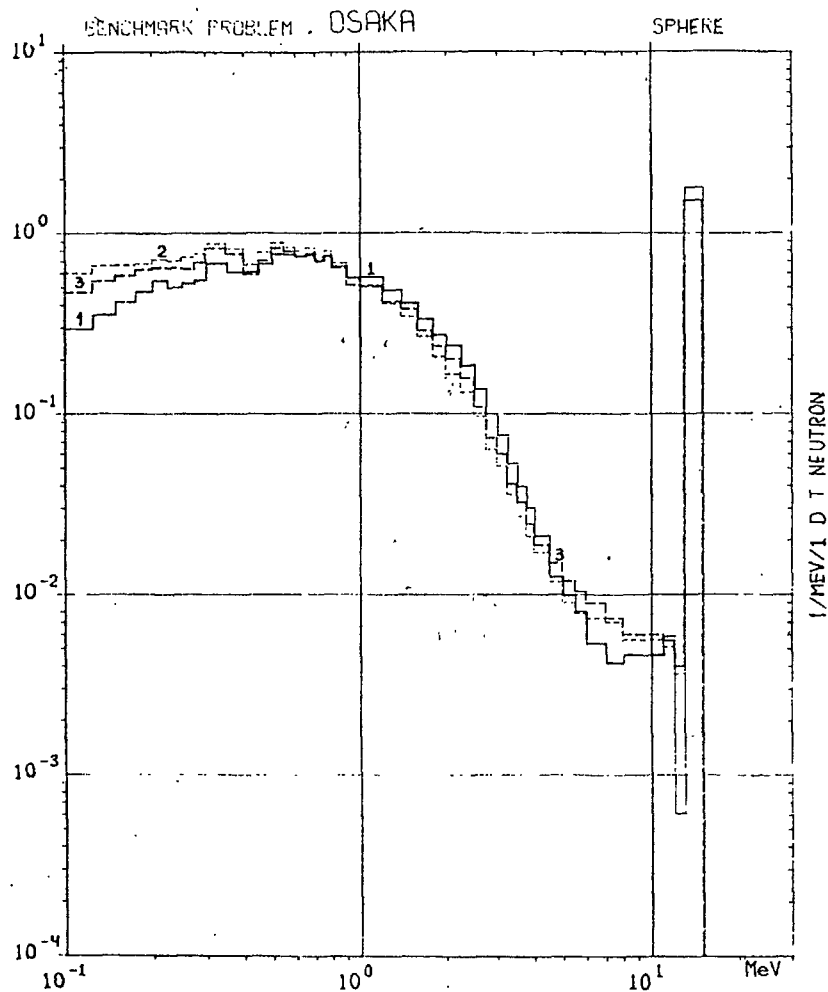


Fig. 9 Neutron leakage spectrum from PB sphere

$E=13.5-14.92$ MeV, thickness-12.00 cm, BLANK - 1×10^5 histories

| source | M_{TOT} | L_{TOT} | c/e | $L^{>0.00}$ | $L^{>0.02}$ | $L^{>0.30}$ | $L^{>1.00}$ |
|------------|-----------|-----------|-------|-------------|-------------|-------------|-------------|
| BROND (1) | 1.594 | 1.589 | 0.883 | 1.589 | 1.588 | 1.479 | 0.377 |
| ENDF-4 (2) | 1.590 | 1.581 | 0.879 | 1.581 | 1.572 | 1.389 | 0.370 |
| EFF-1 (3) | 1.552 | 1.545 | 0.858 | 1.545 | 1.543 | 1.399 | 0.378 |
| EXPER | | 1.800 | | 1.800 | 1.600 | | 0.410 |

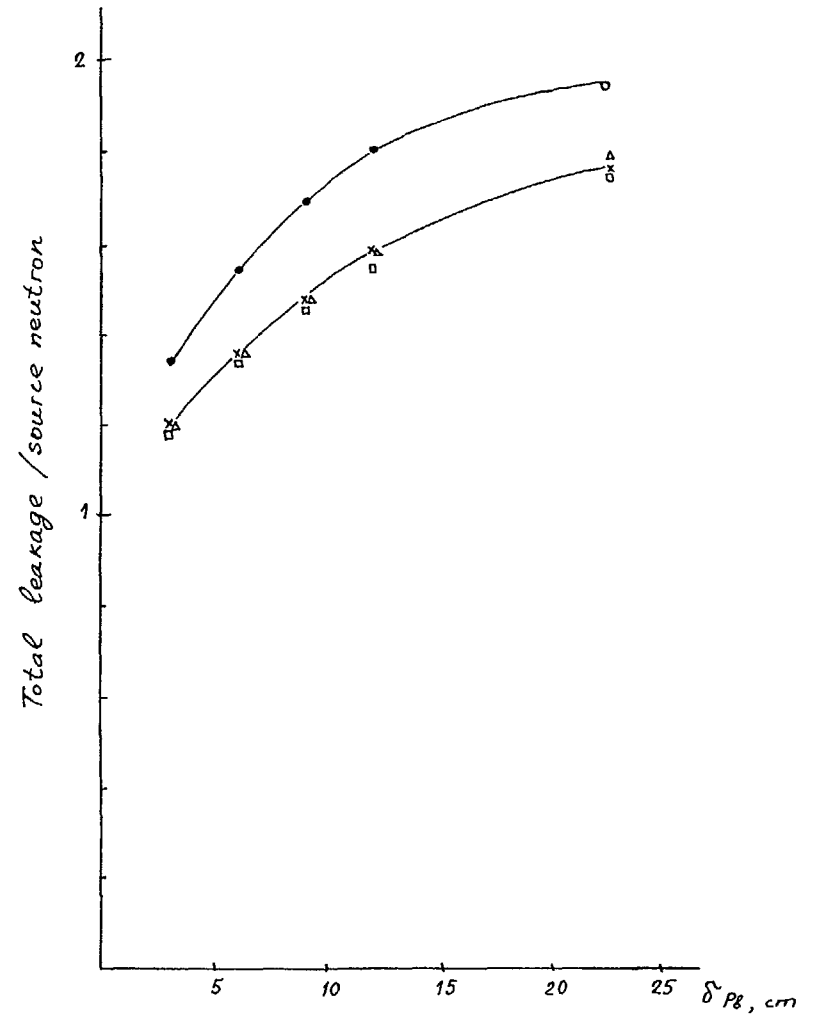


Fig. 10 Total neutron leakage in lead spheres.

x - BROND, Δ - ENDF/B-IV, \square - EFF-1
Experiment \circ [2], \bullet [3].

REFERENCES

1. E.T.Cheng, Specifications on International Comparison of Benchmark calculations. Draft FT/005. January, 20, 1988.
2. T.Efrut et al. Atomkernergie-Kerntechnik, 9, (1987), 3.
3. A.Tokahashi, Integral Measurements and Analysis of Nuclear Data Pertaining to Fusion Reactors. Proc. of the International Conference on Nuclear Data for Basic and Applied Science. Santa Fe, NM, USA, 15-17 May, 1985, p. 59.
4. S.V.Marin, D.V.Markovsky, G.E.Shatalov, Code for Calculation of Spatial Energy Neutron Distribution in One-Dimensional Geometry (BLANK-code modification). Preprint IAE-3044, 1978.
5. L.N.Zakharov, D.V.Markovsky, A.D.Frank-Kamenetsky, G.E.Shatalov Code for Formation of Neutron Microcostants for Calculations by the Monte Carlo method on the basis of evaluated Data Files (NEDAM). Preprint IAE-2994 (1978) - (In Russian).
6. G.E.Shatalov The DENSITY-Code for microscopic cross-section formation VANT. Series: Physics and Nuclear Reactor Technology, 1981, issue 8 (21), (In Russian).

7.16 Results for IAEA Sponsored International Benchmark on 22.5 cm Thick Spherical Lead Shell

Anil Kumar
University of California, Los Angeles, CA 90024-1597, USA
Phone: (213) 825-8627

I. Introduction

The present contribution relates to the international benchmark problem on 22.5 cm thick lead shell as specified by IAEA (see appendix A for details). The experimentally measured values of important parameters of interest are available for this problem. The results from various participants are planned to be discussed during the IAEA specialists' meeting on Fusion Evaluated Neutron Data Library and Benchmark Calculations from May 8 to 11, 1989 in Vienna.

II. Computational Model

The spherically symmetric geometric model recommended by IAEA (see attachment in appendix A) was used with the monte carlo code MCNP (3B version). The material densities and the spatial and energy distributions of the source neutron were also taken as recommended by IAEA. The cross section library is the latest available revision of the continuous ENDF/B-V (file ENDF5T2 on magnetic fusion energy cray computer system). The activation and fission cross sections were taken from the ENDF/B-V dosimetry tape 531 and the LLNL activation library ACTL. Surface detector option was used for tallying of various activation rates. The leakage spectrum from the outer lead surface at 25 cm radius was obtained through surface tally in the forward angular bin spanning from 0° to 90° . The energy bins were so defined as to have their mean energies correspond directly to those where the experimental leakage spectra is provided (see appendix A); it was ensured that both the arithmetic (energy space) and geometric (lethargy space) means stay close to each other. Fifty thousand neutron histories were followed.

III. Results

The results are presented in Tables I to IV and Figure 1. The tables provide the MCNP and the experimental results in the following order:

| | | |
|-----------|---|---|
| Table I | : | Partial and total multiplications per source neutron and nucleus |
| Table II | : | Neutron leakage spectrum per unit lethargy per source neutron |
| Table III | : | Activation rates per source neutron and nucleus for $^{103}\text{Rh}(n,n')$, $^{115}\text{In}(n,n')$, $^{58}\text{Ni}(n,p)$, $^{64}\text{Zn}(n,p)$, $^{27}\text{Al}(n,\alpha)$, $^{203}\text{Tl}(n,2n)$ and $^{65}\text{Cu}(n,2n)$ |
| Table IV | : | Fission rates per source neutron and nucleus for $^{235}\text{U}(n,f)$, $^{238}\text{U}(n,f)$, $^{237}\text{Np}(n,f)$, $^{232}\text{Th}(n,f)$ and $^{239}\text{Pu}(n,f)$ |
| Figure 1 | : | Neutron leakage spectrum per unit lethargy from thick lead shell |

Table I

Partial and total neutron multiplications per source neutron and nucleus [s⁻¹]
(22.5 cm thick lead shell IAEA benchmark)

| Energy range (MeV) | MCNP (C) | Experimental (E) | C/E |
|-----------------------|--------------|--------------------------|------------------------|
| 1 : 5 | 0.549±0.003 | 0.676 | 0.81±0.01 |
| 5 :10 | 0.0210±0.001 | 0.0190 | 1.11±0.05 |
| 10 :15 | 0.134±0.002 | 0.144 | 0.93±0.01 |
| total | 1.749±0.002 | 1.944±0.233 ⁺ | 0.90±0.11 [@] |

+ The error on total multiplication is supposed to be 12%. The errors on the partial multiplications were not provided.

@ 80 group matxs6d cross-section library with ANISN yields total multiplication of 1.746. It also gives C/E of 0.90.

IV. Discussion

For the partial multiplications (Table I), the largest difference between the calculated (C) and the experimental (E) values is found for 1 to 5 MeV energy range where C/E is 0.81. It is to be noted that the errors on the experimental values for all the partial multiplications are entered as zeroes as they were not provided (see appendix A). The C/E for the total multiplication is 0.90±0.11.

The C/E for the neutron leakage spectrum (Table II, Figure 1) varies from 0.71±0.10 at 3.0 MeV to 1.42±0.19 at 6.5 MeV. It is to be noted that $\Delta N_c(u)$ and $\Delta N_e(u)$ stand for the standard deviations on the calculated and the experimental spectral values respectively at lethargy u (energy E). Generally, C/E is less than 1. This trend is in agreement with that for the total multiplication.

Regarding foil activation rates given in Table III, it should be noted that there is a large difference in the $^{58}\text{Ni}(n,p)$ activation rates by t531 (ENDF/B-V dosimetry tape 531) and act1 libraries; it results from the fact that t531 cross-section, unlike that of act1 (^{58}Co product), is for both the ground state and the metastable products, namely, ^{58}Co and ^{58m}Co . The C/E ratios for most of the activation rates are closest to unity at the surface of the sphere; it appears that the $^{203}\text{Tl}(n,2n)$ is as much as 30% or more overpredicted in act1; the $^{58}\text{Ni}(n,p)^{58}\text{Co}+^{58m}\text{Co}$ (by t531) is closer to the experimental value at the surface. All C/E values are higher at inner locations. From the trend of C/E for these detectors with a large range of effective thresholds, one can probably hypothesize that the calculated secondary neutron energy distribution from the (n,2n) reactions in the lead is overpredicted than the actual one in the energy range at least below 3 MeV. This hypothesis can explain very large values of C/E for the activation rates of lower threshold detectors (^{103}Rh , ^{115}In , ^{58}Ni , ^{64}Zn) at 5, 10, 15 and 20 cm; the relatively large reduction in the C/E over next 5 cm for these same

Table II

**Neutron leakage spectrum per unit of lethargy per source
neutron
(22.5 cm thick lead shell IAEA benchmark)**

| E (MeV) | MCNP (ENDF/B-V) | | Experimental | | C/E | ±Δ(C/E) |
|---------|--------------------|----------------------|--------------------|----------------------|------|---------|
| | N _c (u) | ±ΔN _c (u) | N _e (u) | ±ΔN _e (u) | | |
| 0.05 | 0.038 | 0.002 | 0.048 | 0.005 | 0.79 | 0.09 |
| 0.06 | 0.049 | 0.002 | 0.057 | 0.006 | 0.86 | 0.11 |
| 0.07 | 0.057 | 0.003 | 0.069 | 0.007 | 0.83 | 0.11 |
| 0.08 | 0.062 | 0.003 | 0.080 | 0.008 | 0.78 | 0.11 |
| 0.09 | 0.077 | 0.004 | 0.091 | 0.009 | 0.85 | 0.11 |
| 0.10 | 0.091 | 0.004 | 0.098 | 0.010 | 0.93 | 0.11 |
| 0.12 | 0.104 | 0.005 | 0.125 | 0.013 | 0.83 | 0.11 |
| 0.15 | 0.142 | 0.006 | 0.170 | 0.017 | 0.84 | 0.11 |
| 0.18 | 0.193 | 0.008 | 0.215 | 0.022 | 0.90 | 0.11 |
| 0.20 | 0.233 | 0.008 | 0.241 | 0.024 | 0.97 | 0.11 |
| 0.30 | 0.341 | 0.007 | 0.370 | 0.037 | 0.90 | 0.10 |
| 0.40 | 0.397 | 0.007 | 0.550 | 0.055 | 0.72 | 0.10 |
| 0.50 | 0.793 | 0.011 | 0.725 | 0.073 | 1.09 | 0.10 |
| 0.60 | 0.765 | 0.012 | 0.805 | 0.081 | 0.95 | 0.10 |
| 0.70 | 0.812 | 0.014 | 0.810 | 0.095 | 1.00 | 0.12 |
| 0.80 | 0.782 | 0.014 | 0.850 | 0.110 | 0.92 | 0.13 |
| 0.90 | 0.767 | 0.015 | 0.880 | 0.120 | 0.87 | 0.14 |
| 1.00 | 0.740 | 0.015 | 0.865 | 0.120 | 0.86 | 0.14 |
| 1.2 | 0.708 | 0.017 | 0.800 | 0.100 | 0.89 | 0.13 |
| 1.5 | 0.576 | 0.013 | 0.745 | 0.090 | 0.77 | 0.12 |
| 1.8 | 0.460 | 0.013 | 0.590 | 0.070 | 0.78 | 0.12 |
| 2.0 | 0.388 | 0.009 | 0.495 | 0.050 | 0.78 | 0.10 |
| 2.5 | 0.249 | 0.008 | 0.293 | 0.030 | 0.85 | 0.11 |
| 3.0 | 0.118 | 0.006 | 0.167 | 0.015 | 0.71 | 0.10 |
| 3.5 | 0.095 | 0.006 | 0.099 | 0.009 | 0.96 | 0.11 |
| 4.0 | 0.062 | 0.005 | 0.066 | 0.006 | 0.94 | 0.12 |
| 4.5 | 0.033 | 0.004 | 0.046 | 0.004 | 0.72 | 0.15 |
| 5.0 | 0.026 | 0.002 | 0.036 | 0.003 | 0.72 | 0.11 |
| 5.5 | 0.025 | 0.002 | 0.029 | 0.003 | 0.86 | 0.13 |
| 6.0 | 0.031 | 0.004 | 0.026 | 0.003 | 1.19 | 0.17 |
| 6.5 | 0.034 | 0.005 | 0.024 | 0.003 | 1.42 | 0.19 |
| 7.0 | 0.024 | 0.004 | 0.026 | 0.003 | 0.92 | 0.20 |
| 7.5 | 0.028 | 0.005 | 0.027 | 0.004 | 1.04 | 0.23 |
| 8.0 | 0.029 | 0.005 | 0.028 | 0.004 | 1.04 | 0.22 |
| 8.5 | 0.027 | 0.005 | 0.032 | 0.004 | 0.84 | 0.22 |
| 9.0 | 0.030 | 0.005 | 0.034 | 0.004 | 0.88 | 0.20 |
| 9.5 | 0.034 | 0.006 | 0.036 | 0.005 | 0.94 | 0.22 |
| 10.0 | 0.032 | 0.003 | 0.033 | 0.005 | 0.97 | 0.18 |
| 10.5 | 0.029 | 0.006 | 0.031 | 0.004 | 0.94 | 0.24 |
| 11.0 | 0.035 | 0.006 | 0.032 | 0.004 | 1.09 | 0.21 |
| 11.5 | 0.035 | 0.003 | 0.033 | 0.004 | 1.06 | 0.15 |
| 12.0 | 0.034 | 0.003 | 0.033 | 0.004 | 1.03 | 0.15 |
| 12.2 | | | | | | |
| to 14.9 | 0.633 | 0.007 | 0.670 | 0.067 | 0.94 | 0.10 |

detectors could be explained from the enhanced capture and inelastic scattering in the lead at lower neutron energies. The higher values of C/E for 12.4 MeV effective threshold ⁶⁵Cu(n,2n) reaction at the inner locations could then be explained by the overprediction of forward anisotropy of the elastically scattered neutrons (from incident 14 MeV source neutrons) in the calculations, that leads to larger neutron fluxes at higher energies in the inner locations.

Table III

**Activation rates per source neutron and nucleus [s⁻¹]
(22.5 cm thick lead shell IAEA benchmark)**

III.1. Location = 5 cm

| Nuclide | Reaction | MCNP | | Experimental (E) | C/E |
|---------|----------|--------------------|--------------------------------|--------------------------------|-----------|
| | | act. xs. | C | | |
| 103Rh | (n, n') | t531 ⁺ | (4.24±0.04) x10 ⁻²⁷ | (2.89±0.45) x10 ⁻²⁷ | 1.47±0.16 |
| 115In | (n, n') | t531 | (8.60±0.09) x10 ⁻²⁸ | (4.94±0.79) x10 ⁻²⁸ | 1.74±0.16 |
| 58Ni | (n, p) | t531 | (1.37±0.01) x10 ⁻²⁷ | (6.96±1.18) x10 ⁻²⁸ | 1.97±0.17 |
| | | act1 ⁺⁺ | (5.80±0.04) x10 ⁻²⁷ | (6.96±1.18) x10 ⁻²⁸ | 0.83±0.17 |
| 64Zn | (n, p) | act1 | (6.22±0.03) x10 ⁻²⁸ | (5.84±0.99) x10 ⁻²⁸ | 1.07±0.17 |
| 27Al | (n, α) | t531 | (3.25±0.01) x10 ⁻²⁸ | (1.97±0.30) x10 ⁻²⁸ | 1.65±0.15 |
| | | act1 | (3.24±0.01) x10 ⁻²⁸ | (1.97±0.30) x10 ⁻²⁸ | 1.64±0.15 |
| 203Tl | (n, 2n) | act1 | (5.66±0.02) x10 ⁻²⁷ | (4.08±0.65) x10 ⁻²⁷ | 1.39±0.16 |
| 65Cu | (n, 2n) | t531 | (2.25±0.01) x10 ⁻²⁷ | (1.78±0.36) x10 ⁻²⁷ | 1.26±0.20 |
| | | act1 | (2.46±0.01) x10 ⁻²⁷ | (1.78±0.36) x10 ⁻²⁷ | 1.38±0.20 |

III.2. Location = 10 cm

| Nuclide | Reaction | MCNP | | Experimental (E) | C/E |
|---------|----------|-------------|--------------------------------|--------------------------------|-----------|
| | | act. xs. | C | | |
| 103Rh | (n, n') | t531 | (1.73±0.01) x10 ⁻²⁷ | (1.09±0.17) x10 ⁻²⁷ | 1.59±0.16 |
| 115In | (n, n') | t531 | (3.23±0.03) x10 ⁻²⁸ | (2.12±0.34) x10 ⁻²⁸ | 1.52±0.16 |
| 58Ni | (n, p) | t531 | (2.87±0.02) x10 ⁻²⁷ | (1.86±0.32) x10 ⁻²⁸ | 1.54±0.17 |
| | | act1 | (1.26±0.01) x10 ⁻²⁷ | (1.86±0.32) x10 ⁻²⁸ | 0.68±0.17 |
| 64Zn | (n, p) | act1 | (1.25±0.01) x10 ⁻²⁸ | (1.16±0.20) x10 ⁻²⁸ | 1.08±0.15 |
| 27Al | (n, α) | t531 | (5.60±0.03) x10 ⁻²⁹ | (4.52±0.68) x10 ⁻²⁹ | 1.24±0.15 |
| | | act1 | (5.59±0.03) x10 ⁻²⁹ | (4.52±0.68) x10 ⁻²⁹ | 1.24±0.15 |
| 203Tl | (n, 2n) | act1 | (9.70±0.06) x10 ⁻²⁸ | (5.65±0.90) x10 ⁻²⁸ | 1.72±0.16 |
| 65Cu | (n, 2n) | t531 | (3.78±0.02) x10 ⁻²⁸ | (3.62±0.72) x10 ⁻²⁸ | 1.04±0.20 |
| | | act1 | (4.12±0.02) x10 ⁻²⁸ | (3.62±0.72) x10 ⁻²⁸ | 1.14±0.20 |

III.3. Location = 15 cm

| Nuclide | Reaction | MCNP | | Experimental (E) | C/E |
|---------|----------|--------------------|--------------------------------|--------------------------------|-----------|
| | | act. xs. | C | | |
| 103Rh | (n, n') | t531 ⁺ | (8.55±0.05) x10 ⁻²⁸ | (6.54±1.01) x10 ⁻²⁸ | 1.31±0.15 |
| 115In | (n, n') | t531 | (1.50±0.01) x10 ⁻²⁸ | (1.10±0.18) x10 ⁻²⁸ | 1.36±0.16 |
| 58Ni | (n, p) | t531 | (9.84±0.08) x10 ⁻²⁹ | (6.32±1.07) x10 ⁻²⁹ | 1.54±0.17 |
| | | act1 ⁺⁺ | (4.45±0.04) x10 ⁻²⁹ | (6.32±1.07) x10 ⁻²⁹ | 0.70±0.17 |
| 64Zn | (n, p) | act1 | (4.14±0.03) x10 ⁻²⁹ | (3.88±0.66) x10 ⁻²⁹ | 1.07±0.17 |
| 27Al | (n, α) | t531 | (1.66±0.01) x10 ⁻²⁹ | (1.35±0.20) x10 ⁻²⁹ | 1.23±0.15 |
| | | act1 | (1.66±0.01) x10 ⁻²⁹ | (1.35±0.20) x10 ⁻²⁹ | 1.23±0.15 |
| 203Tl | (n, 2n) | act1 | (2.87±0.02) x10 ⁻²⁸ | (1.37±0.22) x10 ⁻²⁸ | 2.09±0.16 |
| 65Cu | (n, 2n) | t531 | (1.10±0.01) x10 ⁻²⁸ | (1.20±0.24) x10 ⁻²⁸ | 0.92±0.20 |
| | | act1 | (1.20±0.01) x10 ⁻²⁸ | (1.20±0.24) x10 ⁻²⁸ | 1.00±0.20 |

III.4. Location = 20 cm

| Nuclide | Reaction | MCNP | | Experimental (E) | C/E |
|---------|----------|-------------|--------------------------------|--------------------------------|-----------|
| | | act. xs. | C | | |
| 103Rh | (n, n') | t531 | (4.21±0.03) x10 ⁻²⁸ | (2.77±0.43) x10 ⁻²⁸ | 1.52±0.16 |
| 115In | (n, n') | t531 | (7.13±0.06) x10 ⁻²⁹ | (5.31±0.85) x10 ⁻²⁹ | 1.34±0.16 |
| 58Ni | (n, p) | t531 | (3.99±0.04) x10 ⁻²⁹ | (3.09±0.53) x10 ⁻²⁹ | 1.29±0.17 |
| | | act1 | (1.83±0.02) x10 ⁻²⁹ | (3.09±0.53) x10 ⁻²⁹ | 0.59±0.17 |
| 64Zn | (n, p) | act1 | (1.65±0.02) x10 ⁻²⁹ | (1.50±0.28) x10 ⁻²⁹ | 1.10±0.19 |
| 27Al | (n, α) | t531 | (6.20±0.07) x10 ⁻³⁰ | (5.04±0.76) x10 ⁻³⁰ | 1.23±0.15 |
| | | act1 | (6.20±0.07) x10 ⁻³⁰ | (5.04±0.76) x10 ⁻³⁰ | 1.23±0.15 |
| 203Tl | (n, 2n) | act1 | (1.06±0.01) x10 ⁻²⁸ | (6.05±0.97) x10 ⁻²⁹ | 1.75±0.20 |
| 65Cu | (n, 2n) | t531 | (4.02±0.05) x10 ⁻²⁹ | (4.59±0.92) x10 ⁻²⁹ | 0.88±0.20 |
| | | act1 | (4.38±0.05) x10 ⁻²⁹ | (4.59±0.92) x10 ⁻²⁹ | 0.95±0.20 |

(Table III continued)

III.5. Location = 25 cm

| Nuclide | Reaction | MCNP | | Experimental (E) | C/E |
|-------------------|----------|--------------------|-------------------------------|-------------------------------|-----------|
| | | act. xs. | C | | |
| ¹⁰³ Rh | (n,n') | t531 ⁺ | (1.38±0.01)×10 ⁻²⁸ | (1.34±0.21)×10 ⁻²⁸ | 1.03±0.16 |
| ¹¹⁵ In | (n,n') | t531 | (2.37±0.01)×10 ⁻²⁹ | (2.46±0.39)×10 ⁻²⁹ | 0.96±0.16 |
| ⁵⁸ Ni | (n,p) | t531 | (1.45±0.01)×10 ⁻²⁹ | (1.69±0.29)×10 ⁻²⁹ | 0.86±0.17 |
| | | act1 ⁺⁺ | (6.60±0.06)×10 ⁻³⁰ | (1.69±0.29)×10 ⁻²⁹ | 0.39±0.17 |
| ⁶⁴ Zn | (n,p) | act1 | (6.07±0.06)×10 ⁻³⁰ | (7.79±1.32)×10 ⁻³⁰ | 0.78±0.17 |
| ²⁷ Al | (n,α) | t531 | (2.44±0.03)×10 ⁻³⁰ | (2.39±0.36)×10 ⁻³⁰ | 1.02±0.15 |
| | | act1 | (2.44±0.03)×10 ⁻³⁰ | (2.39±0.36)×10 ⁻³⁰ | 1.02±0.15 |
| ²⁰³ Tl | (n,2n) | act1 | (4.20±0.05)×10 ⁻²⁹ | (3.12±0.50)×10 ⁻²⁹ | 1.35±0.16 |
| ⁶⁵ Cu | (n,2n) | t531 | (1.59±0.02)×10 ⁻²⁹ | (2.26±0.45)×10 ⁻²⁹ | 0.70±0.20 |
| | | act1 | (1.73±0.02)×10 ⁻²⁹ | (2.26±0.45)×10 ⁻²⁹ | 0.77±0.20 |

+ t531 stands for ENDF/B-V dosimetry file no. 531

++ act1 is an evaluated neutron activation cross section library from Lawrence Livermore National Laboratory

Table IV

Fission rates per source neutron and nucleus [s⁻¹]
(22.5 cm thick lead shell IAEA benchmark)

IV.1. Location = 5.25 cm

| Nuclide | Reaction | MCNP | | Experimental (E) | C/E |
|-------------------|----------|-------------------|-------------------------------|-------------------------------|-----------|
| | | act. xs. | C | | |
| ²³⁵ U | (n,f) | act1 ⁺ | (1.38±0.01)×10 ⁻²⁶ | (9.76±0.63)×10 ⁻²⁷ | 1.41±0.06 |
| ²³⁸ U | (n,f) | act1 | (3.73±0.02)×10 ⁻²⁷ | (3.05±0.27)×10 ⁻²⁷ | 1.22±0.09 |
| ²³⁷ Np | (n,f) | act1 | (1.14±0.01)×10 ⁻²⁶ | (8.66±1.82)×10 ⁻²⁷ | 1.32±0.21 |
| ²³² Th | (n,f) | act1 | (1.12±0.01)×10 ⁻²⁷ | (6.34±0.54)×10 ⁻²⁸ | 1.77±0.09 |
| ²³⁹ Pu | (n,f) | act1 | (1.72±0.01)×10 ⁻²⁶ | - | - |

IV.2. Location = 10.25 cm

| Nuclide | Reaction | MCNP | | Experimental (E) | C/E |
|-------------------|----------|-------------|-------------------------------|-------------------------------|-----------|
| | | act. xs. | C | | |
| ²³⁵ U | (n,f) | act1 | (5.63±0.05)×10 ⁻²⁷ | (3.59±0.46)×10 ⁻²⁷ | 1.57±0.13 |
| ²³⁸ U | (n,f) | act1 | (9.27±0.06)×10 ⁻²⁸ | (8.12±0.54)×10 ⁻²⁸ | 1.14±0.14 |
| ²³⁷ Np | (n,f) | act1 | (4.04±0.02)×10 ⁻²⁷ | (2.84±0.22)×10 ⁻²⁷ | 1.42±0.17 |
| ²³² Th | (n,f) | act1 | (2.63±0.01)×10 ⁻²⁸ | (1.27±0.12)×10 ⁻²⁸ | 1.77±0.09 |
| ²³⁹ Pu | (n,f) | act1 | (7.17±0.05)×10 ⁻²⁷ | - | - |

IV.3. Location = 15.25 cm

| Nuclide | Reaction | MCNP | | Experimental (E) | C/E |
|-------------------|----------|-------------|-------------------------------|-------------------------------|-----------|
| | | act. xs. | C | | |
| ²³⁵ U | (n,f) | act1 | (2.87±0.02)×10 ⁻²⁷ | (1.77±0.31)×10 ⁻²⁷ | 1.62±0.18 |
| ²³⁸ U | (n,f) | act1 | (3.56±0.02)×10 ⁻²⁸ | (2.55±0.45)×10 ⁻²⁸ | 1.40±0.18 |
| ²³⁷ Np | (n,f) | act1 | (1.91±0.01)×10 ⁻²⁷ | (1.31±0.13)×10 ⁻²⁷ | 1.46±0.10 |
| ²³² Th | (n,f) | act1 | (9.68±0.06)×10 ⁻²⁸ | (8.58±0.73)×10 ⁻²⁹ | 1.13±0.09 |
| ²³⁹ Pu | (n,f) | act1 | (3.68±0.02)×10 ⁻²⁷ | - | - |

(Table IV continued)

IV.4. Location = 20.25 cm

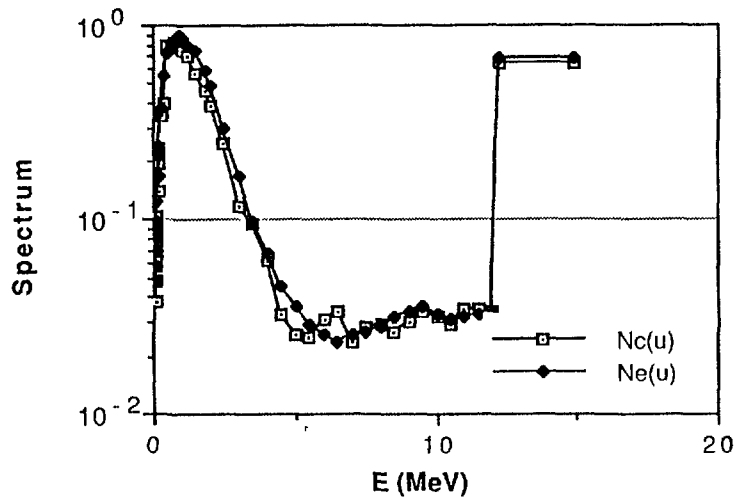
| Nuclide | Reaction | MCNP | | Experimental (E) | C/E |
|-------------------|----------|-------------------|---------------------------------|---------------------------------|-----------|
| | | act. xs. | C | | |
| ²³⁵ U | (n, f) | act1 ⁺ | (1.41±0.01) × 10 ⁻²⁷ | (9.98±1.09) × 10 ⁻²⁸ | 1.41±0.11 |
| ²³⁸ U | (n, f) | act1 | (1.53±0.01) × 10 ⁻²⁸ | (1.21±0.08) × 10 ⁻²⁸ | 1.26±0.07 |
| ²³⁷ Np | (n, f) | act1 | (9.15±0.05) × 10 ⁻²⁸ | (6.82±0.69) × 10 ⁻²⁸ | 1.34±0.10 |
| ²³² Th | (n, f) | act1 | (4.08±0.03) × 10 ⁻²⁹ | (3.47±0.35) × 10 ⁻²⁹ | 1.18±0.10 |
| ²³⁹ Pu | (n, f) | act1 | (1.81±0.01) × 10 ⁻²⁷ | - | - |

IV.5. Location = 25.25 cm

| Nuclide | Reaction | MCNP | | Experimental (E) | C/E |
|-------------------|----------|-------------|---------------------------------|---------------------------------|-----------|
| | | act. xs. | C | | |
| ²³⁵ U | (n, f) | act1 | (4.09±0.01) × 10 ⁻²⁸ | (3.44±0.41) × 10 ⁻²⁸ | 1.19±0.12 |
| ²³⁸ U | (n, f) | act1 | (5.35±0.03) × 10 ⁻²⁹ | (4.93±0.35) × 10 ⁻²⁸ | 1.09±0.07 |
| ²³⁷ Np | (n, f) | act1 | (3.00±0.01) × 10 ⁻²⁸ | (2.56±0.21) × 10 ⁻²⁸ | 1.17±0.08 |
| ²³² Th | (n, f) | act1 | (1.46±0.01) × 10 ⁻²⁹ | (1.42±0.16) × 10 ⁻²⁹ | 1.03±0.11 |
| ²³⁹ Pu | (n, f) | act1 | (5.39±0.01) × 10 ⁻²⁷ | (5.61±0.67) × 10 ⁻²⁸ | 0.96±0.12 |

+ act1 is an activation cross section library from Lawrence Livermore National Laboratory

spectrum per unit lethargy from 22.5 cm thick lead shell



The fission rates for ^{238}U , ^{237}Np and ^{232}Th at different locations (Table IV) follow largely the pattern for lower threshold detectors like ^{103}Rh and ^{115}In . Even the fission rate profile for zero threshold ($1/v$ cross section) ^{235}U behaves like the low threshold detectors thus hinting at the presence of larger number of low energy neutrons in the calculation.

V. Conclusion

Even though the C/E ratio for the total neutron multiplication, being 0.90 ± 0.11 , in the 22.5 cm thick spherical lead shell is probably acceptably close to unity, rather large discrepancies are observed for C/E for the leakage spectrum and the reaction rate profiles. It is important to carry out (i) the sensitivity to the energy distribution of secondary neutrons (SED) from (n,2n) reaction in lead, and (ii) the sensitivity to the angular distribution of the secondary neutrons (SAD) from elastic scattering in the lead, on the leakage spectrum and the reaction rate profiles to establish if indeed these two effects can help explain the observed discrepancies between the calculated and the experimental quantities.

7.17 TUD-Pb CALCULATIONAL BENCHMARK WITH 14MeV NEUTRONS

S.Antonov, K.Ilieva, J.Jordanova, K.Pavlova, I.Popova
Institute of Nuclear Research and Nuclear Energy
Bulgarian Academy of Sciences, Sofia

For testing lead cross section data a comparative benchmark calculations was proposed at IAEA Advisory Group Meeting on Nuclear Data for Fusion Reactor Technology [1]. The University of Dresden /TUD/ lead sphere experiment was recommended as a reference because of its simple geometry, single material set /Pb/ and high precision of the experimental results and because lead is a candidate for neutron multiplier [2]. Time-of-flight /TOF/ and proton recoil spectrometer /PRS/ techniques (stilbene scintillator and hydrogen proportional spherical chambers) were employed for leakage spectrum measurements. Reaction rates of activation detectors and fission chambers were also measured. These results are important in obtaining dosimetry information. In this way the TUD experiment also appears as a reference for neutron dosimetry in fusion systems. Namely, neutron distribution in fusion material test facilities, fusion blanket systems and fusion processes in burning plasma could be studied only by using activation detectors.

Results for TUD lead sphere benchmark problem calculated by using ANISN[4], MCNP[5] and MORSE[6] transport codes and different cross section data are presented in this report.

The 1-D calculational model and nuclide densities used in calculations are shown in Figure 1 and Table 1 respectively. Neutron source is described as isotopic in the energy range 13.5-14.92 MeV and is placed at the center of the sphere. Target support and water cooling system are presented as a homogeneous mixture with nuclide densities given in Table 1. A lead shell with thickness of 25 cm is placed next to the void spherical shell adjacent to the source. Activation and fission detectors positions are

Table 1. Nuclide density

| Region | Target | Lead | Air† |
|--------------|----------|----------|---------|
| Outer Radius | 25 cm | 25 cm | 500 cm |
| H | 2.043-3* | | |
| N | | | 3.909-5 |
| O | 1.021-3 | | 1.048-5 |
| Cu | 9.412-3 | | |
| Pb | | 3.2988-2 | |

*Read as 2.043×10^{-3} [10^{24} atoms /cm³]

†Normal air at 300°K. Elements except N and O are ignored.

Table 2 Partial and total neutron multiplications of the sphere

| Method | M(E ₁ /MeV ... E _n /MeV) | | | | |
|--------------------------|--|-------|--------|---------|--------|
| | 0 - 1 | 1 - 5 | 5 - 10 | 10 - 15 | 0 - 15 |
| exp. TOF | - | 0.653 | 0.0190 | 0.144 | - |
| exp. PRS | 1.160 | 0.701 | 0.0234 | 0.143 | 2.031 |
| TOF - PRS | 1.105 | 0.676 | 0.0190 | 0.144 | 1.944 |
| MCNP | 1.063 | 0.529 | 0.0195 | 0.126 | 1.740 |
| ENDF/4 | 0.2% | 0.3% | 1.8% | 0.6% | 0.1% |
| ANISN DLC37F | 1.060 | 0.520 | 0.0178 | 0.161 | 1.760 |
| ANISN EFF (Pb99S) | 1.020 | 0.600 | 0.0219 | 0.128 | 1.750 |
| ANISN Pb175F6 | 1.111 | 0.600 | 0.0167 | 0.075 | 1.803 |
| MORSE | 1.098 | 0.535 | 0.0127 | 0.145 | 1.830 |
| EURLIB | 1.6% | 2.4% | 16.9% | 11.5% | 0.1% |
| MORSE | 1.001 | 0.595 | 0.0189 | 0.135 | 1.750 |
| EFF (Pb99S) | 0.4% | 0.7% | 5.1% | 1.7% | 0.2% |
| MORSE | 0.988 | 0.592 | 0.022 | 0.133 | 1.735 |
| Pb, Cu, H ₂ O | 0.4% | 0.7% | 4.5% | 1.7% | 0.2% |
| EFF (Pb99S) | 0.972* | | | | |

* - this value is for the energy region 0.05-1.0 MeV

shown in Tables 3 and 4. The TOF and PRS detectors are at distance of 431 cm from the center of the sphere.

Multigroup neutron constants used in calculations are given in the first column of Table 2. The MCNP code utilizes

Table 3 Fission rates per source neutron and nucleus

| Distance from the sphere centre [cm] | | | | | | |
|--------------------------------------|--|----------------------------------|----------------------------------|----------------------------------|----------------------------------|----------------------------------|
| Element | Method | 5.25 | 10.25 | 15.25 | 20.25 | 25.25 |
| ^{235}U - | exp. | $(9.76 \pm 0.63) \cdot 10^{-27}$ | $(3.59 \pm 0.46) \cdot 10^{-27}$ | $(1.77 \pm 0.31) \cdot 10^{-27}$ | $(9.98 \pm 1.09) \cdot 10^{-28}$ | $(3.44 \pm 0.41) \cdot 10^{-28}$ |
| | MORSE (ENDF/5-D) EFF (Pb99S) | $1.37 \cdot 10^{-26}$ (1.0%) | $5.46 \cdot 10^{-27}$ (0.8%) | $2.85 \cdot 10^{-27}$ (0.8%) | $1.38 \cdot 10^{-27}$ (1.1%) | $4.32 \cdot 10^{-28}$ (1.1%) |
| | ANISN (ENDF/4) EFF (Pb99S) | $1.44 \cdot 10^{-26}$ | $5.61 \cdot 10^{-27}$ | $2.86 \cdot 10^{-27}$ | $1.40 \cdot 10^{-27}$ | $4.38 \cdot 10^{-28}$ |
| | ANISN (ENDF/4) DLC37F | $1.53 \cdot 10^{-26}$ | $6.12 \cdot 10^{-27}$ | $3.14 \cdot 10^{-27}$ | $1.53 \cdot 10^{-27}$ | $4.62 \cdot 10^{-28}$ |
| ^{238}U 1,5MeV | exp. | $(3.05 \pm 0.27) \cdot 10^{-27}$ | $(8.12 \pm 0.54) \cdot 10^{-28}$ | $(2.55 \pm 0.45) \cdot 10^{-28}$ | $(1.21 \pm 0.08) \cdot 10^{-28}$ | $(4.93 \pm 0.35) \cdot 10^{-29}$ |
| | MORSE (ENDF/5-D) EFF (Pb99S) (P, Cu, H ₂ O) | $3.92 \cdot 10^{-27}$ (0.4%) | $1.00 \cdot 10^{-27}$ (0.7%) | $3.92 \cdot 10^{-28}$ (1.7%) | $1.65 \cdot 10^{-28}$ (1.5%) | $5.90 \cdot 10^{-29}$ (1.1%) |
| | ANISN (ENDF/4) EFF (Pb99S) | $4.24 \cdot 10^{-27}$ | $1.00 \cdot 10^{-27}$ | $3.81 \cdot 10^{-28}$ | $1.61 \cdot 10^{-28}$ | $6.04 \cdot 10^{-29}$ |
| | ANISN (ENDF/4) DLC37F | $4.04 \cdot 10^{-27}$ | $9.24 \cdot 10^{-28}$ | $3.45 \cdot 10^{-28}$ | $1.44 \cdot 10^{-28}$ | $5.48 \cdot 10^{-29}$ |
| | MCNP (ENDF/4) | $2.56 \cdot 10^{-27}$ (0.59%) | $6.89 \cdot 10^{-28}$ (0.7%) | $2.81 \cdot 10^{-28}$ (0.8%) | $1.25 \cdot 10^{-28}$ (0.8%) | $4.24 \cdot 10^{-29}$ (0.5%) |
| ^{237}Np 1,6MeV | exp. | $(8.66 \pm 1.82) \cdot 10^{-27}$ | $(2.84 \pm 0.22) \cdot 10^{-27}$ | $(1.31 \pm 0.13) \cdot 10^{-27}$ | $(6.82 \pm 0.62) \cdot 10^{-28}$ | $(2.56 \pm 0.21) \cdot 10^{-28}$ |
| | ANISN (ENDF/4) EFF (Pb99S) | $1.37 \cdot 10^{-26}$ | $4.52 \cdot 10^{-27}$ | $2.10 \cdot 10^{-27}$ | $9.99 \cdot 10^{-28}$ | $3.50 \cdot 10^{-28}$ |
| | ANISN (ENDF/4) DLG37F | $1.33 \cdot 10^{-26}$ | $4.35 \cdot 10^{-27}$ | $2.02 \cdot 10^{-27}$ | $9.59 \cdot 10^{-28}$ | $3.36 \cdot 10^{-28}$ |

Table 3

Continuation

| Element | Method | 5.25 | 10.25 | 15.25 | 20.25 | 25.25 |
|-----------------------------|--|----------------------------------|----------------------------------|----------------------------------|----------------------------------|----------------------------------|
| ^{239}Pu - | exp. | - | - | - | - | $(5.61 \pm 0.67) \cdot 10^{-28}$ |
| | MORSE (ENDF/4) EFF (Pb99S) | $1.80 \cdot 10^{-26}$ (2.0%) | $7.28 \cdot 10^{-27}$ (1.1%) | $3.75 \cdot 10^{-27}$ (0.9%) | $1.85 \cdot 10^{-27}$ (1.3%) | $5.84 \cdot 10^{-28}$ (0.5%) |
| | ANISN (ENDF/4) EFF (Pb99S) | $1.91 \cdot 10^{-26}$ | $7.45 \cdot 10^{-27}$ | $3.79 \cdot 10^{-27}$ | $1.86 \cdot 10^{-27}$ | $5.91 \cdot 10^{-28}$ |
| | ANISN (ENDF/4) DLC37F | $1.97 \cdot 10^{-26}$ | $7.81 \cdot 10^{-27}$ | $3.98 \cdot 10^{-27}$ | $1.94 \cdot 10^{-28}$ | $6.06 \cdot 10^{-28}$ |
| ^{232}Th 1,4MeV | exp. | $(6.34 \pm 0.54) \cdot 10^{-28}$ | $(1.24 \pm 0.12) \cdot 10^{-28}$ | $(8.58 \pm 0.73) \cdot 10^{-29}$ | $(3.47 \pm 0.35) \cdot 10^{-29}$ | $(1.42 \pm 0.16) \cdot 10^{-29}$ |
| | MORSE (ENDF/4) EFF (Pb99S) (P, Cu, H ₂ O) | $1.16 \cdot 10^{-27}$ (0.4%) | $2.73 \cdot 10^{-28}$ (0.6%) | $1.01 \cdot 10^{-28}$ (1.4%) | $4.17 \cdot 10^{-29}$ (1.6%) | $1.52 \cdot 10^{-29}$ (1.3%) |
| | ANISN (ENDF/4) EFF (Pb99S) | $1.23 \cdot 10^{-27}$ | $2.71 \cdot 10^{-28}$ | $9.85 \cdot 10^{-29}$ | $4.06 \cdot 10^{-29}$ | $1.56 \cdot 10^{-29}$ |
| | ANISN (ENDF/4) DLC37F | $1.18 \cdot 10^{-27}$ | $2.54 \cdot 10^{-28}$ | $9.05 \cdot 10^{-29}$ | $3.70 \cdot 10^{-29}$ | $1.44 \cdot 10^{-29}$ |

Table 4 Activation Rates

| Distance from the sphere centre [cm] | | | | | | | |
|--|--|-------------------------------|----------------------------|----------------------------|----------------------------|----------------------------|----------------------------|
| Element | Method | 5 | 10 | 15 | 20 | 25 | |
| ⁶⁵ Cu (n, 2n) 12, 4MeV | exp. | (1.78±0.36) ⁻²⁷ | (3.62±0.72) ⁻²⁸ | (1.20±0.24) ⁻²⁸ | (4.52±0.92) ⁻²⁹ | (2.26±0.45) ⁻²⁹ | |
| | MORSE (ENDF/4) EFF (Pb99S) | 2.44 ⁻²⁷ (0.5%) | 4.06 ⁻²⁸ (0.8%) | 1.18 ⁻²⁸ (1.1%) | 4.50 ⁻²⁹ (0.1%) | 1.64 ⁻²⁹ (1.2%) | |
| | MORSE (ENDF/5-D) EFF (Pb99S) | 2.37 ⁻²⁷ (0.4%) | 3.94 ⁻²⁸ (0.6%) | 1.14 ⁻²⁸ (1.3%) | 4.04 ⁻²⁹ (1.7%) | 1.60 ⁻²⁹ (1.9%) | |
| | MORSE (ENDF/5-D) (P, Cu, H ₂ O) EFF (Pb99S) | 2.26 ⁻²⁷ (0.5%) | 3.85 ⁻²⁸ (0.8%) | 1.11 ⁻²⁸ (0.9%) | 4.08 ⁻²⁹ (2.1%) | 1.59 ⁻²⁹ (1.9%) | |
| | ANISN (ENDF/4) EFF (Pb99S) | 2.47 ⁻²⁷ | 4.01 ⁻²⁸ | 1.15 ⁻²⁸ | 4.07 ⁻²⁹ | 1.61 ⁻²⁹ | |
| | ANISN (ENDF/4) DLC37F | 2.47 ⁻²⁷ | 4.02 ⁻²⁸ | 1.15 ⁻²⁸ | 4.08 ⁻²⁹ | 1.61 ⁻²⁹ | |
| | MCNP (ENDF/4) | 1.99 ⁻²⁷ (0.3%) | 2.82 ⁻²⁸ (0.5%) | 0.82 ⁻²⁸ (0.7%) | 2.96 ⁻²⁸ (1.0%) | 1.17 ⁻²⁹ (1.1%) | |
| | ⁵⁸ Ni (n, p) 2, 8MeV | exp. | (6.96±1.18) ⁻²⁸ | (1.86±0.32) ⁻²⁸ | (6.32±1.07) ⁻²⁹ | (3.09±0.53) ⁻²⁹ | (1.69±0.29) ⁻²⁹ |
| | | MORSE (ENDF/4) EFF (Pb99S) | 18.9 ⁻²⁸ (1.3%) | 4.69 ⁻²⁸ (1.0%) | 1.80 ⁻²⁸ (1.1%) | 7.92 ⁻²⁹ (2.2%) | 2.64 ⁻²⁹ (0.9%) |
| MORSE (ENDF/5-D) EFF (Pb99S) | | 14.6 ⁻²⁸ (0.6%) | 3.07 ⁻²⁸ (0.9%) | 1.07 ⁻²⁸ (1.0%) | 4.23 ⁻²⁹ (3.0%) | 1.50 ⁻²⁹ (1.4%) | |
| MORSE (ENDF/5-D) (P, Cu, H ₂ O) EFF (Pb99S) | | 14.4 ⁻²⁸ (1.8%) | 3.05 ⁻²⁸ (0.9%) | 1.05 ⁻²⁸ (1.0%) | 4.16 ⁻²⁹ (1.6%) | 1.53 ⁻²⁹ (1.5%) | |
| ANISN (ENDF/4) EFF (Pb99S) | | 19.4 ⁻²⁸ | 4.74 ⁻²⁸ | 1.80 ⁻²⁸ | 7.63 ⁻²⁹ | 2.62 ⁻²⁹ | |
| ANISN (ENDF/4) DLC37F | | 18.3 ⁻²⁸ | 4.32 ⁻²⁸ | 1.62 ⁻²⁸ | 6.81 ⁻²⁹ | 2.36 ⁻²⁹ | |

Table 4

Continuation

| Element | Method | 5 | 10 | 15 | 20 | 25 |
|--|--|----------------------------------|----------------------------------|----------------------------------|----------------------------------|----------------------------------|
| ^{64}Zn (n,p) 2,8MeV | exp. | $(5.84 \pm 0.99) \cdot 10^{-28}$ | $(1.16 \pm 0.20) \cdot 10^{-28}$ | $(3.88 \pm 0.66) \cdot 10^{-29}$ | $(1.50 \pm 0.28) \cdot 10^{-29}$ | $(7.79 \pm 1.32) \cdot 10^{-30}$ |
| | MORSE (ENDF/4) EFF (Pb99S) | 8.22-28 (1.0%) | 1.84-28 (0.8%) | 6.57-29 (0.9%) | 2.69-29 (1.3%) | 9.47-30 (1.2%) |
| | MORSE (ENDF/5-D) EFF (Pb99S) | 8.20-28 (0.7%) | 1.83-28 (0.9%) | 6.62-29 (1.1%) | 2.82-29 (2.6%) | 9.57-30 (1.0%) |
| | ANISN (ENDF/4) EFF (Pb99S) | 8.40-28 | 1.84-28 | 6.57-29 | 2.68-29 | 9.44-30 |
| | ANISN (ENDF/4) DLC37F | 8.04-28 | 1.71-28 | 6.00-29 | 2.43-29 | 8.63-30 |
| | | | | | | |
| ^{103}Rh (n,n') | exp. | $(2.89 \pm 0.45) \cdot 10^{-27}$ | $(1.09 \pm 0.17) \cdot 10^{-27}$ | $(6.54 \pm 1.01) \cdot 10^{-28}$ | $(2.77 \pm 0.43) \cdot 10^{-28}$ | $(1.34 \pm 0.21) \cdot 10^{-28}$ |
| | MORSE (ENDF/4) EFF (Pb99S) | 5.69-27 (1.1%) | 1.84-27 (0.9%) | 1.26-27 (0.9%) | 6.17-28 (0.9%) | 1.99-28 (0.4%) |
| | MORSE (ENDF/5-) EFF (Pb99S) | 5.73-27 (0.6%) | 2.44-27 (1.0%) | 1.20-27 (0.9) | 6.24-28 (1.0%) | 2.01-29 (1.4%) |
| | ANISN (ENDF/4) EFF (Pb99S) | 5.97-27 | 2.51-27 | 1.27-27 | 6.28-28 | 2.02-29 |
| | ANISN (ENDF/4) DLC37F | 5.75-27 | 2.42-27 | 1.23-27 | 6.08-28 | 1.95-29 |
| | | | | | | |
| ^{27}Al (n, α) 7,2MeV | exp. | $(1.97 \pm 0.30) \cdot 10^{-28}$ | $(4.52 \pm 0.68) \cdot 10^{-29}$ | $(1.35 \pm 0.20) \cdot 10^{-29}$ | $(5.04 \pm 0.76) \cdot 10^{-30}$ | $(2.39 \pm 0.36) \cdot 10^{-30}$ |
| | MORSE (ENDF/5-D) EFF (Pb99S) | 3.41-28 (0.4%) | 5.83-29 (0.6%) | 1.73-29 (1.5%) | 6.13-30 (1.8%) | 2.42-30 (1.9%) |
| | MORSE (ENDF/5-D) (P, Cu, H ₂ O) EFF (Pb99S) | 3.27-28 (0.6%) | 5.69-29 (0.8%) | 1.68-29 (1.0%) | 6.21-30 (2.2%) | 2.43-30 (1.9%) |
| | MCNP (ENDF/4) | 3.40-28 (0.15%) | 5.86-29 (0.5%) | 1.74-29 (0.7%) | 6.41-30 (1.0%) | 2.53-30 (1.1%) |

point cross sections. Multigroup cross sections in P5 approximation referred as Pb995 were calculated by using SUPERTOG-B[7] code and the following cross section data:EFF[8] for Pb[MAT.4820] and ENDF/B4 for H[MAT.1276],O[MAT.1269] and Cu[MAT.1295]. Data for lead from DLC37F[9] cross section library [MAT....], Pb[MAT139001] from EURLIB[10] and Pb[MAT205EFF1] from [12] in VITAMIN -J group presentation and P5 approximation have been also used in calculations.

Multigroup response functions for activation and fission detectors have been prepared by means of SUPERTOG code -on the base of ENDF/B4 and ENDF/B5-D dosimetry files. In Tables 3 and 4 the response functions libraries are indicated in brackets a long with the transport code used. Data used for lead are shown in the following row.

Neutron leakage flux integrated in wide energy intervals is shown in Table 2. Experimental results are higher than calculated ones in all intervals which is in agreement with benchmark authors calculations [9]. The greatest discrepancy (~20%) is obtained in the low energy range(0-1MeV). The difference in the total flux reaches 25-30%. The influence of the neutron absorption in the target material (Cu&H₂O) is negligible. It brings the result for total flux down with no more than 1% on the account of the neutron absorption (see the last two rows in Table 2). The low energy part of neutrons (0-0.05)MeV which is excluded in the experiment, amounts to only 1% from the total leakage (see the last row in Table 2).

Calculations with cross section data from EURLIB and Pb175F6 are closer to the experimental results but there is still 10% disagreement in total leakage estimation. The discrepancy one can see from Figure 2 (Table 5) where the thick line represents the experimental spectrum, long dashed line is the MORSE result and short dashed line is the ANISN calculation.

Calculational results for activation and fission rates are shown in Table 3 and 4. Reaction thresholds are given below detector designation.

Table 5 Neutron leakage spectrum per unit of lethargy and source neutron

| E(MeV) | N(u) (_ N(u)) Experiment | N(u) ANISN Pb99S | N(u) (_ N, %) MORSE Pb99S, Cu |
|---------|------------------------------|------------------------|--------------------------------------|
| 0.05 | 0.048 (0.005) | | |
| 0.06 | 0.057 (0.006) | 0.045 | 0.045 (6) |
| 0.07 | 0.069 (0.007) | | |
| 0.08 | 0.080 (0.008) | 0.052 | 0.049 (5.3) |
| 0.09 | 0.091 (0.009) | | |
| 0.10 | 0.098 (0.010) | 0.079 | |
| 0.12 | 0.125 (0.013) | 0.099 | 0.105 (7.1) |
| 0.15 | 0.170 (0.017) | 0.136 | 0.139 (4.9) |
| 0.18 | 0.215 (0.020) | 0.175 | 0.191 (5) |
| 0.20 | 0.241 (0.024) | 0.226 | 0.235 (3.4) |
| 0.30 | 0.370 (0.037) | 0.334 | 0.366 (3.5) |
| 0.40 | 0.550 (0.055) | 0.434 | |
| 0.50 | 0.725 (0.073) | 0.693 | 0.676 (2.4) |
| 0.60 | 0.805 (0.081) | 0.706 | |
| 0.70 | 0.810 (0.095) | 0.759 | 0.779 (1.9) |
| 0.80 | 0.850 (0.110) | 0.809 | 0.839 (2.1) |
| 0.90 | 0.880 (0.120) | 0.735 | |
| 1.00 | 0.865 (0.120) | 0.751 | 0.733 (2.3) |
| 1.2 | 0.800 (0.100) | 0.668 | 0.604 (2.6) |
| 1.5 | 0.745 (0.090) | 0.659 | 0.626 (2.8) |
| 1.8 | 0.590 (0.070) | 0.505 | 0.564 (2.5) |
| 2.0 | 0.495 (0.050) | 0.465 | 0.473 (2.7) |
| 2.5 | 0.293 (0.030) | 0.270 | 0.268 (4) |
| 3.0 | 0.167 (0.015) | 0.152 | 0.132 (5.2) |
| 3.5 | 0.099 (0.009) | 0.090 | 0.088 (7.4) |
| 4.0 | 0.066 (0.006) | | 0.056 (9.7) |
| 4.5 | 0.046 (0.004) | 0.042 | 0.046 (10) |
| 5.0 | 0.036 (0.003) | 0.055 | |
| 5.5 | 0.029 (0.003) | | 0.033 (9.8) |
| 6.0 | 0.026 (0.003) | | 0.028 (13.2) |
| 6.5 | 0.024 (0.003) | 0.032 | |
| 7.0 | 0.026 (0.003) | 0.030 | 0.024 (13.2) |
| 7.5 | 0.027 (0.004) | 0.029 | 0.031 (13.5) |
| 8.0 | 0.028 (0.004) | | |
| 8.5 | 0.032 (0.004) | 0.031 | 0.033 (13.8) |
| 9.0 | 0.034 (0.004) | | |
| 9.5 | 0.036 (0.005) | 0.032 | 0.042 (12.1) |
| 10.0 | 0.033 (0.005) | | |
| 10.5 | 0.031 (0.004) | 0.027 | 0.029 (13.1) |
| 11.0 | 0.032 (0.004) | | |
| 11.5 | 0.033 (0.004) | 0.028 | 0.035 (14.7) |
| 12.0 | 0.033 (0.004) | | |
| 12.2 to | | | |
| 14.9 | 0.670 (0.067) | 0.617 | 0.635 |

²³⁸U reaction rate values calculated with ENDF/B5-D cross sections are 1.3-1.6 times greater than experimental ones and those calculated with ENDF/B4 are even another 10% greater than that. The similarity of the curves shape shows systematic deviation between the experimental and calculated results. Reaction rates results for ²³⁸U calculated with

Model for IAEA Sponsored International Comparison of Benchmark Calculations

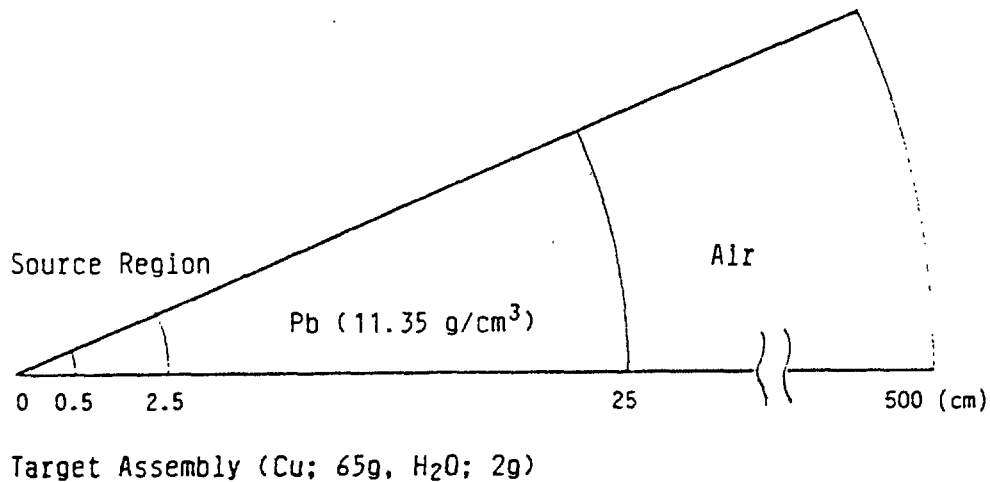
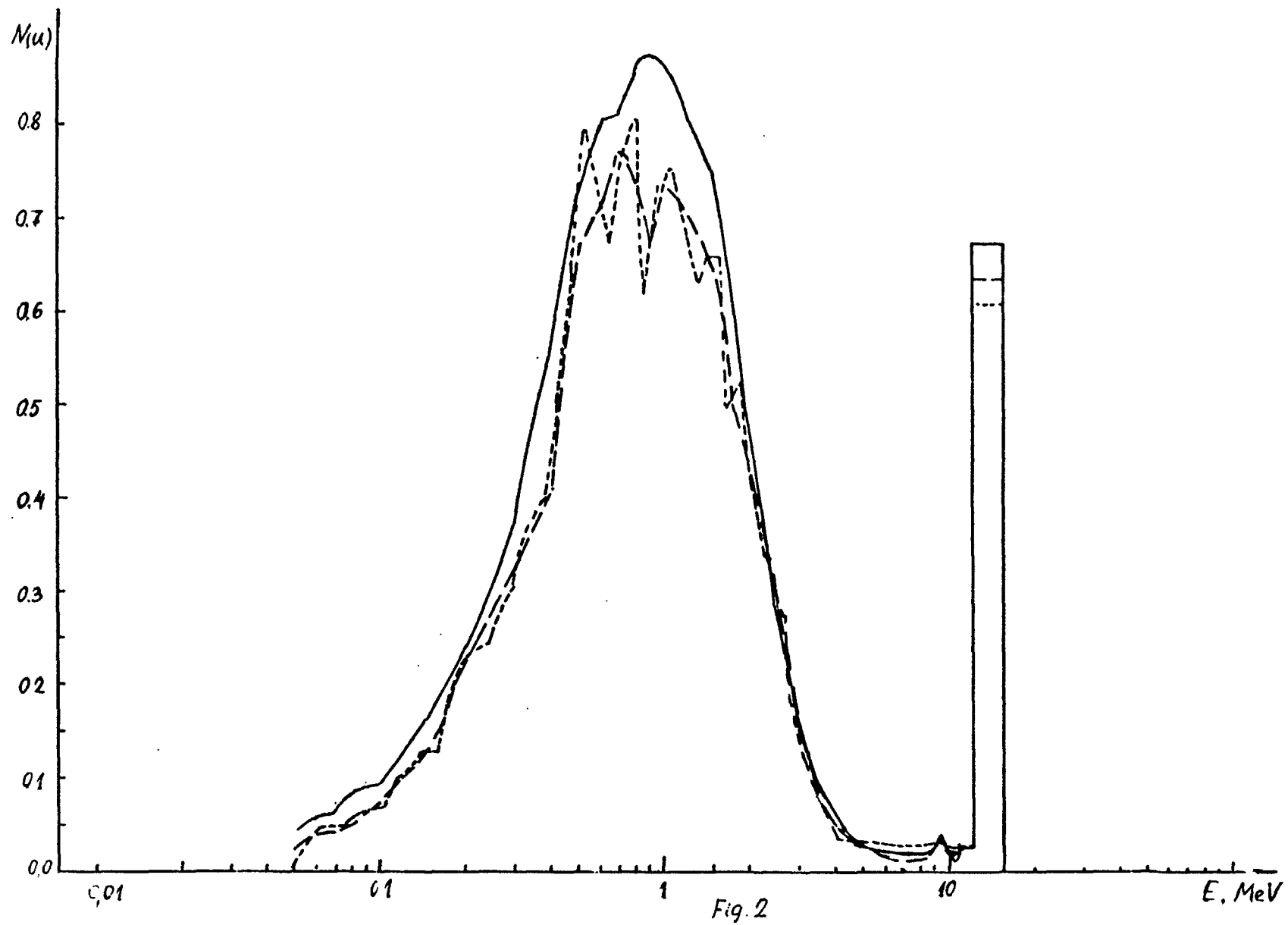


Figure 1 Model for 1-D Calculation

MORSE and ANISN show the same trend. The MCNP results are relatively closer to the experiment but are out of the error corridor. Reaction rates for ²³²Th are twice different at the sphere center and are almost equal (10% difference) at the surface. The greatest discrepancy for ²⁷Al is at the sphere center (twice) and goes down towards the surface where the results coincide within the error. For ⁶⁰Cu there is coincidence only at distance of 15cm. The results for ⁵⁹Ni calculated with ENDF/B5-D are closer to the experiment than those with ENDF/B4-D but at the sphere center they are as high as twice. The difference also diminishes towards the surface where it is negligible. Calculated results for ⁶⁴Zn (n,p) are at average of 1.4 times systematically higher than experimental ones. The results for ¹⁰³Rh are about twice higher than experimental ones.

In conclusion it could be pointed out that the experimentally obtained functionals of neutron spectrum in the lead sphere, i.e. activation and fission reaction rates of have lower values than calculated results. It is in contradiction with TOF and PRS experimental spectrum which is higher than calculated one.



REFERENCES

- [1] Goulo, V.: Report on the IAEA AGM on Nuclear Data for Fusion Reactor Technology, Gaussig, GDR, 1-5 December 1986, INDC/P(87)-3, IAEA Nuclear Data Section, 3 March 1987.
- [2] Cheng E.T. Review of the Nuclear Data Status and Requirements for Fusion Reactors General Atomics, August 1988, GA-A19369.
- [3] Elfruth T., et al The Neutron Multiplication of Lead at 14 MeV Neutron Incidence Energy, Atomkernenergie. Kerntechnik, vol.49(1987), No 3, 121-125.
- [4] Engle, W.W, Jr.: ANISN, A.E.C. Research and Development Report K-1693 (1967).
- [5] J.E.Briesmeister (Ed.): MCNP - A General Monte Carlo Code for Neutron and Photon Transport, Version 3A, LA-7396-M, Sept. 1986.
- [6] Fraley, S.K: Users Guide to MORSE-SGC. ORNL 1976.
- [7] G.Voykov, K.Ilieva, V.Gadjokov. Legendre Series Development of the Anisotropy Density of Neutron Elastic Scattering by Means of Cubic Splines INDC (BUL)-11, May 1986.
- [8] ZZ-EFF-1-Pb-NEA 1050/02, received from IAEA, News from the NEA DATA BANK (Dr. V.Goulo).
- [9] L.J.Baker, N.P.Taylor. The Harwell Version of the DLC37F Nuclear Data L.Labr.Harwell Laboratory, July 1985.
- [10] ZZ-EURLIB NEA 0794/01
- [11] Seidel K., Additional Informations to the Dresden Lead Sphere Benchmark., Memorandum to Benchmark Participants, July 8, 1988.
- [12] 205EFF1 PBNAT MAT=4820. Tape No RL334, received from NDS, desp. 87/06/26, file 4.(Dr. V.Goulo).

IAEA Specialists' Meeting on
THE FUSION EVALUATED NUCLEAR DATA LIBRARY (FENDL)
AND BENCHMARK CALCULATION

IAEA Headquarters, Vienna, 8-11 May 1989

LIST OF PARTICIPANTS

AUSTRIA

H.K. Vonach
Institut für Radiumforschung
und Kernphysik
Boltzmannngasse 3
A-1090 Vienna

R. Feldbacher
Institut für Theoretische Physik
Technische Universität Graz
Petersgasse 16
A-8010 Graz

BULGARIA

K. Ilieva
Institute of Nuclear Research
and Nuclear Energy
Bulgarian Academy of Sciences
72 Lenin Blvd.
1184 Sofia

CHINA, People's Rep.

Zhou Delin
Chinese Nuclear Data Centre (CNDC)
Institute of Atomic Energy
P.O. Box 275 (41)
Beijing

GERMAN Dem. Rep.

D. Seeliger
Sektion Physik
Technische Universität Dresden
Mommensenstrasse 13
DDR-8051 Dresden

GERMANY, Fed. Rep.

V. Fischer
Kernforschungszentrum Karlsruhe
Postfach 3640
D-7500 Karlsruhe

ITALY

G. Reffo
ENEA - Centro Ricerche
Energia "E. Clementel"
Div. Fis. e Calcolo Scientifico
Via Mazzini 2
I-40138 Bologna

G.C. Panini
ENEA - Centro Ricerche Energia
"E. Clementel"
Div. Fis. e Calcolo Scientifico
Via Mazzini 2
I-40138 Bologna

JAPAN

S. Igarasi
Physics Department
Japan Atomic Energy Research
Institute (JAERI)
Tokai-mura, Naka-gun
Ibaraki-ken 319-11

K. Sumita
Department of Nuclear Engineering
Osaka University
Faculty of Engineering
2-1 Yamadaoka
Suita-shi 565

H. Maekawa
FNS, Division of Reactor Engineering
Japan Atomic Energy Research
Institute (JAERI)
Tokai-mura, Naka-gun
Ibaraki-ken 319-11

NETHERLANDS

H. Gruppelaar
Department of Physics
Netherlands Energy Research
Foundation (ECN)
P.O.B. 1, 3 Westerduinweg
NL-1755 ZG Petten

J. Kopecky
Department of Physics
Netherlands Energy Research
Foundation (ECN)
P.O.B. 1, 3 Westerduinweg
NL-1755 ZG Petten

SWITZERLAND

S. Pelloni
Eidgenossisches Institut für
Reaktorforschung
CH-5305 Würenlingen

U.S.S.R.

V.G. Pronyaev
Centr po Jadernym Dannym
Fiziko-Energeticheskij Institut
Ploschad Bondarenko
249 020 Obninsk, Kaluga Region

D.V. Markovskij
Institut Atomnoi Energii
I.V. Kurchatova
Ploschad Kurchatova
Moscow D-182, 123182

UNITED KINGDOM

R. Forrest
Atomic Energy Research
Establishment (AERE)
Harwell, Didcot, OXON. OX11 0RA

U.S.A.

C.L. Dunford
National Nuclear Data Center
Brookhaven National Laboratory
Upton, New York 11973

D.W. Muir
T-2 Nuclear Data, MS-243
Los Alamos National Laboratory
P.O. Box 1663
Los Alamos, New Mexico 87545

D.C. Larson
Eng. Physics and Math. Division
Bldg. 6010, MS-356
Oak Ridge National Laboratory
P.O. Box 2008
Oak Ridge, TN 37831

F.M. Mann
L7-29
Hanford Engineering Development
Laboratory
Westinghouse Hanford
P.O. Box 1970
Richland, WA 99352

E.T. Cheng
GA Technologies Inc.
P.O. Box 85608
San Diego, CA 92138

I.A.E.A.

V. Konshin
IAEA Nuclear Data Section
Wagramerstr. 5, P.O. Box 100
A-1400 Vienna

Wang Dahai
IAEA Nuclear Data Section
Wagramerstr. 5, P.O. Box 100
A-1400 Vienna

J.J. Schmidt
IAEA Nuclear Data Section
Wagramerstr. 5, P.O. Box 100
A-1400 Vienna

K. Okamoto
IAEA Nuclear Data Section
Wagramerstr. 5, P.O. Box 100
A-1400 Vienna

V.G. Goulo (Scientific Secretary)
IAEA Nuclear Data Section
Wagramerstr. 5, P.O. Box 100
A-1400 Vienna

J. Kupitz
IAEA
Wagramerstr. 5, P.O. Box 100
A-1400 Vienna

N. Kocherov
IAEA Nuclear Data Section
Wagramerstr. 5, P.O. Box 100
A-1400 Vienna

V. Demchenko
IAEA
Wagramerstr. 5, P.O. Box 100
A-1400 Vienna

9. Reports submitted for the IAEA Specialists'
meeting on FENDL, 14-16 November 1987

**A COMPARATIVE STUDY OF TRITIUM BREEDING CALCULATIONS
USING EFF-1 AND ENDF/B-V BASED NUCLEAR DATA LIBRARIES**

**S. PELLONI
SWISS FEDERAL INSTITUTE FOR REACTOR RESEARCH (EIR)
WUERENLINGEN, SWITZERLAND**

**E.T. CHENG
GA TECHNOLOGIES INC.
SAN DIEGO, CALIFORNIA, USA**

NUCLEAR DATA LIBRARIES AND TRANSPORT CALCULATIONS

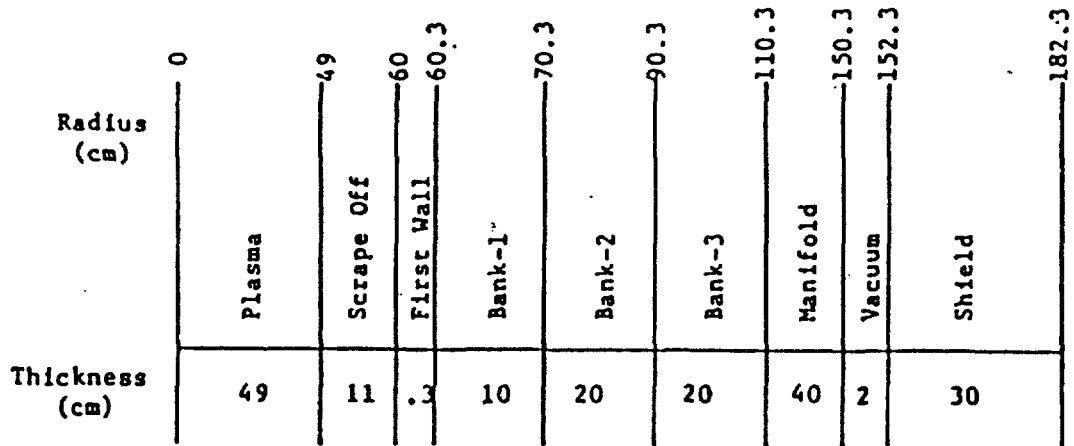
*** EIR, SWITZERLAND**

**NUCLEAR DATA FILE : EFF-1
PROCESSING CODE : NJOY
GROUP STRUCTURE : 175 GROUP VITAMIN-J
TRANSPORT CODE : ONEDANT**

*** GA TECHNOLOGIES, USA**

**NUCLEAR DATA FILE : ENDF/B-V
PROCESSING CODE : NJOY
GROUP STRUCTURE : CONTINUOUS
TRANSPORT CODE : MCNP (MONTE CARLO)**

SYSTEM DESCRIPTION OF THE LI17PB83 BCSS BLANKET



Material Compositions (vol-%)

| | V15Cr5Ti | | 17Li83Pb* | Fel422 |
|------------|----------------|--------------------------|-----------|--------|
| First Wall | 100 | | --- | --- |
| Bank-1 | 7.1 | | 73.7 | --- |
| Bank-2 | 7.1 | | 73.7 | --- |
| Bank-3 | 7.1 | | 73.7 | --- |
| Manifold | 10 | | 20 | 70 |
| Shield | 80 (Fel422) | 20 (H ₂ O) | | |

*17Li83Pb density = 100% of T.D.; ⁶Li enrichment = 30%.

**COMPARISON OF CALCULATED REACTION RATES
IN LITHIUM-LEAD BCSS BLANKET USING EFF-1
AND ENDF/B-V LIBRARIES (30% Li-6 IN LITHIUM)**

| LIBRARY | Li17Pb83 BREEDING ZONE THICKNESS (m) | | | | | |
|------------|--------------------------------------|----------|-------|----------|-------|----------|
| | 0.2 | | 0.5 | | 0.6 | |
| | EFF-1 | ENDF/B-V | EFF-1 | ENDF/B-V | EFF-1 | ENDF/B-V |
| T6 | 0.718 | 0.769 | 1.122 | 1.169 | 1.225 | 1.282 |
| T7 | 0.014 | 0.015 | 0.017 | 0.018 | 0.018 | 0.018 |
| TBR | 0.732 | 0.784 | 1.149 | 1.187 | 1.243 | 1.300 |
| Pb (n, 2n) | 0.585 | 0.625 | 0.706 | 0.714 | 0.714 | 0.714 |
| Pb (n, γ) | 0.027 | 0.032 | 0.053 | 0.057 | 0.059 | 0.064 |

**COMPARISON OF CALCULATED REACTION RATES
IN LITHIUM-LEAD BCSS BLANKET USING EFF-1
AND ENDF/B-V LIBRARIES (90% Li-6 IN LITHIUM)**

| LIBRARY | Li17Pb83 BREEDING ZONE THICKNESS (m) | | | | | |
|------------|--------------------------------------|----------|--------|----------|--------|----------|
| | 0.2 | | 0.5 | | 0.6 | |
| | EFF-1 | ENDF/B-V | EFF-1 | ENDF/B-V | EFF-1 | ENDF/B-V |
| T6 | 1.085 | 1.138 | 1.448 | 1.495 | 1.520 | 1.560 |
| T7 | 0.0020 | 0.0022 | 0.0025 | 0.0025 | 0.0025 | 0.0026 |
| TBR | 1.087 | 1.140 | 1.451 | 1.498 | 1.522 | 1.563 |
| Pb (n, 2n) | 0.584 | 0.621 | 0.705 | 0.712 | 0.712 | 0.712 |
| Pb (n, γ) | 0.0203 | 0.0229 | 0.0339 | 0.0366 | 0.0368 | 0.0389 |

DESCRIPTION OF EVALUATIONS FOR $^{50,52,53,54}\text{Cr}$
PERFORMED FOR ENDF/B-VI*

D. C. Larson, D. M. Hetrick, and C. Y. Fu
Oak Ridge National Laboratory
Oak Ridge, Tennessee 37831-6356
U. S. A.

ABSTRACT

Isotopic evaluations for $^{50,52,53,54}\text{Cr}$ performed for ENDF/B-VI are briefly reviewed. The evaluations are based on analysis of experimental data and results of model calculations which reproduce the experimental data. Evaluated data are given for neutron induced reaction cross sections, angular and energy distributions, and for gamma-ray production cross sections associated with the reactions. File 6 formats are used to represent energy-angle correlated data and recoil spectra. Uncertainty files are included for the major cross sections. Detailed evaluations are given for $^{52,53}\text{Cr}$, and results of calculations for reactions with large cross sections are used for evaluation of the minor isotopes.

1. INTRODUCTION

Separate evaluations have been done for each of the stable isotopes of chromium. In this report we briefly review the structure of the evaluations, describe how the evaluations were done, and note the major pieces of data considered in the evaluation process. Experimental data references were obtained primarily from CINDA, but also from the literature and reports. The data themselves were mostly obtained from the National Nuclear Data Center at Brookhaven National Laboratory and, occasionally, from the literature and reports. The TNG nuclear model code (FU80,SH86), a multistep Hauser-Feshbach code which includes precompound and compound contributions to cross sections, angular, and energy distributions in a self-consistent manner, calculates gamma-ray production, and conserves angular momentum in all steps, was the primary code used for these evaluations. Extensive model calculations were performed for each isotope with the goal of simultaneously reproducing experimental data for all reaction channels with one set of parameters. This ensures internal consistency and energy conservation within the evaluation. In the case of reactions for which sufficient data were available, a Bayesian analysis using the GLUCS code (HE80) was frequently done, using ENDF/B-V or the TNG results as the prior. In cases where insufficient data were available for a GLUCS analysis and the available data were deemed to be accurate, but in disagreement with the TNG results, a line was drawn through the data and used for the evaluation. A hand-drawn line was also used for cross sections where resonant structure was felt to be important, but resonance parameters were not included. The final evaluation is thus a combination of TNG results (used where extrapolation and interpolation was required and where data sets were badly discrepant), GLUCS results (used where sufficient data existed to do an analysis), and hand-drawn curves. In the case of the isotopic chromium evaluations, no reaction was deemed to have enough appropriate data for a GLUCS analysis, so the evaluations depend upon TNG results and hand-drawn curves.

*Research sponsored by the Office of Basic Energy Sciences, U.S. Department of Energy, under contract DE-AC05-84OR21400 with Martin Marietta Energy Systems, Inc.

In Section 2 the resonance parameters are discussed; Section 3 contains a description of the major cross sections included in the evaluation; Section 4 is devoted to angular distributions; and Section 5 to energy-angle correlated distributions. Section 6 describes the uncertainty files.

Much of this information is abstracted from Ref. HE87, a report devoted to a description of the calculations for ^{52}Cr , and Ref. SH87, a similar report for ^{53}Cr . As of this writing, the various pieces of the evaluations are being reviewed, modified if necessary, and assembled into full evaluations using the ENDF/B-VI formats, and will be submitted by May 1988 to the Cross Section Evaluation Working Group (CSEWG) for use in ENDF/B-VI.

2. RESONANCE PARAMETERS

Resonance parameters are taken from Mughabghab (MU81) for energies below about 15 keV. From 15 keV to about 900 keV, the parameters are taken from recent ORNL (AG84) and Geel (BR85) transmission data. Capture resonance parameters are taken from MU81, with average parameters used where individual parameters are not available. The resonance parameters should be processed with the Reich-Moore formalism.

3. CROSS SECTIONS

In this section the evaluation of reactions with large cross sections is presented. The total cross section above the resonance region is taken from recent ORELA transmission measurements on a natural sample. However, if the high-resolution isotopic transmission data from Geel (BR85) are available, it will be used for the evaluation. Experimental data for cross sections describing inelastic scattering to discrete levels in ^{52}Cr are available for only the first two levels at incident neutron energies >4 MeV, and no data are available at 14 MeV. Thus, results of the TNG model calculations, including direct reaction contributions, were used for the evaluation. The calculations were in good agreement with available data, and with a recent measurement of the total inelastic scattering cross section from 1 to 40 MeV (LA85). Figure 1 shows a comparison of the calculated total inelastic cross section with the experimental data. Cross sections for inelastic scattering in the minor isotopes were also taken from the TNG calculations. In all cases a continuum was used to describe inelastic scattering for excitation energies above the discrete levels.

The calculated (n,p) cross sections are in acceptable agreement with the experimental data for both $^{52,53}\text{Cr}$ from 6 to 8 MeV, and around 14 MeV. The calculated values of the total proton emission cross sections for ^{52}Cr are in good agreement with the data of Smith and Meadows (SM80), Grimes et al. (GR79), Colli et al. (CO62) and Barschall (BA82). Since the (n,α) reaction on both $^{52,53}\text{Cr}$ leads to a stable nucleus, no activation data are available, only alpha production data from measured alpha spectra. For ^{52}Cr the TNG results agree within uncertainties with the data of Paulsen et al (PA81) up to 10 MeV, but are at the lower limit of the experimental uncertainties at 14 MeV for the data of Grimes et al. (GR79), Dolja et al. (DO73), and Barschall (BA82). Since much of the energy range to 20 MeV has no data, the calculated results were again taken for the evaluation. For ^{53}Cr , there is only one data point, at 14 MeV, and the calculated result is low.

Available data for the $^{52}\text{Cr}(n,2n)$ reaction are in disagreement near 14 MeV. The calculated results from TNG provide a reasonable compromise near 14 MeV, and are about 15% larger than the measurement of Bormann et al. (BO68) from 13 to 20 MeV. Since no data are available for the $^{53}\text{Cr}(n,2n)$ cross

section, the calculated results were used in the evaluation. Combining the TNG results for $^{52,53}\text{Cr}$ give results which are in good agreement with the $(n,2n)$ natural sample data of Auchampaugh et al. (AU77), Frehaut et al. (FR80), and Frehaut and Mosinski (FR75).

4. ANGULAR DISTRIBUTIONS

Elastic scattering angular distributions generated from the Wilmore-Hodgson potential (WI64) (used for all calculations for chromium) are in good agreement with the measured data and are given as Legendre coefficients in File 4/2. All other angular distribution information is given in File 6.

5. ENERGY-ANGLE CORRELATED DISTRIBUTIONS

Particle emission spectra are often measured as a function of outgoing particle angle, and this correlation of outgoing angle with measured energy spectra can now be represented in File 6. However, often these distributions are measured only at one incident energy, and we must rely upon model calculations to reproduce the available energy and angular distribution information so it can be calculated for the evaluation at other incident energies. File 6 is extensively used in this evaluation to represent energy-angle correlated data. Energy spectra for all outgoing particles, including photons, are given in this file. Angular distributions are given for the neutron emission spectra; for this evaluation angular distributions for all other particles are assumed to be isotropic. Figure 2 (HE87) shows a comparison of the calculated and measured angular distributions for three outgoing neutron energy bins, and Figure 3 (HE87) shows a comparison of the measured and calculated neutron emission spectra around 14 MeV incident neutron energy. These energy-angle distributions were calculated with TNG and entered in File 6 for $^{52,53}\text{Cr}$ at several incident neutron energies between 1 and 20 MeV.

Figures 4 and 5 (HE87) show a comparison of the measured and calculated emission spectra for the $^{52}\text{Cr}(n, xp)$ and $^{52}\text{Cr}(n, \alpha)$ reactions around 14 MeV. These calculated results, at several incident energies between 1 and 20 MeV, have been adopted for the evaluation and put in File 6.

Figure 6 (HE87) shows a comparison of the calculated gamma-ray emission spectrum at 9.5 MeV with the measurement of Morgan and Newman (MO76) for the bin covering incident neutron energies from 9 to 10 MeV. Calculated results from TNG at several incident neutron energies between 1 and 20 MeV were used for the evaluation, with File 6 being used for ease in calculating energy balance.

As an example of the usage of File 6, consider the $^{52}\text{Cr}(n, n\alpha)$ reaction. In File 6/22, constant yields are given for the outgoing neutron, alpha, and ^{48}Ti residual, and an energy-dependent yield is used for the gamma rays associated with the $(n, n\alpha)$ reaction. Normalized energy distributions are given for each outgoing product, but only the outgoing neutron has a non-isotropic angular distribution. The cross section to be used for normalization is taken from File 3/22.

Capture gamma-ray cross sections and spectra are given in Files 13 and 15 respectively and are based on a combination of experimental data and calculated results.

6. UNCERTAINTY INFORMATION

Uncertainty files are given only for the cross sections in File 3, and not for the resonance parameters, energy distributions or angular

distributions. Fractional and absolute components, correlated only within a given energy interval, are based on scatter in experimental data and estimates of uncertainties associated with the model calculations.

REFERENCES

- AG84 H. M. Agrawal, J. B. Garg, and J. A. Harvey, *Phys. Rev. C* 30(6), 1880 (1984).
- AU77 G. F. Auchampaugh, D. M. Drake, and L. R. Veesser, *Neutron Cross Section Programs in the Energy Region from 1 to 24 MeV at the LASL Van de Graaff Facilities*, BNL-NCS-50681, pp. 231-246 (May 1977).
- BA82 H. H. Barschall, *Europhys. Topical Conf. on Neutron Induced Reactions, Smolenice* (June 1982); Proceedings published by Slovak Acad. Sciences as *Physics and Applications*, 10, 279 (1982).
- BO68 M. Bormann, A. Behrend, I. Riehle, and O. Vogel, *Nucl. Phys.* A115, 309 (July 1968).
- BR85 A. Brusegan, R. Buyl, F. Corvi, L. Mewissen, F. Poortmans, G. Rohr, R. Shelley, T. Van der Veen, I. Van Marcke, "High Resolution Neutron Capture and Total Cross Section Measurements of ^{50}Cr , ^{52}Cr , and ^{53}Cr ," p. 633 in *Proc. Int. Conf. Nuclear Data for Basic and Applied Science, Vol. 1, Santa Fe, N. M., May 13-17, 1985*.
- CO62 L. Colli, I. Iori, S. Micheletti, and M. Pignanelli, *Nuovo Cimento* 21, 966 (1962).
- DO73 G. P. Dolja, V. P. Bozhko, V. Ja. Golovnja, A. P. Kljucharev, and A. I. Tutubalin, *Proc. Nejtronnaja Fizika* 3, 131 Kiev (1973).
- FR75 J. Frehaut and G. Mosinski, 5th Int. Seminar on Interaction of Fast Neutrons with Nuclei, Gaussig, (November 1975).
- FR80 J. Frehaut, A. Bertin, R. Bois, and J. Jary, *Status of (n,2n) Cross Section Measurements at Bruyeres-Li-Chatel*, BNL-NCS-51245, pp. 399-411 (May 1980).
- FU80 C. Y. Fu, "A Consistent Nuclear Model for Compound and Precompound Reactions with Conservation of Angular Momentum," p. 757 in *Proc. Int. Conf. Nuclear Cross Sections for Technology, Knoxville, TN, Oct. 22-26, 1979*, NBS-594, U.S. National Bureau of Standards. Also, ORNL/TM-7042 (1980).
- GR79 S. M. Grimes, R. C. Haight, K. R. Alvar, H. H. Barschall, and R. R. Borchers, *Phys. Rev. C* 19, 2127 (June 1979).
- HE75 D. Hermsdorf, A. Meister, S. Sassonoff, D. Seeliger, K. Seidel, and F. Shahin, *Zentralinstitut fur Kernforschung Rossendorf Bei Dresden, Zfk-277 (U)* (1975).
- HE80 D. M. Hetrick and C. Y. Fu, *GLUCS: A Generalized Least-Squares Program for Updating Cross Section Evaluations With Correlated Data Sets*, ORNL/TM-7341, ENDF-303 (October 1980).
- HE87 D. M. Hetrick, C. Y. Fu, and D. C. Larson, *Calculated Neutron-Induced Cross Sections for ^{52}Cr from 1 to 20 MeV and Comparisons with Experiments*, ORNL/TM-10417, ENDF-346 (September 1987).

- LA85 D. C. Larson, "High-Resolution Structural Material $(n,x\gamma)$ Production Cross Sections for $0.2 < E_n \leq 40$ MeV," p. 71 in *Proc. Conf. on Nuclear Data for Basic and Applied Science, Santa Fe, New Mexico, Vol. 1, 1985*.
- MO76 G. L. Morgan and E. Newman, *The Cr(n,x γ) Reaction Cross Section for Incident Neutron Energies Between 0.2 and 20.0 MeV*, ORNL/TM-5098, ENDF-222 (January 1976).
- MU81 S. F. Mughabghab, M. Divadeenam, and N. E. Holden, *Neutron Cross Sections, Vol. 1, Neutron Resonance Parameters and Thermal Cross Sections, Part A, Z=1-60*, Academic Press (1981).
- PA81 A. Paulsen, H. Liskien, F. Arnotte, and R. Widera, *Nucl. Sci. and Eng.* **78**, 377 (1981).
- SA72 O. A. Salnikov, G. N. Lovchikova, G. V. Kotelnikova, A. M. Trufanov, and N. I. Fetisov, *Differential Cross Sections of Inelastic Scattering Neutrons on Nuclei Cr, Mn, Fe, Co, Ni, Cu, Y, Zr, Nb, W, Bi*, Report Jadernye Konstanty -7, 102 (March 1972).
- SH86 K. Shibata and C. Y. Fu, *Recent Improvements of the TNG Statistical Model Code*, ORNL/TM-10093 (August 1986).
- SH87 K. Shibata and D. M. Hetrick, *Calculated Neutron-Induced Cross Sections for ^{53}Cr from 1 to 20 MeV*, ORNL/TM-10381 (1987).
- SM80 D. L. Smith and J. W. Meadows, *Nucl. Sci. and Eng.* **76**, 43 (September 1980).
- TA65 S. Tagesen and P. Hille, *Oesterr. Akad. Wiss., Math. Naturwiss. Kl., Sitz. Abt. 2*, **174**, 85 (March 1965).
- TA83 A. Takahashi, J. Yamamoto, T. Murakami, K. Oshima, H. Oda, K. Fujimoto, M. Ueda, M. Fukazawa, Y. Yanagi, J. Miyaguchi, and K. Sumita, Oktavian Report A-83-01, Osaka University, Japan (June 1983).
- VA62 D. M. Van Patter, N. Nath, S. M. Shafroth, S. S. Malik, and M. A. Rothman, *Phys. Rev.* **128**, 1246 (1962).
- VO80 H. Vonach, A. Chalupka, F. Wenninger, and G. Staffel, "Measurement of the Angle-Integrated Secondary Neutron Spectra from Interaction of 14 MeV Neutrons with Medium and Heavy Nuclei," *Proc. Symp. on Neutron Cross-Sections from 10 to 50 MeV*, BNL-NCS-51245, Brookhaven National Laboratory (July 1980).
- WI64 D. Wilmore and P. E. Hodgson, *Nucl. Phys.* **55**, 673 (1964).

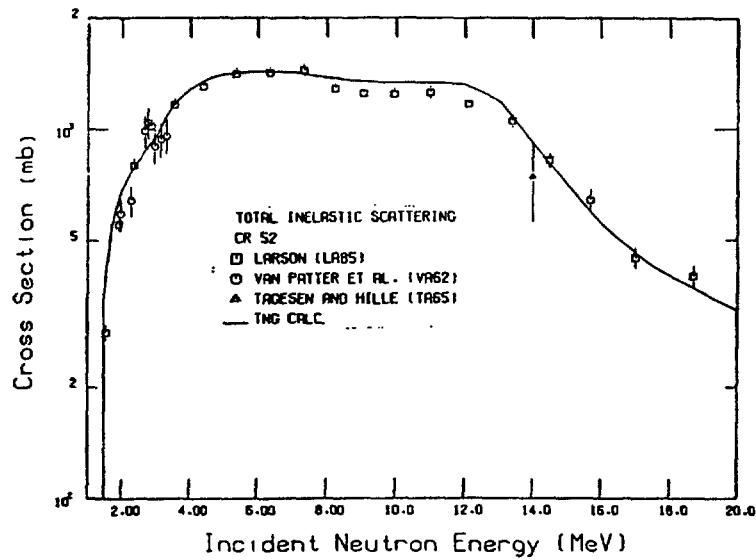


Fig. 1. Comparison of calculated and experimental total inelastic scattering cross sections for ^{52}Cr .

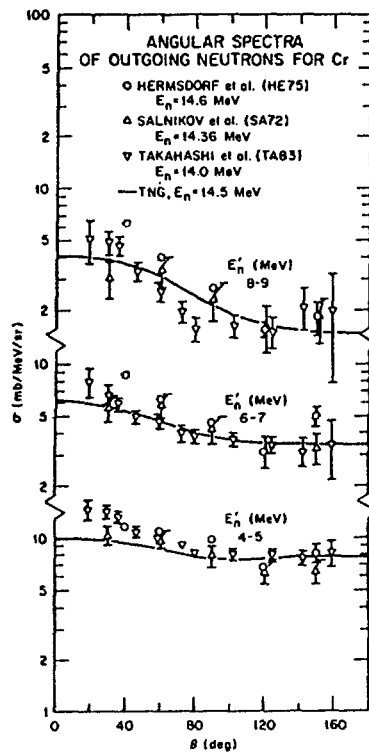


Fig. 2. Comparison of calculated and experimental neutron production cross sections.

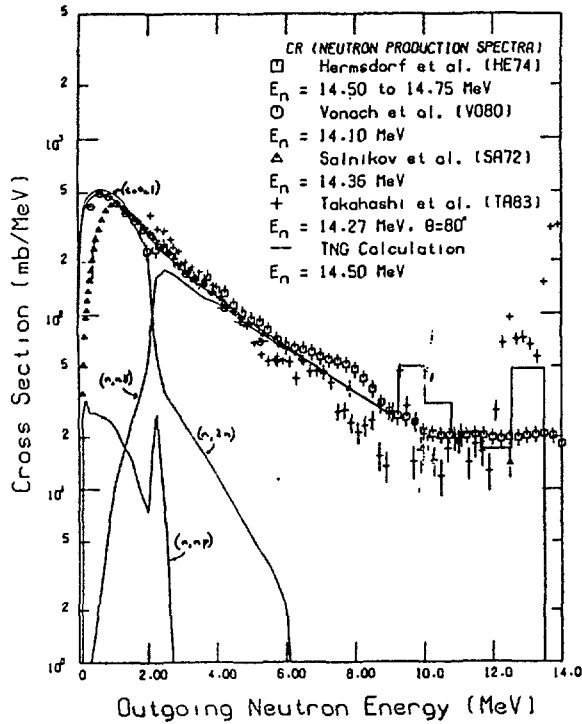
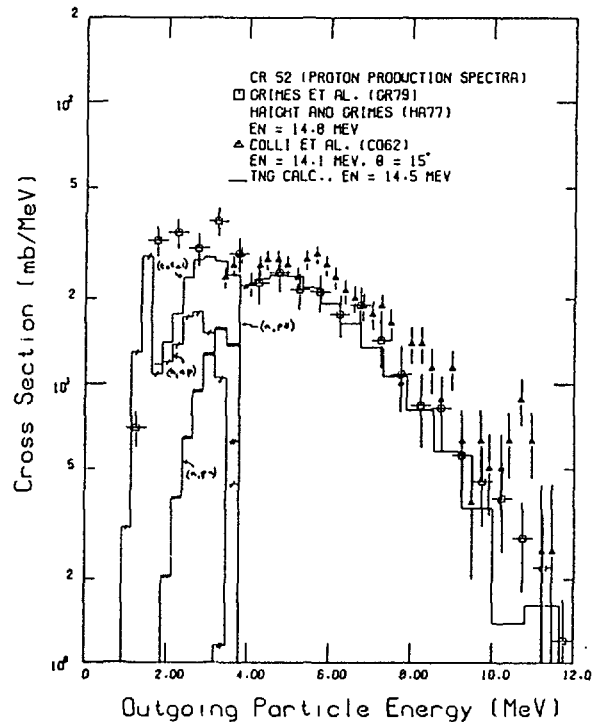


Fig. 3. Neutron emission spectra from the TNG calculation compared with experimental data. The data of Takahashi et al. (TA83) were taken at 80° , and the other measured data sets shown (HE74, V080, and SA72) are angle integrated. Contributions from the various neutron-producing components are shown (they sum to the total). The curve labeled (n,np) includes the (n,pn) component. The (n,na) and (n,an) components were also calculated, but fall below the bottom of the plot.

Fig. 4. Comparison of calculated experimental proton production spectra for ^{52}Cr . The measurements were taken at incident energies of 14.8 and 14.1 MeV; the TNG calculation was for $E_n = 14.5$ MeV. The data of Grimes et al. (GR79, HA77) are angle integrated; the data of Colli et al. (C062) were taken at 15° .



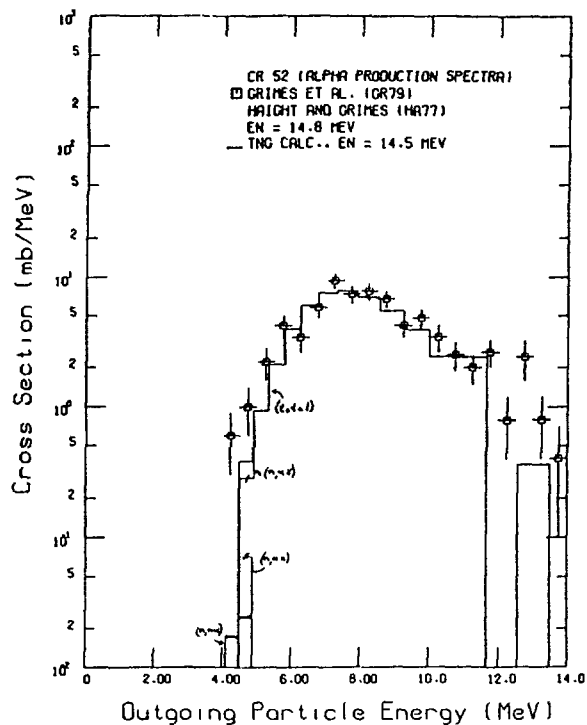
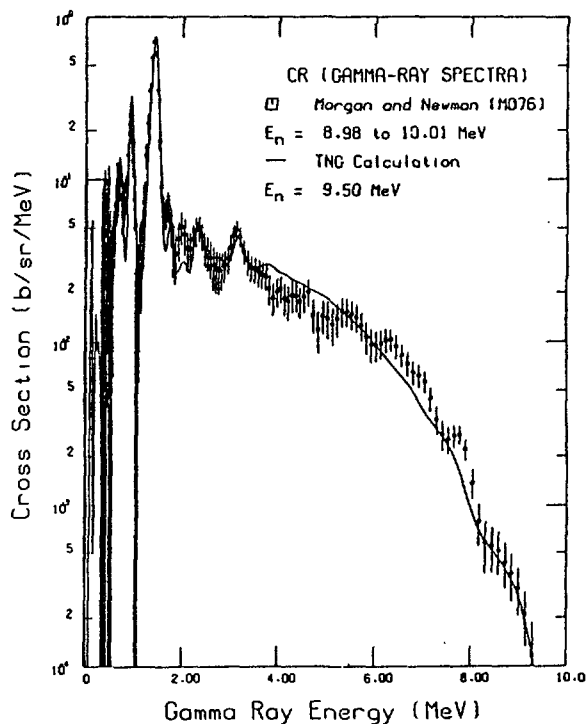


Fig. 5. Comparison of calculated and experimental alpha production spectra for ^{52}Cr . The measurement was taken at an incident energy of 14.8 MeV, the TNG calculation was for $E_n = 14.5$ MeV.

Fig. 6. Secondary gamma-ray spectra versus gamma-ray energy from the TNG calculation (incident energy $E_n = 9.5$ MeV) compared with the data of Morgan and Newman (M076).



DESCRIPTION OF EVALUATIONS FOR $^{58,60,61,62,64}\text{Ni}$
PERFORMED FOR ENDF/B-VI*

D. C. Larson, D. M. Hetrick, and C. Y. Fu
Oak Ridge National Laboratory
Oak Ridge, Tennessee 37831-6356
U. S. A.

ABSTRACT

Isotopic evaluations for $^{58,60,61,62,64}\text{Ni}$ performed for ENDF/B-VI are briefly reviewed. The evaluations are based on analysis of experimental data and results of model calculations which reproduce the experimental data. Evaluated data are given for neutron induced reaction cross sections, angular and energy distributions, and for gamma-ray production cross sections associated with the reactions. File 6 formats are used to represent energy-angle correlated data and recoil spectra. Uncertainty files are included for the major cross sections. Detailed evaluations are given for $^{58,60}\text{Ni}$, and results of calculations for the major reactions are used for evaluations of the minor isotopes.

1. INTRODUCTION

Separate evaluations have been done for each of the stable isotopes of nickel. In this report, we briefly review the structure of the evaluations, describe how the evaluations were done, and note the major pieces of data considered in the evaluation process. Experimental data references were obtained primarily from CINDA, but also from the literature and reports. The data themselves were mostly obtained from the National Nuclear Data Center at Brookhaven National Laboratory and, occasionally, from the literature and reports. The TNG nuclear model code (FU80,SH86), a multistep Hauser-Feshbach code which includes precompound and compound contributions to cross sections, angular, and energy distributions in a self-consistent manner, calculates gamma-ray production, and conserves angular momentum in all steps, was the primary code used for these evaluations. Extensive model calculations were performed with the goal of simultaneously reproducing experimental data for all reaction channels with one set of parameters. This ensures internal consistency and energy conservation within the evaluation. In the case of reactions for which sufficient data were available, a Bayesian analysis using the GLUCS code (HE80) was frequently done, using ENDF/B-V or the TNG results as the prior. In cases where insufficient data were available for a GLUCS analysis, and the available data were deemed to be accurate, but in disagreement with the TNG results, a line was drawn through the data and used for the evaluation. A hand-drawn line was also used for cross sections where resonant structure was felt to be important, but resonance parameters were not included. The final evaluation is thus a combination of TNG results (used where extrapolation and interpolation was required and where data sets were badly discrepant), GLUCS results (used where sufficient data existed to do an analysis), and hand-drawn curves.

In Section 2 the resonance parameters are discussed; Section 3 contains a description of the major cross sections included in the evaluation; Section 4 is devoted to angular distributions; and Section 5 to energy-angle correlated distributions. Section 6 describes the uncertainty files.

*Research sponsored by the Office of Basic Energy Sciences, U.S. Department of Energy, under contract DE-AC05-84OR21400 with Martin Marietta Energy Systems, Inc.

Much of this information is abstracted from Ref. HE87, a report devoted to a description of the calculations for $^{58,60}\text{Ni}$. As of this writing, the various pieces of the evaluations are being reviewed, modified if necessary, and assembled into full evaluations using the ENDF/B-VI formats, and will be submitted by May 1988 to the Cross Section Evaluation Working Group (CSEWG) for inclusion in ENDF/B-VI.

2. RESONANCE PARAMETERS

Resonance parameters for ^{58}Ni from 10 to 810 keV were taken from a recent SAMMY analysis (PE87) of ORELA transmission, scattering, and capture data. Sixty-two $\ell=0$ and 410 $\ell>0$ resonances were identified and are included, using the Reich-Moore formats. Resonance parameters for ^{60}Ni cover the energy range from 1 to 450 keV and were also taken from a SAMMY analysis of ORELA transmission and capture data (PE83). Thirty $\ell=0$ and 227 $\ell>0$ resonances were identified and included in the ^{60}Ni evaluation. For the $^{61,62,64}\text{Ni}$ evaluations, the resonance parameters were taken from the compilation of Mughabghab (MU81).

3. CROSS SECTIONS

In this section we briefly describe the contents of the files containing cross sections for the more important reactions. The total cross section for ^{58}Ni above the resonance region was taken from a high-resolution measurement (PE87) up to 20 MeV. For $^{60,61,62,64}\text{Ni}$ the total cross section above the resonance region was taken from a high-resolution measurement of natural nickel (LA83). Cross sections for inelastic scattering to discrete levels in $^{58,60}\text{Ni}$ were taken from the model calculations which compared favorably with numerous data sets available for these levels. Direct interaction contributions were included for many of the levels. Agreement with experimental data is generally favorable; however, the experimental uncertainties are often rather large. Figures 1 and 2 show a comparison of the TNG results with experimental data for the total inelastic scattering cross section for $^{58,60}\text{Ni}$, respectively. For $^{61,62,64}\text{Ni}$ the cross sections for the lowest few levels were included from the calculations, and a continuum was used to represent the remainder of the inelastic scattering cross section.

Abundant data are available to define the $^{58,60}\text{Ni}(n,p)$ reaction cross sections. Figure 3 shows a comparison of the available data, and the TNG and GLUCS results for the $^{58}\text{Ni}(n,p)$ cross section. The evaluated $^{58}\text{Ni}(n,p)$ cross section was taken from a Bayes' simultaneous analysis of several correlated cross sections (FU82), while the $^{60,61,62,64}\text{Ni}(n,p)$ cross sections were taken from the model calculations. Data for the (n,α) reactions are sparse, and the evaluations are based on calculated results, which were compared with available experimental data. Total proton and alpha emission cross sections for $^{58,60}\text{Ni}$ were also taken from the model calculations and agreed well with the integrated data at 14 MeV of Grimes et al. (GR79) and Kneff et al. (KN86), and with the data of Qaim et al. (QA84) at lower energies.

There is abundant cross section data for the $^{58}\text{Ni}(n,2n)$ reaction, but no data for the $(n,2n)$ cross section on any of the other isotopes. Results of the TNG model calculations were in good agreement with the available $(n,2n)$ data, as well as the neutron emission spectra for natural Ni; thus results of the model calculations were used for the $(n,2n)$ cross sections for all of the isotopes. It should be noted that the $(n,2n)$ cross sections are large for the minor isotopes $^{61,62,64}\text{Ni}$, and were explicitly included in the reactions for these minor isotopes.

Cross sections for all significant binary and tertiary reactions are given for each isotopic evaluation. See the detailed description in Ref. (HE87) for $^{58,60}\text{Ni}$.

4. ANGULAR DISTRIBUTIONS

Calculated elastic scattering angular distributions using the Wilmore-Hodgson optical model potential (WI64) are in good agreement with abundant experimental data and are given as Legendre coefficients in File 4/2. Disagreements in experimental angular distribution data sets for inelastic scattering to discrete levels are often outside rather large uncertainties. Model calculations including direct interaction and compound reaction contributions were compared with available data and used for the evaluations. These data are also entered as Legendre coefficients in File 6/51-90 in each evaluation for as many levels as discrete information is available. Only the few lowest levels were used for the minor isotopes, and isotropic angular distributions were assumed.

5. ENERGY-ANGLE CORRELATED DISTRIBUTIONS (FILE 6)

Often, neutron, proton, alpha, and gamma-ray emission spectral data are measured as a function of outgoing particle angle, and this correlation of outgoing angle with measured spectra can now be represented in File 6. However, generally these distributions have only been measured at one or at most a few incident energies, thus we rely upon the TNG model calculations to reproduce the available data as a function of outgoing energy and angle, and then extrapolate to other incident neutron energies. Figure 4, taken from Ref. HE87, shows a comparison of the experimental data with the calculated results for the natural $\text{Ni}(n,xn)$ cross section, and Figure 5 (HE87) shows a comparison of the measured and calculated angular distributions for three outgoing neutron energy bins. These calculated energy-angle distributions have been taken from the TNG calculations and entered in File 6 for the $^{58,60}\text{Ni}$ evaluations for a number of incident energies between 1 and 20 MeV. Cross sections associated with these distributions are given in File 3.

Figures 6 and 7 (HE87) show comparisons of calculated results with experimental data for the $^{58}\text{Ni}(n,xp)$ and $^{60}\text{Ni}(n,x\alpha)$ reactions near 14 MeV, respectively. These energy distributions, with isotropic angular distributions assumed, have been entered in File 6. Recoil spectra for the heavy residual nuclei have also been included in File 6. Since the angular distributions are given as isotropic, File 5 could have been used for all charged particle spectra with the exception of the recoil spectra, but for ease of energy balance and KERMA calculations, a consistent File 6 usage is desirable. Cross sections associated with these distributions are given in File 3.

File 6 was also chosen to represent the gamma-ray production energy distributions, for consistency with the neutron and charged particle distributions. Isotropic angular distributions were used for the gamma rays. Figure 8 (HE87) shows a comparison of measured gamma-ray spectra around 14 MeV with the TNG calculation at 14.5 MeV. Note that without use of the calculated results, a significant amount of cross section below about 1-MeV gamma-ray energy would be missing. Calculated distributions are given in File 6 for several incident neutron energies from 1 to 20 MeV. Cross sections associated with these distributions are given in File 3.

Capture gamma-ray cross sections and spectra are given in File 13 and 15, respectively, and are based on a combination of experimental data and calculation.

As an example of the usage of File 6, consider the $^{58}\text{Ni}(n,n\alpha)$ reaction. In File 6/22, constant yields are given for the outgoing neutron, alpha and ^{54}Fe residual, and an energy dependent yield is used for the gamma rays associated with the $(n,n\alpha)$ reaction. Normalized energy distributions are given for each outgoing product, but only the outgoing neutron has a non-isotropic angular distribution. The cross section to be used for normalization is taken from File 3/22.

6. UNCERTAINTY INFORMATION

Uncertainty files are given only for the cross sections in File 3 and not for the resonance parameters, energy distributions or angular distributions. Fractional and absolute components, correlated only within a given energy interval, are based on scatter in experimental data and estimates of uncertainties associated with the model calculations.

REFERENCES

- BR71 W. Breunlich and G. Stengel, *Z. Naturforsch. A* **26**, 451 (March 1971).
- CL72 G. Clayeux and J. Voignier, *Centre d' Etudes de Limeil*, CEA-R-4279 (1972).
- CO62 L. Colli, I. Iori, S. Micheletti, and M. Pignanelli, *Nuovo Cimento* **21**, 966 (1962).
- DI73 J. K. Dickens, T. A. Love, and G. L. Morgan, *Gamma-Ray Production From Neutron Interactions with Nickel for Incident Neutron Energies Between 1.0 and 10 MeV: Tabulated Differential Cross Sections*, ORNL/TM-4379 (November 1973). (Title has error; should read 1.0 and 20 MeV.)
- FI84 R. Fischer, G. Traxler, M. Uhl, and H. Vonach, *Phys. Rev. C* **30**, 72 (1984).
- FU80 C. Y. Fu, "A Consistent Nuclear Model for Compound and Precompound Reactions with Conservation of Angular Momentum," p. 757 in *Proc. Int. Conf. Nuclear Cross Sections for Technology, Knoxville, TN, Oct. 22-26, 1979*, NBS-594, U.S. National Bureau of Standards. Also, ORNL/TM-7042 (1980).
- FU82 C. Y. Fu and D. M. Hetrick, "Experience in Using the Covariances of Some ENDF/B-V Dosimetry Cross Sections: Proposed Improvements and Addition of Cross-Reaction Covariances," p. 877 in *Proc. Fourth ASTM-EURATOM Symp. on Reactor Dosimetry, Gaithersburg, Maryland, March 22-26, 1982*, U.S. National Bureau of Standards.
- GR79 S. M. Grimes, R. C. Haight, K. R. Alvar, H. H. Barschall, and R. R. Borchers, *Phys. Rev. C* **19**, 2127 (June 1979).
- HA77 R. C. Haight and S. M. Grimes, Lawrence Livermore Laboratory, Report UCRL-80235 (1977).
- HE75 D. Hermsdorf, A. Meister, S. Sassonoff, D. Seeliger, K. Seidel, and F. Shahin, *Zentralinstitut Fur Kernforschung Rossendorf Bei Dresden*, Zfk-277 (U) (1975).
- HE87 D. M. Hetrick, C. Y. Fu, and D. C. Larson, *Calculated Neutron-Induced Cross Sections for $^{58,60}\text{Ni}$ from 1 to 20 MeV and Comparisons with Experiments*, ORNL/TM-10219 (ENDF-344) (June 1987).

- HE80 D. M. Hetrick and C. Y. Fu, *GLUCS: A Generalized Least-Squares Program for Updating Cross Section Evaluations with Correlated Data Sets*, ORNL/TM-7341, ENDF-303 (October 1980).
- JO69 B. Joensson, K. Nyberg, and I. Bergqvist, *Ark. Fys.* **39**, 295 (1969).
- KN86 D. W. Kneff, B. M. Oliver, H. Farrar IV, and L. R. Greenwood, *Nucl. Sci. Eng.* **92**, 491-524 (1986).
- LA83 D. C. Larson, N. M. Larson, J. A. Harvey, N. W. Hill, and C. H. Johnson, *Application of New Techniques to ORELA Neutron Transmission Measurements and Their Uncertainty Analysis: The Case of Natural Nickel From 2 keV to 20 MeV*, ORNL/TM-8203, ENDF-333, Oak Ridge National Laboratory, Oak Ridge, Tenn. (October 1983).
- LA85 D. C. Larson, "High-Resolution Structural Material (n,x γ) Production Cross Sections for $0.2 < E_n \leq 40$ MeV," *Proc. Conf. on Nucl. Data for Basic and Applied Science, Santa Fe, New Mexico*, **1**, 71 (1985).
- MA69 S. C. Mathur, P. S. Buchanan, and I. L. Morgan, *Phys. Rev.* **186**, 1038 (October 1969).
- MU81 S. F. Mughabghab, M. Divadeenam, and N. E. Holden, *Neutron Cross Sections, Vol. 1, Neutron Resonance Parameters and Thermal Cross Sections, Part A, Z=1-60*, Academic Press (1981).
- PE70 F. G. Perey, C. O. LeRigoleur, and W. E. Kinney, *Nickel-60 Neutron Elastic- and Inelastic-Scattering Cross Sections from 6.5 to 8.5 MeV*, ORNL-4523 (April 1970).
- PE83 C. M. Perey, J. A. Harvey, R. L. Macklin, and F. G. Perey, *Phys. Rev. C* **27**, 2556 (June 1983).
- PE87 C. M. Perey, F. G. Perey, J. A. Harvey, N. W. Hill, N. M. Larson, and R. L. Macklin, *$^{58}\text{Ni} + n$ Transmission, Capture and Differential Elastic Scattering Data Analysis from 6 to 810 keV*, to be published.
- QA84 S. M. Qaim, R. Wolfle, M.M. Rahman, and H. Ollig, *Nucl. Sci. Eng.* **88**, 143-153 (1984).
- SA72 O. A. Salnikov, G. N. Lovchikova, G. V. Kotelnikova, A. M. Trufanov, and N. I. Fetisov, *Differential Cross Sections of Inelastic Scattering Neutrons on Nuclei Cr, Mn, Fe, Co, Ni, Cu, Y, Zr, Nb, W, Bi*, Report Jadernye Konstanty -7, 102 (March 1972).
- SH86 K. Shibata and C. Y. Fu, *Recent Improvements of the TNG Statistical Model Code*, ORNL/TM-10093 (August 1986).
- TA83 A. Takahashi, J. Yamamoto, T. Murakami, K. Oshima, H. Oda, K. Fujimoto, M. Ueda, M. Fukazawa, Y. Yanagi, J. Mizaguchi, and K. Sumita, *Oktavian Report A-83-01*, Osaka University, Japan (June 1983).
- TO67 J. H. Towle and R. O. Owens, *Nucl. Phys.* **A100**, 257 (1967).
- VO80 H. Vonach, A. Chalupka, F. Wenninger, and G. Staffel, "Measurement of the Angle-Integrated Secondary Neutron Spectra from Interaction of 14 MeV Neutrons with Medium and Heavy Nuclei," *Proc. Symp. on Neutron Cross-Sections from 10 to 50 MeV*, BNL-NCS-51245, Brookhaven National Laboratory (July 1980).

WI64 D. Wilmore and P. E. Hodgson, *Nucl. Phys.* 55, 673 (1964).

XI82 S. Xiamin, W. Yongshun, S. Ronglin, X. Jinqiang, and D. Dazhav, *Proc. Int. Conf. on Nuclear Data for Science and Technology*, Antwerp, 373 (Sept. 6-10, 1982).

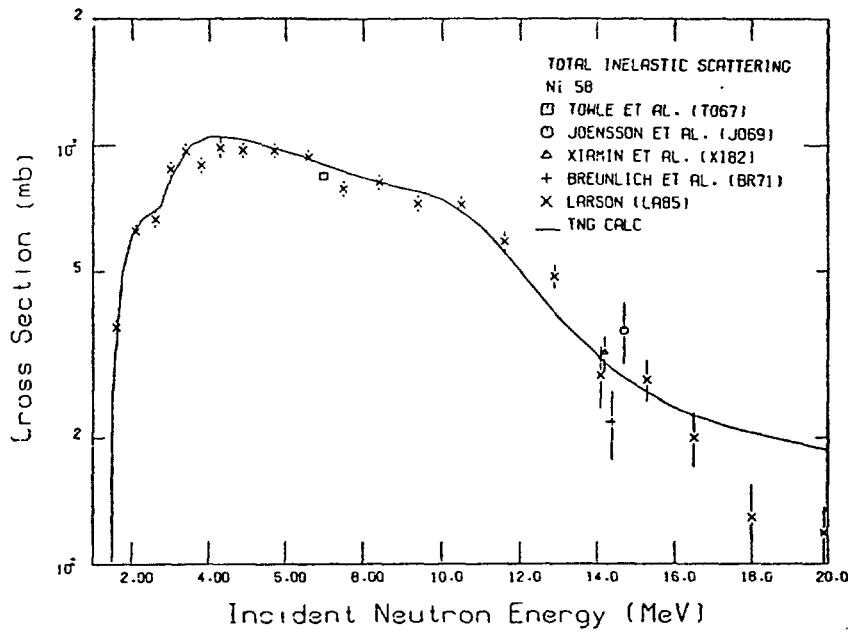


Fig. 1. Comparison of calculated and experimental total inelastic scattering cross sections for ^{58}Ni .

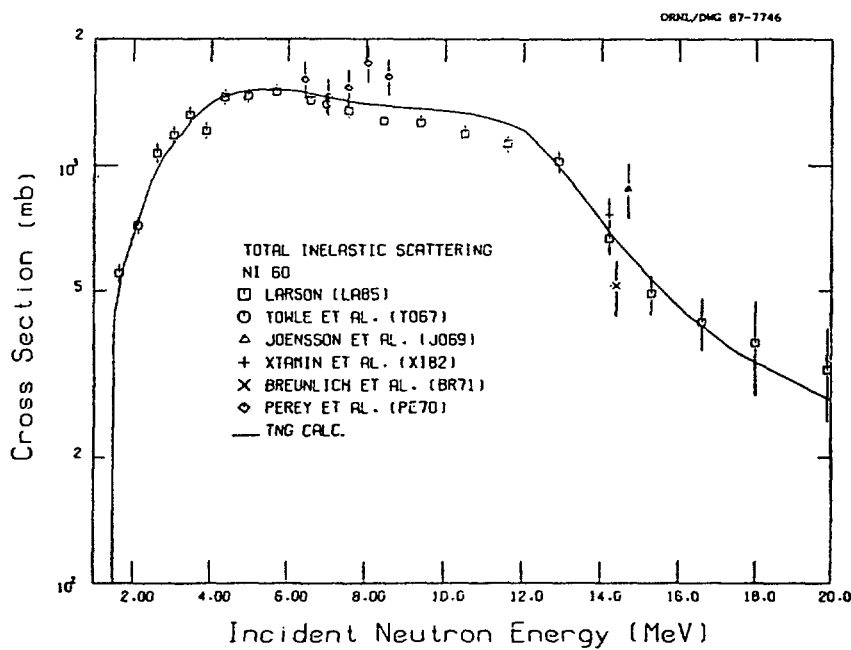


Fig. 2. Comparison of calculated and experimental total inelastic scattering cross sections for ^{60}Ni .

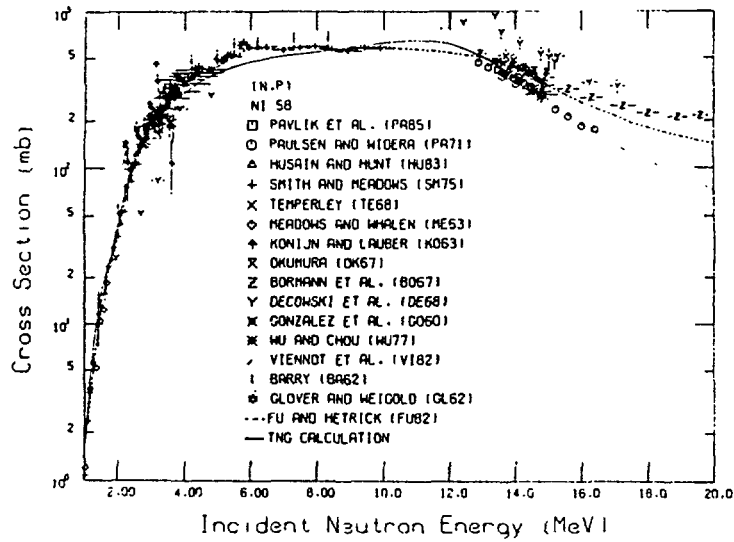


Fig. 3. Comparison of $^{58}\text{Ni}(n,p)$ cross sections with TNG results (HE87) and GLUCS results (FU82). (See Ref. HE87 for references.)

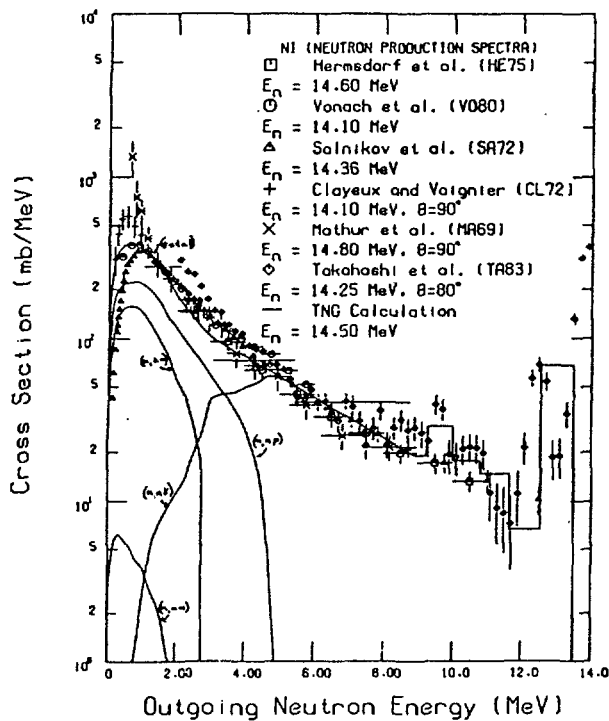


Fig. 4. Neutron emission spectra for the TNG calculation compared with experimental data. The data of Clayeux and Voignier (CL72) and Mathur et al. (MA69) were taken at 90° , the data of Takahashi et al. (TA83) were taken at 80° , and the other measured data sets shown (HE75, V080, and SA72) are angle integrated. Contributions from the various neutron-producing components are shown (they sum to the total). The curves labeled (n,n) and (n,α) include the (n,pn) and $(n,\alpha n)$ components, respectively.

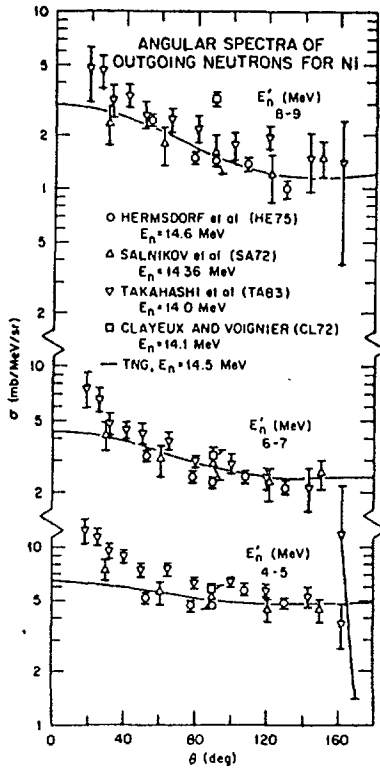
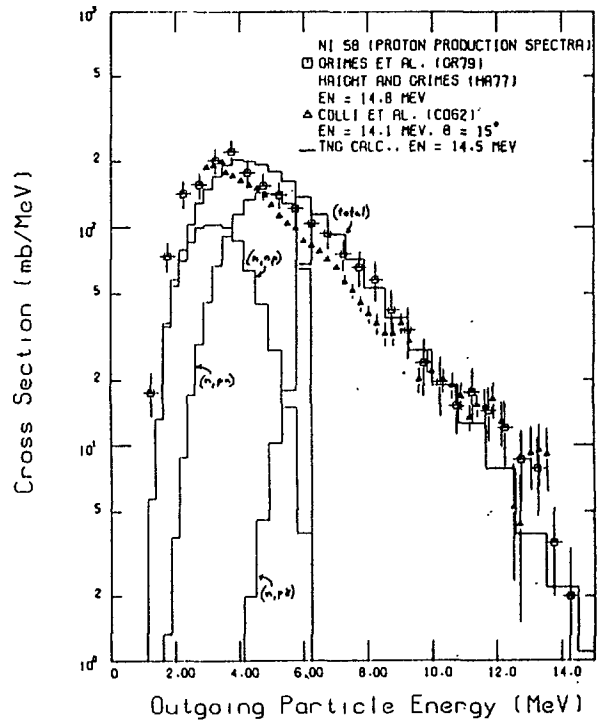


Fig. 5. Comparison of calculated and experimental neutron production cross sections.

Fig. 6. Comparison of calculated experimental proton production spectra for ^{58}Ni . The measurements were taken at incident energies of 14.8 and 14.1 MeV; the TNG calculation was for $E_n = 14.5$ MeV. The data of Grimes et al. (GR79, HA77) are angle integrated; the data of Colli et al. (CO62) were taken at 15° .



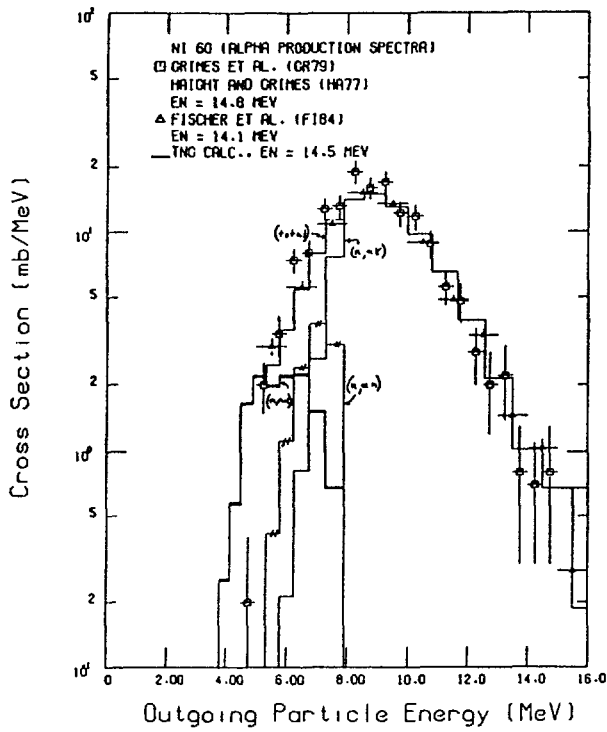
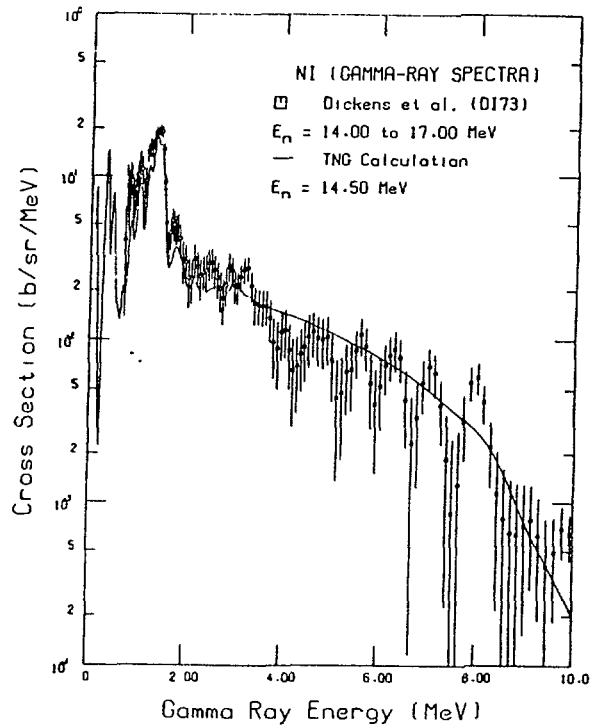


Fig. 7. Comparison of calculated and experimental alpha production spectra for ^{60}Ni . The measurements were taken at incident energies of 14.8 and 14.1 MeV and are angle integrated; the TNG calculation was for $E_n = 14.5$ MeV.

Fig. 8. Secondary gamma-ray spectra versus gamma-ray energy from the TNG calculation (incident energy $E_n = 14.5$ MeV) compared with the data of Dickens et al. (DI73).



DESCRIPTION OF EVALUATIONS FOR $^{54,56,57,58}\text{Fe}$
PERFORMED FOR ENDF/B-VI*

D. C. Larson, C. Y. Fu, and D. M. Hetrick
Oak Ridge National Laboratory
Oak Ridge, Tennessee 37831-6356
U. S. A.

ABSTRACT

Isotopic evaluations for $^{54,56,57,58}\text{Fe}$ performed for ENDF/B-VI are briefly reviewed. The evaluations are based on analysis of experimental data and results of model calculations which reproduce the experimental data. Evaluated data are given for neutron induced reaction cross sections, angular and energy distributions, and for gamma-ray production cross sections associated with the reactions. File 6 formats are used to represent energy-angle correlated data and recoil spectra. Uncertainty files are included for the major cross sections. A detailed evaluation is given for ^{56}Fe and results of calculations for the major reactions are used for evaluations of the minor isotopes, with particular attention paid to inelastic scattering to the low-lying levels in ^{57}Fe .

1. INTRODUCTION

Separate evaluations have been done for each of the stable isotopes of iron. In this report, we briefly review the structure of the evaluations, describe how the evaluations were done, and note the major pieces of data considered in the evaluation process. Experimental data references were obtained primarily from CINDA, but also from the literature and reports. The data themselves were mostly obtained from the National Nuclear Data Center at Brookhaven National Laboratory and, occasionally, from the literature and reports. The TNG nuclear model code (FU79,SH86), a multistep Hauser-Feshbach code which includes precompound and compound contributions to cross sections, angular, and energy distributions in a self-consistent manner, calculates gamma-ray production, and conserves angular momentum in all steps, was the primary code used for these evaluations. Extensive model calculations were performed with the goal of simultaneously reproducing experimental data for all reaction channels with one set of parameters. This ensures internal consistency and energy conservation within the evaluation. In the case of reactions for which sufficient data were available, a Bayesian analysis using the GLUCS code (HE80) was frequently done, using ENDF/B-V or the TNG results as the prior. In cases where insufficient data were available for a GLUCS analysis, and the available data were deemed to be accurate, but in disagreement with the TNG results, a smoothed-curve representation of the data was used for the evaluation. A similar method was also used for cross sections where resonant structure was felt to be important, but resonance parameters were not used. The final evaluation is thus a combination of TNG results (used where extrapolation and interpolation was required, and where data sets were badly discrepant), GLUCS results (used where sufficient data existed to do an analysis), and smoothed curves. Since iron is a very important material in fission and fusion reactors, much effort has gone into its evaluation (and analysis of the evaluations) over the past years, and results of this effort are reflected in the fine tuning done for ENDF/B-VI.

*Research sponsored by the Office of Basic Energy Sciences, U.S. Department of Energy, under contract DE-AC05-84OR21400 with Martin Marietta Energy Systems, Inc.

In Section 2 the resonance parameters are discussed; Section 3 contains a description of the major cross sections included in the evaluation; Section 4 is devoted to angular distributions; Section 5 to energy-angle correlated distributions; Section 6 to gamma-ray production cross sections; and Section 7 describes the uncertainty files.

Much of this information is abstracted from Refs. FU80, FU82, FU86, and FU87. As of this writing, the various pieces of the evaluations are being reviewed, modified if necessary, and assembled into full evaluations using the ENDF/B-VI formats, and will be submitted by May 1988 to the Cross Section Evaluation Working Group (CSEWG) for inclusion in ENDF/B-VI.

2. RESONANCE PARAMETERS

Resonance parameters for $^{54,56,57}\text{Fe}$ were taken from an evaluation of iron resonance parameters up to 400 keV by Perey and Perey (PE80). A total of 312 *s*-, *p*-, and *d*-wave resonances were included. The analysis was based on sets of existing resonance parameters, and an attempt was made to sort out the resonances seen in transmission measurements with different energy resolution, and reconcile them with resonances seen in capture measurements. Spin and parity information was available for some resonances in ^{56}Fe from high-resolution scattering measurements. Resonances in ^{58}Fe were taken from the ENDF/B-V dosimetry file.

Recent high resolution transmission, capture and scattering data for ^{56}Fe are available from ORELA and are currently being analyzed with the R-Matrix code SAMMY to obtain a consistent set of resonance parameters. This work will be incorporated in the ENDF/B-VI ^{56}Fe evaluation as late as possible, to allow the analysis to be pushed to as high a neutron energy as time permits. Resonance parameters for the other isotopes will be unchanged.

3. CROSS SECTIONS

In this section we briefly describe contents of the files containing cross sections for the more important reactions. The total cross section for the minor isotopes above the resonance region was taken from an ORELA measurement for natural iron. For ^{56}Fe , results of an ORELA high-resolution transmission measurement (which covered the energy range from 5 keV to 40 MeV and was used for the resonance parameter analysis) were used to 20 MeV. There are many data sets available for inelastic scattering to the first excited level in ^{56}Fe at 847 keV, including high resolution data showing resonant structure. Below 2 MeV the evaluation is based on the data of Kinney and Perey (KI77) and Voss et al. (VO71). Above 2 MeV several data sets were used, and the evaluated curve was adjusted within experimental uncertainties based on integral results and a consistent nuclear model analysis with TNG. Inelastic scattering cross sections to higher-lying levels in ^{56}Fe are based on a TNG analysis of experimental data and include a direct-reaction contribution to many of the levels. Inelastic scattering to the lowest few levels of $^{54,57,58}\text{Fe}$ is also included in evaluations of those isotopes. In particular, inelastic scattering to the first three levels in ^{57}Fe occurs at neutron energies below the first level in ^{56}Fe and is known to be an important energy loss mechanism when neutrons impinge upon natural iron. Above the discrete levels, inelastic scattering is represented by a continuum given in 3/91. Precompound effects are included both in the cross section and the angular and energy distributions.

The $^{56}\text{Fe}(n,p)$ reaction has several data sets available, and a GLUCS analysis was done which included this reaction. Results of that analysis were used in the evaluation of this cross section. This cross section was

also well reproduced by the TNG results. Evaluation of the (n,p) reaction for the minor isotopes was taken from TNG results. There are no measurements of the $^{56}\text{Fe}(n,\alpha)$ cross section via activation, since the product ^{53}Cr is stable. Thus, this cross section is taken from results of the TNG analysis, which is in good agreement with measured alpha production spectra, and agrees well with measured fission-spectrum averages. Cross sections for the (n,α) reaction on the minor isotopes were also taken from the TNG calculations.

Experimental data for the $(n,2n)$ reaction are available for natural iron. Figure 1 shows results of the TNG calculations for ^{56}Fe compared with available data and with earlier evaluations. The TNG calculated result is used for the present evaluation.

Cross sections for important tertiary reactions are given for ^{56}Fe , based on results of the TNG calculations.

4. ANGULAR DISTRIBUTIONS

High resolution elastic scattering data is available up to 1.23 MeV (KI77) and is used for the evaluation. A Legendre polynomial representation in the center-of-mass system is used. From 1.23 to 20 MeV the evaluation is based on a number of data sets and results of optical model calculations (FU80). Angular distributions are given for inelastic scattering to each level in ^{56}Fe , are taken from the TNG calculations, and most include a direct interaction component. Inelastic scattering to low-lying levels in the minor isotopes are assumed isotropic. Angular distributions for inelastic scattering from the continuum and for other neutron-producing reactions are correlated with outgoing energy and given in File 6.

5. ENERGY-ANGLE CORRELATED DISTRIBUTIONS (FILE 6)

Perhaps the major improvement in the iron evaluation for ENDF/B-VI is the use of correlated energy-angle distributions, obtained from TNG calculations. A revision to ENDF/B-V, incorporating these correlations for inelastic scattering from the continuum (crudely, however, due to format limitations), was quite successful in improving agreement of calculated results with measured values for several reactor problems. ENDF/B-VI uses these results, translated into File 6 formats which allow for more precise representation of the evaluated distributions. Energy-angle correlations in the secondary neutron spectra from the $(n,2n)$, (n,np) , and $(n,n\alpha)$ reactions are incorporated, using File 6. Variable bin widths (SH86) have been used for the neutron emission spectra to faithfully represent the peak area of the spectra. These correlations are particularly important since it is known that the angular distributions vary strongly with outgoing neutron energy (FU86). Energy-angle correlations were also used for the secondary neutrons from the $(n,\alpha n)$ and (n,pn) reactions. All File 6 evaluated data are taken from the TNG calculations, which have been compared with available data. Figure 2 shows a comparison of the TNG results with available neutron emission data as a function of angle for four outgoing neutron energy bins. Figure 3 shows a comparison of several measured neutron emission spectra with the TNG results. The calculated spectrum is broken down into its components $(n,n\gamma) + (n,2n) + ((n,n\alpha)+(n,\alpha n)) + ((n,np)+(n,pn))$.

Charged-particle and recoil spectra are also given in File 6, with isotropic angular distributions assumed. Figure 4 shows a comparison of the measured proton production spectrum of Grimes et al. (GR79) with the TNG results. Again, the proton emission spectrum is broken down into its components $(n,p\gamma) + ((n,np)+(n,pn))$. Figure 5 shows a similar comparison;

this time for the alpha production spectrum. In all cases, the calculated spectra are in good agreement with measured spectra.

As an example of the usage of File 6, consider the $^{56}\text{Fe}(n,n\alpha)$ reaction. In File 6/22, constant yields are given for the outgoing neutron, alpha and ^{52}Cr residual, and an energy dependent yield is used for the gamma rays associated with the $(n,n\alpha)$ reaction. Normalized energy distributions are given for each outgoing product, but only the outgoing neutron has a non-isotropic angular distribution. The cross section to be used for normalization is taken from File 3/22.

6. GAMMA-RAY-PRODUCTION CROSS SECTIONS

One of the major problems with earlier ENDF/B evaluations was a lack of energy balance between gamma rays and particle production. For ENDF/B-VI an effort has been made to alleviate this difficulty. Often the problem has arisen because experimentally measured gamma-ray-production spectra have been used directly in evaluations, without checking for energy balance with other outgoing particles. A typical case existed for iron, where three major sets of gamma-ray-production data existed as a function of neutron energy: that of Orphan, et al. (OR75), Dickens et al. (DI72), and Chapman et al. (CH76). However, the measured data sets disagreed by as much as a factor of two at some energies. A careful evaluation of the data, based on a TNG analysis which attempted to simultaneously fit data for all neutron-induced reactions as a function of incident energy, showed little room for changing neutron production cross sections, secondary neutron energy distributions, or secondary gamma-ray energy distributions. Results of these calculations produced gamma-ray-production cross sections that, while not in good agreement with any single measurement over the entire energy range, were in reasonable average agreement and removed the energy balance problem. Results of the TNG calculation were used for the evaluation.

Gamma-ray-production cross sections have been given separately for each reaction for ^{56}Fe . Gamma rays originating from discrete inelastic scattering in ^{56}Fe are given by branching ratios for exact energy balance. The same discrete gamma rays, arising from cascades of the continuum inelastic gamma rays, are separately given in section 91. This allows checking of energy balance for each individual reaction which could not be done with past evaluations since gamma-ray-production spectra were given only for the nonelastic reaction. File 6 was also chosen to represent the continuum gamma-ray production energy distributions for consistency with the neutron and charged-particle distributions. Isotropic angular distributions were assumed for the gamma rays.

Capture gamma-ray yields, distributions, and recoil distributions are given in File 6 and are based on a combination of experimental data and calculation.

7. UNCERTAINTY INFORMATION

Uncertainty files are given only for the cross sections in File 3 and for the resonance parameters. They are not given for energy distributions or angular distributions. Fractional and absolute components, correlated only within a given energy interval, are based on scatter in experimental data and estimates of uncertainties associated with the model calculations.

REFERENCES

- AS58 V. J. Ashby, H. C. Catron, and L. L. Newkirk, *Phys. Rev.* 111, 616 (1958).
- CH76 G. T. Chapman and G. L. Morgan, Oak Ridge National Laboratory ORNL/TM-5416 (1976).
- CL72 G. Clayeux and J. Voignier, Centre d'Etudes de Limeil CEA-R-4279 (1972).
- CO78 V. Corcalciuc, B. Holmqvist, A. Marcinkowski, and G. A. Prokopets, *Nucl. Phys.* A307(3), 445 (1978).
- DI72 J. K. Dickens, G. L. Morgan, and F. G. Perey, *Gamma-Ray Production Due to Neutron Interactions with Iron for Incident Neutron Energies Between 0.8 and 20 MeV: Tabulated Differential Cross Sections*, ORNL-4798, Oak Ridge National Laboratory, 1972.
- FR80 J. Frehaut, A. Bertin, R. Bois, and J. Jary, *Symp. on Neutron Cross Sections from 10-50 MeV*, Brookhaven National Laboratory, May 12-14, 1980.
- FU79 C. Y. Fu, "A Consistent Nuclear Model for Compound and Precompound Reactions with Conservation of Angular Momentum," p. 757 in *Proc. Int. Conf. Nuclear Cross Sections for Technology*, National Bureau of Standards Special Publication 593, 1979. See also ORNL/TM-7042, Oak Ridge National Laboratory, 1980.
- FU80 C. Y. Fu and F. G. Perey, *Evaluation of Neutron and Gamma-Ray Production Cross Sections for Natural Iron (ENDF/B-V MAT 1326)*, ORNL/TM-7523, ENDF-302, Oak Ridge National Laboratory, 1980.
- FU82 C. Y. Fu, *Summary of ENDF/B-V Evaluations for Carbon, Calcium, Iron, Copper, and Lead and ENDF/B-V Mod-3 for Calcium and Iron*, ORNL/TM-8283, ENDF-325, Oak Ridge National Laboratory, 1982.
- FU86 C. Y. Fu and D. M. Hetrick, *Update of ENDF/B-V Mod-3 Iron: Neutron-Producing Reaction Cross Sections and Energy-Angle Correlations*, ORNL/TM-9964, ENDF-341 (July 1986).
- FU87 C. Y. Fu and D. M. Hetrick, "Preliminary Summary Documentation for Iron Evaluation for ENDF/B-VI" (in preparation).
- GR79 S. M. Grimes, R. C. Haight, K. R. Alvar, H. H. Barschall, and R. R. Borchers, *Phys. Rev.* C19, 2127 (1979).
- HA77 R. C. Haight and S. M. Grimes, LLL Report UCRL-80235 (1977).
- HE75 D. Hermsdorf et al., *Differential Neutron Emission Cross Sections from Iron by 14.6-MeV Neutrons*, ZfK-277, Institute of Nuclear Physics, University of Dresden (East Germany), 1975.
- HE80 D. M. Hetrick and C. Y. Fu, *GLUCS: A Generalized Least-Squares Program for Updating Cross Section Evaluations with Correlated Data Sets*, ORNL/TM-7341, ENDF-303 (October 1980).
- KA72 J. L. Kammerdiener, *Neutron Spectra Emitted by ^{239}Pu , ^{238}U , ^{235}U , Pb, Nb, Ni, Fe, Al, and C Irradiated by 14 MeV Neutrons*, UCRL-51232, Lawrence Livermore Laboratory, 1972.

- KI77 W. E. Kinney and F. G. Perey, *Nucl. Sci. Eng.* 63, 418 (1977).
- OR75 V. G. Orphan, C. G. Hoot, and V. C. Rogers, *Nucl. Sci. Eng.* 57, 309 (1975).
- PE80 C. M. Perey and F. G. Perey, *Evaluation of Resonance Parameters for Neutron Interaction with Iron Isotopes for Energies up to 400 keV*, ORNL/TM-6405, ENDF-298 (September 1980).
- QA77 S. M. Qaim and N. I. Molla, *Nucl. Phys.* A283, 269 (1977).
- SA72 O. A. Salnikov, G. N. Lovchikova, G. V. Kotelnikova, A. M. Trufanov, and N. I. Fetisov, *Jadernye Konstanty* - 7, 102 (1972).
- SH86 K. Shibata and C. Y. Fu, *Recent Improvements of the TNG Statistical Model Code*, ORNL/TM-10093 (1986).
- TA83 A. Takahashi et al., *Double Differential Neutron Emission Cross Sections, Numerical Tables and Figures (1983)*, A-83-01, Intense 14-MeV Neutron Source Facility, Osaka University, 1983.
- VE79 L. R. Veesser, Figure 61 in "Evaluated Neutron-Induced Cross Sections for $^{54,56}\text{Fe}$ to 40 MeV," by E. D. Arthur and P. G. Young, LA-8626-MS, ENDF-304 (1980).
- VO71 F. Voss et al., USAEC CONF-710310, p. 218 (1971).
- WE62 R. Wenusch and H. Vonach, *Anz. Oesterr. Akad. Wiss., Math-Naturwiss. Kl.* 99 1 (1962).

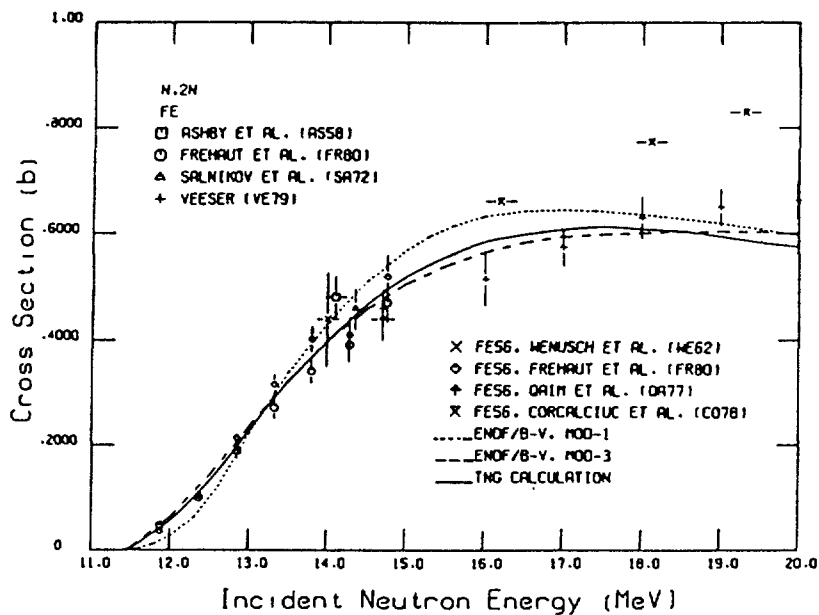


Fig. 1. Comparisons of the Fe(n,2n) cross sections of ENDF/B-V Mod-1, ENDF/B-V Mod-3, and the present calculation with measurements.

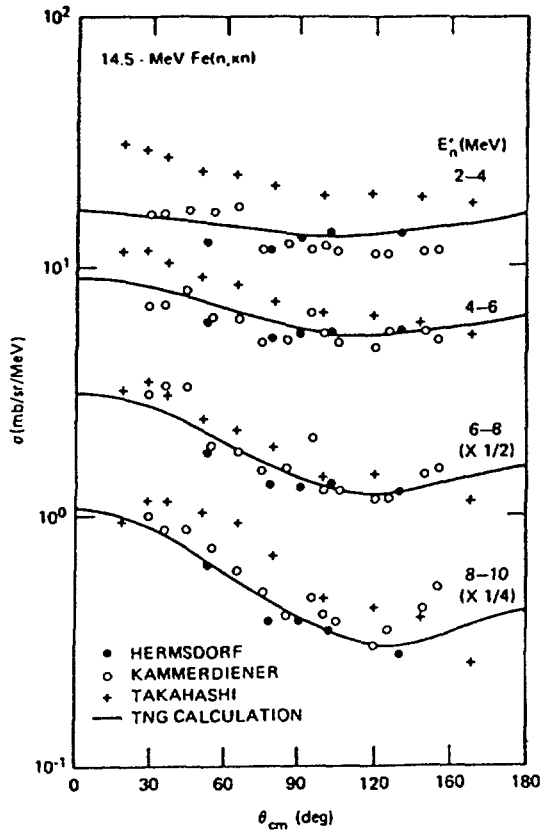
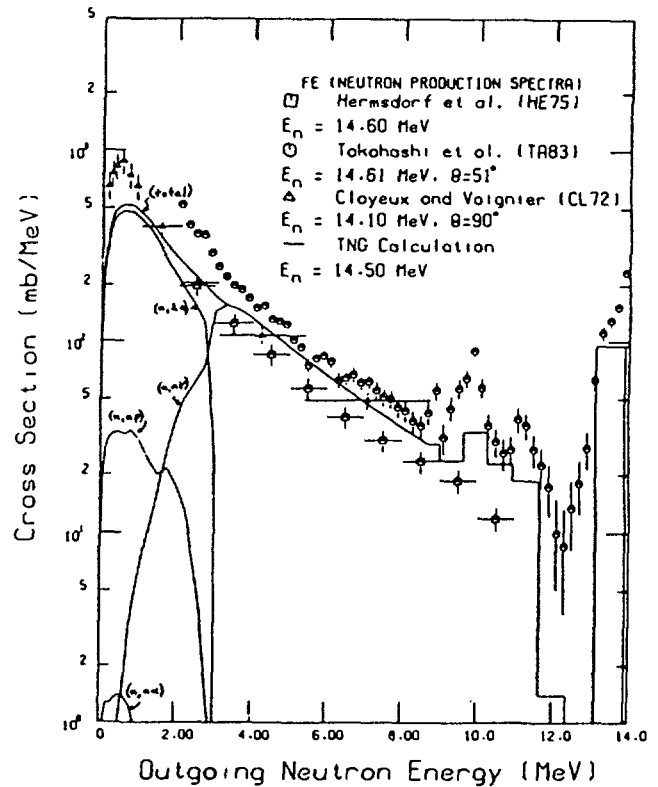


Fig. 2. Calculated and experimental (HE75, KA72, TA83) double differential Fe(n,xn) cross sections for 14.5-MeV incident neutrons and several secondary energy ranges.

Fig. 3. Comparison of the neutron production spectrum of the present calculation with measurements. Various contributing components in the calculation are shown.



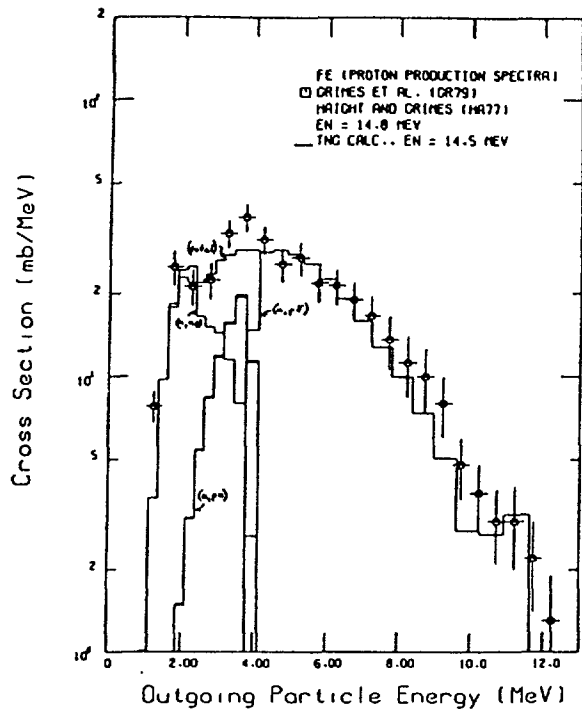
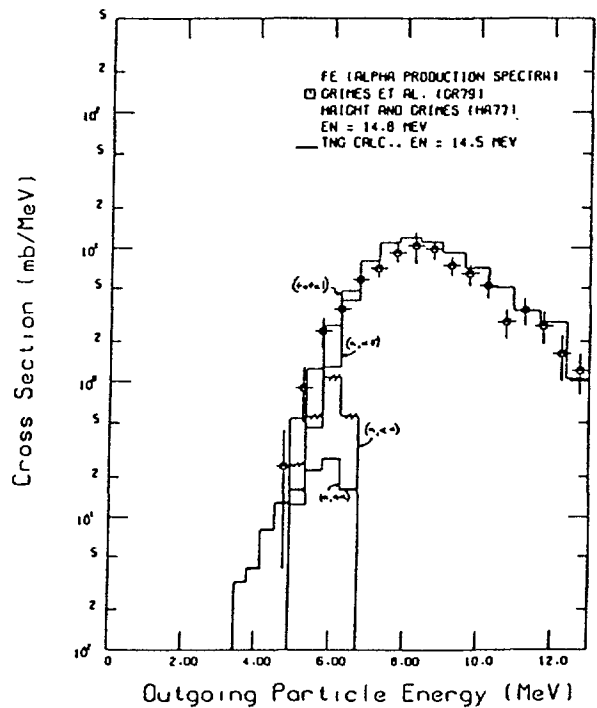


Fig. 4. Comparison of the proton production spectrum of the present calculation with measurements. Various contributing components in the calculation are shown.

Fig. 5. Comparison of the alpha-particle production spectrum of the present calculation with measurements. Various contributing components in the calculation are shown.



D. C. Larson, D. M. Hetrick and C. Y. Fu
Oak Ridge National Laboratory
Oak Ridge, Tennessee 37831-6356
U. S. A.

ABSTRACT

Isotopic evaluations for $^{63,65}\text{Cu}$ performed for ENDF/B-VI are briefly reviewed. The evaluations are based on analysis of experimental data and results of model calculations which reproduce the experimental data. Evaluated data are given for neutron-induced reaction cross sections, angular and energy distributions, and for gamma-ray production cross sections associated with the reactions. File 6 formats are used to represent energy-angle correlated data and recoil spectra. Uncertainty files are included for the major cross sections. Full evaluations are given for $^{63,65}\text{Cu}$.

1. INTRODUCTION

Separate evaluations have been done for each of the stable isotopes of copper. In this report we briefly review the structure of the evaluations, describe how the evaluations were done, and note the major pieces of data considered in the evaluation process. Experimental data references were obtained primarily from CINDA, but also from the literature and reports. The data themselves were mostly obtained from the National Nuclear Data Center at Brookhaven National Laboratory and, occasionally, from the literature and reports. The TNG nuclear model code (FU80,SH86), a multistep Hauser-Feshbach code which includes precompound and compound contributions to cross sections, angular, and energy distributions in a self-consistent manner, calculates gamma-ray production, and conserves angular momentum in all steps, was the primary code used for these evaluations. Extensive model calculations were performed with the goal of simultaneously reproducing experimental data for all reaction channels with one set of parameters. This ensures internal consistency and energy conservation within the evaluation. In the case of reactions for which sufficient data were available, a Bayesian analysis using the GLUCS code (HE80) was frequently done, using ENDF/B-V or the TNG results as the prior. In cases where insufficient data were available for a GLUCS analysis and the available data were deemed to be accurate, but in disagreement with the TNG results, a line was drawn through the data and used for the evaluation. A hand-drawn line was also used for cross sections where resonant structure was felt to be important, but resonance parameters were not included. The final evaluation is thus a combination of TNG results (used where extrapolation and interpolation was required and where data sets were badly discrepant), GLUCS results (used where sufficient data existed to do an analysis), and hand-drawn curves.

In Section 2 the resonance parameters are discussed; Section 3 contains a description of the major cross sections included in the evaluation; Section 4 is devoted to angular distributions; and Section 5 to energy-angle correlated distributions. Section 6 describes the uncertainty files.

Much of this information is abstracted from Ref. HE84, a report devoted to a description of the calculations for $^{63,65}\text{Cu}$. As of this writing, the

*Research sponsored by the Office of Basic Energy Sciences, U.S. Department of Energy, under contract DE-AC05-84OR21400 with Martin Marietta Energy Systems, Inc.

various pieces of the evaluations are being reviewed, modified if necessary, and assembled into full evaluations using the ENDF/B-VI formats, and will be submitted by May 1988 to the Cross Section Evaluation Working Group (CSEWG) for use in ENDF/B-VI.

2. RESONANCE PARAMETERS

Resonance parameters for $^{63,65}\text{Cu}$ are taken from the compilation of Mughabghab (MU81). They cover the energy range from 0.402 to 153 keV for ^{63}Cu and 0.230 to 149 keV for ^{65}Cu . Average capture widths are used for neutron energies above about 50 keV. The resonance parameters should be processed with the Reich-Moore formalism.

3. CROSS SECTIONS

This section contains a brief discussion of the cross section files in the evaluations for $^{63,65}\text{Cu}$. The total cross section above the resonance region was taken from the isotopic experimental data described in Ref. PA77. Cross sections for inelastic scattering to discrete levels are taken from the model calculations, which included a direct interaction component and generally are in good agreement with the available experimental data. A continuum was used to represent the inelastic scattering cross section for excitation energies above the discrete levels.

The $^{63}\text{Cu}(n,p)$ reaction has very little data, but the calculated result agrees with the data of Qaim and Molla (QA77) and Allan (AL61). The $^{63}\text{Cu}(n,\alpha)$ reaction has much data and is a common dosimetry cross section. The evaluated cross section for this reaction is taken from the results of a generalized least squares analysis (FU82) of twelve dosimetry reactions, which included ratio data and covariance information. The $^{65}\text{Cu}(n,p)$ cross section has abundant data and is well reproduced by the TNG calculations, which are used for the evaluation. The $^{65}\text{Cu}(n,\alpha)$ cross section is small, and the experimental data are in disagreement. The calculated results are used for the evaluation.

The $^{63,65}\text{Cu}(n,2n)$ cross sections are well defined by experimental data, and the results of a GLUCS analysis was used for the evaluation. Other tertiary reaction cross section data are reproduced by the TNG calculations and are included in each evaluation.

The capture cross sections for $^{63,65}\text{Cu}$ are defined by the resonance parameters and a smooth background below 150 keV, and by smooth experimental data above the resonance region. Guided by experimental data and the TNG calculation, a smooth line was drawn through the data and used for the evaluation.

4. ANGULAR DISTRIBUTIONS

Elastic scattering angular distributions were obtained from an optical potential derived by fitting experimental angular distribution data for $^{63,65,\text{nat}}\text{Cu}$ with GENOA (PE67). A compound elastic term was included for neutron energies below 5 MeV. Since very little difference was observed between the experimental data for ^{63}Cu and ^{65}Cu , one potential was derived and used for both evaluations. Figures 1 and 2 show a comparison of the calculated and experimental data for $E_n = 8.05$ and 14.5 MeV. The angular distributions are represented as Legendre coefficients and given in File 4/2. Angular distributions for inelastic scattering to excited levels and the continuum are given as Legendre coefficients in File 6.

5. ENERGY-ANGLE CORRELATED DISTRIBUTIONS (FILE 6)

Neutron emission spectra, as a function of outgoing energy and angle, are given in File 6. For copper, the measurements of Morgan et al. (MO79) give the outgoing neutron spectra at one angle for several incident neutron energies between 1 and 20 MeV, while the measurements of Hermsdorf et al. (HE75), Salnikov et al. (SA75) and Takahashi et al. (TA83) give the outgoing spectra at several angles but only near 14.5-MeV incident energy. Such complementary measurements allow a good determination of the model parameters for the calculations and, thereby, reliable interpolation and extrapolation to energies where there are no data. For these reasons, as well as ensuring energy conservation, results of the model codes, expressed in File 6 formats, were used for the evaluations. The angular distributions were expressed in terms of Legendre coefficients, while the energy distributions were expressed as tabulated probability distributions. Figures 3 and 4 show the neutron emission data of Morgan et al. (MO79) compared with the TNG calculated results for the incident neutron-energy bins from 9 to 10 MeV and 12.5 to 15 MeV, respectively. The data of Takahashi et al. (TA83) became available after the evaluation was done but are found to be in good agreement with the evaluation.

Proton and alpha emission spectra for both isotopes are available (GR79) at an incident energy of 14 MeV. The calculations are in excellent agreement with the measured spectra, including reproducing the observed sub-coulomb emission of protons. Figure 5 shows a comparison of the measured data for proton emission from ^{63}Cu with the TNG results. However, the observed sub-coulomb emission of alphas is not well reproduced by the TNG calculations. Figure 6 shows a comparison of the measured data for ^{63}Cu alpha emission, compared with the TNG results. These calculated results (at several incident neutron energies) are used for the evaluation and are placed in File 6, with isotropic angular distributions assumed.

Tabulated energy distributions for the recoil spectra associated with the various particle producing reactions are also given in File 6, and isotropic angular distributions are assumed.

Gamma-ray production spectra were also calculated as part of the TNG calculations, and compared with data sets of Rogers et al. (RO77), Morgan (MO79), Dickens et al. (DI73), and Chapman (CH76) (see Ref. HE84). Figure 7 shows a comparison of the measured data of Dickens et al. with the TNG results around 14-MeV incident energy. Note that without the use of the calculated results, a significant amount of cross section below 700-keV gamma-ray energy would not be accounted for due to gamma rays from the $(n,2n)$ reaction. Since calculated results are generally used for the evaluation, energy conservation is ensured. Sections of File 6 were used to represent the gamma-ray emission spectra for the individual reactions, and isotropic angular distributions were assumed. The cross sections for the gamma-ray production are given in corresponding sections of File 3.

As an example of the usage of File 6, consider the $^{65}\text{Cu}(n,n\alpha)$ reaction. In File 6/22, constant yields are given for the outgoing neutron, alpha and ^{61}Co residual, and an energy dependent yield is used for the gamma rays associated with the $(n,n\alpha)$ reaction. Normalized energy distributions are given for each outgoing product, but only the outgoing neutron has a non-isotropic angular distribution. The cross section to be used for normalization is taken from File 3/22.

Capture gamma-ray cross sections and spectra are given in Files 13 and 15, respectively, and are based on a combination of experimental data and calculation.

6. UNCERTAINTY INFORMATION

Uncertainty files are given only for the cross sections in File 3, and not for the resonance parameters, energy distributions or angular distributions. Fractional and absolute components, correlated only within a given energy interval, are based on scatter in experimental data and estimates of uncertainties associated with the model calculations.

REFERENCES

- AL61 D. L. Allan, *Nuclear Physics* 24, 274 (April 1961).
- CH76 G. T. Chapman, *The Cu(n,xy) Reaction Cross Section for Incident Energies Between 0.2 and 20.0 MeV*, ORNL/TM-5215 (1976).
- CO58 J. H. Coon, R. W. Davis, H. E. Felthouser, D. B. Nicodemus, *Phys. Rev.* 111, 250 (1958).
- DI73 J. K. Dickens, T. A. Love, and G. L. Morgan, *Gamma-Ray Production Due to Neutron Interactions with Copper for Incident Neutron Energies Between 1.0 and 20.0 MeV: Tabulated Differential Cross Sections*, ORNL-4846 (1973).
- FU80 C. Y. Fu, "A Consistent Nuclear Model for Compound and Precompound Reactions with Conservation of Angular Momentum," p. 757 in *Proc. Int. Conf. Nuclear Cross Sections for Technology*, Knoxville, TN, Oct. 22-26, 1979, NBS-594, U.S. National Bureau of Standards. also, ORNL/TM-7042 (1980).
- FU82 C. Y. Fu and D. M. Hetrick, "Experience in Using the Covariance of Some ENDF/B-V Dosimetry Cross Sections: Proposed Improvements and Addition of Cross-Reaction Covariances," p. 877 in *Proc. Fourth ASTM-EURATOM Symp. on Reactor Dosimetry*, Gaithersburg, Md., March 22-26, 1982, U.S. National Bureau of Standards.
- GR79 S. M. Grimes, R. C. Haight, K. R. Alvar, H. H. Barschall, and R. R. Borchers, *Phys. Rev.* C19, 2127 (1979).
- HA77 R. C. Haight and S. M. Grimes, Lawrence Livermore Laboratory Report UCRL-80235 (1977).
- HE75 D. Hermsdorf, A. Meister, S. Sassonoff, D. Seeliger, K. Seidel, and F. Shahin, *Zentralinstitut Fur Kernforschung Rossendorf Bei Dresden*, Zfk-277 (U), (1975).
- HE80 D. M. Hetrick and C. Y. Fu, *GLUCS: A Generalized Least-Squares Program for Updating Cross Section Evaluations with Correlated Data Sets*, ORNL/TM-7341, ENDF-303 (October 1980).
- HE84 D. M. Hetrick, C. Y. Fu, D. C. Larson, *Calculated Neutron-Induced Cross Sections for $^{63,65}\text{Cu}$ from 1 to 20 MeV and Comparisons with Experiments*, ORNL/TM-9083, ENDF-337 (August 1984).
- HO69 B. Holmqvist and T. Wiedling, Atomic Energy Company, Studsvik, Nykoping, Sweden, Report AE-366 (1969).
- MO79 G. L. Morgan, *Cross Sections for the Cu(n,xn) and Cu(n,x α) Reactions Between 1 and 20 MeV*, ORNL-5499, ENDF-273 (1979).

- MU81 S. F. Mughabghab, M. Divadeenam, and N. E. Holden, *Neutron Cross Sections, Vol. 1, Neutron Resonance Parameters and Thermal Cross Sections, Part A, Z=1-60*, Academic Press (1981).
- PA77 M. S. Pandey, J. B. Garg, and J. A. Harvey, *Phys. Rev. C15*, 600 (February 1977).
- PE67 F. G. Perey, Computer code GENOA, Oak Ridge National Laboratory, unpublished (1967).
- QA77 S. M. Qaim and N. I. Molla, *Nucl. Phys. A283*, 269 (June 1977).
- RO77 V. C. Rogers, D. R. Dixon, C. G. Hoot, D. Costello, and V. J. Orphan, *Nucl. Sci. Eng. 62*, 716 (1977).
- SA75 O. A. Salnikov, G. N. Lovchikova, G. V. Kotelnikova, A. M. Trufanov, N. I. Fetisov, *Energy Spectra of Inelastically Scattered Neutrons for Cr, Mn, Fe, Co, Ni, Cu, Y, Zr, Nb, W, and Bi*, IAEA Nuclear Data Section, Karntner Ring 11, A-1010 Vienna (July 1974).
- SH86 K. Shibata and C. Y. Fu, *Recent Improvements of the TNG Statistical Model Code*, ORNL/TM-10093 (1986).
- TA83 A. Takahashi, J. Yamamoto, T. Murakami, K. Oshima, H. Oda, K. Fujimoto, M. Ueda, M. Fukazawa, Y. Yanagi, J. Miyaguchi, and K. Sumita, Oktavian Report A-83-01, Osaka University, Japan (June 1983).

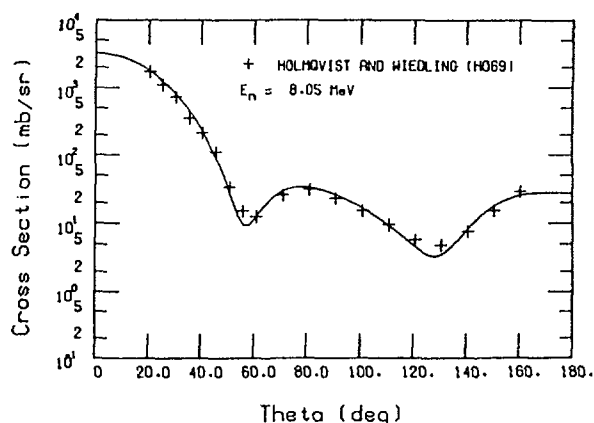


Fig. 1. Comparison of final optical-model fit with elastic scattering data of Holmquist and Wiedling (HO69) for Cu at 8.05 MeV.

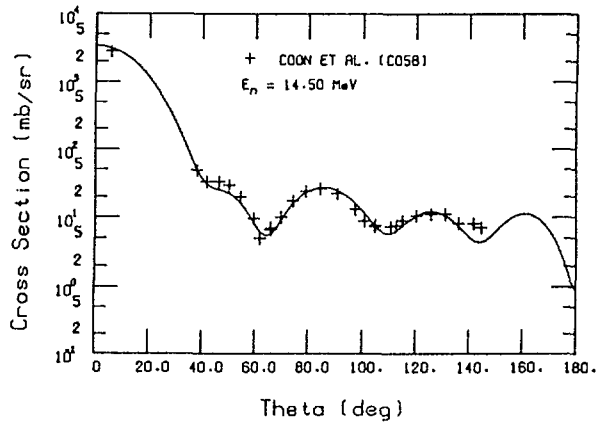


Fig. 2. Comparison of final optical-model fit with elastic scattering data of Coon et al. (C058) for Cu at 14.5 MeV.

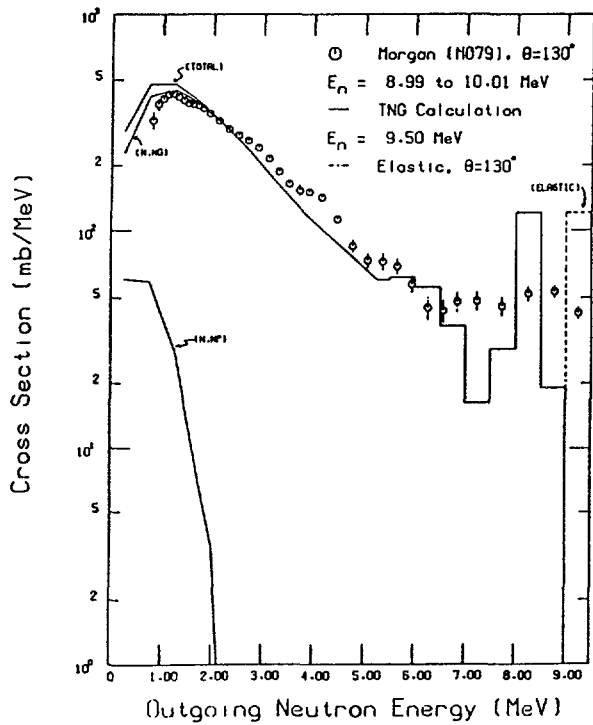


Fig. 3. Neutron emission spectra from the TNG calculation compared with the data of Morgan (M079). The calculated elastic cross section ($\theta=130^\circ$) is not smeared and is not in phase with the data. Contributions from the various neutron-producing components are shown (they sum to the total). The curve labeled (n,np) includes the (n,pn) component.

Fig. 4. Neutron emission spectra from the TNG calculation compared with the data of Morgan (M079). Also shown is the calculation for $\theta=130^\circ$. The calculated elastic cross section is not smeared and is not in phase with the data. Contributions from the various neutron-producing components are shown (they sum to the total). The curves labeled (n,np) and (n,α) include the (n,pn) and $(n,\alpha n)$ components, respectively.

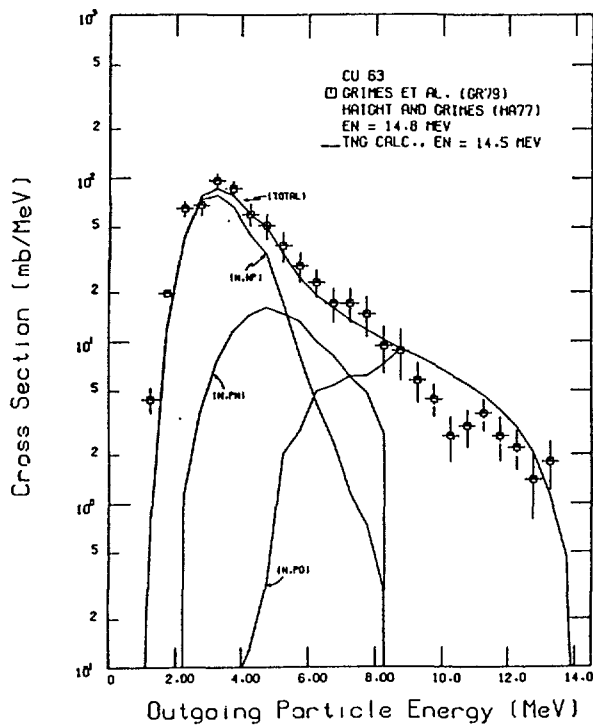
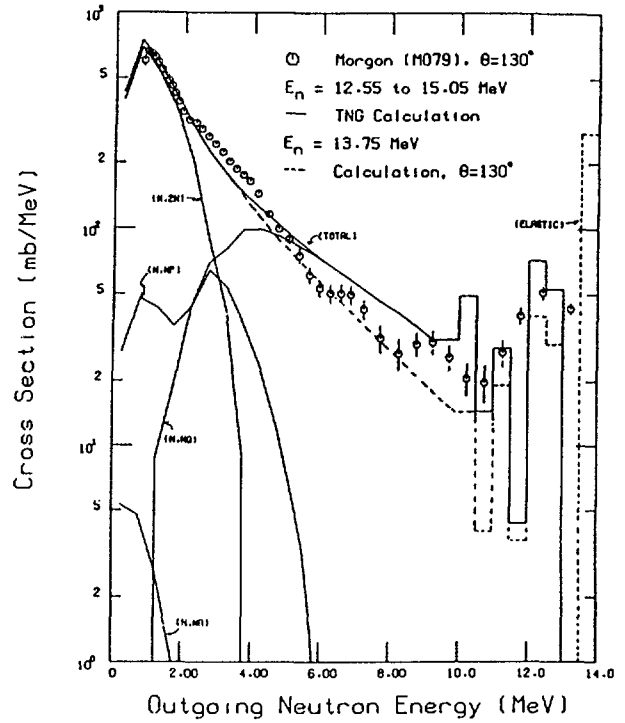


Fig. 5. Comparison of calculated and experimental proton production spectra for ^{63}Cu . The measurement was taken at an incident energy of 14.8 MeV; the TNG calculation was for $E_n = 14.5$ MeV.

Fig. 6. Comparison of calculated and experimental alpha production spectra for ^{65}Cu . The measurement was taken at an incident energy of 14.8 MeV; the TNG calculation was for $E_n = 14.5$ MeV.

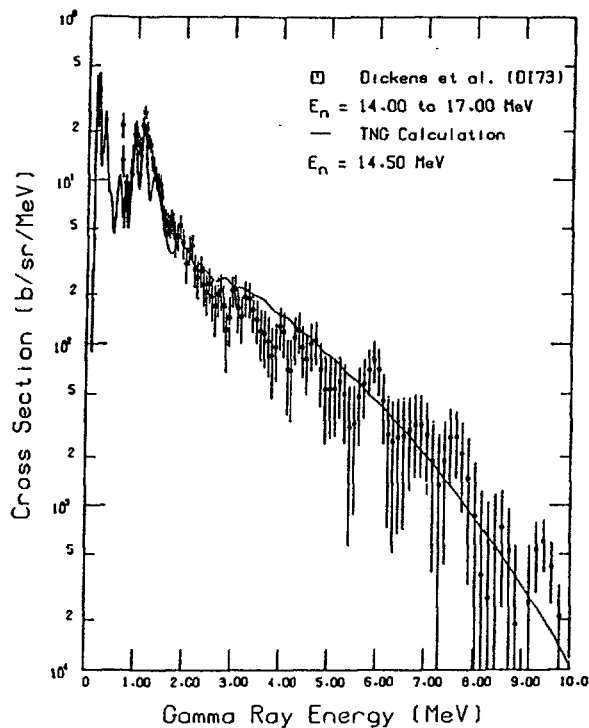
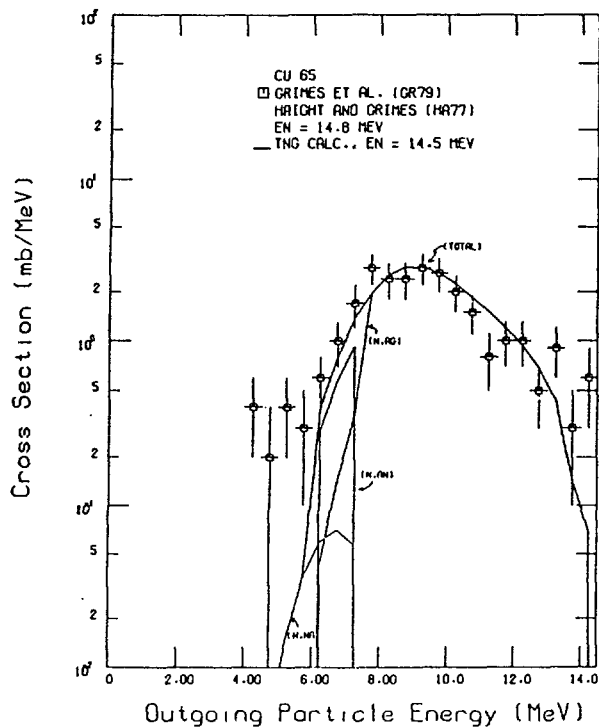


Fig. 7. Secondary gamma-ray spectra versus gamma-ray energy from the TNG calculation (incident energy $E_n = 14.5$ MeV) compared with the data of Dickens et al. (1973).

D. C. Larson, C. Y. Fu and D. M. Hetrick
Oak Ridge National Laboratory
Oak Ridge, Tennessee 37831-6356
U. S. A.

ABSTRACT

The model code TNG has been extensively used in evaluation work of structural materials for ENDF/B-VI performed at Oak Ridge National Laboratory. A new aspect of ENDF/B-VI is the use of File 6 formats for energy-angle correlated data. Such data are generally calculated, anchored by experimental data. In this informal note we outline how the TNG results are calculated and entered in the File 6 formats.

The TNG code is a multistep Hauser-Feshbach code (FU80,SH86,FU87) which calculates precompound and compound contributions to the cross sections, energy and angular distributions in a self-consistent manner, computes gamma-ray production cross sections, and conserves energy and angular momentum in all steps. It is extensively used for evaluations being done for ENDF/B-VI at ORNL.

In the following discussion a binary reaction will refer to a reaction with one outgoing particle; the three normally considered in evaluation work are the (n,n') , (n,p) , and (n,α) reactions. When the incident energy becomes high enough, a second particle is energetically able to be emitted, and this is referred to as a tertiary reaction. Each binary channel can break up into several tertiary channels, two examples being $(n,n') = (n,n'\gamma) + (n,2n) + (n,np) + (n,n\alpha)$, and $(n,p) = (n,p'\gamma) + (n,pn) + (n,2p) + (n,p\alpha)$. For a binary reaction, TNG calculates both the compound and precompound contributions to the cross section and energy distribution (and optionally, the compound and/or precompound contribution to the angular distribution) for each outgoing particle, whether it be neutron, proton or alpha. For a tertiary reaction, TNG calculates both the compound and precompound contributions to the cross section, as well as the energy distribution of both outgoing particles, and optionally the compound and/or precompound contribution to the angular distribution for the first outgoing particle only. The angular distribution is not calculated for the second outgoing particle. This is reasonable at the energies for which we use TNG since the second outgoing particle usually has low energy, and an isotropic angular distribution is adequate. In other words, TNG calculates the precompound angular distribution information only for the binary reaction. Thus, precompound angular distribution information is available for the (n,n') , (n,p) , and (n,α) reactions, and (for example) the first neutron in the $(n,2n)$ reaction, and the neutron in the (n,np) , $(n,n\alpha)$, and $(n,n\gamma)$ reactions.

Now consider how this information is placed in File 6. In our evaluations, File 6 contains separate contributions for all reaction components, which

*Research sponsored by the Office of Basic Energy Sciences, U.S. Department of Energy, under contract DE-AC05-84OR21400 with Martin Marietta Energy Systems, Inc.

must be summed to compare with a neutron, proton, alpha or gamma emission spectrum. For example, (MF/MT) = 6/16 contains angle and energy distribution information for the $(n,2n)$ reaction, 6/22 for the $(n,\alpha)+(n,\alpha n)$ reaction, and 6/28 for the $(n,np)+(n,pn)$ reaction. Looking closer at 6/28, it contains energy distribution data for the outgoing neutron, proton, recoil nucleus, and gamma-ray production from the $(n,np)+(n,pn)$ reaction. In addition, it contains the angular information for the first neutron emitted, calculated with TNG. Since the (n,np) and (n,pn) reactions are combined for this file, the first neutron (i.e., from the (n,np) reaction) has a precompound (non-isotropic) angular distribution, while the neutron from the (n,pn) reaction, being the second particle, has no calculated contribution to the angular distribution, and is assumed to be isotropic. In combining these cross sections for 6/28, the energy distributions for the neutrons (as for all outgoing particles) are weighted by the cross sections. In principle, the non-isotropic angular distribution for the neutron from the (n,np) reaction should be combined with the (assumed) isotropic angular distribution for the neutron from the (n,pn) reaction, in a similar weighted manner. However, for convenience, and since the experimental angular distribution data are not adequate to tell the difference, the angular distribution for the neutron from the (n,np) reaction is also used for the neutron from the (n,pn) reaction. A similar argument is made for 6/22 and 6/16. For the $(n,2n)$ reaction, one energy distribution is given, since the first neutron emitted is assumed indistinguishable from the second. File 6/91 contains the distributions for neutrons emitted from the continuum. So, to get the energy distribution spectrum to compare with the neutron emission spectrum experimentally measured at a given angle, the neutron energy spectra from the 6/16, 6/22, 6/28 and 6/91 files (calculated at the desired angle from the Legendre coefficients in File 6) are weighted by the cross sections from 3/16, 3/22, 3/28 and 3/91, and added. Since the angular distributions are all for the 'first' neutron out, (or the binary (n,n') channel) they are the same for each of the tertiary reactions. The only approximation is the previously noted assumption regarding distributions for the (n,pn) and $(n,\alpha n)$ outgoing neutrons. The energy distributions are given as tabulated probability distributions, and the angular information is given as Legendre coefficients; coefficients a_3 and above are assumed zero. All distributions in File 6 are given in the laboratory frame of reference.

Angular distribution information is normally calculated and included in File 6 for outgoing neutrons. Outgoing protons, alphas, recoil nuclei, and gamma rays are assumed to have isotropic angular distributions. Thus, this energy-angle distribution information is uncorrelated and, with the exception of the recoil spectra, could be included in File 4 (isotropic angular distributions) and File 5 (energy distributions). However, File 6 was chosen so that the recoil spectra could be included and for ease in calculating and checking energy balance for each reaction.

Recoil spectra are calculated from the particle spectra output from TNG. For binary reactions, this calculation can be done exactly. For tertiary reactions, it is based on the high-energy particle approximation. The high-energy particle is the first neutron in the $(n,2n)$ reaction, the proton in (n,np) , and the alpha particle in $(n,n\alpha)$. No low-energy protons and alphas are emitted due to inhibition by the Coulomb barrier, so they have a higher average energy than the competing neutrons. An approximation to take into account the recoil effect of the low-energy particle has been developed (FU87a) and is being applied to the evaluation for iron for ENDF/B-VI. Exact calculation of the recoil spectra for tertiary reactions has to be done in the model code where correlation between the energies of the two outgoing particles is known. Energy balance is calculated and normally checks to better than 1%.

TNG does not calculate the angular distribution for the (first particle) precompound component unless requested, since the calculation is rather time consuming. For a given incident energy, the Legendre coefficients a_1 and a_2 are calculated only for a few selected outgoing particle energy bins, and the Legendre coefficients are plotted as a function of outgoing energy. Interpolation procedures are then used to obtain coefficients for other outgoing energy bins. The code is run at several incident energies, and the values of the Legendre coefficients a_1 and a_2 are plotted as a function of incident energy. Interpolation procedures are then used to obtain the coefficients at other incident energies.

REFERENCES

- FU80 C. Y. Fu, "A Consistent Nuclear Model for Compound and Precompound Reactions with Conservation of Angular Momentum," p. 757 in *Proc. Int. Conf. Nuclear Cross Sections for Technology, Knoxville, TN, Oct. 22-26, 1979*, NBS-594, U.S. National Bureau of Standards. Also, ORNL/TM-7042 (1980).
- FU87 C. Y. Fu, "Approximation of Precompound Effects in Hauser-Feshbach Codes for Calculating Double Differential (n, xn) Cross Sections," submitted for publication in *Nucl. Sci. Eng.* (October 1987).
- FU87a C. Y. Fu, Informal memorandum (September, 1987).
- SH86 K. Shibata and C. Y. Fu, *Recent Improvements of the TNG Statistical Model Code*, ORNL/TM-10093 (August 1986).

**"The Lawrence Livermore National Laboratory ^9Be Evaluation"
by S. T. Perkins, E. F. Plechaty, and R. J. Howerton**

**Roger M. White
Nuclear Data Group**

**Currently available for use in the Livermore
Evaluated Neutron Data Library (ENDL)
and will be used in ENDF/B-VI**

Evaluation History

- 1965 Angle integrated spectra based on narrow level, time sequential reactions. Used for ENDL and ENDF/B-III.
- 1973 Up to four time-sequential reactions of the form $^9\text{Be}(n,n_1)$
 $^9\text{Be}(W_9)(n_2)^8\text{Be}(W_8)$ with neglect of the energy-angle correlation for the second neutron. Used in ENDL and ENDF/B-IV.
- 1976 Double differential measurement of Drake, et al. Large discrepancies with ENDF/B-IV.
- 1976 Five levels in ^9Be (four being wide) used in ENDL. CSEWG did not approve format change so ENDF/B-V same as ENDF/B-IV.
- 1979 Bulk leakage multiplication experiment of Basu, et al. Results 20% lower than calculation.
- 1982 Double differential measurement of Takahashi, et al. Large discrepancies with ENDF/B-IV.
- 1980-83 New evaluation which reproduced double differential measurements and Livermore integral experiments. Used in ENDL and has been accepted for ENDF/B-VI.

Description of evaluation in details was published in
Nuclear Science and Engineering: 90, 83-98 (1985).

The ${}^9\text{Be}$ reaction proceeds by transitions through levels in ${}^9\text{Be}$, ${}^8\text{Be}$, ${}^6\text{He}$, and ${}^5\text{He}$.

The end product is always two neutrons and two alpha particles.

10 levels are observed in ${}^9\text{Be}$ between the G.S. and 14 MeV. Except for the 2.43-MeV level, the widths of these states range from 0.2 to > 1 MeV. They decay by either neutron or alpha-particle emission.

${}^8\text{Be}$ is unstable (10^{-16} s) and has two wide levels of interest decaying by alpha-particle emission.

The first excited state of ${}^6\text{He}$ decays by neutron emission; hence, transitions through this level are a component of the (n,2n) reaction.

${}^5\text{He}$ is unstable (10^{-21} s) with a very wide level at 4 MeV. Both this level and the G.S. decay to a neutron and an alpha particle.

Using these level transitions, the ${}^9\text{Be}(n,2n)$ reaction can be described by the following four sequences of two-body reactions and supplemental decays:

1. ${}^9\text{Be}(n, n_1) {}^9\text{Be}(n_2) {}^8\text{Be}(\alpha_1) \alpha_2$
2. ${}^9\text{Be}(n, n_1) {}^9\text{Be}(\alpha_1) {}^5\text{He}(n_2) \alpha_2$
3. ${}^9\text{Be}(n, \alpha_1) {}^6\text{He}(n_1) {}^5\text{He}(n_2) \alpha_2$
4. ${}^9\text{Be}(n, {}^5\text{He}_1) {}^5\text{He}_2, {}^5\text{He}_1(n_1) \alpha_1, {}^5\text{He}_2(n_2) \alpha_2.$

EXPERIMENTAL DATA

Relatively few microscopic nuclear data are available for ${}^9\text{Be}(n,2n)$ reaction and its decay channels.

A principal decay channel is through (n,n') with one of the strongest transitions through the 2.43 level.

The angular distribution for (n,n') through this level is known.

Measurements for $E_n > 10$ MeV exist for (n,alpha) to the 1st excited state of ${}^6\text{He}$.

Alpha-alpha particle correlation spectra at 14 MeV indicate dominant transitions are through sequential decay (rather than 4-body breakup).

Recent double-differential measurements have been made:

Drake, et al., $E_n = 5.9, 10.1, \& 14.2$ MeV at 7-8 angles from 20 to 145 degrees,

Baba, et al. at 6 energies between 3.25 and 15.4 MeV at 1 to 6 angles between 25 and 135 degrees, and

Takahashi, et al., 1 angle for 12 incident neutron energies between 13.42 and 14.84 MeV.

COMMENTS ABOUT LEVEL EXCITATION IN ^9Be

1. Little if any excitation is observed for the 1.68-MeV level.
2. At a 5- to 6-MeV incident energy, the 3.04-MeV state is seen, but not at 7 MeV.
3. For 10.1-MeV incident neutrons, the 6.76-MeV state is populated. At 14.2 MeV, neutrons from both this state and the state at 7.94 MeV were observed. This may be compared with the measurement in which no population of the 6.76-MeV level at a neutron energy of 12.1 MeV was noted.

These comments briefly cover the recent microscopic nuclear data pertaining to the $^9\text{Be}(n,2n)$ reaction.

TECHNIQUE OF EVALUATION

- Use double differential measurements as experimental basis and devise method for interpolating and extrapolating those (partial) data to obtain complete set of evaluated data.
- Formulate a kinematics model which describes the various excitations and modes of breakup - and then calculate the double differential cross sections.
- Within uncertainty of known structure information, input to model was varied until agreement between calculation and experiment was satisfactory.
- A Monte Carlo technique was employed which requires as input a description of various nuclei, level energies, level widths, decay modes, and the number of neutrons to be followed.
- It then tallies the number of secondary neutrons and alphas in specified energy and angular bins.

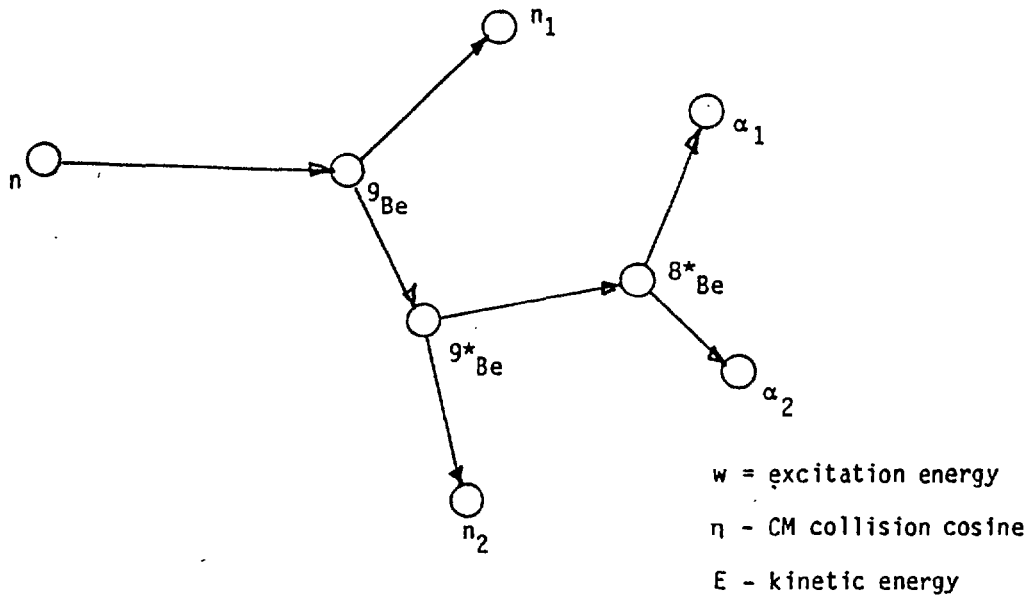
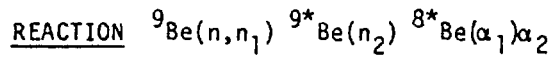
Assume kinematics can be described as a series of time-sequential reactions.

Criteria specified:

1. kinematics of various reactions
2. sampling technique from wide level distributions
3. specification of allowable bounds on excitation energy
4. resolution broadening for comparison to experiment

Nonrelativistic kinematics used.

MONTE CARLO ANALYSIS



| Given | Calculate |
|---|----------------------------|
| $\sigma(E_n), E_n, p(w_{9*}), p(\eta_{n1})$ | E_{n1}, E_{9*} |
| $E_{9*}, p(w_{8*}), p(\eta_{n2})$ | E_{n2}, E_{8*} |
| $E_{8*}, p(\eta_{\alpha1})$ | $E_{\alpha1}, E_{\alpha2}$ |

- Start at lowest incident energy and work upwards.
- Iterate as necessary.
- Output is double-differential cross section.

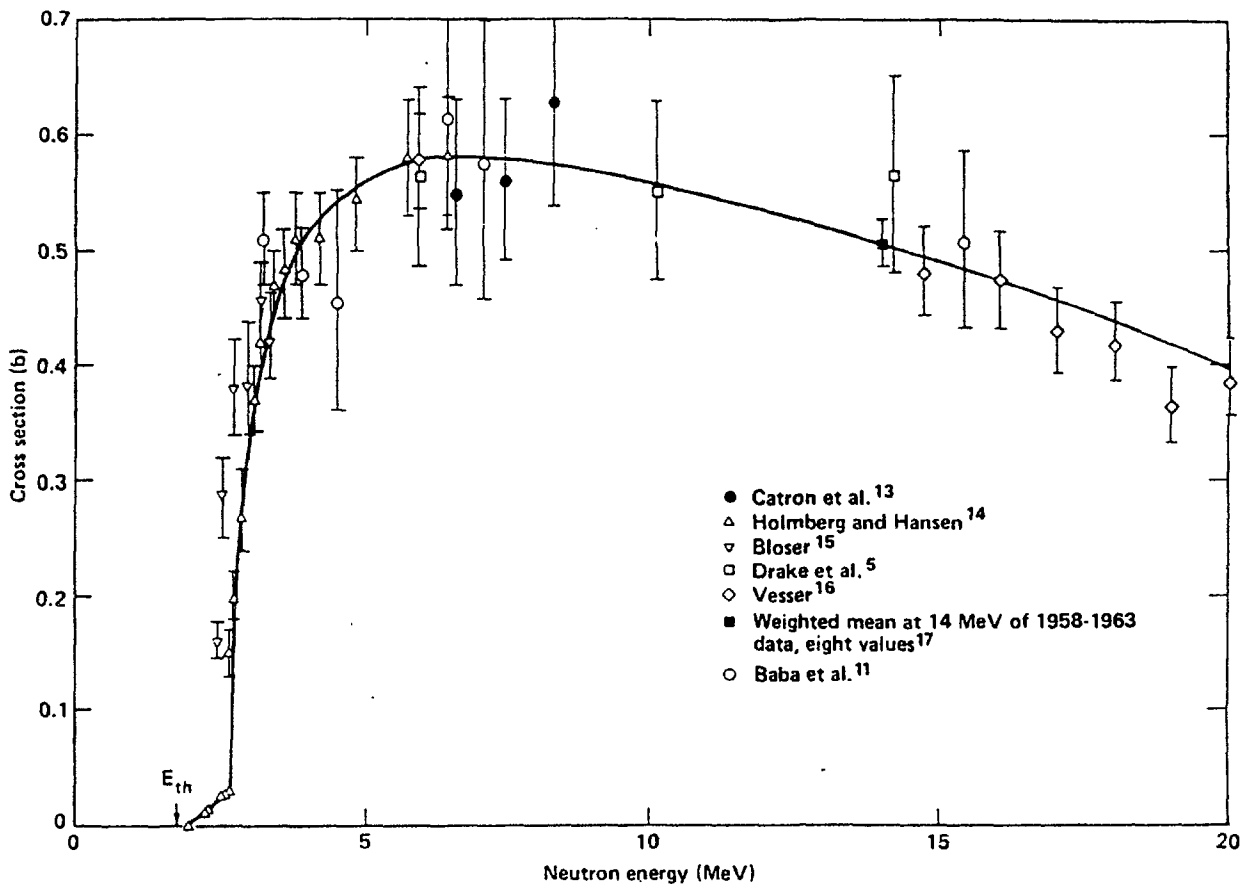


Fig. 1. The ${}^9\text{Be}(n,2n)2\alpha$ cross section. The line represents the results used in the present work.

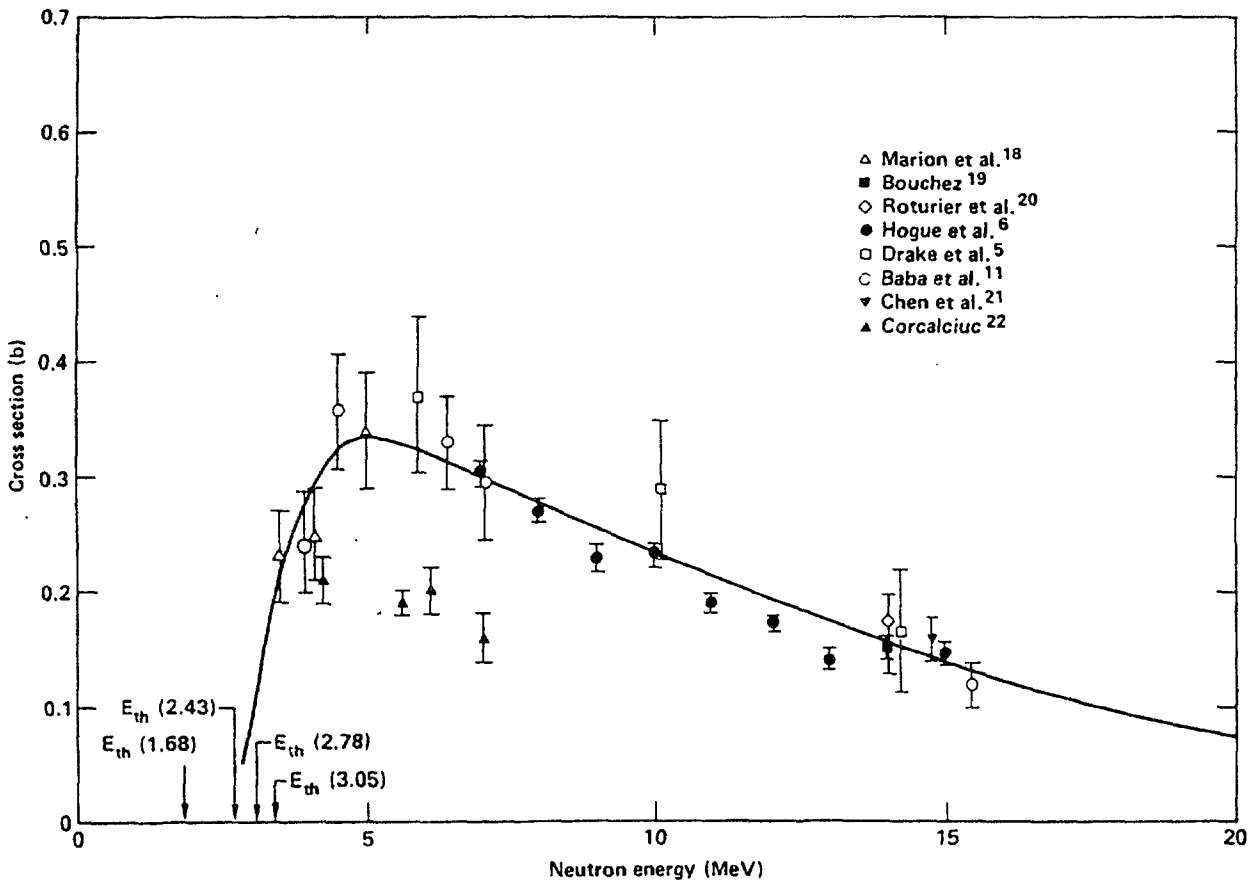


Fig. 2. The (n,n') cross section through the 2.43-MeV level in ${}^9\text{Be}$. The line is that used in the present work.

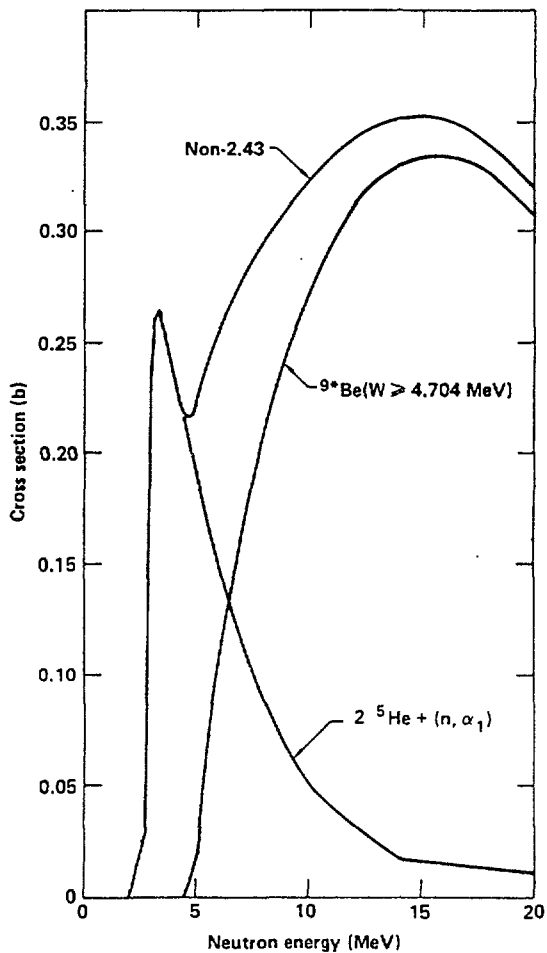


Fig. 3. The non-2.43-MeV component of the $(n,2n)$ cross section and its further decomposition.

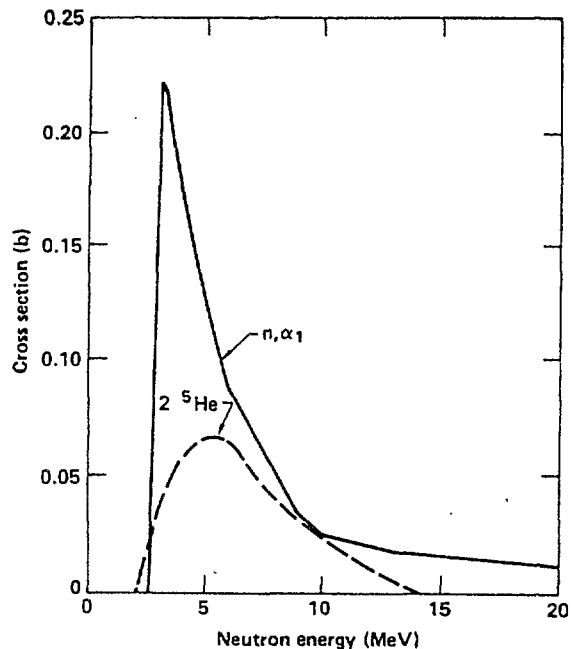


Fig. 4. Decomposition in the $2(^5\text{He}) + (n, \alpha_1)$ cross section shown in Fig. 3.

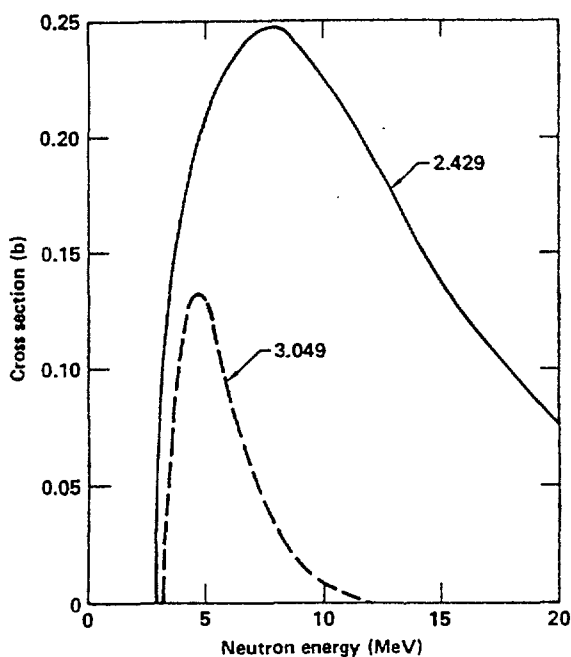


Fig. 5. Decomposition in the 2.43-MeV cross section of Fig. 2 into specific level excitations in ^9Be .

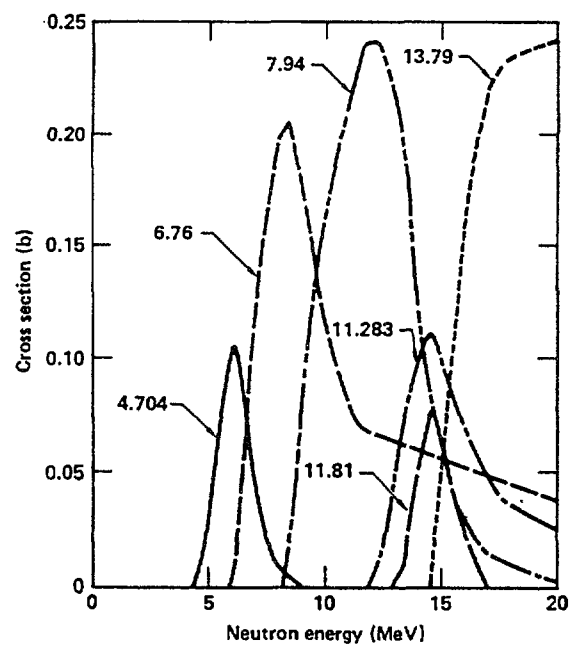


Fig. 6. Excitation of higher level excitations in ^9Be as obtained from the decomposition of the $^9\text{Be}(W \geq 4.704 \text{ MeV})$ cross section of Fig. 3.

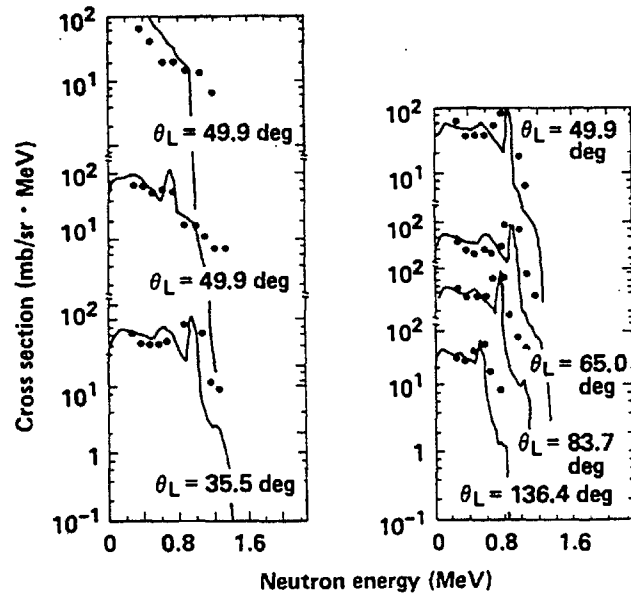


Fig. 7. Comparison of our evaluated double-differential cross sections (line) with data of Baba et al.¹¹ (points). The upper left results (49.9 deg) are at a 3.25-MeV incident energy, the middle left results (49.9 deg), at a 3.9-MeV incident energy, and all remaining results, at a 4.5-MeV incident energy.

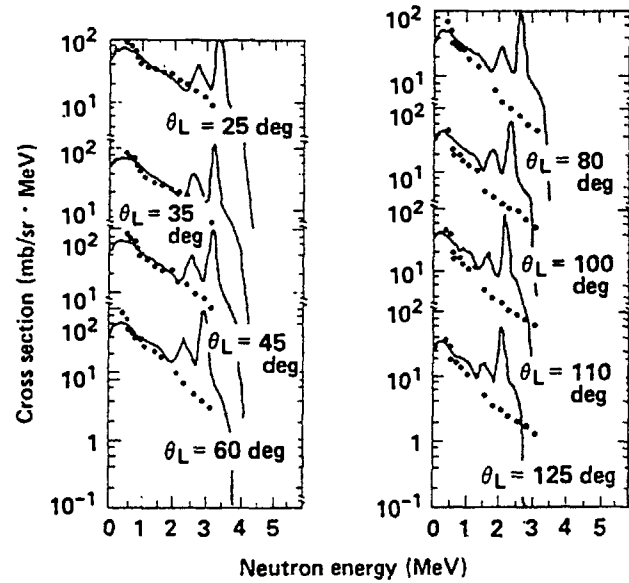


Fig. 8. Comparison of our evaluated double-differential cross sections (line) with the data of Drake et al.⁵ at a 5.9-MeV incident neutron energy. The 2.43-MeV inelastic peak has been subtracted from the experimental data for this reference at this and all higher incident neutron energies.

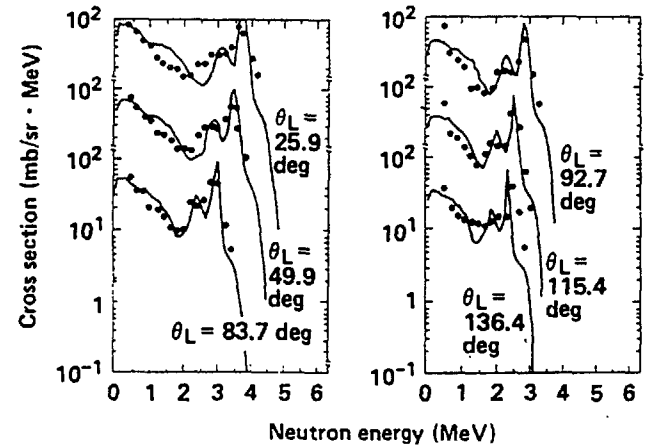


Fig. 9. Comparison of our evaluated double-differential cross sections (line) with the data of Baba et al.¹¹ at a 6.4-MeV incident neutron energy.

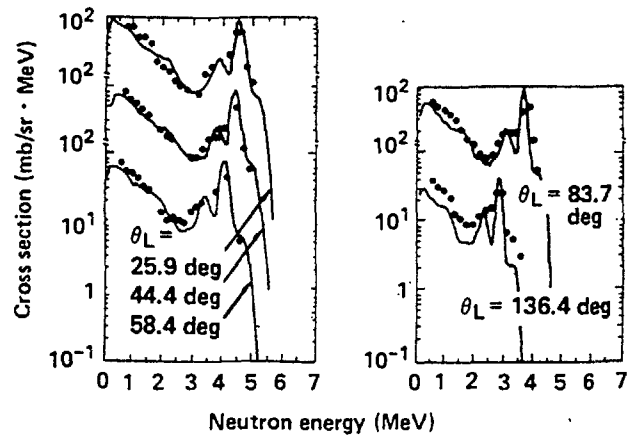


Fig. 10. Comparison of our evaluated double-differential cross sections (line) with the data of Baba et al.¹¹ at a 7.05-MeV incident neutron energy.

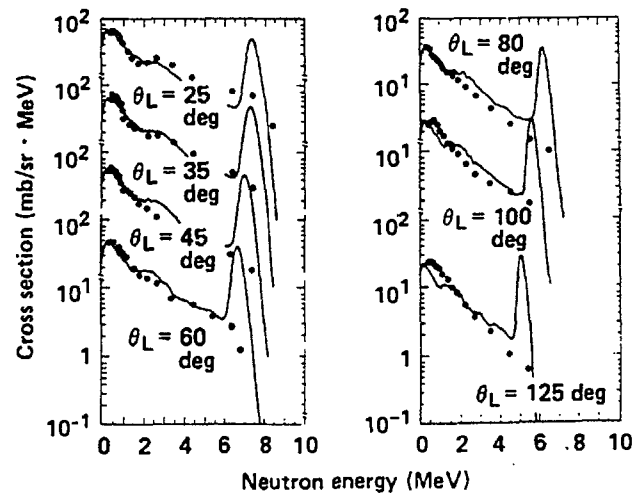


Fig. 11. Comparison of our evaluated double-differential cross sections (line) with the data of Drake et al.⁵ at a 10.1-MeV incident neutron energy.

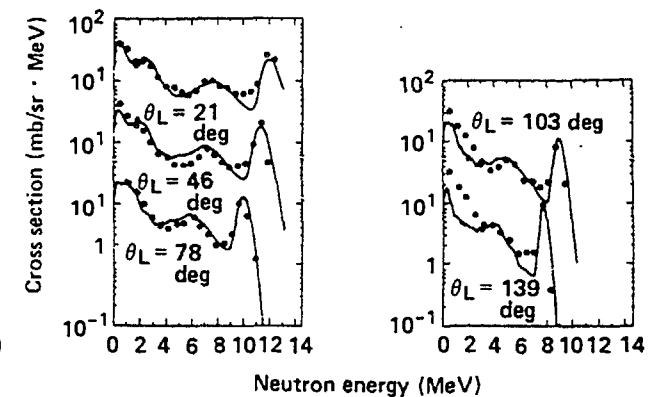


Fig. 12. Comparison of our evaluated double-differential cross sections (line) with the data of Takahashi et al.¹² at a 14.0-MeV nominal incident neutron energy. For each angle of the measured secondary neutron spectrum, the incident energy is unique (see text). The incident neutron energies corresponding to the angles shown are: 21 deg (14.82 MeV), 46 deg (14.66 MeV), 78 deg (14.30 MeV), 103 deg (13.97 MeV), and 139 deg (13.52 MeV). No multiple scattering corrections have been made of these data.

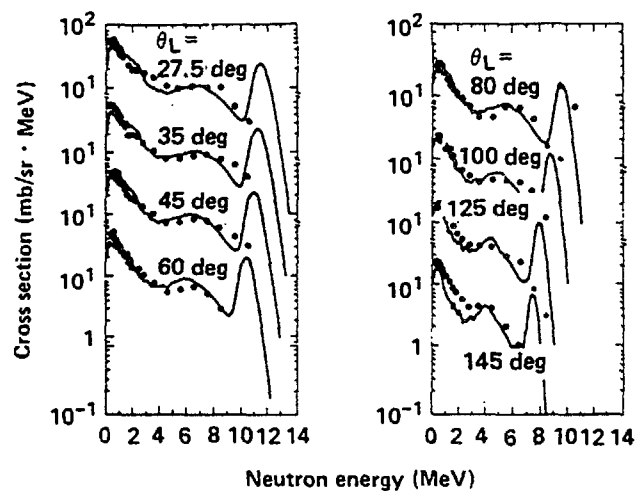


Fig. 13. Comparison of our evaluated double-differential cross sections (line) with the data of Drake et al.⁵ for 14.2-MeV incident neutrons.

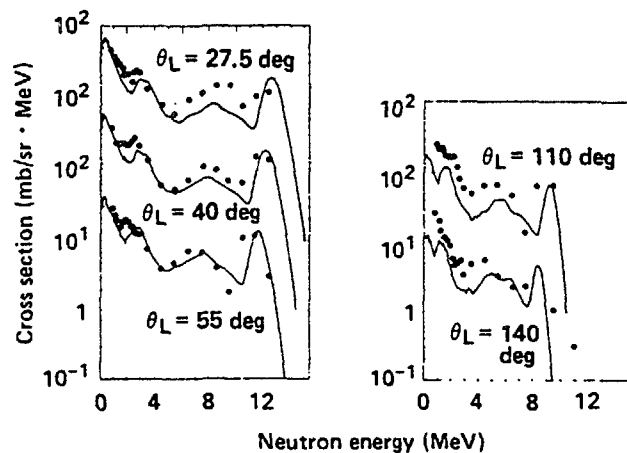


Fig. 14. Comparison of our evaluated double-differential cross sections (line) with the data of Baba et al.¹¹ for 15.4-MeV incident neutrons.

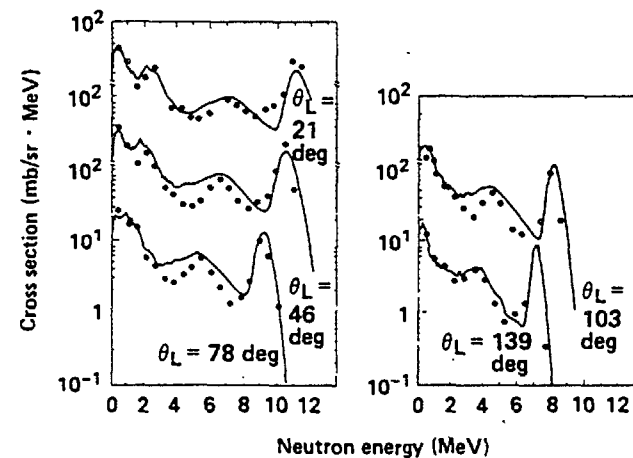


Fig. 15. Comparison of our evaluated double-differential cross sections (line) with the data of Takahashi et al.¹² for nominal 14.0-MeV incident neutrons (see Fig. 12 for actual incident neutron energies). These data include multiple scattering corrections.

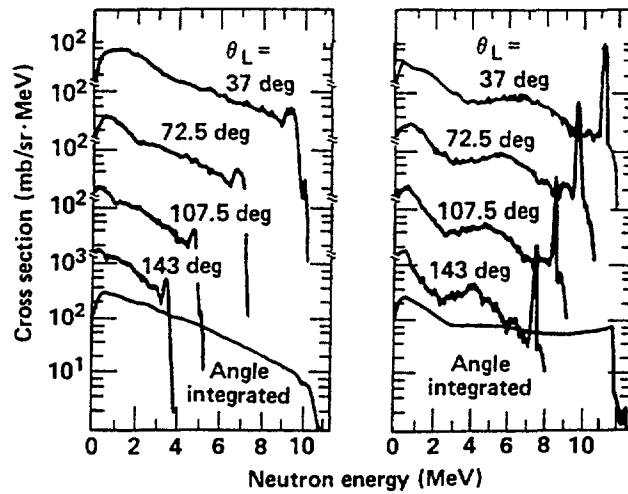


Fig. 16. Evaluated cross sections for 14.2-MeV incident neutrons. The left plot is for outgoing alpha particles and the right plot is for outgoing neutrons. The angle-integrated cross section (in millibarns per mega-electron-volts) is shown at the lower part of each plot.

INTEGRAL EXPERIMENTS

1. Series of measurements performed at Jülich in which leakage multiplication was measured for various beryllium blanket thickness.
2. LLNL pulsed-sphere program where the time spectra of neutrons leaking from a sphere are measured.
3. Nominal 14-MeV neutron sources used for both measurements.

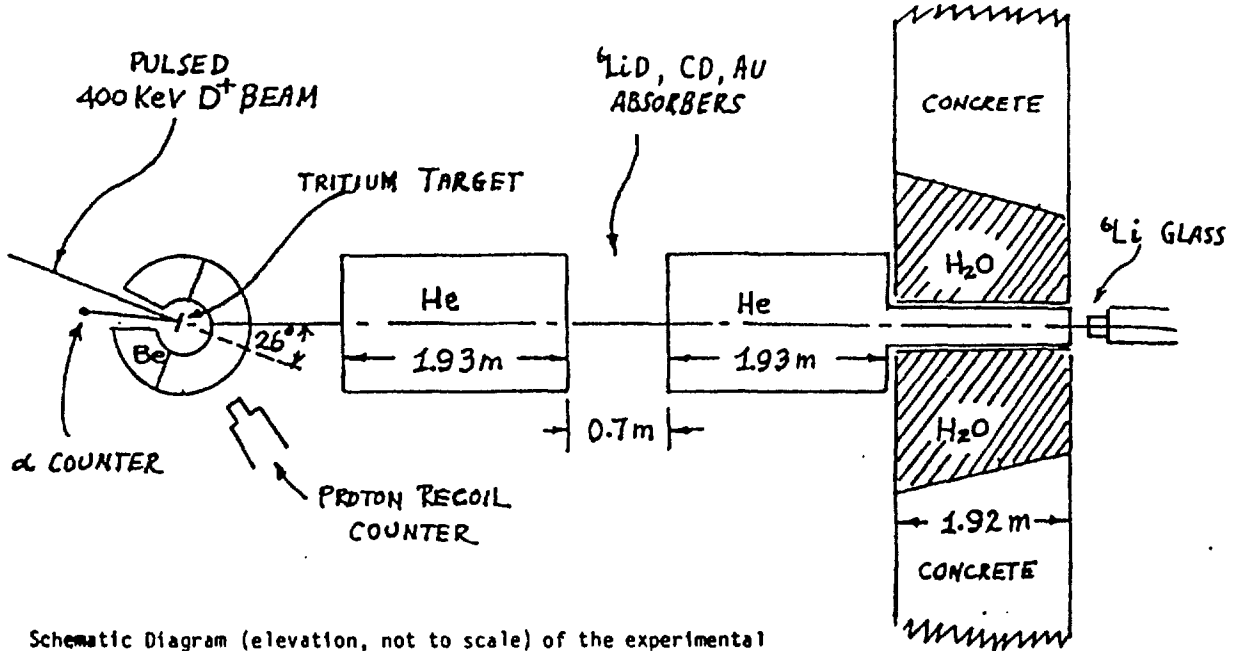
JÜLICH EXPERIMENT

- 14-MeV source surrounded by 8 to 20 cm of beryllium which was in turn surrounded by a large volume of polyethylene.
- Neutrons leaking from beryllium were captured in polyethylene allowing direct determination of leakage multiplication of the system (by use of BF_3 counters and numerical volume integration).
- Three dimensional geometry used in Monte Carlo (TART) calculation employing this evaluation.
- 20-25% disagreement between experiment and calculation not understood.

Multiplication in the Jülich Experiment

| Beryllium Thickness (cm) | Leakage Multiplication | | | |
|--------------------------|------------------------|------------------|--------------------------------|---------------------------|
| | Experimental Value | Calculated Value | | Calculated / Experimental |
| | | Bare Beryllium | Beryllium with CH ₂ | |
| 8 | 1.35 | 1.696 ± 0.008 | 1.705 ± 0.005 | 1.26 |
| 12 | 1.58 | 1.904 ± 0.009 | 1.901 ± 0.006 | 1.20 |
| 20 | 1.62 | 2.024 ± 0.014 | --- | 1.25 |

LIVERMORE PULSED-SPHERE MEASUREMENTS



Schematic Diagram (elevation, not to scale) of the experimental geometry for the low energy neutron spectra measurements.

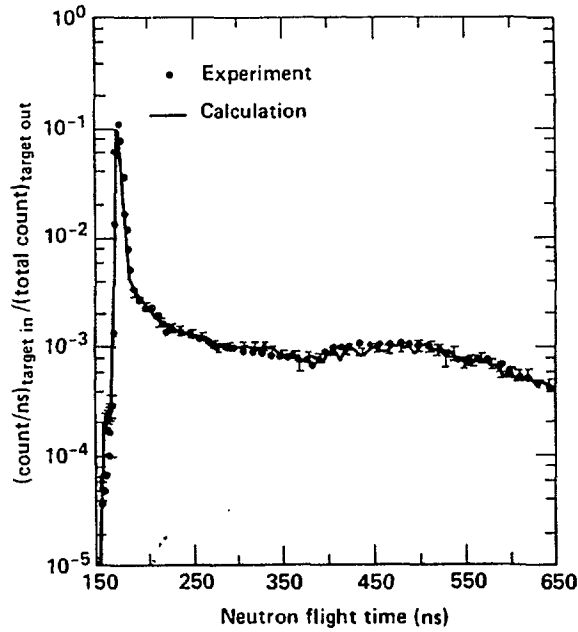


Fig. 18. Comparison between measured and calculated (ENDL84 library) neutron spectra for the 0.8-mfp beryllium sphere.

Time Integrals of Emergent Neutrons from the Beryllium Pulsed Sphere

| E_{min} (MeV) | E_{max} (MeV) | Experiment | Calculated ENDL80 | Error ^a (%) | Calculated ENDL84 | Error (%) |
|--------------------|--------------------|------------|----------------------|---------------------------|----------------------|--------------|
| 1 | 5 | 0.2876 | 0.3265 | +13.5 | 0.2789 | -3.0 |
| 5 | 10 | 0.1066 | 0.1047 | -1.8 | 0.1070 | +0.3 |
| ≥10 | | 0.7379 | 0.7328 | -0.7 | 0.7481 | +1.4 |
| ≥1 | | 1.132 | 1.164 | +2.8 | 1.134 | +0.2 |

^aError = (calculated - experiment) × 100/experiment.

SUMMARY OF LIVERMORE EXPERIMENTS - 1985

Measured and Calculated Integrals (counts/source count) for NE213 at 1 MeV Detector Bias using ENDL-84

| Shell Thickness | E>10MeV | 5<E<10 | 1<E<5 | Total |
|-----------------|---------|--------|-------|-------|
| 0.8 MFP | | | | |
| Calc. | .724 | .118 | .321 | 1.163 |
| Exp. | .743 | .114 | .312 | 1.169 |
| Ratio | .974 | 1.035 | 1.029 | .995 |
| 2.5 MFP | | | | |
| Calc. | .350 | .134 | .386 | .870 |
| Exp. | .373 | .127 | .372 | .872 |
| Ratio | .938 | 1.055 | 1.038 | .998 |
| 3.5 MFP | | | | |
| Calc. | .207 | .114 | .337 | .658 |
| Exp. | .225 | .106 | .322 | .653 |
| Ratio | .920 | 1.076 | 1.047 | 1.008 |

THICK-BLANKET CALCULATIONS

We calculated the leakage multiplication in spherical geometry for thicker beryllium blankets.

The average energy of the leakage neutrons, which is only weakly dependent on void radius, is approximately 4.5 MeV for a beryllium thickness of 10 cm and is 1.75 MeV for 20-cm thickness.

In the latter case, 50% of the leakage neutrons are below 250 eV. Thus, the thicker the blanket, the more degraded in energy are the leakage spectra.

This results in a larger calculational uncertainty for thick blankets as no low-energy spectral measurements are available for comparison with the calculated values.

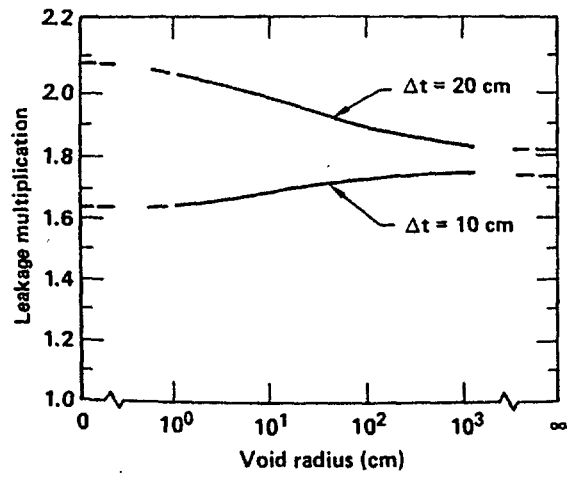


Fig. 19. Calculated (ENDL84 library) leakage multiplication for spherical shells around an interior void. Here, Δt is the shell thickness.

Keiichi SHIBATA

Japan Atomic Energy Research Institute
Tokai-mura, Ibaraki-ken, Japan

Abstract

Nuclear data evaluations have been performed for the third version of Japanese Evaluated Nuclear Data Library (JENDL-3). In the JENDL-3 evaluation, much emphasis was placed on the application to fusion neutronics. This paper gives a brief review of the evaluations of light nuclides and structural materials. Post JENDL-3 activities are also described.

1. Introduction

Much effort has been made by Japanese Nuclear Data Committee (JNDC) to prepare JENDL-3. A tentative library, which will be a base of JENDL-3, has been compiled, and it is being used for various benchmark tests. The evaluated data will be modified according to the results of benchmark tests, and then they will be made available as JENDL-3. In the JENDL-3 project, emphasis was put on the following subjects:

- 1) improvements of high-energy data,
- 2) inclusion of photon-production data,
- 3) consideration of measured double-differential cross section (DDX) data.

In JENDL-2, the direct-interaction process was not considered for almost all nuclides but nickel. Thus, it was necessary to improve the evaluated data by taking account of direct and precompound processes. Photon-production data are important for assessment of γ -ray heating. In order to investigate how to evaluate photon-production data, the working group on nuclear data for photon production was organized in JNDC. Moreover, the Tokyo Institute of Technology group has actively measured γ -ray spectrum from various nuclides below 1 MeV, and their data were utilized for the evaluation. The DDX data provide detailed information on neutron scattering processes required for transport calculations. In Japan, the DDX data have been being measured by two groups, i. e., Osaka University and Tohoku University.

The number of nuclides to be included in the JENDL-3 general purpose file is given in Table 1, together with those in JENDL-2 and ENDF/B-V. The total number will exceed that of ENDF/B-V. Concerning structural materials, JENDL-3 will include isotopic data as well as elemental data.

Section 2 gives a brief review of the evaluations of light nuclides (^2H , ^6Li , ^7Li and ^{12}C) and structural-material nuclides (Cr, ^{55}Mn , Fe, Ni and Cu) with stress on fusion applications. As mentioned above, the presently evaluated data may be modified as a result of the benchmark tests. Therefore, it should be noted that the evaluated data given in this paper are preliminary and should not be referred to as the JENDL-3 data. JENDL-3 will be released by March 1989. The post JENDL-3 activities are described in Sect. 3.

2. Evaluations for JENDL-3

2.1 Light nuclides

1) Deuterium

The data were taken from the JENDL-2 evaluation¹⁾ except that the File 6 part was removed. The evaluated (n, 2n) cross section is consistent with a recent measurement of Fréhaut et al.²⁾, as shown in Fig. 1. The elastic angular distribution and emitted neutron spectra from the (n, 2n) reaction were calculated with the three-body model based on the Faddeev equation. Figure 2 indicates that a simple phase-space distribution, shown by the dashed line, cannot reproduce the measured (n, 2n) spectrum.

As mentioned above, the File 6 part was removed, because JENDL-3 will be compiled in the ENDF/B-V format and use of File 6 is not recommended. It is, however, obvious that combination of Files 4 and 5 is inadequate for representing the (n, 2n) spectrum, since reaction kinematics cannot be taken into account. Therefore, it is required to make File 6 within the framework of the ENDF/B-VI format.

2) Lithium

The ^6Li (n, t) ^4He reaction cross section was calculated³⁾ with the R-matrix theory below 1 MeV, together with the total and elastic scattering cross sections. The calculated thermal cross section is 940.33 barns, in good agreement with the value of 940 ± 4 barns recommended by Mughabghab et al.⁴⁾ In the MeV region, the (n, t) cross section was based on the measurements of Bartle et al.⁵⁾ Figure 3 shows the evaluated ^6Li (n, t) ^4He cross section. The ^7Li (n, n't) ^4He reaction

Table 1. Comparison of the number of nuclides to be included in JENDL-3 with those in JENDL-2 and in ENDF/B-V. (General purpose files) The figures in parentheses stand for the number of nuclides with photon-production data.

| Nuclide \ Library | JENDL-2 | JENDL-3 | ENDF/B-V |
|--|---------|----------|----------|
| light nuclides (Z = 1 ~ 19) | 11 | 37 (10) | 25 (20) |
| structural material nuclides (Z = 20 ~ 30) | 30 | 36 (15) | 9 (9) |
| FP nuclides (Z = 31 ~ 69) | 9 | 25 (6) | 45 (5) |
| medium weight nuclides (Z = 70 ~ 89) | 12 | 20 (6) | 19 (6) |
| heavy nuclides (Z = 90 ~ 94) | 19 | 21 (3) | 13 (6) |
| transplutonium (Z = 95 ~) | 8 | 18 (0) | 7 (6) |
| TOTAL | 89 (0) | 157 (40) | 118 (52) |

cross section was evaluated⁶⁾ in 1984. After the evaluation, several measurements⁶⁻¹¹⁾ have been performed and they revealed that the 1984 evaluation was a little bit lower than the experimental data around 14 MeV. Therefore, it was decided to revise the 1984 evaluation by taking account of new measurements. The result is illustrated in Fig. 4.

For the inelastic scattering, four discrete levels were taken into consideration (2.19 MeV, 3.56 MeV, 4.31 MeV and 5.71 MeV for ⁶Li; 0.478 MeV, 4.63 MeV, 6.68 MeV and 7.47 MeV for ⁷Li). The excitation functions of these levels were obtained from experimental data.

Evaluation of neutron emission spectra is important for transport calculation in fusion blanket materials. In lithium, the continuous part of the spectra comes from the reactions ⁶Li (n, n')α, ⁷Li (n, n')α and ^{6,7}Li (n, 2n). The emission spectra from the (n, 2n) reaction were evaluated with the conventional evaporation model. The evaporation temperatures were obtained by Chiba et al.⁹⁾ The Coulomb-corrected phase-space model¹²⁾ was employed to express neutron emission spectra from the ⁶Li (n, n')α and ⁷Li (n, n')α reactions. According to this model, the neutron spectrum is given by

$$d^2\sigma / dE d\Omega \propto C_o^2 \rho,$$

$$\text{where } C_o^2 = 2\pi\eta / [\exp(2\pi\eta) - 1],$$

$$\eta = Z_2 Z_3 e^2 / (\hbar v_{23}),$$

$$\text{and } \rho = [E(E_{\max} - E)]^{1/2}.$$

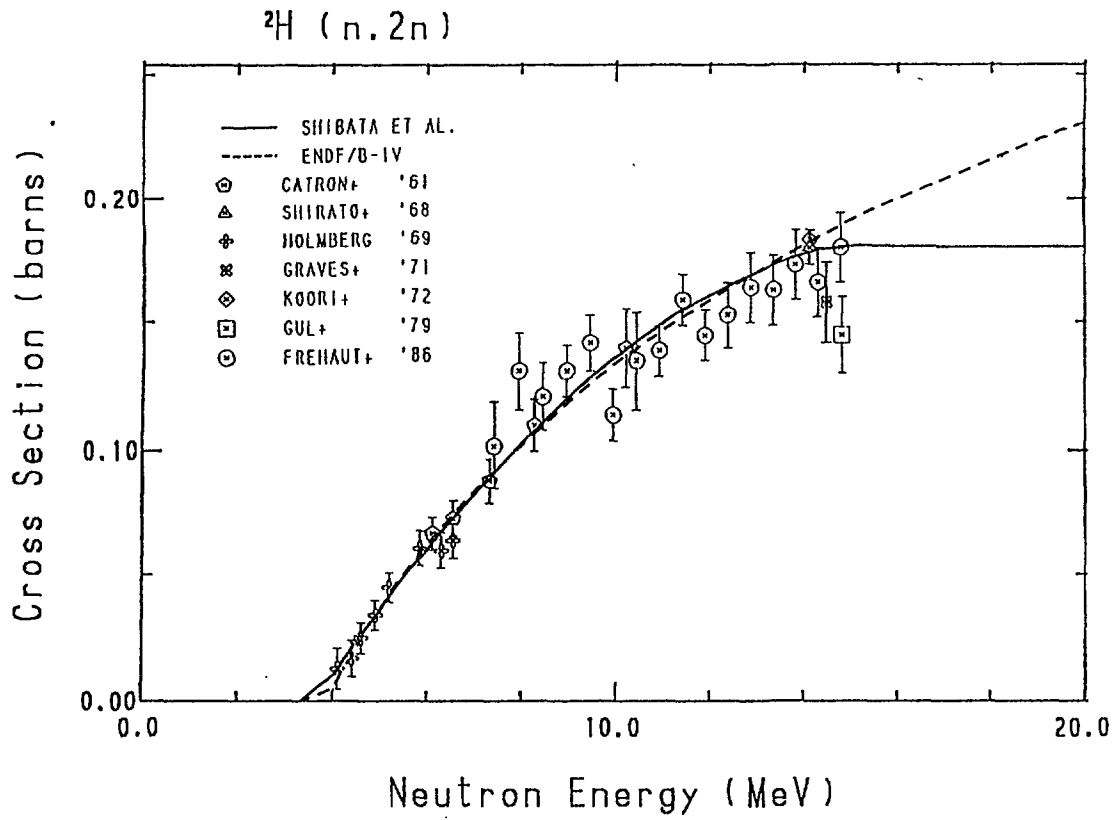


Fig. 1 ${}^2\text{H} (n, 2n)$ cross sections.

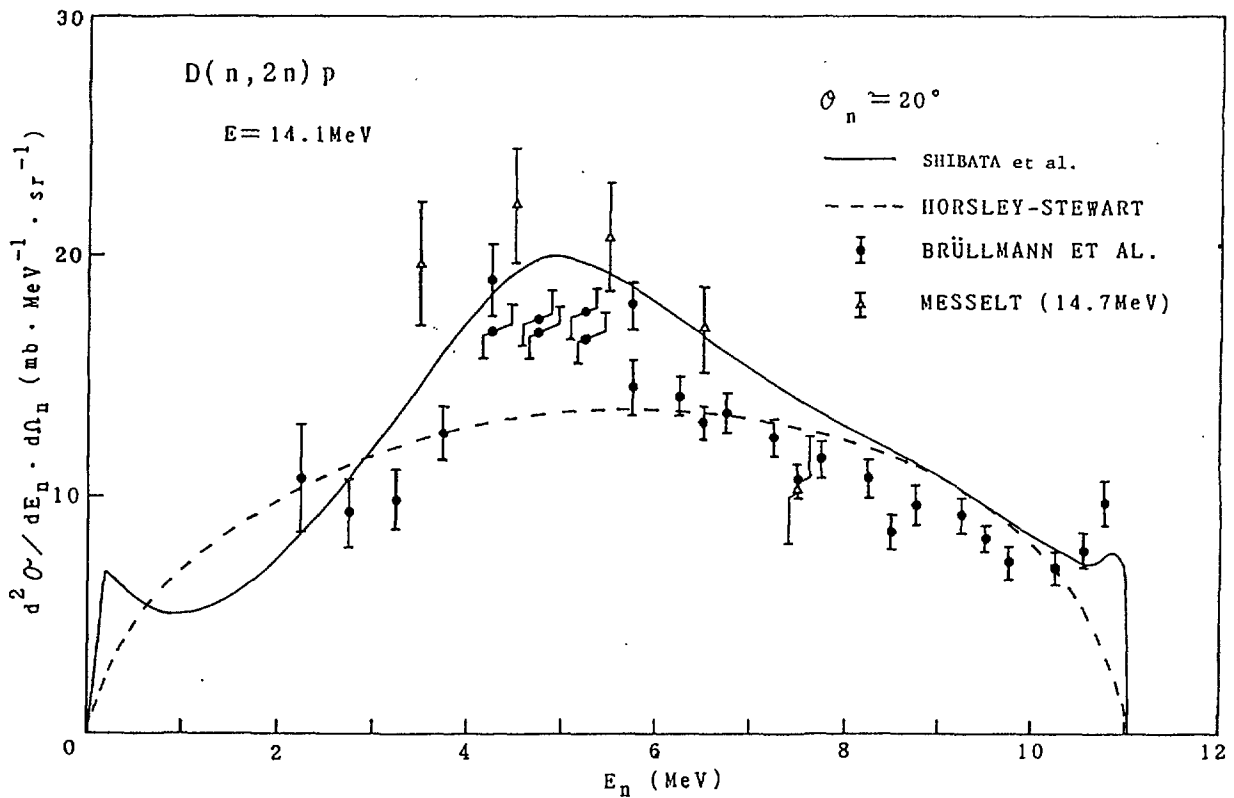


Fig. 2 Neutron emission spectra from the ${}^2\text{H} (n, 2n)$ reaction.

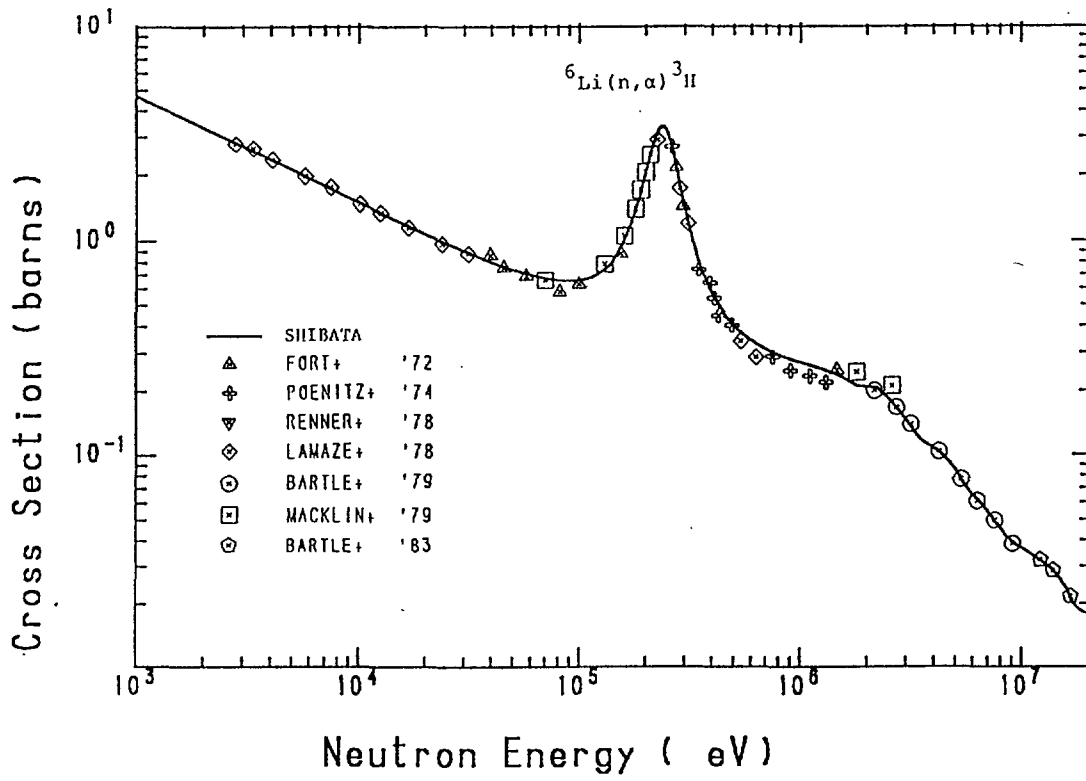


Fig. 3 ${}^6\text{Li}(n, t){}^4\text{He}$ cross sections.

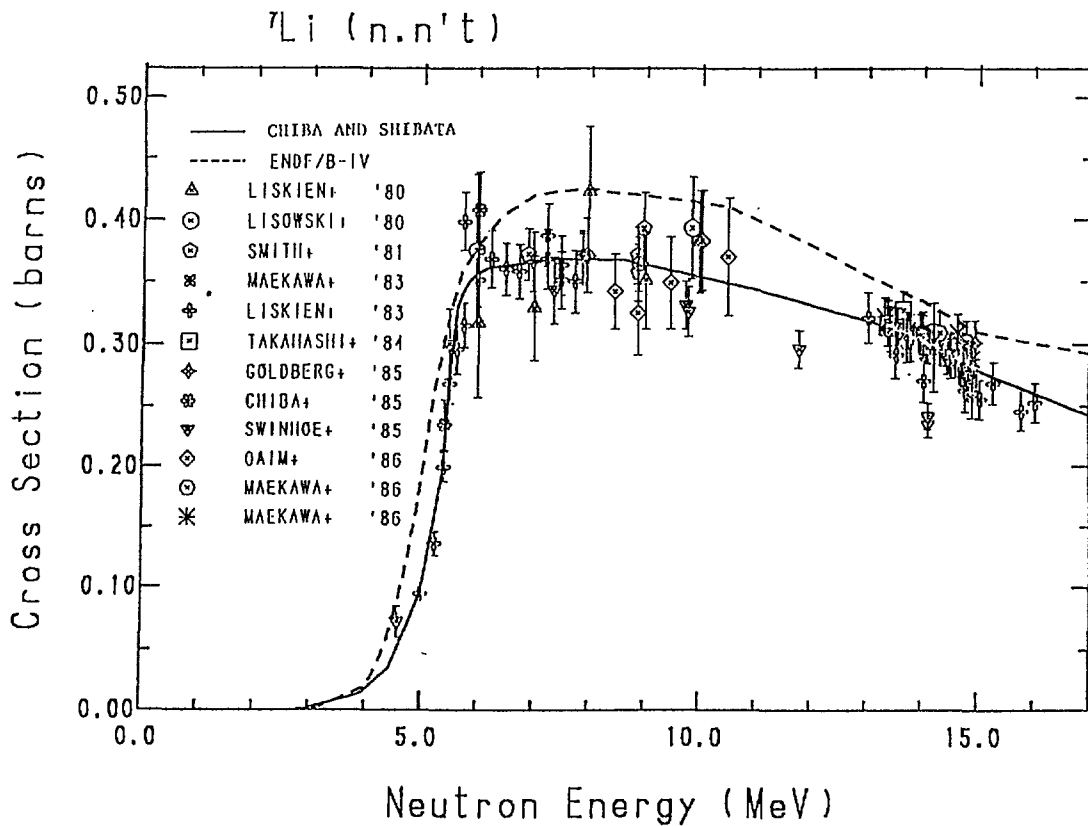


Fig. 4 ${}^7\text{Li}(n, n't){}^4\text{He}$ cross sections.

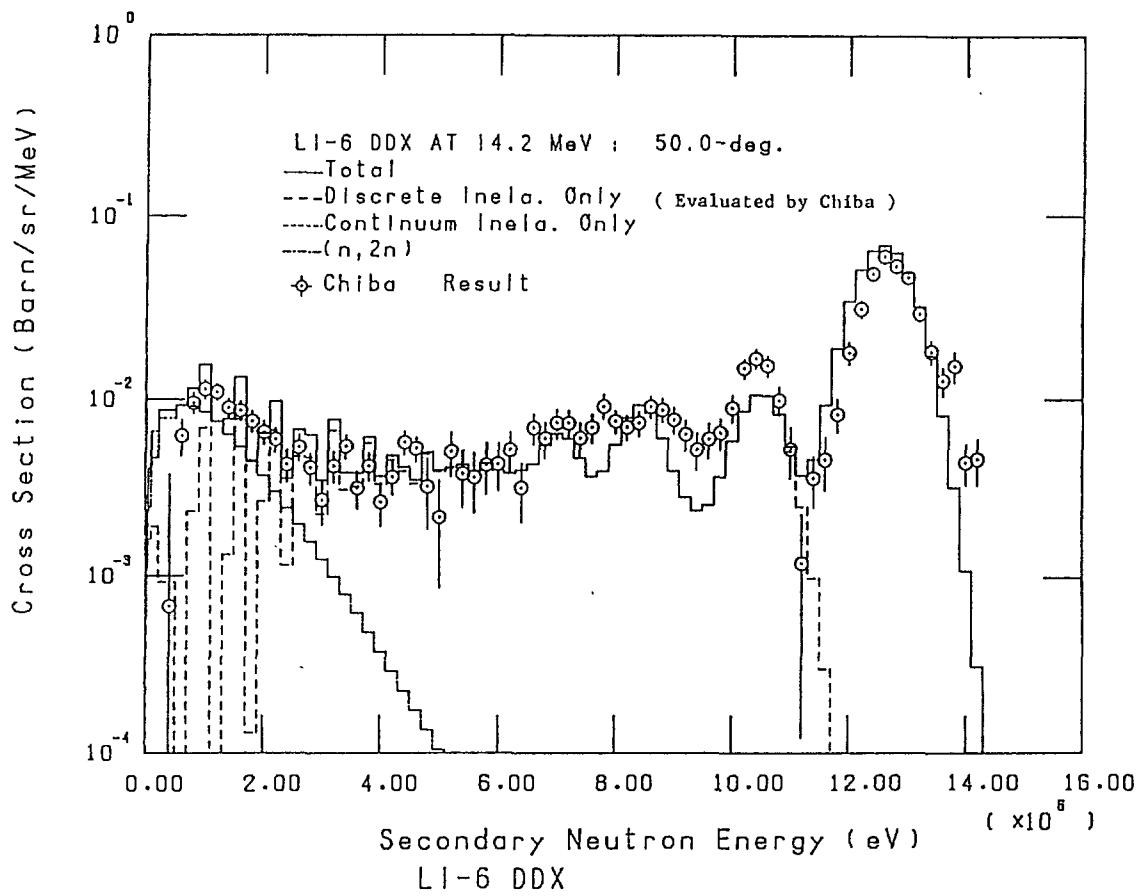


Fig. 5 Neutron emission spectra from ${}^6\text{Li}$.

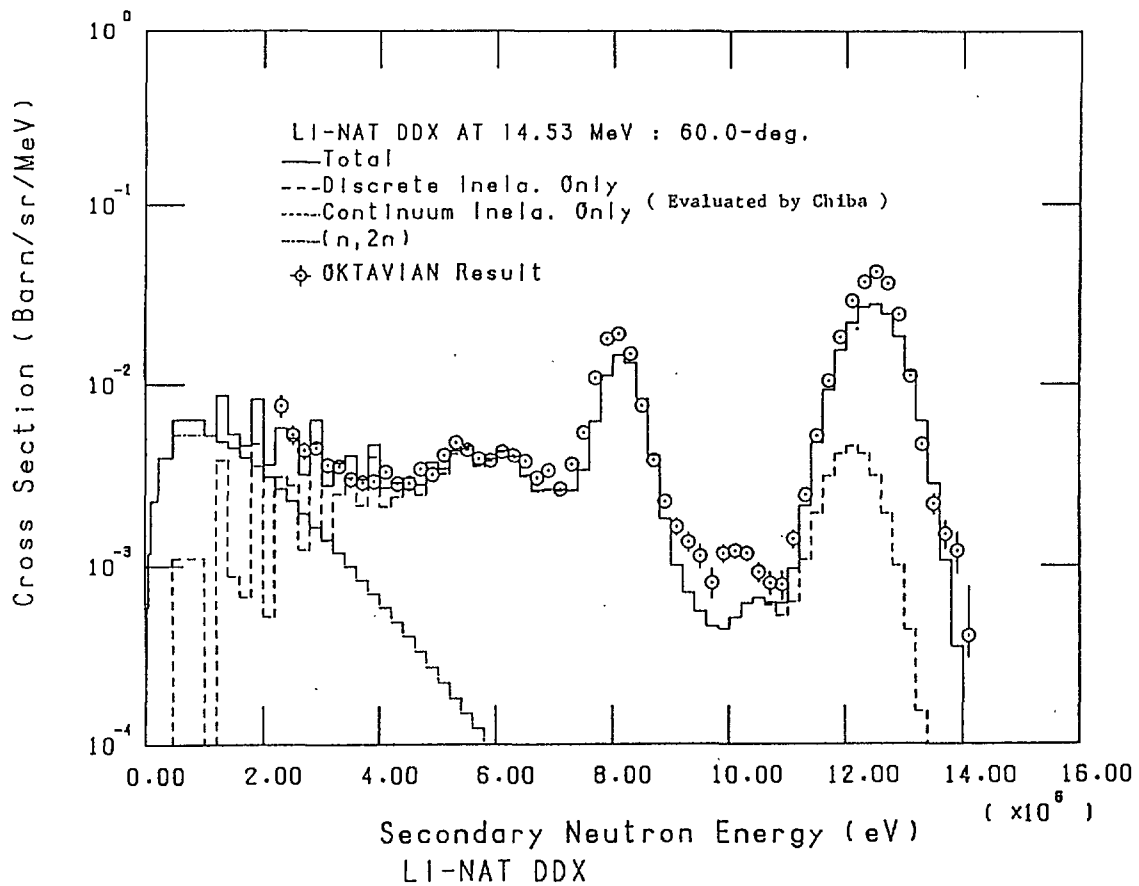


Fig. 6 Neutron emission spectra from ${}^{\text{nat}}\text{Li}$.

Here, E is the secondary-neutron energy in C. M. and E_{\max} its kinematically allowed maximum value. The subscripts 2 and 3 correspond to two unobserved particles, and v_{23} is their relative velocity. The symbol ρ stands for the ordinary phase-space factor. It should be noted that the phase-space distribution with the Coulomb corrections gives softer spectrum than the one without the corrections. In order to incorporate kinematics into actual files, pseudo levels were used¹³⁾ to express the above spectrum. This pseudo-level description is adequate for preserving energy-angle correlation approximately. Figures 5 and 6 show comparison of the evaluated data with measurements.^{9,14)}

3) Carbon-12

The total cross section was analyzed with the R-matrix theory below 4.8 MeV. Above 4.8 MeV, the evaluation was performed on the basis of the experimental data¹⁵⁻¹⁷⁾. Figure 7 shows the total cross section between 1 and 5 MeV.

Three discrete levels (4.44 MeV, 7.65 MeV and 9.64 MeV) were considered for the inelastic scattering. The cross sections for these levels were based on experimental data. The inelastic scattering to the excited states higher than 10.3 MeV and other reactions which lead to the final state of $n+3\alpha$ were regarded as the inelastic scattering to the continuous levels. Antolković et al.¹⁸⁾ measured the $(n, 3\alpha)$ cross section in a kinematically complete experiment, and their data are consistent with early works^{19,20)}. Owing to the experimental energy cut-off, however, the events due to the decay via the second excited state of ^{12}C (7.65 MeV) could not be detected. Accordingly, we considered the contribution from the continuous levels as the difference between the measured $^{12}\text{C}(n, 3\alpha)n$ cross section and the $^{12}\text{C}(n, n')^{12}\text{C}^*$ (9.64 MeV) cross section, since the 9.64-MeV level contributes to the $(n, 3\alpha)$ reaction but it was regarded as a discrete level in the evaluation.

The neutron emission spectrum from the continuous levels was assumed to have a simple evaporation shape. The value of nuclear temperature θ was determined from the DDX data measured at Osaka University¹⁴⁾ using 14 MeV neutrons. For other energies the following expression was assumed:

$$\theta = (E_n/\alpha)^{1/2},$$

where α is a constant. The calculated DDX is shown in Fig. 8.

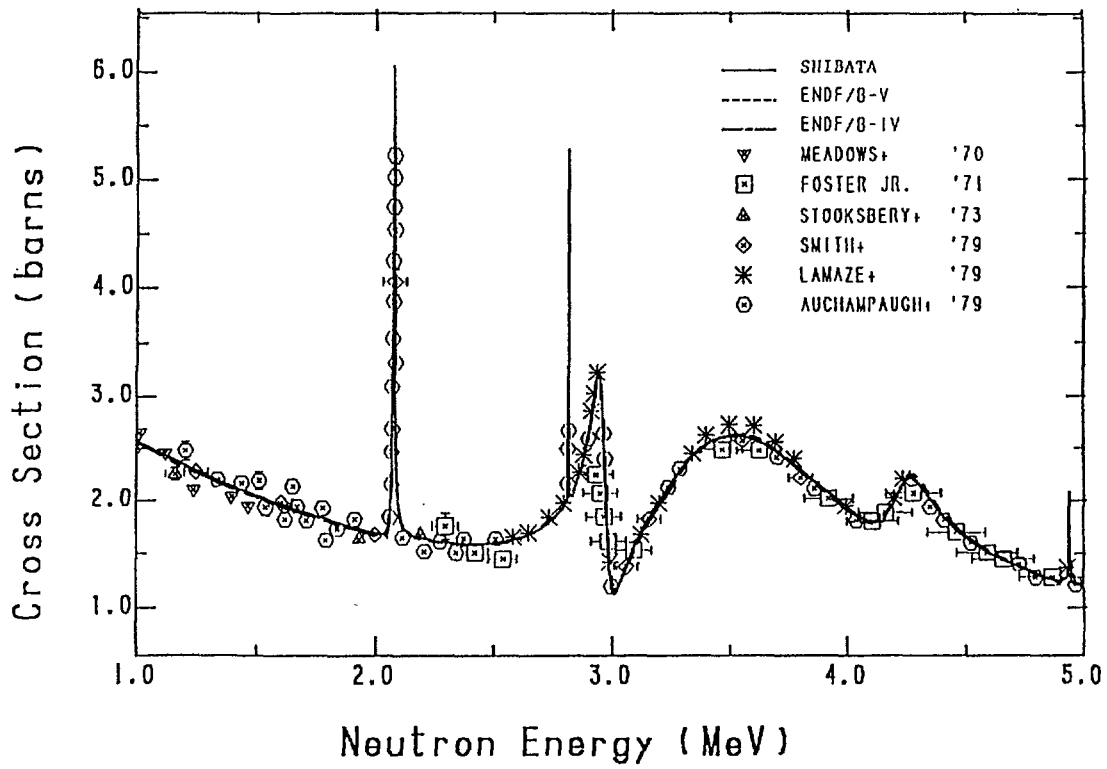


Fig. 7 Total cross sections of ^{12}C .

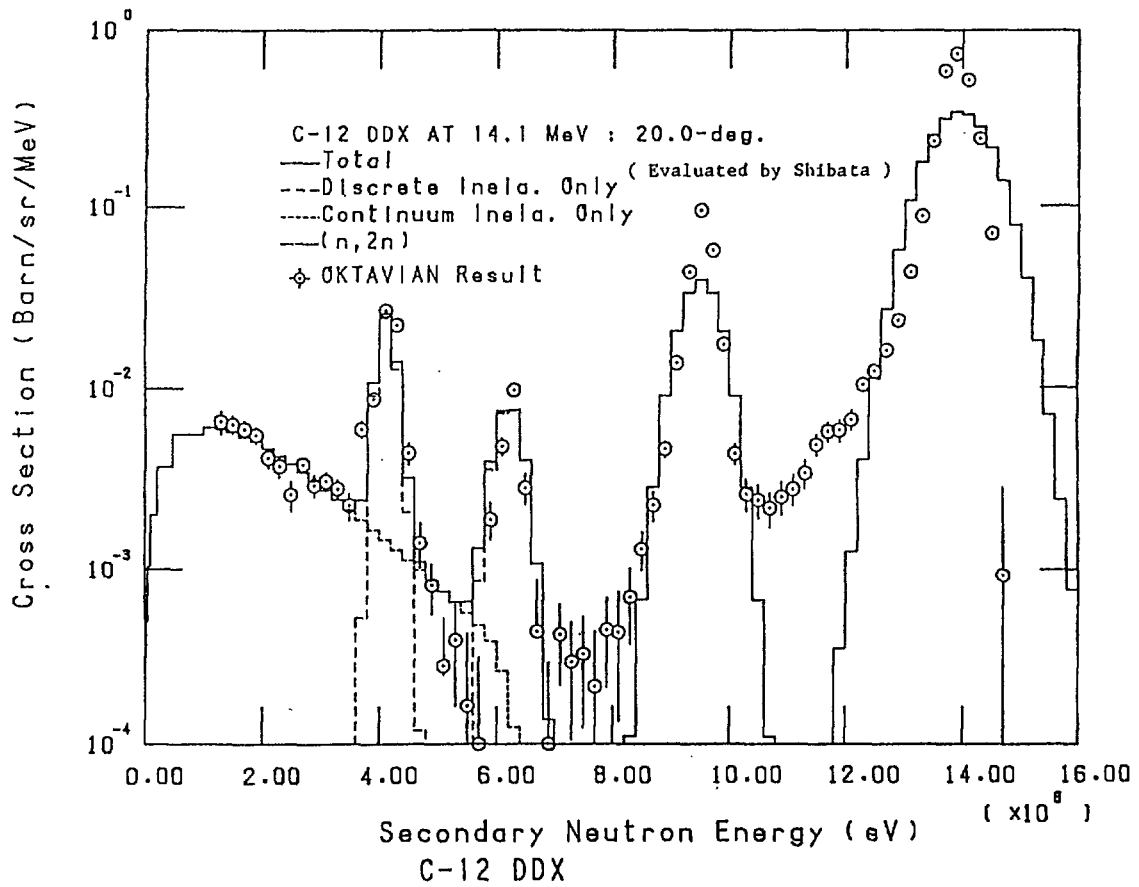


Fig. 8 Neutron emission spectra from carbon.

2.2 Structural-material nuclides

Theoretical calculations played an important role in the evaluation of structural materials. The nuclear model codes CASTHY²¹⁾ and GNASH²²⁾ were mainly used for the evaluations²³⁻²⁶⁾ of Cr, Fe, Ni and Cu. The inelastic scattering cross sections at low incident-energies were calculated using the CASTHY code, because CASTHY is capable of taking account of width-fluctuation corrections which are important at low energies. In the higher energy region, the inelastic scattering cross section was calculated by using GNASH and it was smoothly connected to the low-energy cross section calculated by CASTHY. The evaluation of ⁵⁵Mn was performed²⁷⁾ at ORNL under the cooperative program between JAERI and U.S.D.O.E. The TNG code²⁸⁾ was used to calculate neutron cross section of ⁵⁵Mn. The precompound mode was considered in the GNASH and TNG calculations. The direct-interaction cross sections were calculated with the DWBA theory using the DWUCK code²⁹⁾. For the threshold reactions, Ikeda et al.³⁰⁾ have measured activation cross sections of various nuclides between 13 and 15 MeV. Their experimental data were taken into account in the JENDL-3 evaluation.

Figures 9-13 show the calculated neutron emission spectra together with experimental data. Energy-angle correlation in continuous neutron spectra was neglected in the present work, because JENDL-3 will be compiled in the ENDF/B-V format. Angular distributions of continuum neutrons were calculated by using TNG at 14 MeV, and they are shown in Fig. 14. It is obvious from this figure that a forward peaking increases with outgoing energy. Thus, energy-angle correlation should be properly included in order to reproduce measured DDX data.

Photon-production cross sections were also calculated for the structural materials. The results are illustrated in Figs. 15-17. The Tokyo Institute of Technology group measured capture γ -ray spectra from iron and nickel in the energy range of 20 to 600 keV. The data will be included in JENDL-3.

3. Post JENDL-3 Activities

We have a plan to make the JENDL special purpose data file given as follows:

- (A) Activation cross section and decay data file
- (B) Actinide cross section and decay data file
- (C) Decay data file (not included in (A) and (B))
- (D) Dosimetry cross section file
- (E) Gas production cross section file

- (F) Kerma factor and DPA cross section file
- (G) (α , n) cross section file (including thick target yields)
- (H) Photo reaction data file
- (I) Standard data file

Preparation for the activation file has already started this year. It is planned to include reaction data of 138 nuclides. The number of reactions to be considered amounts to 369 and about 60 percent of the reactions will be covered by the JENDL-3 data. The gas production file will contain cross-section data needed for radiation-damage studies. JENDL-3 will cover 80 percent of the reactions considered. Concerning the items (F) (G) and (H), the working group on special purpose data file has been organized in JNDC. It is necessary to incorporate charged-particle emission spectra for the calculations of Kerma factors and DPA cross sections.

4. Concluding Remarks

The compilation work on JENDL-3 is in the final stage. A tentative library has been made for the benchmark tests. The problems in the JENDL-2 data have been almost resolved by the new evaluations for JENDL-3. The tasks still remained are incorporation of energy-angle correlation into neutron spectra and inclusion of charged-particle emission spectra. To achieve these things, file-making with the ENDF/B-VI format is required for important nuclides.

We have started preparation for special purpose data files. As the first step, the evaluation of activation cross sections is in progress. Furthermore, the evaluation method is being investigated for the nuclear data needed for radiation-damage studies.

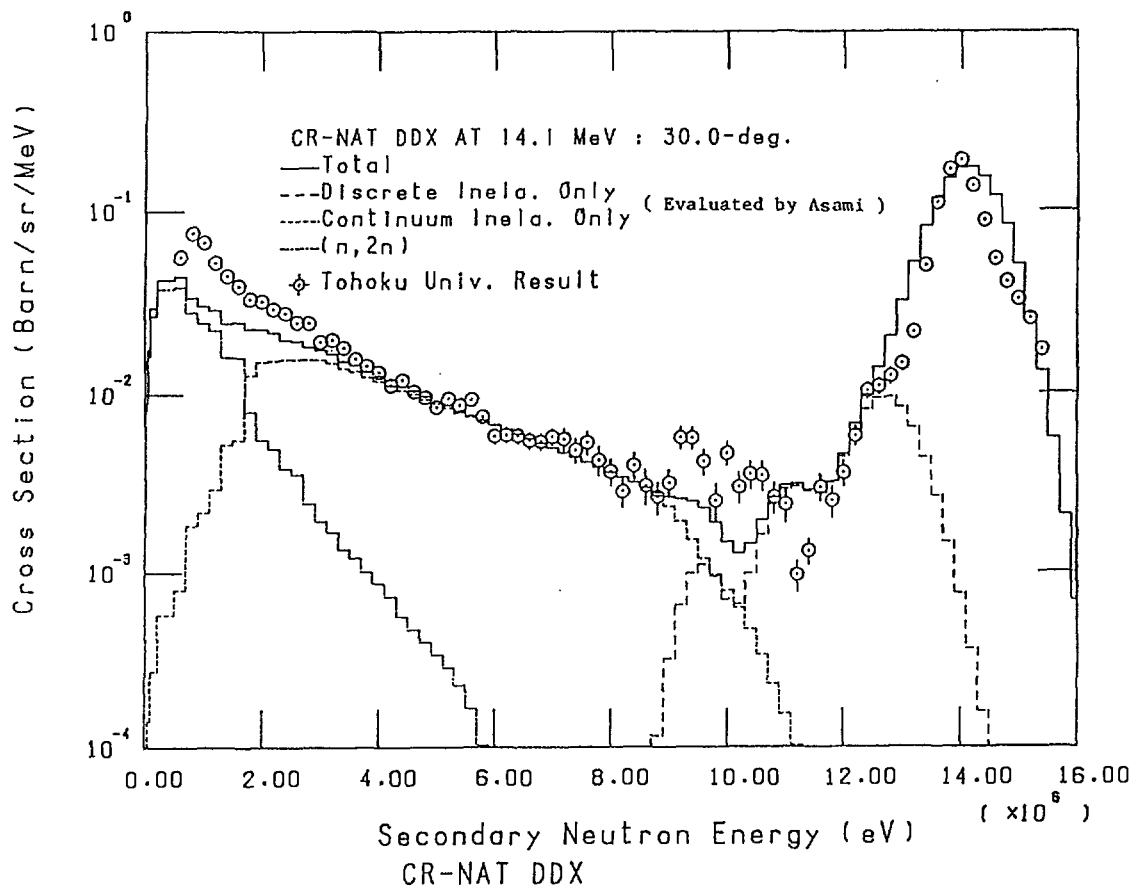


Fig. 9 Neutron emission spectra from chromium.

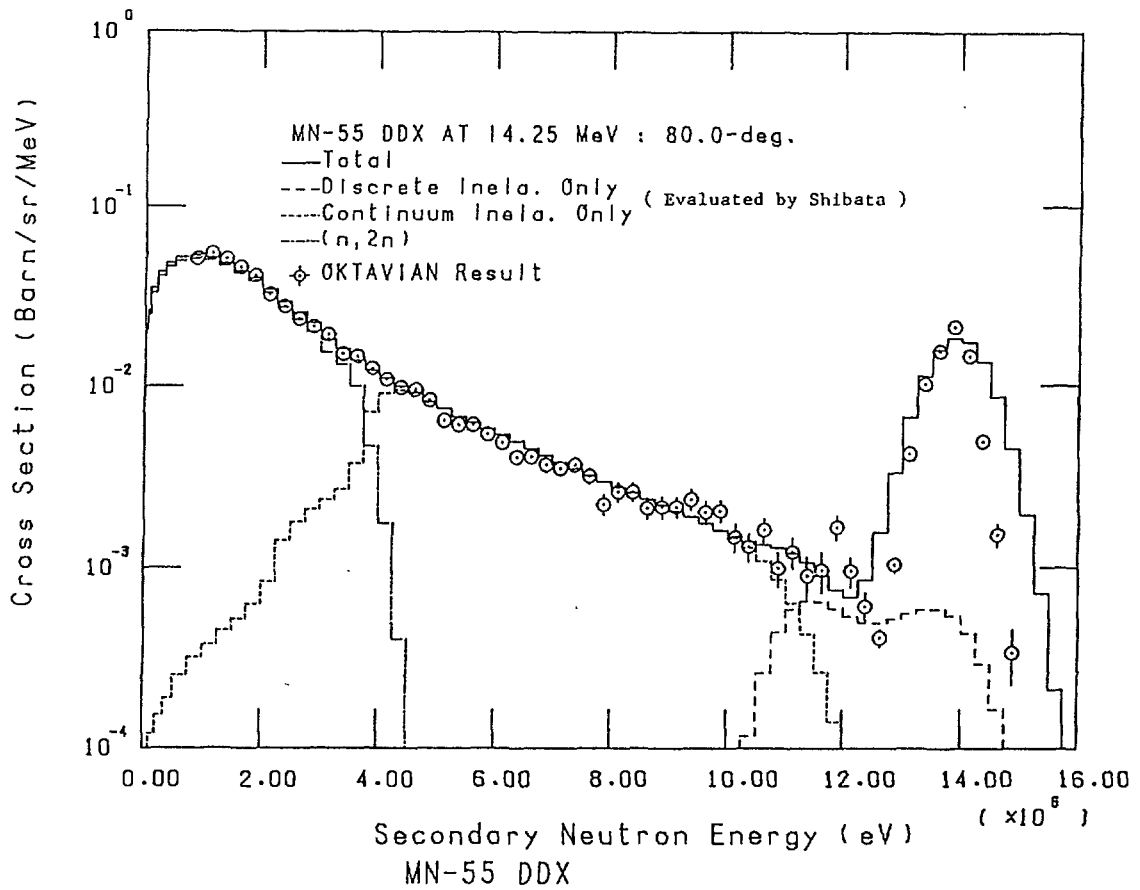


Fig. 10 Neutron emission spectra from manganese.

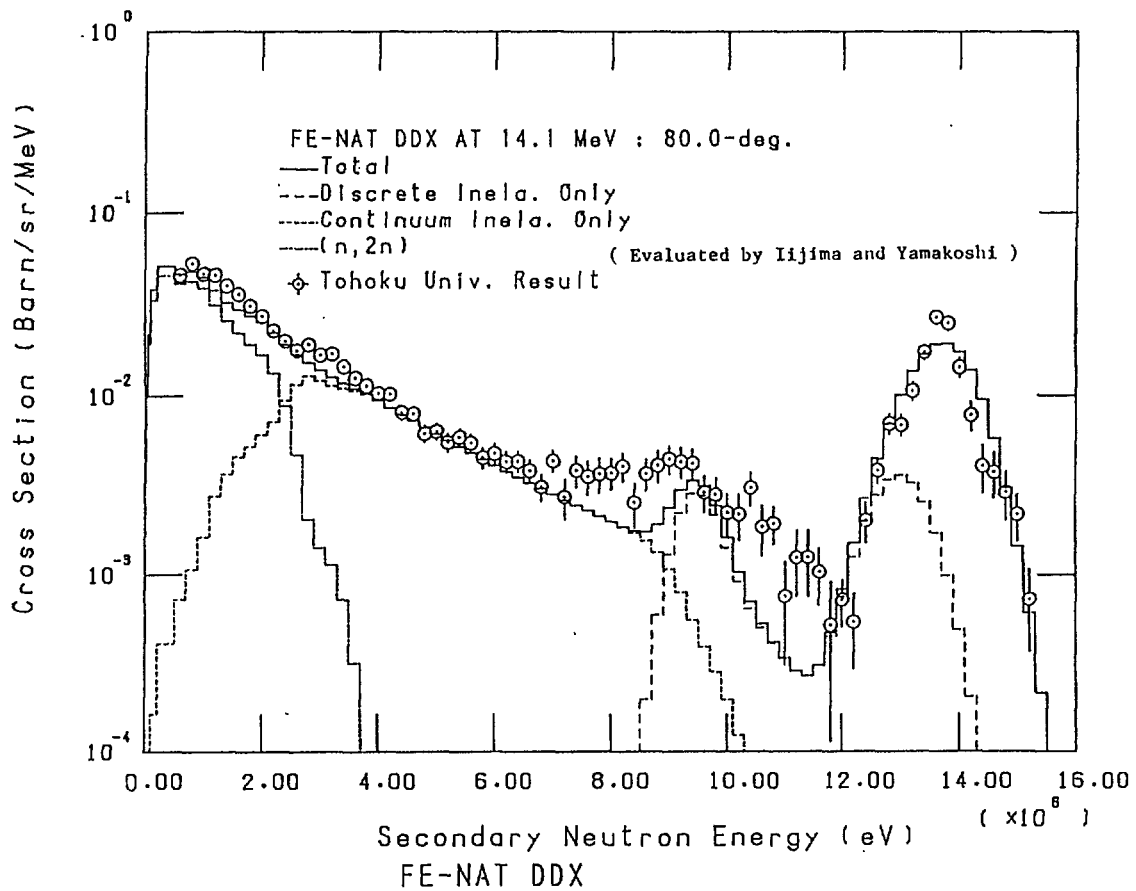


Fig. 11 Neutron emission spectra from iron.

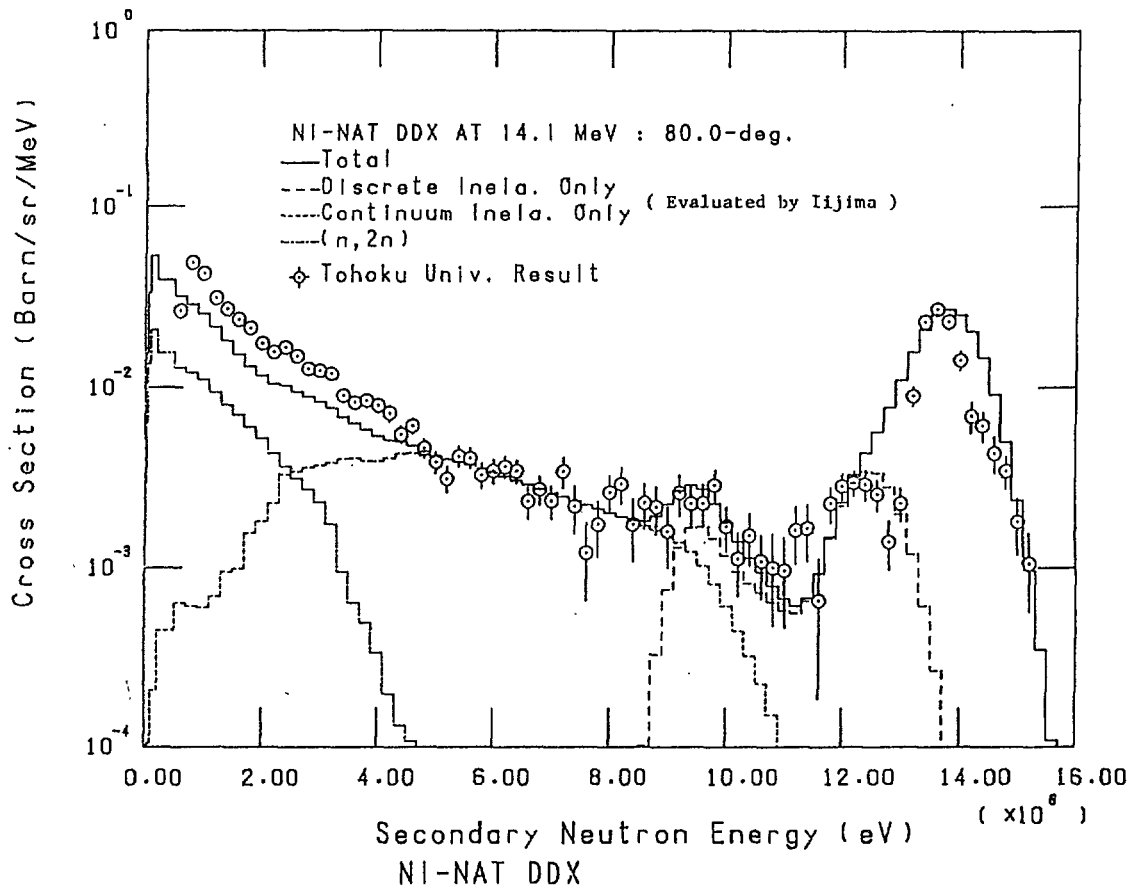


Fig. 12 Neutron emission spectra from nickel.

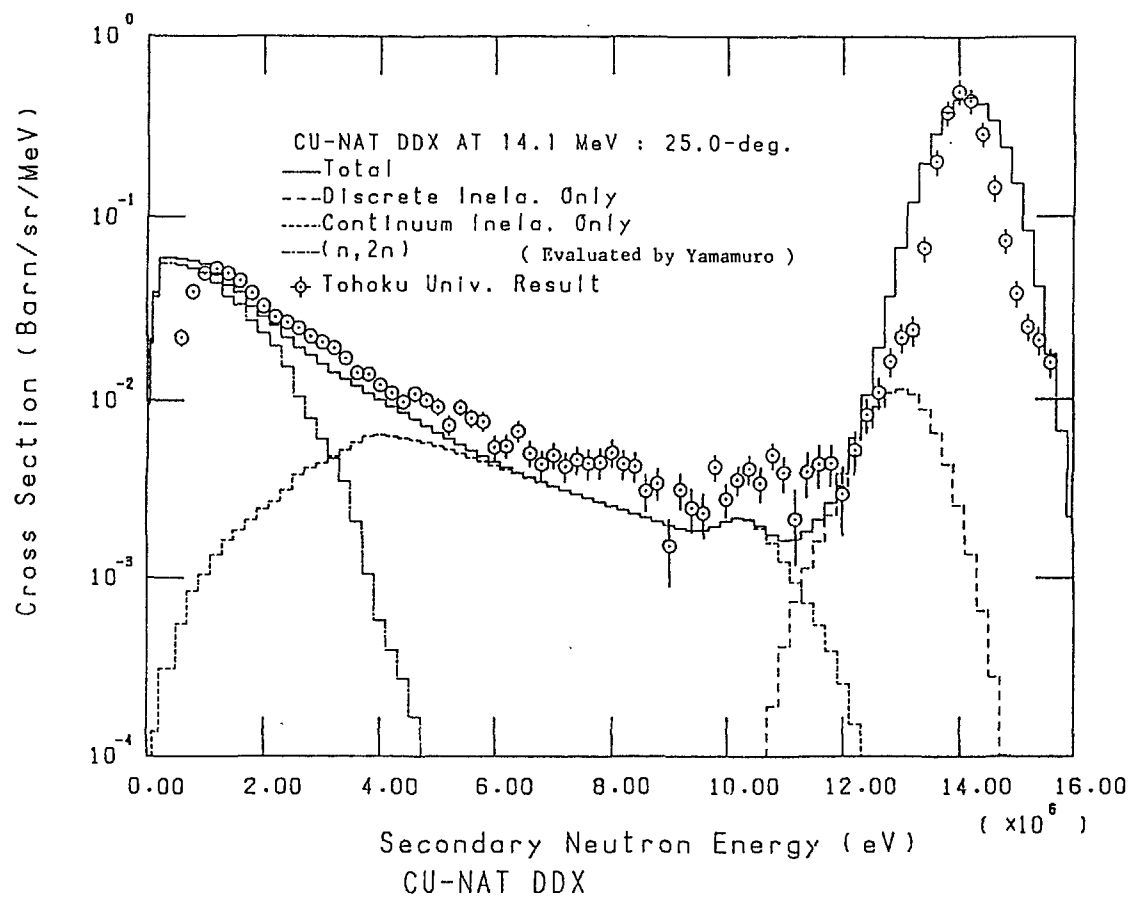


Fig. 13 Neutron emission spectra from copper.

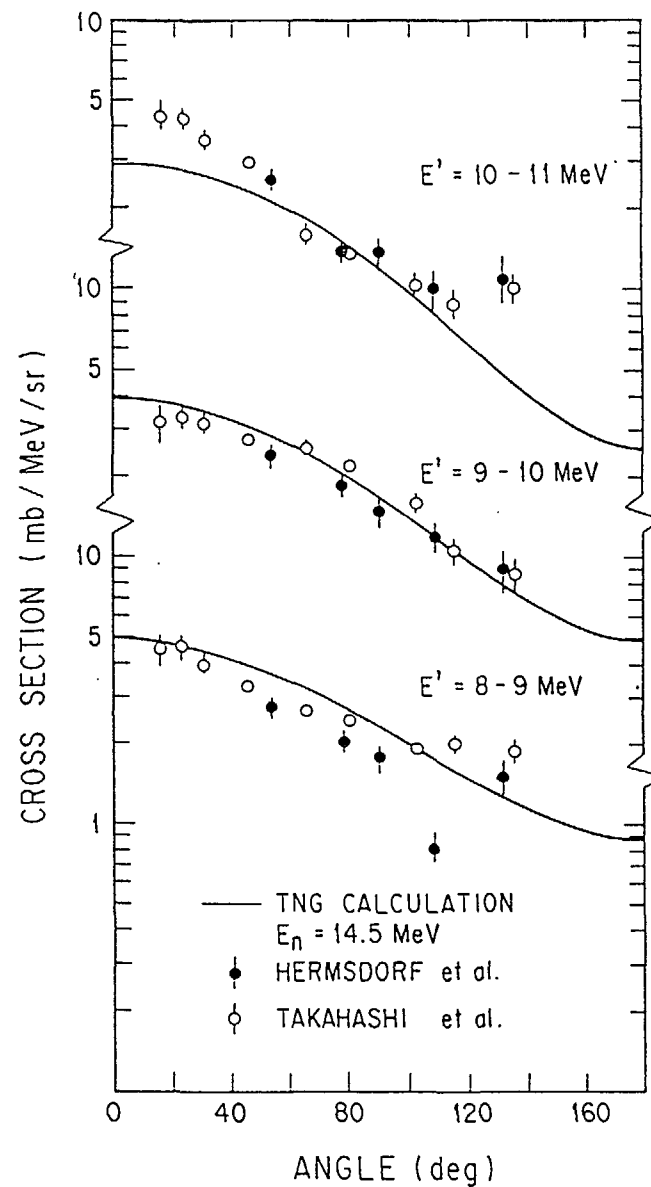


Fig. 14 Angular distributions for the $^{55}\text{Mn} (n, xn)$ reaction.

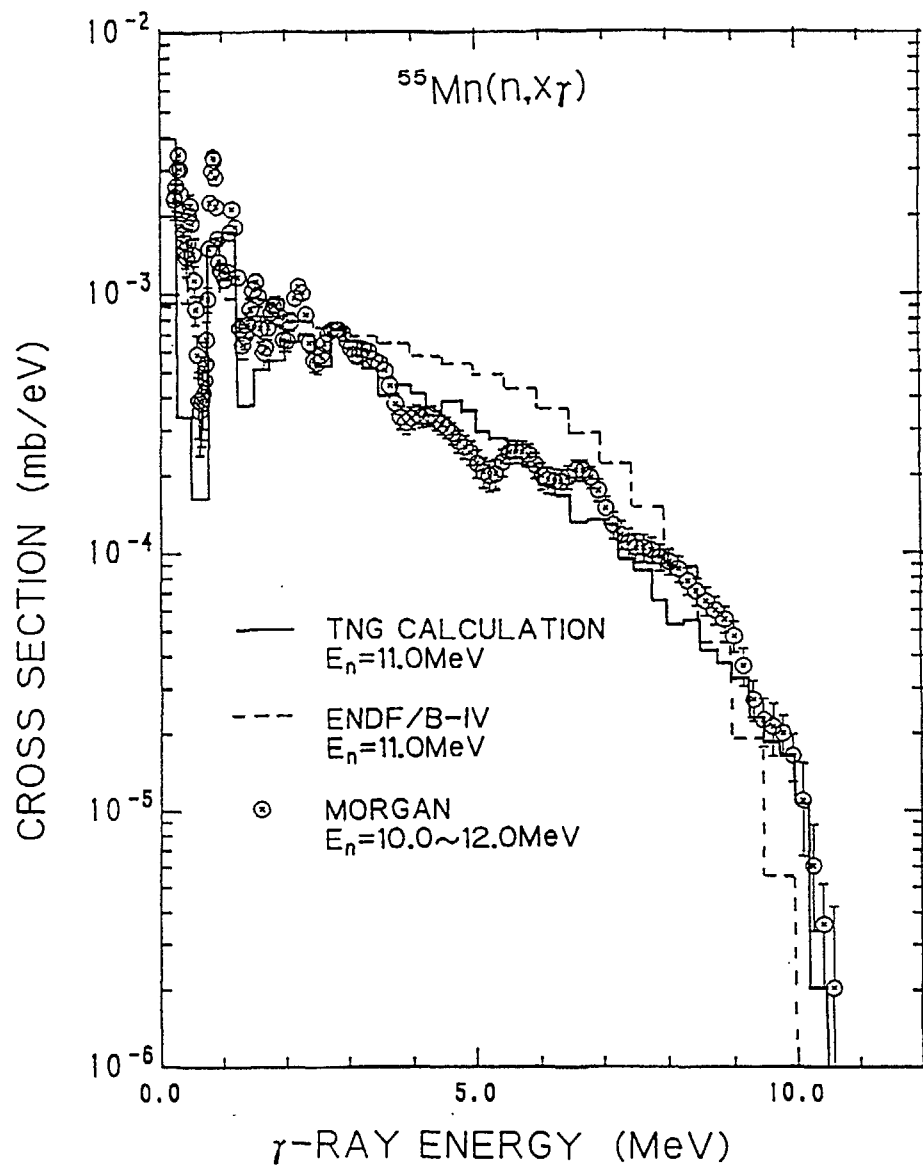


Fig. 15 Gamma-ray spectra from manganese.

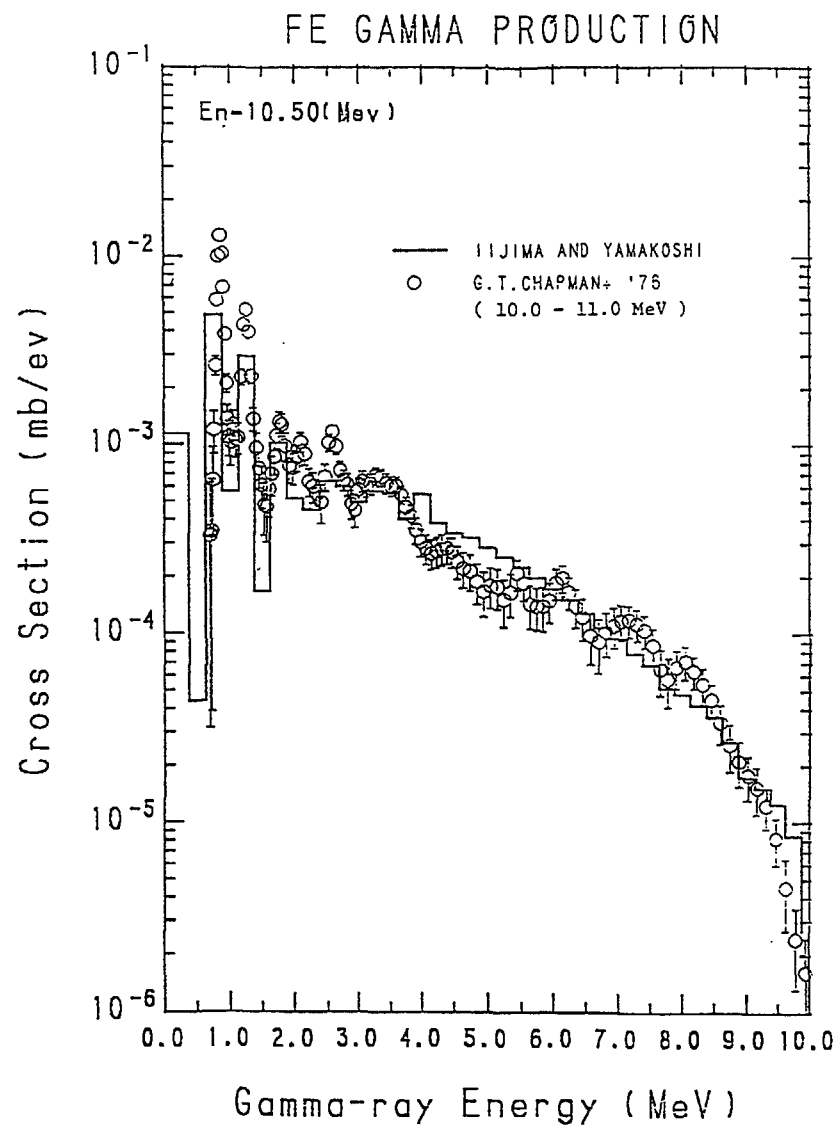


Fig. 16 Gamma-ray spectra from iron.

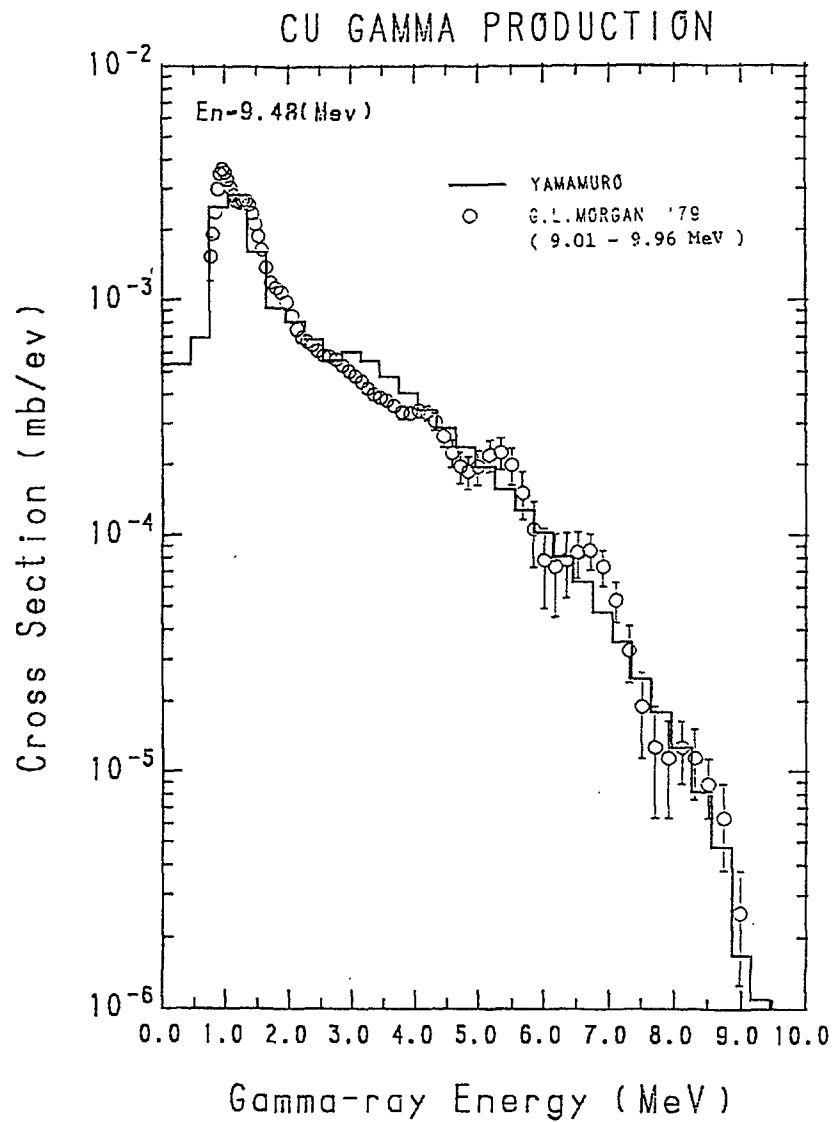


Fig. 17 Gamma-ray spectra from copper.

References

- 1) K. Shibata et al., "Evaluation of Neutron Nuclear Data for Deuterium", JAERI-M 83-006 (1983).
- 2) J. Fréhaut et al., "(n, 2n) Cross Section of ^2H and ^{239}Pu ", Proc. Int. Conf. Nuclear Data for Basic and Applied Science, Santa Fe, 1985, p.1561 (1986), Gordon and Breach Science Publishers.
- 3) K. Shibata, "Evaluation of Neutron Nuclear Data of ^6Li for JENDL-3", JAERI-M 84-198 (1984).
- 4) S.F. Mughabghab et al., "Neutron Cross Sections Vol. 1", Academic Press, 1981.
- 5) C.M. Bartle, Nucl. Phys. A330 (1979) 1,
C.M. Bartle et al., Nucl. Phys. A397 (1983) 21.

- 6) A. Takahashi et al., "Measurements of Tritium Breeding Ratios in Lithium Slabs Using Rotating Neutron Source", Proc. 13th Symp. Fusion Technology, Varese, Italy, 1984, p.1325.
- 7) D.L. Smith et al., "Cross-Section Measurement for the ${}^7\text{Li}$ (n,n't) ${}^4\text{He}$ Reaction at 14.74 MeV", ANL/NDM-87 (1984).
- 8) E. Goldberg et al., Nucl. Sci. Eng. 91 (1985) 173.
- 9) S. Chiba et al., J. Nucl. Sci. Technol. 22 (1985) 771.
- 10) H. Maekawa et al., "Measurement of ${}^7\text{Li}$ (n,n' α) T Cross Section Between 13.3 and 14.9 MeV", JAERI-M 86-125, p.130 (1986).
- 11) S.M. Qaim and R. Wölfle, Nucl. Sci. Eng. 96 (1987) 52.
- 12) R.E. Holland et al., Phys. Rev. C19 (1979) 592.
- 13) S. Chiba, "Revision of the Neutron Nuclear Data of Lithium", JAERI-M 86-029, p.32 (1986).
- 14) A. Takahashi et al., "Measurement of Double Differential Neutron Emission Cross Sections with 14 MeV Source for D, Li, Be, C, O, Al, Cr, Fe, Ni, Mo, Cu, Nb and Pb", Proc. Int. Conf. Nuclear Data for Science and Technology, Antwerp, 1982, p.360 (1983), D. Reidel Publishing Company.
- 15) G.P. Lamaze et al., Bull. Am. Phys. Soc. 24 (1979) 862.
- 16) G.F. Auchampaugh et al., Nucl. Sci. Eng. 69 (1979) 30.
- 17) S. Cierjacks et al., Nucl. Instrum. Methods 169 (1980) 185.
- 18) B. Antolković et al., Nucl. Phys. A394 (1983) 87.
- 19) G.M. Frye, Jr. et al., Phys. Rev. 99 (1955) 1375.
- 20) S.S. Vasil'ev et al., Sov. Phys. -JETP 6 (1958) 1016.
- 21) S. Igarasi, J. Nucl. Sci. Technol. 12 (1975) 67.
- 22) P.G. Young and E.D. Arthur, "GNASH: A Preequilibrium, Statistical Nuclear-Model Code for Calculation of Cross Sections and Emission Spectra", LA-6974 (1977).
- 23) T. Asami, "Evaluation of Neutron Nuclear Data for Chromium", private communication (1987).
- 24) S. Iijima and H. Yamakoshi, "Evaluation of Neutron Nuclear Data for Iron", private communication (1987).
- 25) S. Iijima, "Evaluation of Neutron Nuclear Data for Nickel" private communication (1987).
- 26) N. Yamamuro, "Evaluation of Neutron Nuclear Data for Copper", private communication (1987).
- 27) K. Shibata, "Evaluation of Neutron Nuclear Data for ${}^{55}\text{Mn}$ ", private communication (1987).
- 28) C.Y. Fu, "A Consistent Nuclear Model for Compound and Precompound Reactions with Conservation of Angular Momentum", ORNL/TM-7042 (1980).

29) P.D. Kunz,; unpublished.

30) Y. Ikeda et al., "A Program of Activation Cross Section Measurements on Fusion Reactor Structural Components for 14 MeV Neutrons Using FNS Facility", JAERI-M 87-025, p.244 (1987).

The activation cross section library UKACT1 and the inventory code FISPACT

R.A.Forrest

Nuclear Physics Division
A.E.R.E., Harwell
Didcot, Oxfordshire
OX110RA, England

The UK activation library for fusion applications, UKACT1, supersedes the existing UKCTRIIA library. It contains neutron induced reaction data for 8719 reactions on 625 target nuclides. The library is used by the inventory code FISPACT which is a modified version of the existing code FISPIN. A library of decay information for all the 1314 nuclides involved is also required for calculations and this is also briefly described. UKACT1 will be used for irradiation calculations and as the starting point for a new version which will contain improved data for the most important reactions. These will be identified using the sensitivity subroutine in FISPACT.

1 Introduction

The status of the UK activation library for fusion at the end of 1986 is summarized in reference 1. The present paper reports further progress with the data library and gives details of the inventory code FISPACT which has been developed to use the new library.

2 The data library UKACT1

UKACT1 is an essentially complete library containing activation cross section data for neutron induced reactions with thresholds up to 14.9 MeV. Most of the work on this library has been to ensure completeness rather than in trying to significantly improve the accuracy of the individual reactions. It contains cross section data in 100-group GAM-II format for reactions on 625 target nuclides. These are shown in Table 1 and include all stable isotopes and radionuclides with half lives greater than one day. In addition, some nuclides with shorter half lives have been included (indicated by * in Table 1) where a product formed by a single reaction is a long lived nuclide. These reactions are especially important in some cases *e.g.* $^{45}\text{Ti}(n,2n)^{44}\text{Ti}$ where there is no other route for the production of ^{44}Ti .

The target nuclides include 49 first isomers(m) and 4 second isomers(n). It is extremely important that all the isomers for all elements are included because in some cases such as ^{178}Hf and ^{192}Ir the second isomers are very long lived (31 and 241 years respectively). In addition to the 625 target nuclides a further 689 are required as products of reactions or as decay daughters. The library containing the decay data for all these 1314 nuclides is described in section 3.

UKACT1 is developed from the REAC library produced by Mann *et al*². This was modified by Gruppelaar *et al*³ with the addition of some missing reactions and renormalisation of the reactions to the (then) best systematics. Further changes have been made independently since then by Gruppelaar *et al*, but these have not been incorporated in this version of UKACT. To the interim library the following changes have been made.

1 Addition of THRES-G generated cross sections for 162 reactions. These are normalised using the systematics given by Forrest^{1,4}. THRES-G is a modified version of THRES-F⁵

Table 1 Isotopes considered as targets in UKACT1.

| Element | Atomic Mass | Number |
|---------|---|--------|
| H | 1,2,3 | 3 |
| He | 3 | 1 |
| Li | 6,7 | 2 |
| Be | 9,10 | 2 |
| B | 10,11 | 2 |
| C | 12,13,14 | 3 |
| N | 14,15 | 2 |
| O | 16,17,18 | 3 |
| F | 19 | 1 |
| Ne | 20,21,22 | 3 |
| Na | 22,23 | 2 |
| Mg | 24,25,26 | 3 |
| Al | 26,27 | 2 |
| Si | 28,29,30,31*,32 | 5 |
| P | 31,32,33 | 3 |
| S | 32,33,34,35,36 | 5 |
| Cl | 35,36,37 | 3 |
| Ar | 36,37,38,39,40,41*,42 | 7 |
| K | 39,40,41,42* | 4 |
| Ca | 40,41,42,43,44,45,46,47,48 | 9 |
| Sc | 44m,45,46,47,48 | 5 |
| Ti | 44,45*,46,47,48,49,50 | 7 |
| V | 48,49,50,51 | 4 |
| Cr | 50,51,52,53,54 | 5 |
| Mn | 52,53,54,55 | 4 |
| Fe | 54,55,56,57,58,59,60 | 7 |
| Co | 56,57,58,59,60 | 5 |
| Ni | 56,57,58,59,60,61,62,63,64,66 | 10 |
| Cu | 63,64*,65,67 | 4 |
| Zn | 64,65,66,67,68,70,72 | 7 |
| Ga | 67,69,71 | 3 |
| Ge | 68,69,70,71,72,73,74,76 | 8 |
| As | 71,72,73,74,75,76,77 | 7 |
| Se | 72,73*,74,75,76,77,78,79,80,82 | 10 |
| Br | 77,79,81,82 | 4 |
| Kr | 78,79,80,81,82,83,84,85,86 | 9 |
| Rb | 83,84,85,86,87 | 5 |
| Sr | 82,83,84,85,86,87,88,89,90 | 9 |
| Y | 87,88,89,90,91 | 5 |
| Zr | 88,89,90,91,92,93,94,95,96 | 9 |
| Nb | 91,91m,92,92m,93,93m,94,95,95m | 9 |
| Mo | 92,93,94,95,96,97,98,99,100 | 9 |
| Tc | 95,95m,96,97,97m,98,99 | 7 |
| Ru | 96,97,98,99,100,101,102,103,104,105,106 | 11 |
| Rh | 99,101,101m,102,102m,103,105 | 7 |
| Pd | 100,101*,102,103,104,105,106,107,108,109*,110 | 11 |
| Ag | 105,106m,107,108m,109,110m,111 | 7 |
| Cd | 106,108,109,110,111,112,113,113m,114,115,115m,116 | 12 |
| In | 111,113,114m,115 | 4 |

Table 1 Continued.

| Element | Atomic Mass | Number |
|------------------------|--|--------|
| Sn | 112,113,114,115,116,117,117m,118,119,119m,120,121,121m, 122,123,124,125,126 | 18 |
| Sb | 119,120m,121,122,123,124,125,126,127 | 9 |
| Te | 118,119,119m,120,121,121m,122,123,123m,124,125,125m,126, 127*,127m,128,129*,129m,130,131m,132 | 21 |
| I | 124,125,126,127,128*,129,130*,131 | 8 |
| Xe | 124,125*,126,127,128,129,129m,130,131,131m,132,133,133m,134,136 | 15 |
| Cs | 129,131,132,133,134,135,136,137 | 8 |
| Ba | 128,129*,130,131,132,133,133m,134,135,135m,136,137,138,139*,140 | 15 |
| La | 137,138,139,140,141* | 5 |
| Ce | 136,137m,138,139,140,141,142,143,144 | 9 |
| Pr | 141,142*,143 | 3 |
| Nd | 140,141*,142,143,144,145,146,147,148,149*,150 | 11 |
| Pm | 143,144,145,146,147,148,148m,149,150*,151 | 10 |
| Sm | 144,145,146,147,148,149,150,151,152,153,154 | 11 |
| Eu | 145,146,147,148,149,150,150m,151,152,152m,153,154,155,156 | 14 |
| Gd | 146,147,148,149,150,151,152,153,154,155,156,157,158,159*,160 | 15 |
| Tb | 153,154*,155,156,156n,157,158,159,160,161 | 10 |
| Dy | 154,155*,156,157*,158,159,160,161,162,163,164,165*,166 | 13 |
| Ho | 163,165,166,166m | 4 |
| Er | 162,164,165*,166,167,168,169,170,171*,172 | 10 |
| Tm | 165,166*,167,168,169,170,171,172 | 8 |
| Yb | 166,168,169,170,171,172,173,174,175,176 | 10 |
| Lu | 169,170,171,172,173,174,174m,175,176,177,177m | 11 |
| Hf | 174,175,176,177,178,178n,179,179n,180,180m,181,182 | 12 |
| Ta | 177,179,180,180m,181,182,183 | 7 |
| W | 178,180,181,182,183,184,185,186,187,188 | 10 |
| Re | 181*,182,183,184,184m,185,186,186m,187,188*,189 | 11 |
| Os | 184,185,186,187,188,189,190,191,192,193,194 | 11 |
| Ir | 188,189,190,191,192,192n,193,193m,194,194m | 10 |
| Pt | 190,191,192,193,193m,194,195,195m,196,197*,198 | 11 |
| Au | 194,195,196,197,198,198m,199 | 7 |
| Hg | 194,195*,195m,196,197,198,199,200,201,202,203,204 | 12 |
| Tl | 200,201,202,203,204,205 | 6 |
| Pb | 202,203,204,205,206,207,208,209*,210 | 9 |
| Bi | 205,206,207,208,209,210,210m | 7 |
| Po | 206,207*,208,209,210 | 5 |
| Sum of target isotopes | | 625 |

with new systematics, graphical output and automatic generation of isomeric cross sections in the 100-group format. The latter is achieved by including data on all known isomeric states and checking to see if a product has isomers. If it has, then the total reaction cross section is split by the appropriate isomer ratio and two (or more) cross section records are written. In some cases there is a substantial energy difference between the isomer and ground state and this is taken into account by varying the threshold for the production of the isomer and the ground state. For this version of the library a very simple formula is used to give the isomer ratio. For all reactions it is assumed that the ratio is given by equation 1

$$\sigma^m/\sigma^g = \begin{cases} 1 & , J^m \leq 7 \\ 10^{-2} & , J^m > 7 \end{cases} \quad (1)$$

where J^m is the isomer spin. Equation 1 describes a nuclide where only g and m states exist. If n is also present then similar expressions describe the splitting between the three states.

Better systematic formulae for individual reactions have recently been published by Kopecky and Gruppelaar⁶, and it is planned to incorporate these into THRES-G for future versions of the library.

2 Many more isomeric states have been considered in the present library. This has meant additional THRES-G calculations to replace existing reactions where product isomers were missing. In cases where the product isomer was present in the interim library but set to 1 even when the isomer spin was greater than 7, the cross sections have been rescaled to give an isomer ratio of 10^{-2} . However, when this change was made by the editor program no account was taken of the differing thresholds between the isomer and ground states.

Another problem that has been corrected in UKACT1 is the proper assignment of isomer (m and n) labels. Previous libraries only consider one possible isomer per nuclide. This means that if the second isomer is longer lived than the first, then the first isomer is ignored and the second isomer has the label m.

3 Many new capture reactions have been included. The processing code NJOY⁷ was used to give 100-group cross sections using data from the JEF1 library for 176 nuclides. These include cases where no capture data are present in the interim library or where the data are estimated using capture data from another reaction. In addition some missing reactions were taken from the ACTL⁸ library, after processing to produce the 100-group format. If data are unavailable from either of these sources then data for the nearest target nuclide with the same odd/even structure for number of neutrons and protons are used. In all cases if isomers exist as targets, exactly the same cross section as from the ground state is used. In the case of isomers as products the same isomer ratio as given in equation 1 is used.

4 Excitation of isomers by neutron interaction is calculated using the THRES-G code from the g or m states to the m and n states. However, there is no provision in the code for automatic calculation of superelastic collisions where the incoming neutron de-excites the nucleus from an m or n state to the ground state. These cases are estimated by the following algorithms:

$$\sigma[X^m(n,n')X^g] = \frac{1}{2}\sigma[X^g(n,n')X^m]$$

if only g and m exist, and

$$\sigma[X^n(n,n')X^m] = \sigma[X^n(n,n')X^g] = \frac{1}{3}(\sigma[X^g(n,n')X^m] + \sigma[X^g(n,n')X^n])$$

if g, m and n exist.

5 With a library of such a large size (70161 card records) it is most important to have some systematic check that all possible reactions are included in the library. To provide this a checking program called CHECK has been written. This reads the index of target nuclides (essentially Table 1) and for each target checks that all of the standard twelve reactions shown in Figure 1 are present in the library. It is a reasonably sophisticated in that the 'boxes' generated for each reaction are split into two or three parts if product isomers exist. The 3×3 character symbols indicate whether the cross section in the library is zero (0) or if there are 1,2 or 3 routes. Multiple routes mean for example, that (n,np) and (n,d) cross sections are given separately even though the same product nuclide is formed. An asterisk indicates that the reaction is missing.

Also shown in each box is the source of the decay data for that nuclide. 'STB' indicates a stable nuclide, 'JEF' that the data comes from the JEF1 file and 'TRI' that the data are taken from The Table of Radioactive Isotopes⁹. If no decay data exist in the decay library then the symbol '~~~' is shown. CHECK prints a list of all the missing reactions and gives summary statistics on the whole library.

Table 2 Summary statistics of the library UKACT1 produced by the code CHECK.

STATISTICS FOR LIBRARY

NUMBER OF TARGET NUCLIDES : 625
 NUMBER OF MISSING REACTIONS : 441
 NUMBER OF REACTIONS WITH ZERO CROSS SECTION : 1208
 NUMBER OF REACTIONS WITH ONE ROUTE : 6936
 NUMBER OF REACTIONS WITH TWO ROUTES : 888
 NUMBER OF REACTIONS WITH THREE ROUTES : 1
 NUMBER OF ADDITIONAL REACTIONS : 10
 NUMBER OF NON ZERO REACTIONS IN BOXES : 7825

NUCLIDE : PT195
 MAT NUMBER : 1207

| | | | | | |
|--------------------|-------------------------------------|---|---|---|------------------------|
| M PT193 | G 000 0 0 000 | PT194 1 1 1 | M PT195 | G ##### ##### ##### ##### ##### ##### | PT196 1 1 1 |
| TRI | TRI | STABLE | TRI | STB | STABLE |
| (N,3N) | | (N,2N) | (N,N') | | (N,G) |
| N M G IR192 | 000 000 0 0 0 0 000 000 | M G IR193 222 222 2 2 222 222 | M G IR194 222 222 2 2 222 222 | M G IR195 1 1 1 1 1 1 | |
| JEF JEF JEF | TRI STB | TRI TRI | TRI TRI | TRI TRI | |
| (N,NT) | (N,T) | (N,D) | (N,P) | | |
| M OS191 | G 1 1 1 | M OS192 | G 1 1 1 | M OS193 | G 000 0 0 000 |
| TRI | TRI | TRI | STB | TRI | TRI |
| (N,NA) | (N,A) | (N,H) | | JEF | (N,2P) |

KEY TO BOXES

* REACTION MISSING
 0 REACTION HAS ZERO CROSS SECTION
 1 REACTION HAS ONE ROUTE
 2 REACTION HAS TWO ROUTES
 3 REACTION HAS THREE ROUTES
 ~~~ DECAY DATA MISSING  
 JEF DECAY DATA FROM JEF LIBRARY  
 TIR DECAY DATA FROM TABLE OF RADIOACTIVE ISOTOPES  
 STB STABLE NUCLIDE  
 G M N REFER TO ISOMERS  
 ##### TARGET NUCLIDE

Figure 1 The output of CHECK for <sup>195</sup>Pt, a similar output is produced for each of the other 624 targets.

The listings of the missing reactions for the interim libraries were checked. In many of the cases the reactions had been considered by THRES-G, but had not been printed because they were zero. This indicates that either the threshold is too high or that the cross section is smaller than the built in lower limit of  $10^{-7}$  barns in THRES-G. In a later version it may be sensible to reduce this limit further. In other cases the listed reactions really were missing and these  $(n,\gamma)$ ,  $(n,n')$ , isomer and superelastic reactions were added. The summary statistics produced by CHECK are shown in Table 2. The entry 'additional reactions' refers to reactions which do not fit into the  $3 \times 4$  box format and these are mostly break-up type reactions *e.g.*  $^{12}\text{C}(n,n2\alpha)^4\text{He}$ . Only four out of the ten additional reactions are in fact non-zero.

Within the following constraints it is believed that the 100-group format of UKACT1 is complete. The constraints are: all nuclides with  $Z \leq 84$  and with half lives greater than one day and additional nuclides with long lived reaction products are considered as targets, and cross sections are set to zero by THRES-G if less than  $10^{-7}$  barns. Tests are underway at Imperial College to check whether the criterion for selection of targets of one day half life is adequate. It is however believed that most future effort will be put into an improvement in accuracy rather than an addition of reactions. This will be done by utilizing more sophisticated codes as indicated in reference 1 for important reactions identified by the sensitivity work.

### 3 The decay data library UKDECAY1

In addition to the cross section data for the target nuclides the inventory code also requires radioactive decay data for the target and short lived product nuclides formed either by reactions or by decay. FISPACT reads the decay data in ENDF/BV format and it is therefore possible to use existing JEF1 evaluations for most of the nuclides. In all 1314 nuclides require data, although for the 266 stable isotopes only identifying information is needed. Where data are not available in the JEF1 library, data were extracted by hand from the handbook Table of Radioactive Isotopes<sup>9</sup>. In a very few cases half life data were taken from Tuli<sup>10</sup> and decay energies were estimated from  $Q$ -values. The following data are converted into the ENDF/BV format for the 435 nuclides:

- 1) chemical symbol, mass number and isomeric state,
- 2) half life,
- 3) average gamma, beta and alpha energies,
- 4) number of decay modes,
- 5) branching ratio to each daughter.

For the average energies the following conventions were followed, using the notation of reference 9.

$$\text{Average gamma energy} = \langle \gamma \rangle + \langle IB \rangle$$

$$\text{Average beta energy} = \langle \beta^- \rangle + \langle \beta^+ \rangle + \langle e \rangle$$

$$\text{Average alpha energy} = \langle \alpha \rangle$$

If data are not given then the following rules were applied:

For  $\beta^-$  decay, if  $\langle \gamma \rangle$  is not given then  $\langle \gamma \rangle = \frac{1}{2}Q_{\beta^-}$  and  $\langle \beta \rangle = \langle \gamma \rangle$

if  $\langle \gamma \rangle$  is given then  $\langle \beta \rangle = \frac{1}{2}(Q_{\beta^-} - \langle \gamma \rangle)$ .

For  $\beta^+$  decay, define  $e = \frac{1}{2}(Q_e - 2m_e c^2)$ , from neighbouring nuclides estimate  $f_\beta$  ( $= \% \beta^+$ ) and set  $\langle \gamma \rangle = (1 - f_\beta)e$  and  $\langle \beta \rangle = f_\beta e$ .

If  $e < 0$  then assume  $\langle \beta \rangle = 0$  and choose  $\langle \gamma \rangle$  from available photon data.

For  $\alpha$  decay, define  $\langle \alpha \rangle = \alpha \times$  branching fraction for  $\alpha$  decay.

For these constructed ENDF/BV files no spectral data are included, because of the time required to input so many data by hand, for nuclides that are expected to be of limited importance. However, as discussed in section 4 the spectral data are estimated by FISPACT so that dose rates from the 435 nuclides are not ignored. If subsequent inventory runs indicate that any of these nuclides contribute significantly to the total dose rate, then spectral data will be input or other evaluations used.

In a few cases *e.g.*  $^{172}\text{Ho}$  there are no data available in either references 9 or 10. For these nuclides a suitable value of half life and  $Q_{\beta}$  are estimated. In many decays the daughter can be in either the ground or isomeric state. The branching ratios were calculated using Lederer<sup>11</sup>, although only in a few cases with long lived isomers would this be important. If data are not available in Lederer, it is assumed that all the decays went to the ground or isomeric state depending on spins. All these estimates are unlikely to effect the overall result as the isomers are either short lived or decay by isomeric transition to the ground state.

In the case of  $^{180}\text{Ta}$  the identity of the g and m states as given by reference 9 have been reversed. This is because the long lived state ( $2.8 \cdot 10^{13}$  years) is present in natural Ta, and it is sensible to have the ground state and not the isomer input if natural Ta is present in any material to be irradiated.

#### 4 The inventory code FISPACT

Reference 1 indicates the reasons for the UK changing from the inventory code ORIGEN to FISPIN for calculations using the present library. Many changes have been made to FISPIN to enable the much larger data libraries to be read and stored, and to make the output more relevant to fusion applications. It was decided not to incorporate these changes within the existing version of FISPIN as this would have made the code large and clumsy for users of both the fission and fusion parts. Rather it was decided to put the fusion options in a separate code FISPACT based on the calculational routines of FISPIN but with modified input and output. The new code will be maintained alongside FISPIN so that the codes will remain a closely linked pair for the applications of power reactor and activation calculations.

The most important change has been in the sizes of the internal arrays necessitated by the large size of the activation data libraries. The main array which stores cross section and decay data is now 75000 words, an increase by a factor of more than two from FISPIN. The calculational method of FISPIN is based on the work of Sidell<sup>12</sup> and uses an exponential form in the first order Taylor expansion. This method has been shown to be efficient and reliable for stiff differential equations and the calculational routines are used unchanged in FISPACT. Many new subroutines have been added and these are described in outline below.

**ENDFP** Inputs decay data in ENDF/BV format.

**COLLAP** Uses a 100-group neutron spectrum to collapse the 100-group cross section library into a suitable 1-group library.

**MASSIN** FISPIN needs the material to be specified by the number of atoms of each isotope. This subroutine enables the total mass and percentage of each *element* to be input. It then calculates the number of atoms of each isotope from natural abundance data.

**HAZINP** This reads in information on biological hazards, *i.e.* the committed effective dose equivalent (CEDE) for ingestion and inhalation (Sv/Bq) from an external file. This is derived from the latest version of the RAPID database held by the National Radiological Protection Board and described in references 13 and 14.

**DOSES** The surface contact dose from gamma emissions above 100 keV is calculated in the approximation of contact with an infinite slab of the irradiated material. Both the dose rate due to individual nuclides and the total dose rate are calculated.

**BREM** A correction to the dose rate due to bremsstrahlung radiation from high energy  $\beta$  particles can be calculated for any specified nuclide. This can be important if a nuclide gives very little  $\gamma$  radiation, but has a high energy  $\beta$  emission. The subroutine uses a weighted average  $Z$  value for the whole material to evaluate the correction.

In addition to these new routines, existing routines are modified to give more features, these include the following.

**1** Sensitivity information in the form  $(dN_i/N_i)/(d\sigma_j/\sigma_j)$  for specified nuclide  $N_i$  and cross section  $\sigma_j$ . It has been shown by James<sup>15</sup> that these differential coefficients can be calculated in a very similar fashion as the inventory equations. Thus without much additional computing time the sensitivities can be generated and used to predict the most important reactions in the different pathways to formation of nuclides and also give estimates of the error of nuclide concentrations based on error estimates of the cross sections.

**2** Reading and processing of the data libraries into the internal arrays is a CPU intensive operation. The code therefore writes a very condensed version of the data libraries (basically the data in the main array A) at the same time as doing the initial read. This condensed form can then be used for all subsequent calculations.

**3** Files for nuclides which have been specially made in ENDF/BV format contain no spectral data. In order to estimate the contribution these nuclides make to the total dose rate and so decide if the data are really necessary, a spectrum is calculated based on the averages so as to give an exponentially decreasing intensity as a function of energy. These nuclides are flagged in the output and a percentage of the estimated doses to the total is calculated.

**4** New output more suitable for fusion activation calculations is produced by FISPACT.

FISPACT is presently being documented and tested. It is expected that a first version will be available in the near future for trial use.

## 5 Summary and conclusions

A new inventory code FISPACT based on the calculational methods of FISPIN has been written. This is able to read and process the large cross section and decay data libraries necessary for activation calculations. The cross section library UKACT1 contains 100-group data for 625 targets covering 8719 reactions. This is an initial version and work is in hand to improve the accuracy of the most important reactions based on sensitivity calculations. The decay library UKDECAY1 consists of ENDF/BV files for 1314 nuclides and the file UKDOSE1 contains hazard data for ingestion and inhalation for 241 nuclides.

Inventory calculations for the first wall of a solid breeder DEMO<sup>16</sup> type reactor are due to start soon to ascertain the changes that the larger database has on the conclusions about acceptable amounts of elements in structural materials. Although UKACT1 and FISPACT have been developed for fusion applications, there is no reason why they could not be used with other spectra in fission activation. In these situations with a high proportion of thermal neutrons more effort would be needed to improve the capture reactions in the library.

## 6 References

1. Forrest R.A., 'Status of the UK activation cross section library for fusion', *IAEA Advisory Group Meeting on Nuclear Data for Fusion Reactor Technology, Gaussig*, December 1986.
2. Mann F.M., Lessor D.E. and Pintler J.S., *Nuclear Data for Basic and Applied Science, Santa Fe*, 207, 1986.
3. Gruppelaar H. *et al*, 'Cooperation between ECN Petten and JRC Ispra on the improvement and extension of activation data for fusion reactor technology', (in course of publication), 1986.
4. Forrest R.A., 'Systematics of neutron-induced threshold reactions with charged products at about 14.5 MeV', *AERE – R12419*, 1986.
5. Giancarli L. and Gruppelaar H., 'User Manual for THRES-F Code', *Culham Report CLM-R 261*, 1985.
6. Kopecky J. and Gruppelaar H., *ECN Report ECN 200*, 1987.
7. MacFarlane R.E., Muir D.W. and Bolcourt R.M., 'The NJOY Nuclear Data Processing System'. *LA-9303-M, Vol.1*. Los Alamos National Laboratory (1982).
8. Gardner M.A. and Howerton R.J., 'ACTL: Evaluated neutron activation cross-section library – evaluation techniques and reaction index'. *UCRL-50400 (vol.18)*. Lawrence Livermore Laboratory (1978).
9. Brown E. and Firestone R.B., *Table of Radioactive Isotopes*, John Wiley and Sons, 1986.
10. Tuli J.K., *Handbook on Nuclear Activation Data*, IAEA Technical Report 273, Vienna, 1987.
11. Lederer C.M. and Shirley V.S., *Table of Isotopes, 7th Edition*, John Wiley and Sons, 1978.
12. Sidell J., 'EXTRA: A digital computer program for the solution of stiff sets of ordinary initial value, first order differential equations', *AEEW – R799*, 1972.
13. Greenhalgh J.R., Fell T.P. and Adams N., 'Doses from Intakes of Radionuclides by Adults and Young People', *NRPB – R162*, 1985.
14. Greenhalgh J.R., Kendall G.M., Fell T.P. and Kennedy B.W., 'The RAPID system for information retrieval from the NRPB Internal Dosimetry Database', *NRPB – M133*, 1986.
15. James M., Unpublished, 1981.
16. Baker *et al*, 'A DEMO Tokamak Reactor – Aspects of the Conceptual Design', *Culham Report CLM-R 261*, 1985.

